# MUTATION DETECTION AND THE USE OF TISSUE EXPRESSION PROFILING TO ELUCIDATE THE PATHOGENESIS OF DUCHENNE MUSCULAR DYSTROPHY

by

KUMARI DEVI HALLWIRTH PILLAY

Submitted in partial fulfillment of
the requirements for the degree of

DOCTOR OF PHILOSOPHY

in the
Department of Neurology
University of KwaZulu-Natal
Durban
South Africa
2008

# DECLARATION

This study represents original work by the author and has not been submitted in any form to another University. Where use was made of the work of others it has been duly acknowledged in the text.

The research described in this thesis was carried out in the Department of Neurology, University of KwaZulu-Natal, under the supervision of Professor P.L.A. Bill; the Department of Biological Chemistry, University of California, Irvine, under the supervision of Dr. William Byerley and at the Center for Human and Clinical Genetics, Leiden University Medical Center, the Netherlands under the supervision of Dr. Johan den Dunnen, Professor E. Bakker and Dr. Peter-Bram 't Hoen.

_____

Kumari Devi Hallwirth Pillay

2008

# DEDICATION

Dedicated to my wonderful husband whose unrelenting support made the completion of

this thesis possible.

# PRESENTATIONS

**Personal presentations of this work that was presented in part at congresses**

1. Invited speaker - Oral presentation entitled: Molecular aspects of Duchenne muscular dystrophy. Society of medical laboratory technologists of South Africa meeting, February 2004, Inkosi Albert Luthuli Central Hospital.

2. Oral presentation entitled: Tissue expression profiling in Duchenne muscular dystrophy using microarray analysis and quantitative real-time PCR Faculty research day, September 2005, Nelson R. Mandela School of Medicine, Durban, South Africa.

**Presentation performed on my behalf**

1. Presentation done by Prof. Bill entitled: Gene expression profiling in DMD using microarray analysis and real-time PCR. **Neurology Congress**, March 2006, The Royal Hotel, Durban, South Africa.

# PUBLICATIONS

1. K.D. Hallwirth Pillay, P.L.A Bill, L. Mubaiwa and P. Rapiti. Molecular deletion patterns in Duchenne and Becker muscular dystrophy patients from KwaZulu Natal. 2006. Journal of the Neurological Sciences.

2. In preparation: K.D. Hallwirth Pillay, P.A.C 't Hoen, P.L.A., Bill, E. Bakker and J.T. den Dunnen. Gene profiling analysis in double biopsy dystrophinopathy patients show gene indicators that may assist in elucidation of pathogenesis.

**Other publications**

1. Pillay, K.D., Madurai, S, Bill, P.L.A., Hallwirth, C. Molecular diagnosis of Duchenne muscular dystrophy. Abstract. Neuromuscular Disorders. Vol. 10 (4,5). pp. 379. 2000.

2. K.D. Pillay, S.Madurai, A.L.J.Kneppers, E.Bakker and P.L.A.Bill. Carrier statusdetermination for Duchenne muscular dystrophy using quantitative polymerase chain reaction techniques. Abstract. Journal of the Neurological Sciences. Vol. 199 (Supp.1). 2002.

3. Bhigjee Ahmed, Sablonniere B, Madurai S, Emery-Rouaix N, Stojkovic T, Patel V.B, Bill P.L.A, Pillay K.D. Hereditary neuropathy with liability to pressure palsies: A clinical and molecular study in a South African family of Indian descent. African Journal of Neurological Sciences (online). Vol. 22 (1). 2003.

4. Ahmed Iqbal Bhigjee, Rivashnee Padayachee, Hoosain Paruk, <u>Kumari Devi Hallwirth-Pillay</u>, Suzaan Marais, Cathy Connoly, Lynnette Roux. Diagnosis of tuberculous meningitis: clinical and laboratory parameters. International Journal of Infectious Diseases. 2006, 335; 1-7.

5. **Submitted**: Harriet P. Lo, Sandra T. Cooper, Frances J. Evesson, <u>Kumari D. Hallwirth Pillay</u>, Jane T. Seto, Maria Chiotis, Valerie Tay, Alison G. Compton, Anita G. Cairns, Alistair Corbett, Daniel G. MacArthur, Nan Yang, Katrina Reardon and Kathryn N. North. (2007). Limb-girdle muscular dystrophy: diagnostic evaluation, frequency and clues to pathogenesis. Brain.

6. **Being submitted**: <u>K.D. Hallwirth Pillay</u>, P.L.A. Bill, C.V.Hallwirth and S.Madurai. Detection of novel point mutations in non-deletion patients with Duchenne muscular dystrophy.

# ACKNOWLEDGEMENTS

Peter-Bram, thank you for supervising the microarray aspect of the study at the Center for Human and Clinical genetics, The Netherlands. Your assistance was invaluable and I did not just gain knowledge but also a friend.

Thank you to my family, especially to my parents for your love, encouragement and motivation during my project.

Thank you to my parents-in-law Dr. Horst and Mrs. Helga Hallwirth for the immense interest that was shown in my research as well as your constant love and support.

Dr. Byerley, I express my thanks to you for affording me the opportunity of learning the SSCP technique with the help of research assistant, Brandi at the Department of Biological Sciences, University of California, Irvine.

Wendy Jones, our relationship over the past 7 years has grown into a remarkable friendship. I express my gratitude, for your constant assistance and belief in our research projects.

Muscular dystrophy foundation KwaZulu-Natal branch has provided regular funding for our MD research and has assisted tremendously in making our research endeavours possible. Thank you also to the MDF national body for assisting with funding my PhD project.

# TABLE OF CONTENTS

# LIST OF FIGURES

**CHAPTER 3**

## CHAPTER 4

# LIST OF TABLES

## CHAPTER 5

## CHAPTER 6

# ABBREVIATIONS

| | |
|---|---|
| μg | micro gram |
| μl | micro litre |
| μM | micro Molar |
| μm | micrometre |
| $^{32}$P | radioactively labelled phosphorous 32 |
| AAV | adeno-associated virus |
| $A_{260}$ | absorbance at 260 nm |
| ATF | activating transcription factor |
| ATP | adenosine triphosphate |
| bp | base pairs |
| β-DGN | beta-dystroglycan |
| BMD | Becker muscular dystrophy |
| BSA | bovine serum albumin |
| CE | capillary electrophoresis |
| CINRG | The Cooperative International Neuromuscular Research Group |
| CNS | central nervous system |
| CREB | cyclic AMP response element binding protein |
| cGMP | cyclic guanosine monophosphate |
| DAB | diaminobenzadine |
| DAGC | dystrophin associated glycoprotein complex |
| ddNTP | di-deoxy nucleotide triphosphate |
| DEPC | diethyl pyrocarbonate |
| $dH_2O$ | distilled water |

| DNA | deoxyribonucleic acid |
| DMD | Duchenne muscular dystrophy |
| DMSO | dimethylsulphoxide |
| dNTPs | deoxy nucleotide triphosphates |
| Dp | human dystrophin isoform |
| DRP2 | dystrophin related protein 2 |
| dsDNA | double stranded deoxyribonucleic acid |
| EDTA | ethylene diaminetetra-acetic acid |
| EGFP | enhanced green fluorescent protein |
| ENA | epithelial neutrophil activating peptide |
| FAM | 6-carboyx-fluorescein |
| GAPDH | glyceraldehydes 3-phosphate dehydrogenase |
| Grb2 | growth factor receptor-bound protein 2 |
| H+E | haematoxylin and eosin |
| HCl | hydrochloroic acid |
| HEX | 4,7,2', 4', 5', 7'-hexochloro-6-carboxy-fluorescein |
| HPLC | high performance liquid chromatography |
| Hsp | heat shock protein |
| Igf | insulin-like growh factor |
| IL | interleukin |
| kb | kilobase |
| kDA | kilodalton |
| M | molar |
| mA | milli Amps |
| MAPK | mitogen activated protein kinase |

| | |
|---|---|
| MDSC | muscle-derived stem cell |
| *mdx* | mouse model of Duchenne muscular dystrophy |
| MEF2 | myocyte enhance factor 2 |
| $MgCl_2$ | magnesium chloride |
| mM | milli-molar |
| MSDS | material safety data sheet |
| NaCl | sodium chloride |
| NaOH | sodium hydroxide |
| NFAT | nuclear factor of activated T-cells |
| ng | nano gram |
| nm | nanometer |
| nNOS | neuronal nitric oxide synthase |
| NO | nitric oxide |
| OD | optical density |
| PBS | phosphate buffered saline |
| PCR | polymerase chain reaction |
| PGC-1 | peroxisome proliferator γ coactivator 1 |
| PI3K | phosphatidylinositol-3-kinase |
| pMol | pico moles |
| RFU | relative fluorescence units |
| RNA | ribonucleic acid |
| SCK | serum creatine kinase |
| SDS | sodium dodecyl sulphate |
| SNP | single nucleotide polymorphism |
| SP | muscle-resident side population |

| | |
|---|---|
| SSCP | single stranded conformational polymorphism |
| TAMRA | |
| *Taq* | *Thermus aquaticus* |
| TBE | tris, boric acid, ethylenediamine tetra-acetic acid |
| TE | Tris EDTA buffer |
| $T_m$ | melting temperature |
| TGF | transforming growth factor |
| TNF | tumour necrosis factor |
| UTR | utrophin |
| UV | ultraviolet |
| V | volt |
| v/v | volume per volume |
| w/v | weight per volume |

# ETHICS

This entire study was approved by the Ethics Committee at the Nelson R. Mandela School of

Medicine, University of KwaZulu-Natal, Durban, South Africa.

# ABSTRACT

Duchenne muscular dystrophy (DMD) is an X-linked recessive disorder affecting 1:3500 live male births. Disease manifestations include progressive weakness of predominantly proximal musculature, due to progressive loss and degeneration of muscle fibres, fatty infiltration and fibrosis, resulting in reduced mobility and eventual loss of ambulation. Becker muscular dystrophy (BMD) is the allelic variant of Duchenne muscular dystrophy however the disease course is milder with less severe disease symptoms and progression. In 5-10% of cases, female patients referred to as manifesting carriers have shown characteristic muscle weakness and pseudohypertrophy of gastrocnemius muscles.

The 427 kDa protein product, dystrophin, is composed of 79 exons, containing 3686 amino acids and spanning 2.4 Mb. Dystrophin is a member of the cytoskeletal protein family and early studies localised this protein to the cytoplasmic face at the inner surface of the sarcolemma (Zubrzycka-Gaarn et al., 1988). The dystrophin protein is thought to play a structural role in the cytoskeletal membrane owing to its similarity to structural proteins. Various functional studies performed on dystrophin suggested that the protein has numerous interacting partners involved in the regulatory process with the dystrophin associated glycoprotein complex playing a significant role. Such vast and varied protein interactions highlight the complexity of elucidating the pathogenesis in Duchenne and Becker muscular dystrophy. In order to better understand the pathogenesis of human dystrophinopathies, a diverse range of disease models have been employed in order to unravel the pathophysiology of DMD and BMD.

Mutation detection is an important first step in categorising dystrophinopathy patients into DMD or BMD classes. This study aimed to find methodologies that were efficient, effective as well as cost-effective at producing a definitive result in a resource-limited setting such as South Africa. This was done by initially performing single stranded conformation polymorphism analysis on DNA samples from 20 individuals including both the patient and his mother or female relative that were previously shown to have no deletions using the 18-exon multiplex PCR assay. Their mothers DNA samples were also subjected to the analysis if the DNA was available. "Cold" PCR-SSCP was employed using both a conventional slab gel apparatus and the Novex precast gel apparatus. Various parameters including optimal voltage, the correct circulating device to maintain the temperature, buffer concentrations, gel concentrations, the use of denaturants and the use of appropriate loading buffers were optimised. The Novex system took only 2-3 hours and produced better resolution of bands and product separation than the slab gels. The slab gel system had the advantage of being cheaper to run and the circulating water bath could be easily manufactured thus making all equipment more readily available in South Africa than the expensive Novex apparatus. When all the results were collated, 17 patients showed abnormally migrating bands on visual inspection. On subjecting the DNA samples to DNA sequencing analysis, three SNPs were found in exon 6 and flanking sequence of exon 5, and two insertion mutations were found in exon 52. From these results, the carrier status in the mother of the DMD patient and his female relative can be determined. DNA sequencing analysis revealed that the mother and female relative of the DMD patient have the same nucleotide changes / mutations.

The 30-exon multiplex PCR mutation detection assay aimed to expand the conventional 18-exon multiplex PCR assay and was performed on DNA samples from 24 patients. The

technique incorporated 30 primer pairs into three separate reaction mixes. The assay did not improve the diagnostic efficacy of the 18-exon multiplex PCR. The 30-exon screening method detected the start and end exon of a patient's deletion and therefore proved useful in confirming a clinical diagnosis of dystrophinopathy. One was also able to determine whether a deletion was in-frame or out-of-frame by utilising the reading-frame-checker (www.dmd.nl) and in so doing a diagnosis of DMD or BMD was made.

The next mutation detection method, the multiplex ligation-dependent probe amplification (MLPA) assay was implemented with the aim of detecting deletions and duplications throughout the dystrophin gene. The technique utilised probes instead of primers in the assay therefore a confirmation of any previously detected deletions using other primer based methodologies was achieved. A total of 23 individuals were included, two of which were mothers of DMD patients. Four of the 21 patients included had duplication mutations in the dystrophin gene, with two being in-frame and two being out-of-frame. All patients exhibited a rapidly progressing dystrophinopathy this suggesting that the duplication mutations are far more complex and produce different effects compared to deletion mutations. Duplication mutations were a lot more difficult to analyse using the Genemapper software on the ABI 3100 genetic analyser as dosage quotient analysis and the Excel spreadsheet was required to obtain a definitive answer whereas visual inspection was sufficient to detect deletions. One of the patients with a duplication mutation was shown to have a complex re-arrangement mutation and this was confirmed in the mother.

Following on from the mutation detection analyses, double biopsy samples obtained with informed consent from four dystrophinopathy patients were subjected to gene profiling analysis using spotted oligonucleotide arrays and Illumina bead arrays. By obtaining two

samples from the same patient we were able to remove the element of genetic variability that normally adds bias to gene profiling experiments such as those conducted between normal and diseased tissue samples or pooled samples. This novel aspect of the study was performed at Leiden University in the Netherlands. The gastrocnemius muscle was biopsied from all patients, the biceps muscle was biopsied from 3 patients and the quadriceps muscle was biopsied from one patient. This part of the study aimed to answer the question why specific muscle groups such as the biceps and quadriceps muscles become progressively weaker whereas the gastrocnemius muscle remains invariably strong despite the lack of dystrophin protein in all muscles subjected to immunohistochemical analysis. For the spotted oligonucleotide arrays, dye-swap experiments were performed and P-values were calculated using Rosetta's error model. For beadchip analysis, the Illumina Human Sentrix-6 Beadchip was used. Quantile normalisation was achieved using "R" and Benjamin-Hochberg multiple testing was performed. On evaluation of the microarray data a positive correlation was achieved between the molecular findings and immunohistochemical observations on muscle biopsy. The dysregulated genes included immediate early factors, transcription factors, ECM proteins and IGF binding proteins, whilst the discordant genes were MAP kinase signalling genes (MAPK1, DUSP1, DUSP6, JAK1, GRB2, ILK), immediate early proteins (ZFP36, EGR1), ubiquitin (UBE2D2, UBC), NF-kB, Homeobox proteins (IRX5, MSX1, PRRX1) and some extracelluar matrix proteins.

Interestingly, many transcription factors including TAF15, USF2, CEBPA, RNPS1, SAFB, MEIS1 and HOXC6 were down-regulated in biceps / quadriceps vs. calf in our study. It can be deduced from the results obtained that the homeobox transcription factors that appear to be differentially expressed in our study but not in other studies (DMD vs.

normal), may be responsible for sparing the gastrocnemius muscle in DMD patients when other muscles become progressively weaker.

Another important finding was that Hsp70 (heat shock protein 70) or Hspa1B showed up-regulation in our study with biceps or quadriceps vs. calf muscle, which differed from other studies. It has been documented that the absence of Hsp70 is associated with induction of cardiac hypertrophy and increased MAPK signalling. Our data revealed Hsp70 to be reduced in hypertrophied DMD calf muscle however it is also lower in DMD quadriceps muscle compared to healthy quadriceps. The phenotypic hypertrophy seen in the patients can therefore be attributed to the increased MAPK/p38 signalling in DMD calf muscle.

CYP2J2 was another gene that was found to be dysregulated in our study. CYP2J2, a P450 epoxygenase that synthesizes arachadonic acid is know to activate the p42/p44 MAPK signalling cascade in cardiomyocytes, which in effect provides cardioprotection after ischaemia (DeLozier et al, 2007). The gene has recently been found in skeletal muscle and by extrapolation such a protective effect may also prove to be true.

The results obtained from undertaking this novel gene profiling aspect of the study has far-reaching consequences both for therapy as well as in detecting the molecular signatures that play a role in elucidating the mechanisms involved in Duchenne muscular dystrophy pathogenesis. Large scale gene profiling analyses using both several patients and different platforms are an essential next step into further cement the results obtained from this study.

# CHAPTER 1

## GENERAL INTRODUCTION

Duchenne muscular dystrophy (DMD) is a debilitating X-linked recessive disorder affecting 1:3,500 live male births (Emery, 1993). It is named after Guillaume-Benjamin Duchenne de Boulogne, who was credited as having first described the disease and for the significant contribution he made in the area. However, according to Emery and Emery (1993), Edward Meryon first described DMD in 1851 where it was referred to as "granular degeneration".

## 1.1 CLINICAL MANIFESTATIONS

The disease is characterised by progressive wasting of the proximal musculature. The disease can be detected at birth by performing a serum creatine kinase (SCK) assay however the symptoms only become apparent as the child learns to sit and stand, or even later at ages 3-5 (Dubowitz, 1995). Clinical presentation including delayed motor developmental milestones and walking difficulties are common attributes exhibited by these children. Other manifestations include a waddling gait and difficulty climbing stairs due to proximal muscle weakness, and toe walking due to contracture of the archilles tendons. Gradual and progressive deterioration of muscle strength leading to wheelchair confinement by the age of 12 reflects the nature of the disease.
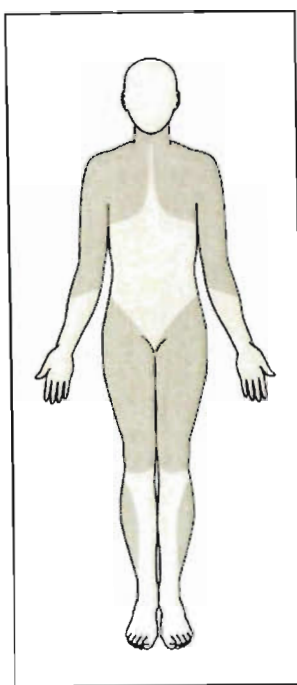
**Figure 1: Diagram highlighting the muscles that are predominantly affected & which become progressively weaker in Duchenne muscular dystrophy patients (adapted from Emery, 2002).**

The milder allelic variant, Becker muscular dystrophy (BMD) has a less severe disease progression. The disease was first brought to light by Becker and Kiener in 1955 as a disorder that closely resembled DMD. It was named Becker muscular dystrophy owing to the classification system proposed by Becker (Bakker, 1989). It is characterised by much later age of onset, usually after age 11. Affected individuals are diagnosed when skeletal muscle symptoms are evident on clinical examination, which can be in their late 20s (Emery, 2002). According to Emery and Skinner (1976), BMD is thought to be 10 times less frequent than DMD with one in 30,000 males being affected. In BMD there exists a broad clinical spectrum with respect to severity of disease state (Blake *et al.*, 2002). Loss of ambulation may occur late in adulthood or not at all, with the patients only suffering milder effects such as myalgia (Emery, 1993).

Dystrophinopathy is the disease manifested by patients that have dystrophin deficient muscle fibres. These patients display an abnormal Gowers' manoeuvre, which occurs as a

direct result of knee and hip extensor weakness. The action may be described as one where the affected child climbs up from the ground using his knees as an aid in rising by pushing down on them, thereby extending the hips and trunk (Emery, 2002). Pseudohypertrophy of the calf muscles is a distinguishing trait in both Duchenne and Becker muscular dystrophy. According to Emery (2002), the disorder was previously known as pseudohypertrophic muscular dystrophy on account of the enlarged calf muscles of affected patients. As the disease progresses the individuals suffer from recurrent respiratory problems due to weakening of the intercostals, which eventually lead to early death caused by pulmonary and other respiratory infections. Presently there is an increasing number of DMD patients who receive respiratory intervention through ventilation support and tracheostomy treatment, which increases their lifespan significantly (Simonds *et al.*, 1998; Emery, 2002). Cardiomyopathy and cardiac conduction defects are other leading causes of death in dystrophinopathies, particularly in BMD patients (Emery, 1993).

Apart from the clinical manifestations affecting dystrophinopathy patients, a recent study (Wicksell *et al.*, 2004) has outlined the specific cognitive defects that are present in these patients. From the 1980s to the present time, this area has been the focus of attention in many studies (Sollee *et al.*, 1985; Billard *et al.*, 1998; Bardoni *et al.*, 2000). Wicksell *et al.* (2004) performed a study on the IQ of DMD patients. No significant difference was found between the IQ scores of DMD affected and normal children, which was in contrast with previous studies (Cotton *et al.*, 2001). They did find that short-term memory was below normal whereas learning ability and long-term memory was not affected (Wicksell *et al.*, 2004). The group suggested that the cognitive differences seen in DMD patients may be attributed to heterogeneity of mutations in the dystrophin gene, which has been previously proposed and reviewed by Anderson *et al.* (2002).

Five to 10% of female carriers show symptoms such as muscle weakness, enlarged calf muscles and cardiomyopathy later in life (Emery, 2002). Grain *et al.* (2001) showed that even though cardiomyopathy does occur in carriers of DMD, the prevalence is lower than was previously reported. Owing to the variable state of progression relating to dystrophic symptoms, a mistaken diagnosis of limb-girdle muscular dystrophy can be made. It is therefore important that a full diagnostic work-up be performed on suspected manifesting carriers.

## 1.2    MOLECULAR GENETICS OF DYSTROPHIN

Mapping of one of the largest genes ever to be characterised, began in 1984 using the technique of positional cloning (Worton *et al.*, 1984; Kunkel *et al.*, 1985; Monaco *et al.*, 1985). The gene was localised to chromosome position Xp21.2 (Verellen-Dumoulin *et al.*, 1984; Worton *et al.*, 1984) and was shown to be allelic to Becker muscular dystrophy (Kingston *et al.*, 1983). The physical mapping was undertaken using pulsed field gel electrophoresis (PFGE) and field inversion gel electrophoresis (FIGE) because the enormous size of the gene prevented the use of conventional restriction endonuclease mapping.

In 1987, the protein product named dystrophin was discovered by Hoffman *et al.* (1987) and the complete dystrophin sequence was elucidated by Koenig *et al.* (1987). It was also revealed that the dystrophin gene spanned approximately 2.4 Mb and further screening using Southern blotting analysis highlighted fragments of the X-chromosome containing dystrophin exons. Gene promoters together with intron/exon boundaries were identified using exon mapping of isolated genomic clones (Worton, 1992). A full description of the

protein was outlined in 1988 by Koenig *et al.* where the muscle dystrophin gene was shown to encode a full-length 14 kb mRNA. The gene is composed of 79 exons. The exon structure was identified by Roberts *et al.* (1993), where a yeast artificial chromosome (YAC) vectorette approach was employed and further analysis on the exon/intron organisation of the gene was accomplished by Nobile *et al.* (1997).

Utilisation of these techniques led to the detection of a myriad of deletions in both DMD and BMD patients' samples. These deletions were found throughout the dystrophin gene with "hot-spots" located at the 5' proximal end and 3' distal end of the gene. The exonic deletion identification process was the first step in implicating the dystrophin gene in the pathogenesis of dystrophinopathies.

## 1.3    THE DYSTROPHIN PROTEIN

The 427 kDa protein contains 3686 amino acids (Koenig *et al.*, 1988) and is expressed in a highly regulated manner utilising approximately eight independent tissue specific promoters (Roberts, 1995). According to RNase protection assays conducted by Nudel *et al.* (1988) transcription was most active in skeletal muscle thus producing the highest level of expression in this region.



**Figure 2: Genomic organisation of the dystrophin gene highlighting the 79 exons of dystrophin (vertical lines) and location of the promoters, particularly brain (B), muscle (M) and purkinje (P) as adapted from Zhou *et al.* (2006).**

## 1.3.1 Dystrophin isoforms and regulated tissue specific expression

There are three promoters that independently regulate the expression of the 427 kDa full-length dystrophin transcripts in brain, muscle and purkinje as shown in the diagram above (figure 2). These full-length isoforms possess a "unique first exon spliced to a common set of 78 exons" (Zhou *et al.*, 2006). The Dp427m transcript is expressed predominantly in skeletal muscle, smooth muscle, cardiomyocytes and to a limited extent in the retina and glial cells (Barnea *et al.*, 1990; Chelly *et al.*, 1990).

The brain (B) promoter or exon 1 is located approximately 130 kb upstream of the Dp427m muscle promoter and drives expression of dystrophin in neurons in the cortex and the CA (*Cornu Ammonis*) regions of the hippocampus.

The Dp427p isoform is expressed in all cerebellar purkinje cells (Gorecki et al., 1992) and to a limited extent in skeletal muscle (Holder *et al.*, 1996). The unique promoter or exon 1 is located in what corresponds to the first intron of the Dp427m isoform.
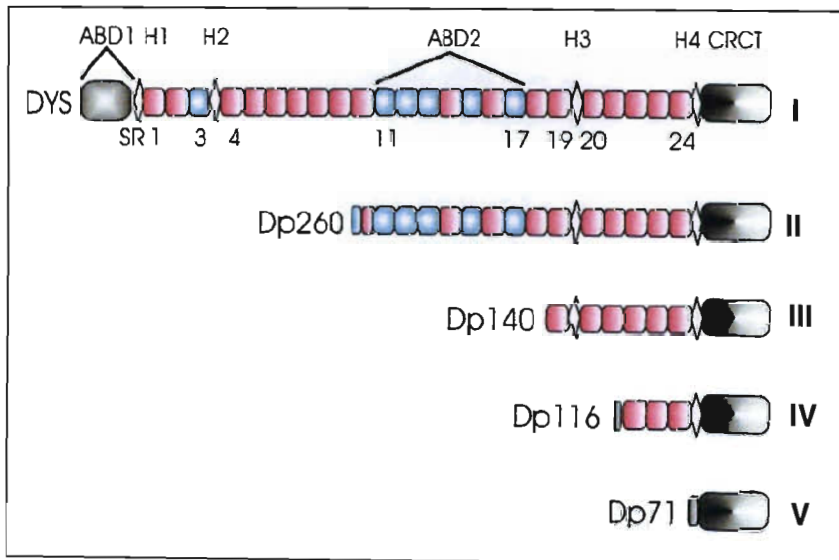


**Figure 3: Dystrophin gene isoforms (as adapted from Ervasti, 2006). Structure of the four dystrophin domains are clearly illustrated in the full-length muscle isoform.**

In the above figure, the dystrophin (DYS) domains are shown, which include the actin-binding domain (ABD1), composed of tandem calponin homology (CH) domains, a triple-helical spectrin-like repeat (SR), together with four hinge regions (H1-H4) located throughout the gene, a cysteine rich domain (CR) essential for binding β-dystroglycan and a carboxy-terminal domain important for binding syntrophins and α-dystrobrevin-2. Acidic spectrin repeats are coloured in pink, basic repeats coloured in cyan, and a cluster of independent acidic repeats form the second actin binding domain (ABD2). Other truncated dystrophin non-muscle isoforms, driven by specific promoters are also shown (Dp260, Dp140, Dp116, Dp71).

Within the dystrophin gene at least four other promoters are found, which give rise to smaller dystrophin transcripts that posses truncated carboxy-terminal regions (shown in figure 3 above). The Dp260 isoform expressed predominantly in the retina utilises exons 30-79 to produce its transcript.

Expression of the Dp140 isoform has been identified in the cerebral cortex, cerebellum, hippocampus, brain stem, spinal cord and olfactory bulb. It has also been detected in the kidney but not in skeletal muscle (Lidov *et al.*, 1990).

The Dp116 isoform was found specifically in adult peripheral nerve, along the Schwann cell membrane. Alternative splicing is also a feature of this isoform, which may also be called apo-dystophin-2 (Byers *et al.* 1993).

The Dp71 isoform is found predominantly in the liver, brain as well as astrocyte and glioma cell cultures. Interestingly, the transcript shares with Dp427m most of the cysteine-

rich and C-terminal domains sequence. Dp71 may also be referred to as apo-dystrophin-1 (Bar *et al.*, 1990).

## 1.3.2 Domain structure

The dystrophin protein belongs to the family of cytoskeletal proteins, which include α-actinin and β-spectrin. They possess a characteristic amino terminal domain followed by repeat units of spectrin-like elements. Dystrophin is composed of four domains, namely the amino terminal actin-binding domain, the central rod domain, the cysteine-rich domain and the carboxy terminal domain, each with highly distinctive affinities. A review of dystrophin's secondary structure revealed that this predominantly hydrophilic molecule (Kyte and Doolittle, 1982) has a propensity to form α-helices throughout the protein.

The actin-binding domain is composed of amino acids 1-220 and exons 2-8 (http://www.dmd.nl). This region in dystrophin is highly homologous to the actin-binding domain of α-actinin however it is not associated with cross-linking F-actin to form bundles (Kuhlman *et al.*, 1992; Roberts, 2001).

The central rod domain comprising 24, triple-helical spectrin-like repeats and incorporating amino acids 338-3,055 and exons 8-61 (http://www.dmd.nl), make up 75% of the protein (Koenig *et al.*, 1988; Roberts, 2001).

The next region initially referred to as the cysteine-rich domain is composed of amino acids 3,056-3,354 and exons 63-69 (Roberts, 2001, http://www.dmd.nl). The domain contains a β-sheet protein binding WW module that is found in other signalling molecules

(Bork *et al.*, 1994). It also has a $Ca^{2+}$ binding helix-loop-helix "EF" hand motif comprising four hairpins of α-helices (Noegel *et al.*, 1987; Brandon & Tooze, 1991) and a zinc-finger ZZ motif found in other nuclear and cytoplasmic proteins (Ponting *et al.*, 1996). According to Andersen *et al.* (1996), the ZZ domain binds calmodulin in a $Ca^{2+}$-dependent manner and this may have implications for calmodulin binding in other dystrophin related proteins (Blake *et al.*, 2002).

The C-terminal domain of dystrophin is comprised of amino acids 3,355-3,685 and exons 70-79 (http://www.dmd.nl). The only other close similarity exists between dystrophin and its homologous relatives, utrophin (Tinsley *et al.*, 1992), dystrophin-related protein and the dystrobrevins (Wagner *et al.*, 1993). The homology exists at a leucine zipper motif, which is well-documented as protein-interaction regions and located at amino acid positions 3,559-3,594. Being a region of protein interaction, the coiled-coil region of dystrophin serves as a binding site for dystrobrevin, syntrophins and perhaps other dystrophin-associated proteins (Suzuki *et al.*, 1994; Sadoulet-Puccio *et al.*, 1997; Blake *et al.*, 1995).

### 1.3.3 Utrophin and dystrophin-related protein 2

Dystrophin and utrophin are analogous in that they both possess the same four domains however utrophin is located on chromosome 6q24 and is 395 kDa whereas dystrophin is 427 kDa. In comparison to dystrophin, the rod domain of utrophin consists of a shorter 22 repeat region with the difference occurring at repeat 14 and 18 (Roberts, 2001) (Figure 4). In foetal and regenerating muscle, utrophin is expressed throughout the sarcolemma (Takemitsu *et al.*, 1991). Utrophin expression is concentrated at the neuromuscular and myotendinous junctions in adult muscle tissue whereas dystrophin has a more varied

expression (Ohlendieck *et al.*, 1991). According to Campanelli *et al.* (1994) utrophin may be involved with post-synaptic membrane maintenance and 'clustering of acetylcholine receptors'.

Many pathogenesis and therapy related studies have been performed to date on unravelling the mechanisms that are involved in utrophin regulation as it has been shown to play a role in compensating for dystrophin in dystrophin-deficient muscle (Rafael & Brown, 2000; Baker *et al.*, 2006). In 2003 an utrophin knockout mouse (UKOex6 - exon 6 was knocked out) was used to analyse and assess the cellular functions in several short isoforms of utrophin. In the same report it was found that full-length utrophin was expressed in 'intertubular tissue of the testis'. The authors speculated that it may be involved with testosterone secretion and that its absence may result in loss of fertility (Jimenez-Mallebrera *et al.*, 2003).

The dystrophin-related protein 2 (DRP2), a 45 kb gene which was localised to chromosome Xq22 (Roberts *et al.*, 1996) has close homology to the C-terminal domain of dystrophin and is 120 kDa in size (Figure 4). It is present in such tissues as the kidney, epididymis, ovary, in many synapses throughout the central nervous system and in Schwann cells (Roberts, 2001). The rod domain of the dystrophin-related protein has two repeats and there is a 75-residue coiled-coil amino terminal region specific to this protein (Roberts, 2001).

### 1.3.4 Sub-cellular location and function of dystrophin

Immunohistochemical studies have localised dystrophin to the cytoplasmic face at the inner surface of the sarcolemma (Zubrzycka-Gaarn *et al.*, 1988). It is confined to

costameres or the cytoskeletal lattice network (Porter *et al.*, 1992; Straub *et al.*, 1992).
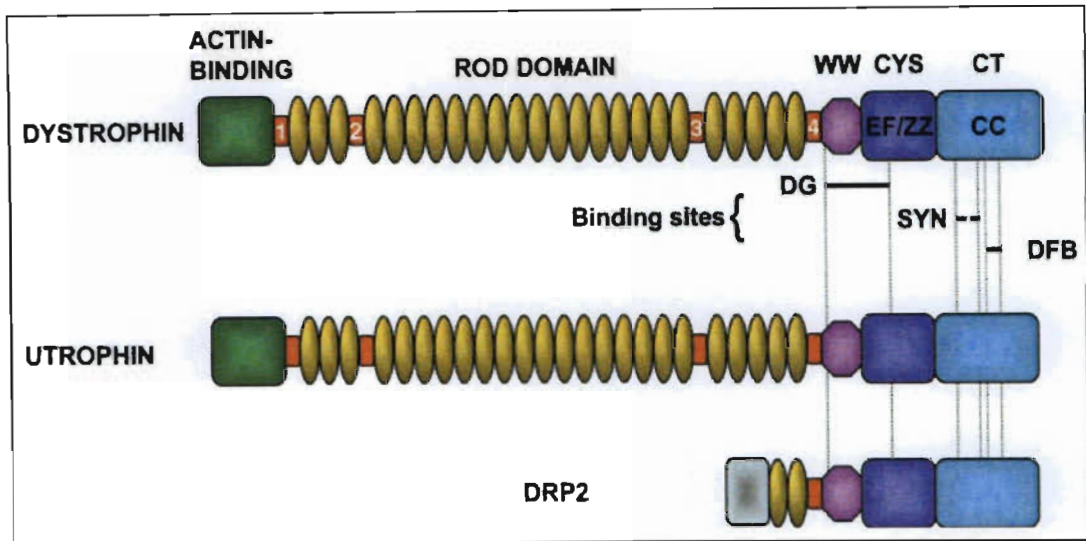


**Figure 4: Schematic diagram showing the similarity & differences between dystrophin (DYS), utrophin (UTR) & dystrophin related protein 2 (DRP) as adapted from Blake *et al.* (2002).**

According to Ervasti (2003), costameres are components that couple the sarcolemma to the Z-disk of muscle fibres with the assistance of many interacting protein partners. The location of dystrophin suggested that it was involved with strengthening the sarcolemmal membrane and mediating its association with the myofibrillar cytoskeleton (Watkins *et al.*, 1988). One of the functional roles played by dystrophin is outlined in the schematic below (Ervasti, 2006).

In figure 5, the three-tiered process is outlined. It comprises a relaxed muscle (I), muscle stretch, which "imposes forces that unwind" spectrin (spring-like) elements within repeats 1-10 and 18-24 (II) and "electrostatic interaction of basic actin-binding repeats 11-17 with acidic actin filaments" that reduces extension of the "spring-like elements" (III). The electrostatic interaction is non-specific and optimal because no specific orientation is required thus allowing sliding between actin and dystrophin. Owing to the shortening of muscle during contraction, electrostatic interaction facilitates a reduction in elastic recoil.
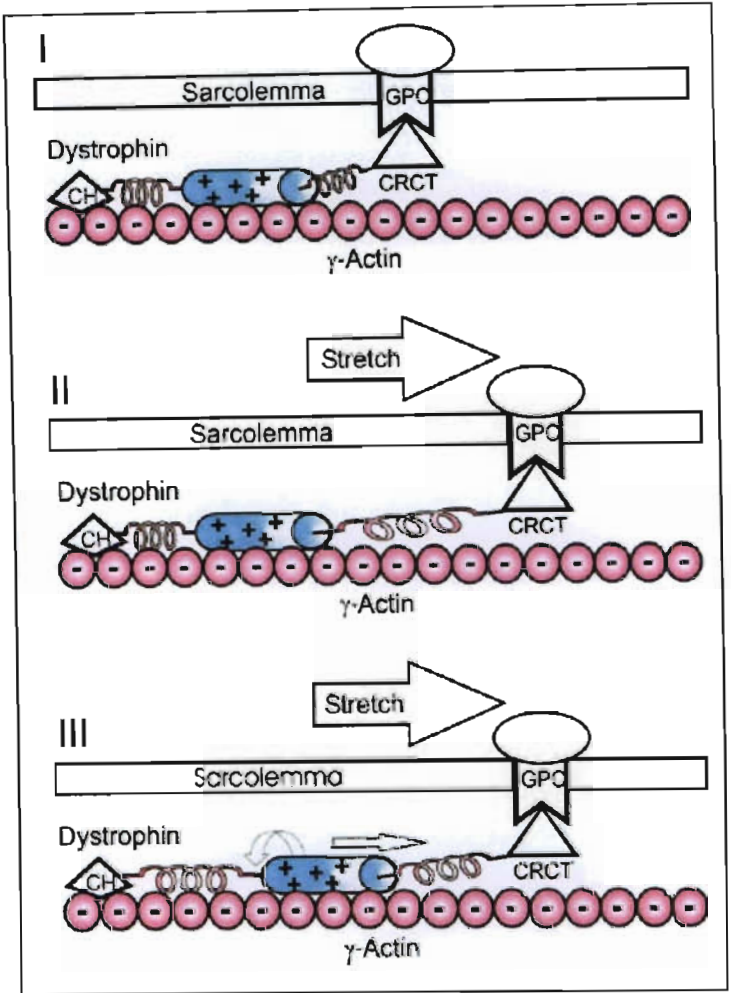
**Figure 5: Schematic model revealing dystrophin's functional role as a "molecular shock absorber" during muscle stretch as adapted from Ervasti (2006).**

## 1.4   DYSTROPHIN ASSOCIATED GLYOCOPROTEIN COMPLEX

In 1989 it was shown that dystrophin co-localised with a series of other proteins when a

dystrophin enriched fraction was isolated from detergent-solubilised skeletal muscle

membranes following chromatographic purification (Campbell & Kahl, 1989). This tightly

bound complex was found to be highly reduced in biopsies from DMD affected individuals

and *mdx* (mouse model of dystrophin) muscle lacking the dystrophin protein (Ervasti *et al.*,

1990; Ervasti & Campbell, 1991). All these findings suggested that this hetero-oligomeric

glycoprotein complex served as a structural link between the actin cytoskeleton and the

extracellular matrix. This stabilises the sarcolemma during repeated stress imposed by the contraction and relaxation process.

The dystrophin-associated glycoprotein complex can be separated into three complexes, namely the dystroglycan complex, the sarcoglycan:sarcospan complex and the cytoplasmic, dystrophin-containing complex (Winder *et al.*, 1995). Alpha and beta dystroglycan together provides the transmembrane link between laminin-$\alpha$-2 and dystrophin. Many extracellular matrix proteins such as the agrins, perlecan and neurexins have been shown to bind $\alpha$- dystroglycan with high affinity however the significance of such interactions is as yet unclear (Blake *et al.*, 2002). Beta-dystroglycan is one of the key players in the DAGC that engages in a direct protein interaction with dystrophin and a defined binding region has been mapped to the cysteine-rich domain of dystrophin (Roberts, 2001). Another binding partner of $\beta$-dystroglycan appears to be the adaptor protein Grb2, which leads one to speculate that it may be involved with the movement of "extracellular mediated signals to the muscle cytoskeleton" (Blake *et al.*, 2002). Another newly discovered player in the protein interaction game is caveolin-3, which also serves as a binding partner for $\beta$-dystroglycan. Studies have revealed that caveolin-3 may compete with dystrophin for the binding site of $\beta$-dystroglycan at the C-terminus (Sargiacomo *et al.*, 2000).
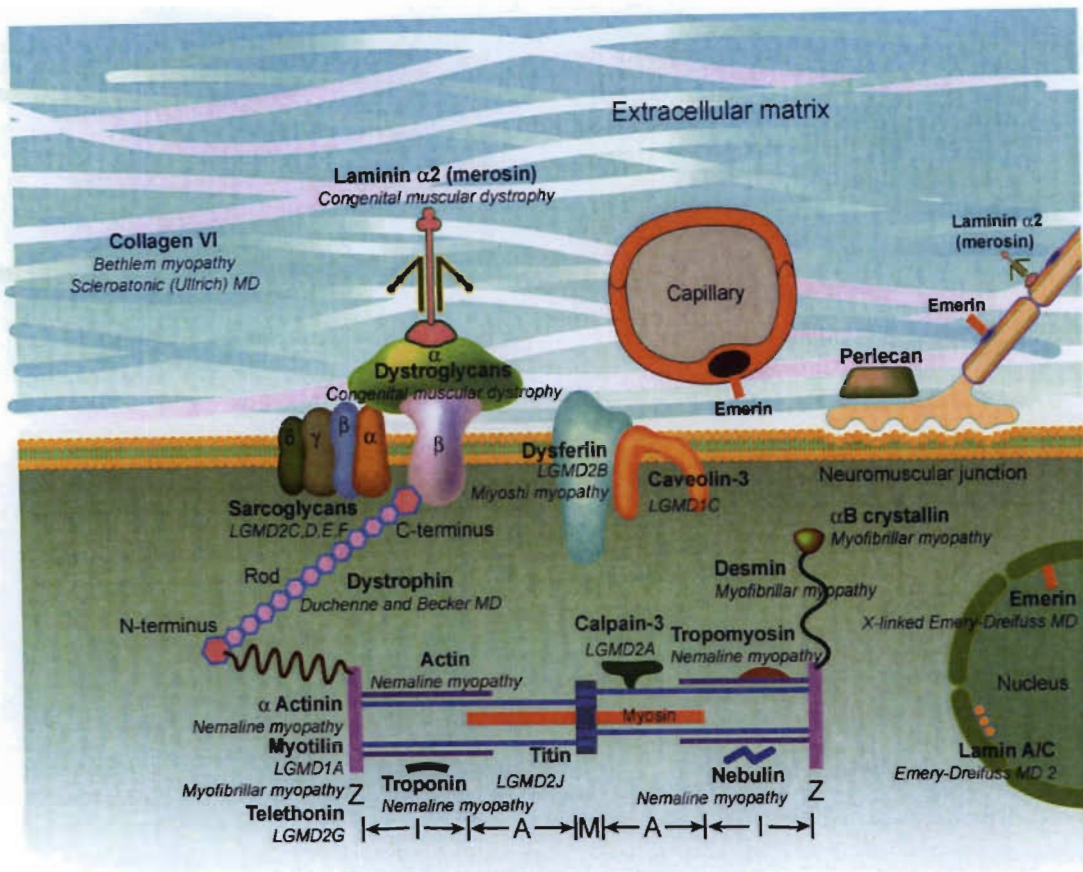
**Figure 6: Image showing the extracellular, sarcolemmal, myofibrillar & nuclear proteins of the dystrophin associated glycoprotein complex & their associated diseases as adapted from Vogel and Zamecnik (2005).**

The sarcoglycan complex comprises six transmembrane glycoproteins, namely, α, β, γ, δ, ε, ζ-sarcoglycan and the 25 kDa membrane protein sarcospan that also has four transmembrane domains. The actual function of these proteins still remains unclear, however studies have revealed that δ plays an integral role in the assembly of the other sarcoglycans as the absence thereof prevented assembly of the remaining glycoproteins in the endoplasmic reticulum (Hack *et al.*, 2000; Lapidos *et al.*, 2004).. The sarcoglycan group also ensures proper functioning and stability of sarcospan at the membrane (Crosbie *et al.*, 1999), however sarcospan null-mice do not exhibit muscle pathology (Lebakken *et al.*, 2000). With dystrophin deficiency as is the case in DMD, the sarcoglycan complex

becomes disrupted and a reduction in some of the glycoproteins is seen on immunohistochemical analyses.

The syntrophins are another important group of dystrophin interacting proteins that also bind neuronal nitric oxide synthase (nNOS), which is found at diminished levels in dystrophinopathy patients. The actual association and functional role has not been elucidated (Blake *et al.*, 2002). It was speculated by Ehmsen *et al.*, (2002) that the abnormal blood vessel constriction seen in DMD patients may be attributed to the lack of nNOS at the sarcolemma. This in itself is not enough to bring about a muscular dystrophy phenotype as has been shown in mouse studies (Crosbie *et al.*, 1998). According to Lapidos *et al.* (2004) "nNOS is responsible for increasing cyclic GMP levels to reduce vasoconstriction of smooth muscle" (Grady *et al.*, 1999).

The dystrobrevins are encoded by two different genes, with the α-dystrobrevin gene located on chromosome 18 (Sadoulet-Puccio *et al.*, 1996) and producing at least five different isoforms. Beta-dystrobrevin is located on chromosome 2 (Peters *et al.*, 1997) and produces C-terminal alternatively spliced forms. Dystrobrevin uses the same strategy employed by dystrophin to bring about expression in different tissues by utilising specific promoters (Lapidos *et al.*, 2004). Three of the α-dystrobrevin isoforms are located in the DAGC of skeletal muscle, with the coiled-coil domain of dystrobrevin interacting with dystrophin whilst a specific binding site exists where interaction with the syntrophins is brought about. It has been documented that the sarcolemmal localisation of α-dystrobrevin is lost in the absence of dystrophin (Metzinger *et al.*, 1997).

The highly arranged network of proteins that make up the DAGC and their complex

interactions are shown in the diagram below (Figure 7).

In the figure below, the core proteins that comprise the dystrophin-glycoprotein complex,

namely α-dystroglycan (α-DG), β-dystroglycan (β-DG), the sarcoglycan complex (SGC),

sarcospan (SPN), α-dystrobrevin-2 (α-Db 2), syntrophin (SYN) and dystrophin are

highlighted in pink. Structural proteins, cytokeratins 8 and 19 (K8/K19) that interact

directly with constituents of the DAGC, their binding partners and location within striated

muscle cells are also shown. Those proteins that are present in increased levels in

dystrophin-deficient muscle are shown in cyan.
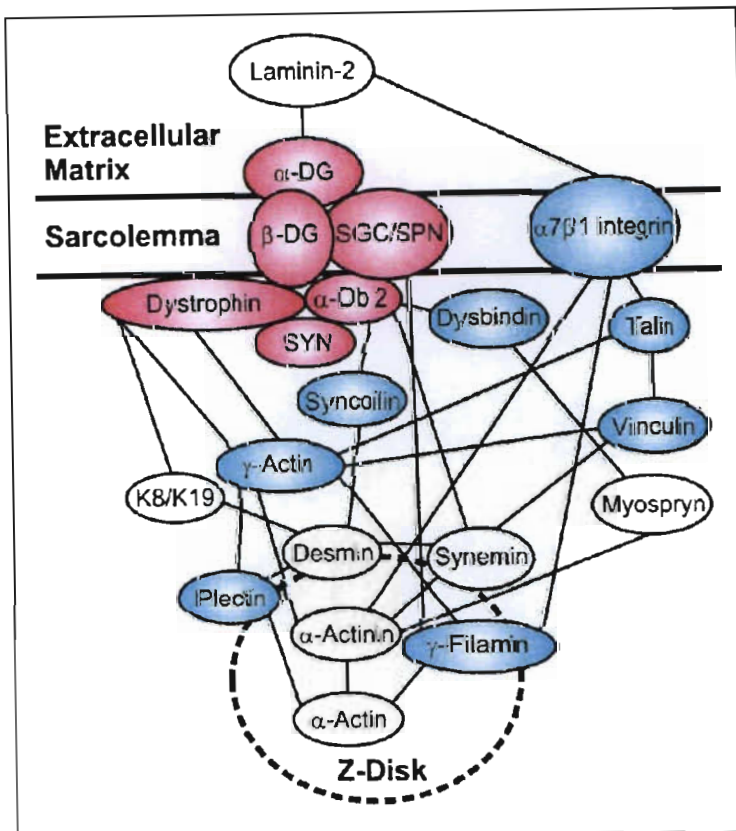


**Figure 7: Associations between the dystrophin associated glycoprotein complex (DAGC) constituents are clearly illustrated (as adapted from Ervasti, 2006).**

Proposed cell survival signalling pathways are shown in the diagrams below (figure 8,

Rando, 2001). In (A) of figure 8, calmodulin plays an active role in the cell survival

strategy. It regulates phosphorylation whilst also binding to dystrophin and α1- syntrophin in a calmodulin-dependent manner. The calmodulin-regulation kinases engage in cell survival pathways such as that brought about by phosphatidylinositol-3-kinase (PI3K) and Akt thereby controlling muscle cell survival.
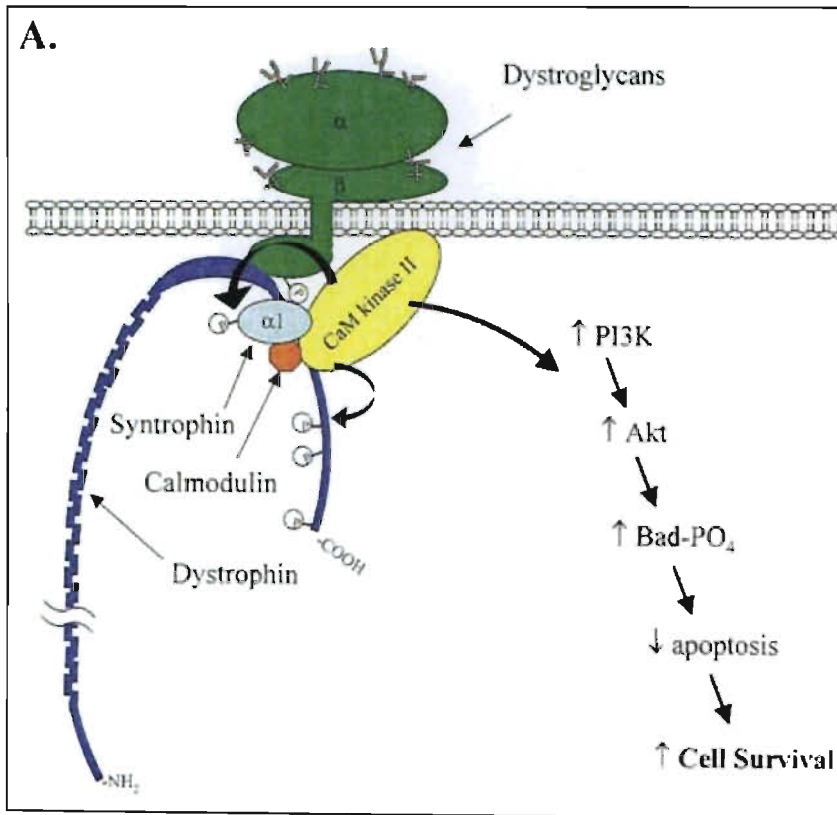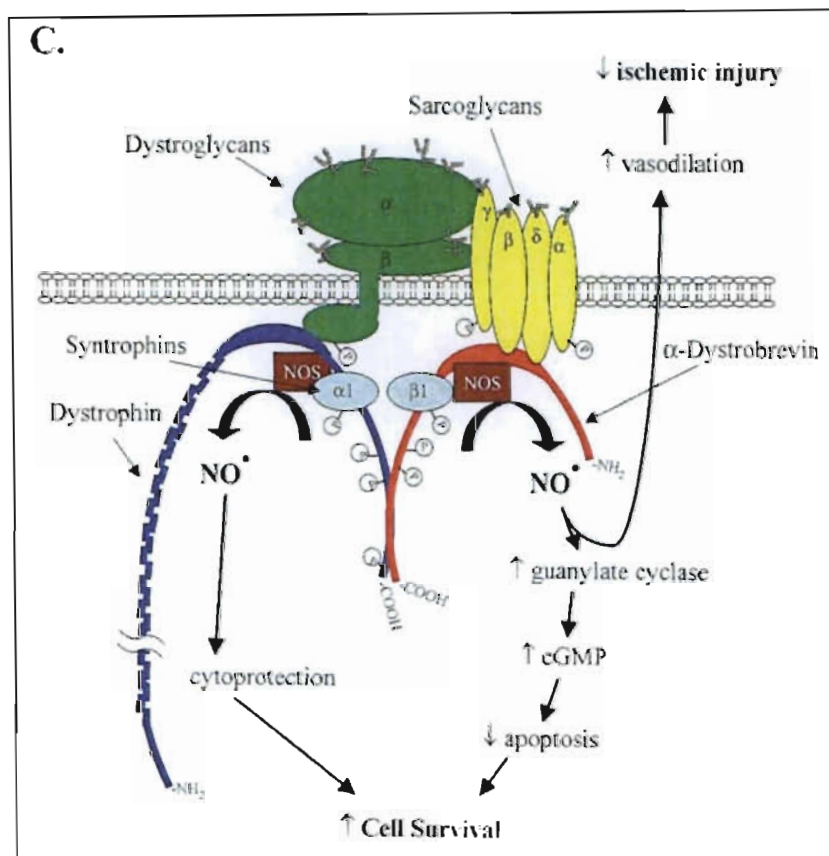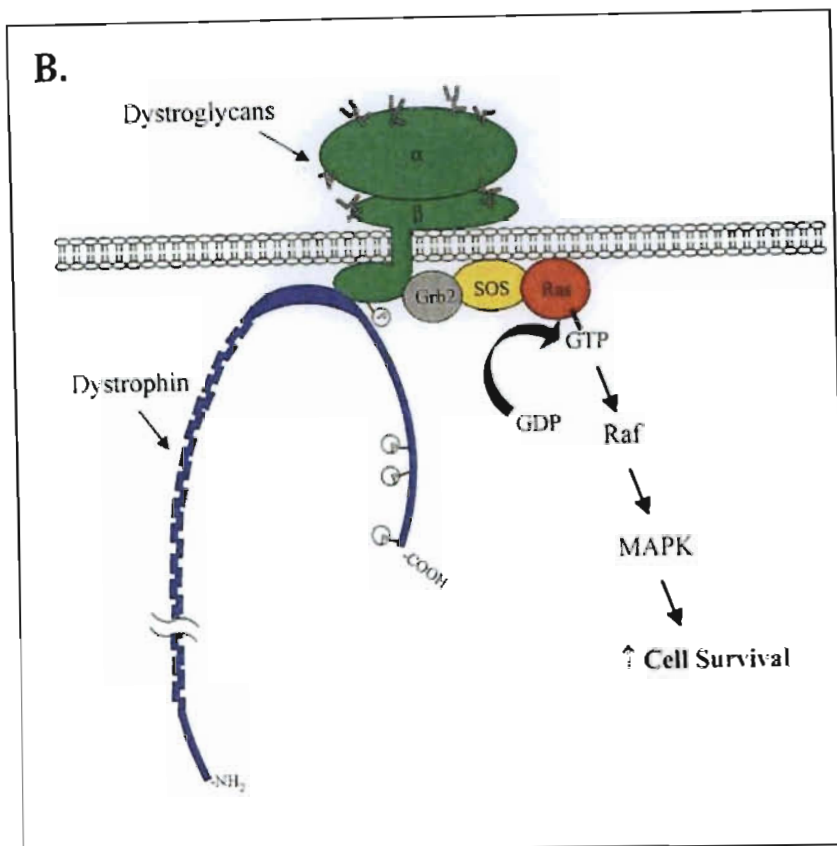
**Figure 8: Diagrams illustrating putative cell survival signalling cascade pathways associated with the dystrophin associated glycoprotein complex (as adapted from Rando, 2001).**

In (B) of figure 8, a cell survival strategy involving growth factor receptor-bound protein 2 (Grb2) is outlined. It has been previously reported that the Ras/MAPK signalling pathways are intimately involved with membrane signalling proteins such as caveolin and integrin in enhancing cell survival (Bonni *et al.*, 1999). This may have implications for the role played by Grb2 in the apoptosis that accompanies the disruption of the DAGC (Tidball *et al.*, 1995; Rando, 2001).

The last putative cell survival pathway utilises nNOS as the key enzyme (C, of figure 8 above), which has many binding sites in the DAGC, the most significant being the syntrophins. The active compound of this enzyme, nitric oxide (NO) has been implicated in many intracellular signalling pathways (Bredt & Snyder, 1994). The role of NO in the pathogenesis of DMD emerged when it was noted that it provides a vasodilatory effect on smooth muscle. Since NO is not present to regulate smooth muscle activity, functional ischemia results in the muscle cells (Sander *et al.*, 2000).

The figure below (Figure 9) shows the many pathways that are initiated and regulated by the nNOS reduction that occurs in dystrophin null mutant muscle (grey shaded boxes). This may be further worsened by muscle disuse. Also highlighted is the role of NO in DMD pathology through the cGMP pathway. Neuronal NOS therefore has a multi-faceted role in the pathophysiology of DMD (Tidball & Wehling-Henricks, 2007).

## 1.5    PATHOPHYSIOLOGY

According to Blake *et al.* (2002), the pathophysiology of dystrophin deficient muscle can be categorised into two parts, the first being abnormalities of the muscle cell and the other
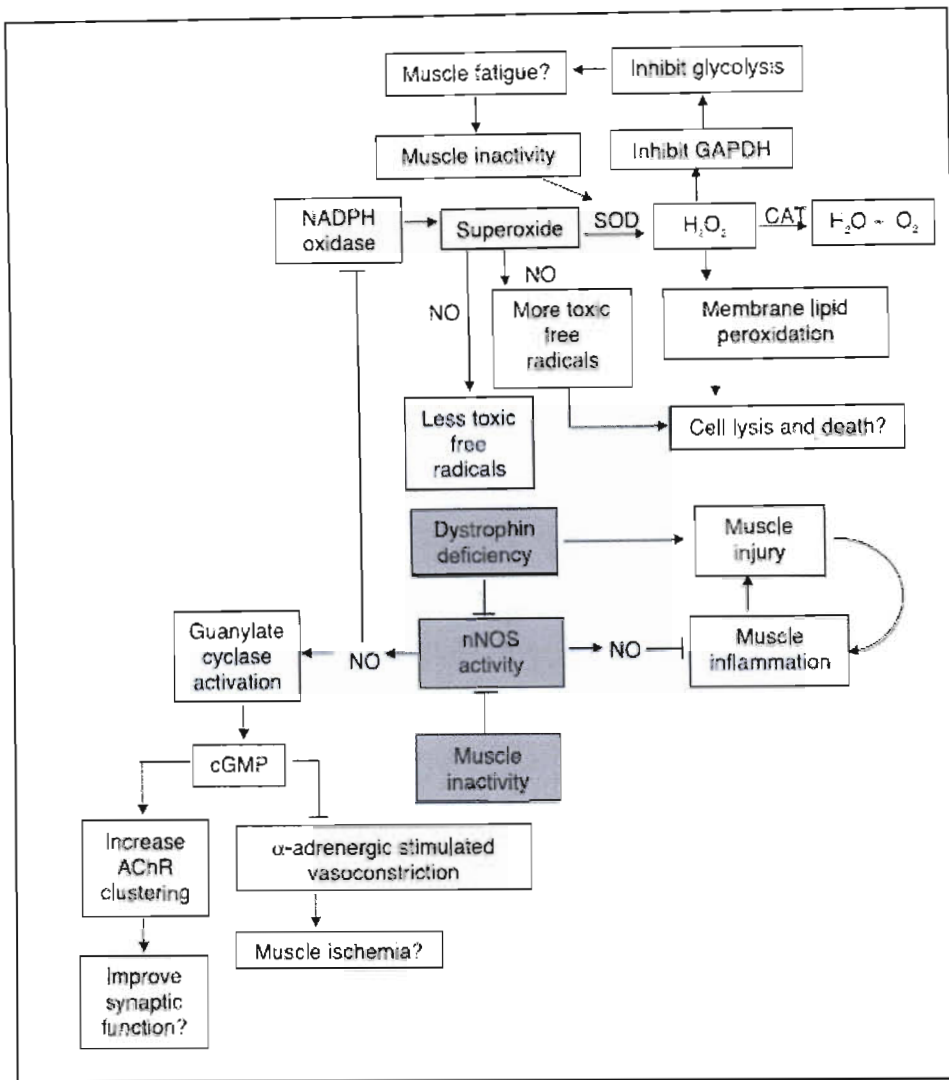
**Figure 9: Schematic showing the various routes through which nNOS contributes to the pathophysiology of Duchenne muscular dystrophy and the pathology seen in dystrophin-deficient muscle fibres (as adapted from Tidball & Wehling-Henricks, 2007).**

being abnormalities of the muscle tissue. A combination of biochemical, physiological and molecular studies has been used to identify the pathophysiological pathways involved in DMD (Figure 10). With respect to the abnormalities of the muscle cell, it appears that molecules that would under normal circumstances be prevented from entering the muscle fibres are allowed free access through the cell membrane in dystrophin-deficient muscle fibres. These muscle fibres exhibit structural and functional defects, thus rendering it vulnerable to mechanical stress (Blake *et al.*, 2002). Other dystrophin-deficient muscle cell abnormalities include inability of the dystrophin-deficient cells to maintain calcium

homeostasis and abnormal expression of proteases such as calpain-3. Oxidative damage and apoptosis have also has been implicated in the pathophysiology of DMD (Figure 10).

Leading on from the abnormalities of the muscle cell are those of the muscle tissue. These include vascular problems, inflammation and fibrosis that are initiated by necrosis and muscle regeneration. The high number of satellite cells in muscle fibres at the early stages of the dystrophic process lead to increased regeneration, which falls rapidly as the disease progresses (Figure 10).

## 1.6 ANIMAL MODELS

The discovery of the dystrophin gene and the effects that it has on dystrophin deficient muscle in humans subsequently led to the identification of dystrophin homologues in other animals. Such animals where similar muscle effects have been noted include the vertebrate species *mdx* mouse, golden retriever dog, cat and zebrafish. The invertebrates include *Caenorhabditis elegans* and *Drosophila melanogaster*, where the disease symptoms have either been spontaneous or a result of targeted disruption of the gene. The most commonly used model to study the disease is the *mdx* mouse owing to the ease with which genome manipulation can be undertaken. It is however not the ideal animal model for human DMD owing to differences in muscle pathology. The Golden retriever dog model appears to be the ideal candidate to study the disease as the symptoms and the effects it produces are very similar to those seen in human DMD. The different animal models have been used extensively to study the pathophysiology of DMD and many potentially useful therapeutic options have been investigated.
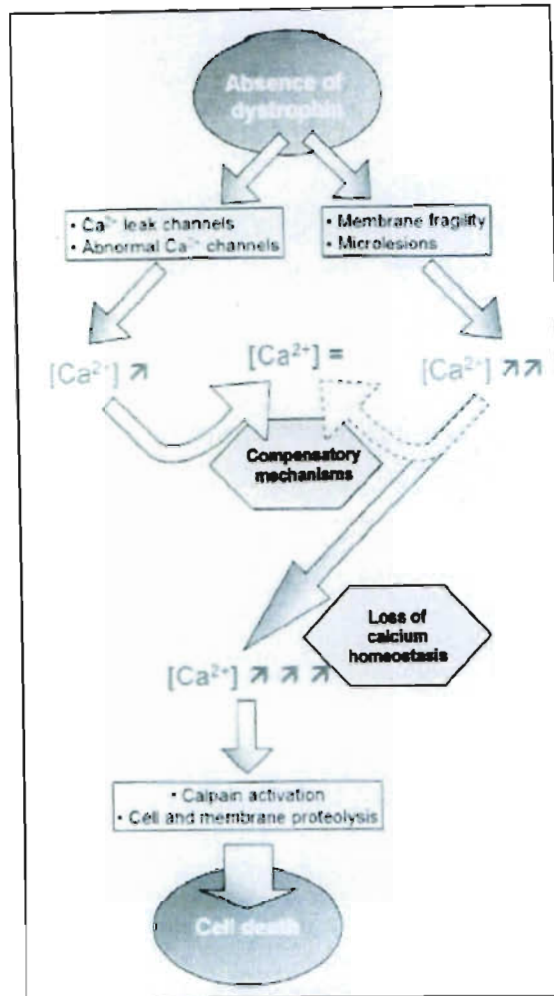
**Figure 10: Proposed pathophysiology of dystrophinopathies (as adapted from Deconinck and Dan, 2007).**

The *mdx* mouse was first discovered by the high serum creatine kinase level that it exhibited (Bulfield *et al.*, 1984). The muscle pathology that it showed made it a useful model in further studying the dystrophin gene. The *mdx* mouse has a point mutation in exon 23 of its dystrophin gene that produces a premature stop-codon thus preventing full-length dystrophin from being expressed (Sicinski *et al.*, 1989). One of the pathological features seen in *mdx* includes its high regenerative capacity of muscle, which is not the case in human DMD. It has also been noted that the 'muscle fibre loss' and 'collagen deposition' in *mdx* occur only later in life (Stedman *et al.*, 1991; Blake *et al.*, 2002). In comparison, these traits affect DMD patients much earlier in the disease. Interestingly, the course of the disease can be hastened by including a moderate exercise regimen in the

activity schedule of the mice (De Luca *et al.*, 2003). Despite these differences, the *mdx* mouse has made significant contributions to the understanding of disease pathology in DMD. *Mdx* has been the model used in many therapeutic intervention trials (Wells & Wells, 2002; Bertoni *et al.*, 2003) to determine whether they would be feasible to implement such interventions in larger models such as the dog. One can therefore call the *mdx* mouse the pioneer in studying treatment options for DMD.

Another mouse model with pathological and clinical features similar to human DMD has recently received much attention (Deconinck *et al.*, 1997). This mouse model is a double dystrophin/utrophin (mdx/utrn$^{-/-}$) knockout. It has long been postulated that utrophin can compensate for the loss of dystrophin and this has been shown to be the case when *mdx* mice were injected with utrophin, with resulting improvement in muscle pathology (Squire *et al.*, 2002). Such results could have wider reaching implications for future therapeutic interventions that may be implemented in DMD patients owing to the similarity that exists at the histological and pathological level.

Several dog models have been studied (Sharp *et al.*, 1992; Winand *et al.*, 1994; Schatzberg *et al.*, 1999) in an attempt to find one that mimics the human DMD phenotype and pathology. The Golden retriever dog appears to be most appropriate as a model for human DMD however the size of the dog and the severe symptoms that it exhibits are points of ethical concern. The muscles of the dog show widespread necrosis from as early on as birth, which increases till day 30 after which time there is a steady decline until adulthood (Nguyen *et al.*, 2002; Cozzi *et al.*, 2001). In much the same way as in human DMD, serum creatine kinase levels are very high with levels reaching 100 × that of normal. There has also been evidence to suggest that utrophin is abnormal, which might account for the

severe symptoms (Wilson *et al.*, 1994). According to Nguyen *et al.* (2002), the dogs often suffer from respiratory distress and cardiac abnormalities leading to their death much like in DMD affected patients. The major limitations of this model appear to be the inability to use the dogs in high-throughput studies owing to size and costs of maintaining such large animals, as well as the extreme variability in severity exhibited by the dogs (Collins & Morgan, 2003).

The term hypertrophic feline muscular dystrophy is used to describe the muscle disease that affects cats. The dystrophy occurs as a result of a deletion in the promoter region of the dystrophin gene (Winand *et al.*, 1994). Muscle pathology is similar to that seen in the *mdx* mouse with the cyclic processes of regeneration and degeneration being prominent. Marked hypertrophy is also a pathological feature. Once again it does not serve as a suitable model for human DMD as it does not show any of the characteristic features of human DMD such as muscle fibrosis. Collins and Morgan (2003) have also pointed out that the large size and emotive nature of cats significantly reduces their usefulness as a model organism.

To date no non-human primates harbouring a dystrophin mutation or exhibiting dystrophin deficiency has been reported.

There are at least three model systems used to study DMD pathogenesis that are non-mammalian. These include the zebrafish (Guyon *et al.*, 2006), the nematode (Baumeister & Ge, 2002) and *Drosophila* (van der Plas *et al.* 2007). Even though the pathology exhibited by these organisms is by no means comparable to that of human DMD, the number of experiments that can be conducted using these simple, small and easily manipulatable

organisms from a genetic point of view makes them useful. Large scale screening of pharmacological therapeutic approaches can be rapidly undertaken thereby reducing costs. The unique trait of optical transparency shown by embryos and young zebrafish makes them suitable models to study dystrophin and other associated proteins. Owing to the synteny that exists between human and zebrafish genomes and since it has been found that orthologous genes in the two organisms regulate similar processes such as T-cell development, their use as a model is warranted. Care should be taken to first replicate experiments that prove to be promising in other larger, vertebrate organisms before any definitive connection can be made with human DMD (Guyon *et al.*, 2006). With respect to *C.elegans* as a model organism for DMD, their ability to undergo parthenogenesis and their high reproductive capacity facilitates the conduction of high-throughput experiments (Baumeister & Ge, 2002; Collins & Morgan, 2003). In order to determine which isoforms were associated with maintenance of muscle integrity in Drosophila, van der Plas *et al.* (2007), utilised RNA interference assays. They found that the Dp117 isoform is required to prevent muscle degeneration. A previous report suggested that the DLP2 orthologue is responsible for maintaining synaptic homeostasis (van der Plas *et al.*, 2000).

## 1.7 VARIOUS FORMS OF THERAPY

### 1.7.1 Gene therapy using viral vectors

Initial gene therapy studies were performed on the *mdx* mouse model using retroviral and adenoviral vectors owing to their sustained level of expression and high transduction rate. These viral vectors served as shuttle vehicles for the delivery of a 6.3 kb mini-dystrophin cDNA (Acsadi *et al.*, 1996; Dunckley *et al.*, 1993; Vincent *et al.*, 1993). Such experiments were successful at expressing dystrophin, albeit for a limited period of time. The next

contender was an adeno-retro viral vector that expressed a 3.7 kb micro-dystrophin. This vector did not solve the previously encountered problems, such as the high immunogenicity of adenoviral vectors and the ability of retroviral vectors to integrate into the host genome (Fassati *et al.*, 1996). The vector system did succeed in obtaining efficient expression of dystrophin in the muscles that were injected; however they also contained retroviral vector sequences (Roberts *et al.*, 2002). According to Roberts *et al.* (2002), designing such hybrid vectors should continue as it may result in the development of a useful vector because researchers would be focusing on the positive attributes of each partner in the vector system.

The group of vectors that has shown promise in gene transfer therapy is the adeno-associated viral vectors. These vectors lack the viral genes that produced immunogenicity in host cells resulting in rejection of the injected dystrophin mini-genes. This attribute is also harboured by helper dependent (gutted) adenoviral vectors (Dickson *et al.*, 2002). Even though the AAV vectors are suitable candidates for gene therapy trials, their one flaw is the inability to house foreign material larger than 5kb. In order to prevent this from being a set-back many groups have designed micro-dystrophins in the range of 3.1 to 4.2 kb in order to harness the potential of these vector systems. These constructs were designed, based on the premise that the central part of the rod domain is dispensable as found in many patients with BMD phenotypes with truncated but functional dystrophin (Passos-Bueno *et al.*, 1994). There have been several studies using the AAV vectors to restore protein expression of dystrophin where it has been expressed at the sarcolemma (Wang *et al.*, 2000) and restored expression at the DAGC (Yuasa *et al.*, 1998; Fabb *et al.*, 2002). It has been documented that even the smallest micro-dystrophin molecules delivered using the AAV vector system were able to prevent and reverse the disease

pathology in the *mdx* mouse (Harper *et al.*, 2002; Dickson *et al.*, 2002; Gregorevic *et al.*, 2008). Such successes make the use of such vectors promising in the battle against muscular dystrophy through gene therapy. There has been much improvement in the area of AAV vectors including serotype analysis and transgene engineering (Blankinship *et al.*, 2006).

## 1.7.2   Utrophin transgenic mice

Another manner in which the *mdx* mouse has been rescued from its dystrophic phenotype was to use utrophin as a means to compensate for dystrophin. Studies were performed using full-length and rod-domain deleted utrophin transgenic mice (Tinsley *et al.*, 1996; Tinsley *et al.*, 1998). Since utrophin is only expressed at the neuromuscular junction in adult skeletal muscle, a specific promoter had to be used to bring about more generalised expression. Using the human skeletal actin (HSA) promoter, utrophin localised to the sarcolemma, restored DAGC functionality and "prevented much of the dystrophic phenotype in *mdx*", with the full-length dystrophin being more efficient (Tinsley *et al.*, 1998). When the double knockout was crossed with a rod-domain deleted utrophin transgenic mouse, utrophin expression was shown to prevent the clinical phenotype and the pathological features in the utrophin-dystrophin double knockout mouse (Rafael *et al.*, 1998). Such data suggests that 'sarcolemmal expression of either protein' is able to restore functionality in the DAGC and can 'compensate for the loss of both proteins' (Rafael & Brown, 2000). In 2008, Odom *et al.* showed that delivery of a micro-utrophin using a recombinant AAV vector was successful in increasing lifespan in dystrophin/utrophin deficient mice.

## 1.7.3  Cell therapy

Cell transplantation in DMD patients started out as a promising therapeutic alternative and has been attempted by different groups. The outcome however has been disappointing (Huard *et al.*, 2003; Urish *et al.*, 2005). The postulated reason for poor response was the lack of migration of the myoblasts (approximately 0.5 mm) away from the site of injection. Also the rapid death of >75% of injected myoblasts on account of an immune response was common. Systemic delivery of myoblast cells produces problems such as the heightened risk of embolism in organs such as the heart, lung, brain, kidneys and liver (Péault *et al.*, 2007). Recent human trials have demonstrated minimal improvements over previous experiments.

Cell transplantation studies have been rapidly replaced by stem cell therapy. Stem cells have the advantage of self-renewal and plasticity or "unlimited potency". In 2005, the isolation of myogenic precursor muscle cells from the satellite cell compartment was undertaken in an attempt to regenerate muscle fibres (Collins *et al.*, 2005; Wagers & Conboy, 2005). Owing to the amount of knowledge that has been accumulated in the field of tissue regeneration, the molecular biology and functional attributes of satellite cells and associated markers has been largely deciphered (Péault *et al.*, 2007).

There are other populations of stem cells that may play a role in muscular dystrophy therapy. These include muscle-resident side population (SP), muscle-derived stem cells (MDSCs) or multipotent adult progenitor cells. Even though all these cell populations have the potential to bring about muscle regeneration, their myogenic capacity appears to be lower than satellite cells (Collins *et al.*, 2005; Urish *et al.*, 2005). Another contender that

may produce a favourable outcome for cell therapy is the embryonic stem cell pool. This group has a high differentiation capability that could be potentially beneficial for muscular dystrophy, particularly DMD. To overcome immune rejection, groups working on stem cell therapy have started looking into the possibility of using the DMD patients' own adult stem cell pool to prevent the immune response reactions (Zhou *et al.*, 2006). A newly discovered stem cell, mesangioblast, has been isolated from blood vessels and their ability to regenerate dystrophic muscle was demonstrated successfully in Golden retriever dogs. More studies on this pool of stem cells are required with a strong focus on how their finite life span can be prolonged since their characteristics make them ideal as candidates for clinical trials (Sampaolesi *et al.*, 2006; Grounds & Davies, 2007; Péault *et al.*, 2007).

### 1.7.4   Aminoglycoside treatment of DMD patients with nonsense mutations

In 1999 it was suggested that DMD patients with a nonsense mutation could be treated with an aminoglycoside antibiotic, gentamicin, to convert a truncated dystrophin protein into a functional one. This was possible owing to the ability of gentamicin to read-through the nonsense mutation. The study was conducted using the *mdx* mouse model (Barton-Davis *et al.*, 1999), and the theory was further investigated by Wagner *et al.* (2001) using aminoglycoside antibiotics on humans. Much interest was sparked by the report as the trial was performed on 2 DMD and 2 BMD patients. The technique was also outlined in the research updates magazine Quest of the muscular dystrophy association in the USA (MDA). The differences obtained in the mouse and human studies may be species dependent with toxicity levels and misreading efficiency being related to the type of organism being used (Karpati & Lochmuller, 2001).
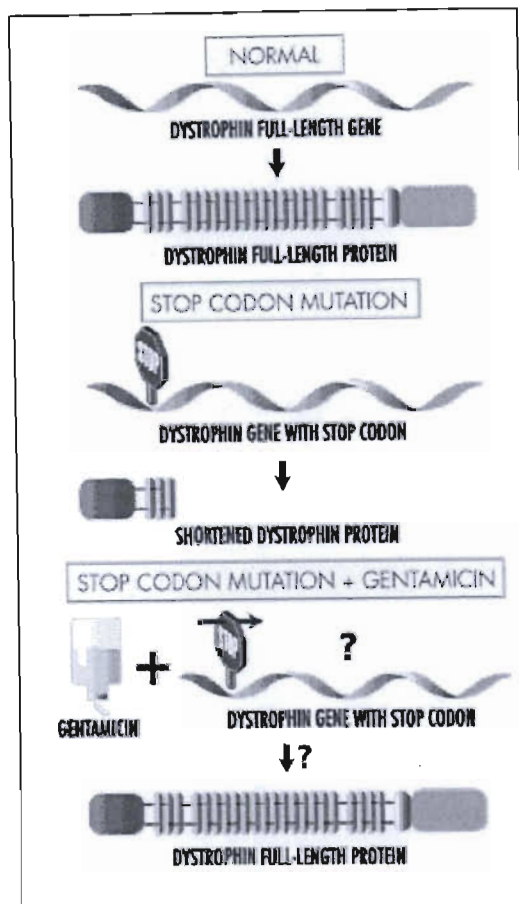
**Figure 11: Schematic representation of the therapeutic approach using aminoglycoside antibiotic, gentamicin to read-through a nonsense mutation found in the dystrophin gene of DMD patients (Quest – MDA, Vol 8, 2001 http://www.mdausa.org).**

According to Karpati and Lochmuller (2001), the brand and composition of the gentamicin sulphate compound also plays a role in inducing misreading. Other aminoglycoside antibiotics such as negamicin and PTC124 have also been used to promote read-through of stop-codons and may be less toxic (Arakawa *et al.*, 2003). It was previously documented that the "efficacy of read-through" was dependent on specific types of nonsense mutations (Howard *et al.*, 2000). According to Kimura *et al.* (2005), a method for identifying the patient and the nonsense mutation amenable to gentamicin treatment has been investigated and proven to be beneficial. The patient was considered for the therapy, if gentamicin "induced dystrophin expression" in the myotubes (Kimura *et al.*, 2005) and in all cases the patients showed a TGA stop codon mutation.

## 1.7.5 Myostatin as a therapeutic avenue

Myostatin was first described in 1997 as a "negative regulator of muscle growth" owing to the increase in skeletal muscle bulk and mass that is exhibited by knock-out mice. This gene is also called growth differentiation factor 8 and forms a part of the transforming growth factor (TGF) β family. Studies conducted in mice have not been clear as to whether the increase in muscle bulk occurred as a result of hyperplasia alone or hypertrophy alone, however there is data to support the theory that both pathways are active (Zhu *et al.*, 2000; Lee & McPherron, 2001; Dominique & Gérard, 2006). The myostatin deletion-mutation appears to not only influence muscle mass positively but there is also evidence to suggest that a decrease in adipose tissue occurs in mice (Lin *et al.*, 2002; McPherron & Lee, 2002). Such results may have a far reaching, positive impact on muscular dystrophy patients since adipose tissue deposition increases with age. This increase in fat places increasing strain on their progressively weakening muscles. Long before the myostatin gene was cloned, naturally occurring mutations resulting in increased muscle mass had been described in cattle (Charlier *et al.*, 1995). The double muscled cattle however also exhibited increases in weight of skin, adipose tissue and bone in contrast to the increase in muscle mass seen in mice. In 2004, a spontaneous mutation in the myostatin gene was found in a child of an athlete. The child showed increase in muscle mass with no negative effects (Schuelke *et al.*, 2004).

According to Wagner *et al.* (2005) studies on myostatin negative mice revealed that regeneration and repair of skeletal muscle was more efficient than in wildtype, with earlier differentiation and greater satellite cell proliferation noted. Myostatin also seems to bring

about muscle repair and regeneration by regulating the movement of macrophages to the site of injury (McCroskery et al., 2005).

In 2006 an extensive gene expression profiling study was performed in myostatin knockout mice by Steelman et al. (2006) where myostatin was shown to be involved with global regulation of various proteins. The report showed that the wnt/calcium signalling pathway was upregulated in the absence of myostatin and wnt4 was shown to increase the proliferation of satellite cells.

Other studies have focussed on hypertrophy as a way to increase muscle mass without inducing pathological changes. In 2001, Musaro et al. produced conditional knockout mice that expressed an insulin-like growth factor (IGF)-1 isoform called mIGF-1, which is normally expressed in skeletal and cardiac muscle. These mice developed hypertrophic skeletal muscle containing "little or no body fat" and no cardiac hypertrophy. In older mice, normal atrophy occurring as a result of senescence was prevented and histological analyses indicated the presence of centralised nuclei, which is a hallmark of regeneration (Musaro et al., 2001). Musaro et al. (2006) showed that IGF-1 plays a crucial role in down-regulating cytokines IL (interleukin) 1, TNF (tumour necrosis factor) α, ENA (epithelial neutrophil activating peptide)-78, and the CC chemokines (β-chemokines possess two cysteine residues near the amino terminal end) at the latter stages of the inflammatory process, during which time necrosis becomes active, and not during the pro-inflammatory stages. Such findings aid in cementing its role in the regeneration of muscle tissue (Pelosi et al., 2007).

In 2004, Lai *et al.* used fluorescently tagged conditional knockout mice to show that activation of the phosphatidylinositol-3-kinase (PI3K)/Akt pathway was sufficient to induce hypertrophy.

All these studies aim to provide mechanisms and pathways that can be activated and in so doing induce skeletal muscle hypertrophy that has already been shown to have beneficial effects in mice. Recent studies have revealed that signalling pathways that regulate hypertrophy are dominant over atrophy mediators, which leaves much hope for muscular dystrophy therapy (Cai *et al.*, 2004; Glass *et al.*, 2005).

Findings that NF-κB, through activation of IκB kinase (IKK) β and to a lesser extent TNF-α are key initiators of atrophy, open up possibilities for studies that aim to down regulate these proteins by biochemically interfering with the pathway (Glass *et al.*, 2005). NF-κB has previously been shown to be upregulated during muscle disuse and sepsis (Hunter *et al.*, 2002; Penner *et al.*, 2001) therefore understanding the functional attributes of NF-κB may assist in opening up potential therapeutic avenues.

There has been one study that focused on myostatin blockade in mouse models of muscular dystrophy and it was shown that the effects of myostatin blockade is variable in different muscle groups (Parsons *et al.*, 2006; Hoffman & Escolar, 2006). Care should be taken to not extrapolate these results to include DMD when reviewing the data, as δ-sarcoglycanopathy (limb-girdle muscular dystrophy) was the disease being subjected to scrutiny. The results of the report make it necessary for similar studies to first be performed on other forms of muscular dystrophy such as DMD before decisions are made regarding the usefulness of such as therapeutic option.

## 1.7.6 Pharmaceuticals as an alternative to mainstream therapy

In a review published by Radley *et al.* in 2007, the benefits and risks of using different drugs to improve patients affected by muscular dystrophy were outlined. The authors highlighted the studies that utilised drug therapy both in *mdx* mice and human trials. The first group of drugs to be evaluated were the corticosteroids, prednisone and Deflazacort whose side-effects of weight gain, asymptomatic cataracts and stunted growth, outweigh their beneficial attributes of delaying muscle wasting. A potentially useful anti-inflammatory drug, pentoxifylline, was shown to reduce TNF-$\alpha$ production, reduce fibrosis and play a "role in normalizing blood flow in dystrophic muscle" (Granchelli *et al.*, 2000). Owing to such positive results, pentoxifylline is the subject of two CINRG (The Cooperative International Neuromuscular Research Group) trials in DMD patients.

Another manner in which drug therapy has proven to be beneficial is in the use of anti-cytokine drugs to bring about targeted blockage of specific aspects in the inflammatory response cascade. This approach has been used successfully in diseases such as rheumatoid arthritis and crohn's disease, where neutralizing antibody called infliximab is used to block the action of TNF-$\alpha$. In *mdx* mice the use of infliximab was shown to "delay and reduce necrosis" associated with the dystrophy (Grounds & Torrisi, 2004).

The next type of pharmaceutical intervention used in DMD and other diseases include antioxidants such as Co-enzyme Q and green tea extract [($-$)-epigallocatechin gallate]. Various studies have revealed green tea extract to be responsible for a reduction in muscle cell damage and improvement in muscle function in the *mdx* mouse (Buetler *et al.*, 2002; Dorchies *et al.*, 2006). Co-enzyme Q has become the subject of CINRG trials on DMD patients where its effectiveness as an adjunct to steroid therapy was assessed. It was shown

to "increase strength in some muscle groups" in DMD patients and a larger follow-up study is underway.

In order to assess the usefulness of an anabolic agent, albuterol, the drug was administered to DMD patients for 28 weeks (Fowler *et al.*, 2004). Anabolic drugs, such as β2-agonists are known to increase protein content and muscle size. The result of the DMD trials was a slight increase in strength with no side-effects. The future use of such drugs in DMD trials looks promising.

### 1.7.7 Antisense oligonucleotide therapy

This form of therapy falls into the category of gene modification where exon-skipping is brought about in the dystrophin gene of an affected DMD child in order to convert the severe phenotype to a more benign BMD phenotype. The procedure is outlined in figure 11 below. By using the antisense oligonucleotide (AON) approach, an out-of-frame deletion can be converted into an in-frame deletion thereby creating a smaller yet functional dystrophin protein. According to Aartsma-Rus *et al.* (2003), a maximum of 20 exons can be targeted by using the AON technique for single-exon skipping (Zhou *et al.*, 2006). AONs could serve as a "molecular patch" to treat patients with different deletions. In order to enhance the delivery of these molecular patches *in vivo*, a non-ionic triblock copolymer F127 was used to efficiently transfect the *mdx* mice, which contain an exon 23 mutation (Lu *et al.*, 2003). The authors found no humoral immune responses to dystrophin after administration of the AON. Later systemic studies using the same methodology induced dystrophin expression in all skeletal muscles except cardiac muscle (Lu *et al.*, 2005). It was later shown that by altering the chemistry of anti-sense oligonucleotides to an ethylene

bridge nucleic acid (ENA) chimera the skipping of exon 19 was induced and a 40 × more efficient expression was achieved, with a reduction in toxicity (Yagi *et al.*, 2004). Using the same antisense chimeric oligonucleotide, impressive results were achieved when the skipping of exon 41 was accomplished with >90% of muscle fibres being dystrophin positive in culture (Surono *et al.*, 2004).
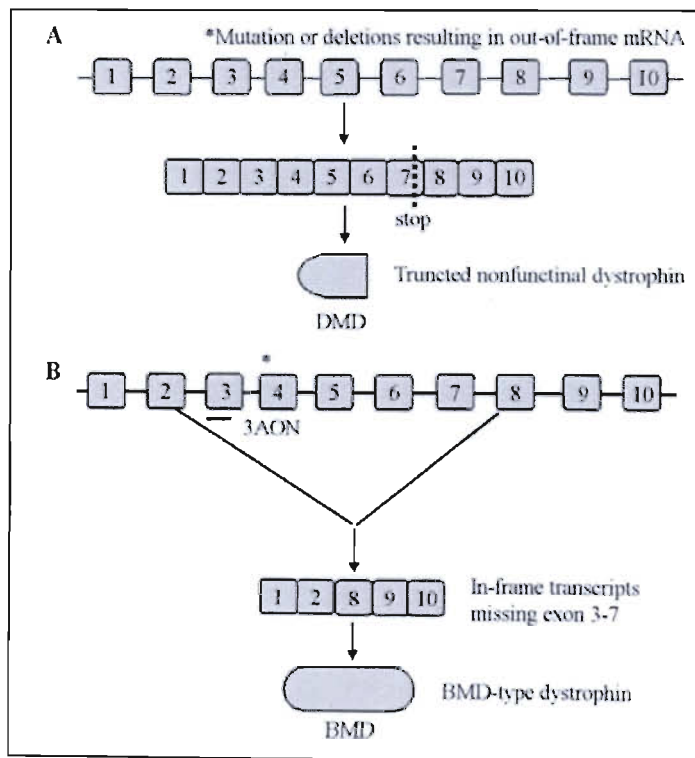


**Figure 12: Illustration of the exon-skipping approach adopted by different groups where antisense-oligonucleotides technology is implemented in Duchenne muscular dystrophy (as adapted from Zhou *et al.*, 2006).**

# CHAPTER 2

## OUTLINE OF STUDY

The study will be divided into two parts.

**Part I:**

- Mutation detection in dystrophinopathy patients and carrier detection in their mothers.

**Part II:**

- Gene profiling analysis using microarray technology to elucidate the pathogenesis in DMD by focussing on two muscle groups from the same patient.

## 2.1    AIMS

a)  Perform immunohistochemistry on all biopsy samples taken from clinically affected dystrophinopathy patients through informed consent.

b)  To expand PCR deletion detection in dystrophinopathy patients to encompass 30 exons within and surrounding the deletion hotspots of the dystrophin gene.

c)  Detect deletions and duplications throughout the 79 exons of dystrophin using a novel technique that combines probe-based methodology with the power of PCR.

d)  To evaluate the usefulness and reproducibility of a point mutation detection technique that uses single stranded conformers to separate normal from

abnormal fragments. Aberrant bands would be confirmed by automated DNA sequencing.

e) To close the mutation gap by conducting reverse-transcription PCR on the RNA samples from dystrophinopathy patients to detect aberrant fragments that were not detected using DNA based methods.

f) Performing gene expression profiling on a selected number of DMD affected patients RNA samples using the spotted oligonucleotide approach to unravel the molecular signatures and regulatory pathways that may be active in different types of muscle biopsy samples (gastrocnemius and biceps/quadriceps). Double-biopsy samples were obtained from the same patient. Such a broad analysis will help us to elucidate the pathogenesis in Duchenne muscular dystrophy.

## 2.2    PATIENT POPULATION

**Table 1: Table showing the Duchenne and Becker muscular dystrophy patients who agreed to have an open muscle biopsy.**

| DNA number | Surname, Initials | Age | Dystrophinopathy status | Mental status |
|---|---|---|---|---|
| 2 | S, W | 8 | DMD | Intellectually impaired |
| 5 | M, B | | DMD | Intellectually impaired |
| 7 | H, J | 8 | DMD | Normal |
| 8 | S, T | 13 | DMD | N/K |
| 9 | S, NM | 17 | DMD | N/K |
| 12 | G, S | 16 | DMD | N/K |
| 14 | N, D | 9 | DMD | N/K |
| 16 | M, T | 14 | DMD | N/K |
| 19 | M, S | 6 | DMD | N/K |
| 20 | M, S | | DMD | N/K |
| 21 | R, S | 8 | DMD | N/K |
| 22 | N, N | 10 | DMD | Normal |
| 23 | H, ZM | 13 | DMD | N/K |
| 24 | P, D | 8 | DMD | N/K |

| | | | | |
|---|---|---|---|---|
| 27 | L, L | | DMD | N/K |
| 28 | M, MB | 10 | DMD | Mentally impaired |
| 29 | N, C | | DMD | N/K |
| 30 | W, R | | DMD | Normal |
| 31 | C, L | 12 | DMD | Normal, CK 5901 |
| 32 | M, NL | 6 | DMD | N/K |
| 33 | G, P | | DMD | N/K |
| 37 | M, G | 8 | DMD | Normal, CK 7815 |
| 38 | N, M | 14 | DMD | Normal, CK 6409 |
| 39 | S, T | 14 | DMD | Normal |
| 40 | S, C | 12 | DMD | Normal |
| 41 | M, S | 10 | DMD | N/K |
| 42 | M, R | 12 | DMD | Normal |
| 43 | S, V | 14 | DMD | Normal |
| 44 | C, L | | DMD | N/K |
| 45 | M, T | 13 | DMD | N/K |
| 46 | M, S | | DMD | N/K |
| 47 | M, ST | | DMD | N/K |
| 48 | M, S | | DMD | N/K |
| 49 | M, W | 7 | DMD | N/K |
| 50 | N, T | 14 | DMD | N/K |
| 52 | K, TP | 18 | DMD | N/K |
| 53 | V, S | 10 | DMD | N/K |
| 54 | B, N | | DMD | N/K |
| 56 | S, T | 12 | DMD | Normal |
| 58 | M, M | 14 | DMD | Normal |
| 59 | B, X | 10 | DMD | Normal |
| 60 | N, S | 12 | DMD | Normal, CK 5177 |
| 61 | L, M | 8 | DMD | Normal |
| 62 | S, S | | DMD | Normal |
| 63 | S, N | 25 | Carrier F | Intellectually impaired |
| 66 | M, R | | DMD | Normal |
| 68 | N, S | | DMD | Normal |
| 18 | R, J | 34 | BMD | Normal |
| 25 | R, D | 35 | BMD | Normal |
| 26 | Z, S | 18 | BMD | Normal |
| 34 | N, M | | BMD | N/K |
| 35 | S, G | | BMD | N/K |
| 36 | H, XV | 22 | BMD | Normal |
| 51 | H, N | 19 | BMD | N/K |
| 55 | F, S | | BMD | Normal |

**Legend: N/K – not known**

**Table 2: Table showing details of mothers and relatives of dystrophinopathy patients who were included in different aspects of the project.**

| DNA number | Surname, Initials | Relationship to dystrophinopathy child |
|---|---|---|
| 1 | S, R | Aunt of 2 |
| 3 | S, DK | Mother of 2 |
| 4 | M, M | Mother of 5 |
| 6 | H, S | Mother of 7 |
| 10 | S, S | Mother of 8 & 9 |
| 11 | S, B | Sister of 8 & 9 |
| 13 | Mrs G | mother of 12 |
| 15 | N, C | Mother of 14 |
| 17 | Mrs M | Mother of 16 |
| 57 | M, T | Mother of DMD child 28 |
| 64 | M, S | Mother of 19 |
| 65 | M, C | Sister of 64 |
| 67 | M, P | Mother of 64 |

## 2.3  METHODS EMPLOYED

### 2.3.1  Immunohistochemistry

Immunohistochemical analyses was performed using H+E staining, staining for dystrophin, the sarcoglycans, α-actinin, merosin (laminin-α-2), dysferlin (hamlet 1 and hamlet 2), spectrin. All the stains were obtained from Novocastra laboratories (UK).

### 2.3.2  30-exon Multiplex PCR

PCR or polymerase chain reaction, which is the rapid amplification of a target DNA strand, was undertaken. Deletion detection by multiplex PCR spanning 30 exons of the dystrophin gene was performed. In the case of multiplex PCR, several PCR primers were included in the same reaction tube. The resultant effect following amplification was the production of several amplicons of differing lengths. The 30 exons were used to cover the regions that

were not amplified using the conventional Chamberlain and Beggs 18 exon multiplex PCR. The 30 exons were tested in an attempt to improve the diagnostic efficacy of multiplex PCR and thereby increase the number of patients that showed deletions.

### 2.3.3  Multiplex ligation-dependent probe amplification assay (MLPA)

Complete deletion and duplication testing of the dystrophin gene was performed using the multiplex ligation-dependent probe amplification assay (MLPA). This novel technique uses commercially available probes that are subsequently amplified in the presence of the patients' DNA. The products are subjected to fragment analysis using a genetic analyser. Genemapper analysis would reveal no peak for a deletion and duplications are noted by an increase in peak area or peak height. Duplications are also confirmed using dosage quotient analysis on a spreadsheet program such as Excel.

### 2.3.4  Single strand conformation polymorphism (SSCP) analysis

Point mutation detection was undertaken using the "Cold" PCR single strand conformation polymorphism (SSCP) analysis assay on the DNA samples of deletion-negative DMD patients. The DNA is PCR amplified, electrophoresed on an agarose gel, purified and subjected to SSCP on a polyacrylamide gel. Visually detected aberrant bands / abnormally migrating bands are subjected to DNA sequencing using the ABI 3100 and analysis is conducted using the Biotools bioinformatics software program.

## 2.3.5   Reverse-transcription PCR

Reverse-transcription PCR was attempted on the RNA samples from dystrophinopathy patients' and controls to detect mutations in the dystrophin gene by using 10 amplified fragments to examine the entire coding region of the gene by nested PCR.

## 2.3.6   Gene profiling using microarrays

Gene profiling analysis was performed using the Sigma-Compugen human 19K 60-mer oligonucleotide collection, spotted at the Leiden Genome Technology Center (LGTC) in the Netherlands. Double biopsy samples were obtained through informed consent from dystrophinopathy patients. These samples were taken from a weak muscle (biceps / quadriceps) and a strong (gastrocnemius) muscle to determine whether differences in gene expression were present. These differences may help to understand why the one muscle remains invariably strong throughout the child's life whereas the other muscle becomes progressively weaker. Such dysregulation of genes may expand therapeutic options for dystrophinopathy patients in the future, which may increase the lifespan and quality of life in the affected child.

# CHAPTER 3

# IMMUNOHISTOCHEMISTRY

## 3.1 INTRODUCTION

The use of immunohistochemistry (IHC) in the diagnosis of muscle disease has served as the gold standard for many years. Even though molecular biology has become popular in diagnosing various muscle diseases owing to the genes responsible for such disorders being mapped out and characterised, the muscle biopsy still proves to be useful in the diagnostic process (Tuffery-Giraud *et al.*, 2004). The success rate in achieving a definitive diagnosis with the aid of immunohistochemistry and histological methods increases when combined with molecular diagnostic assays (Vogel & Zamecnik, 2005).

### 3.1.1 Skeletal muscle

Skeletal muscle, which is also referred to as voluntary muscle, is a type of striated muscle. It is attached to bone by tendons. Skeletal muscle has a multinucleated structure composed of long, cylindrical cells. The nuclei are located at the periphery, under the plasma membrane and this arrangement produces higher efficiency. Muscle is surrounded by three connective tissue components that give strength, protection and rigidity to the fibres. The epimysium is a fibrous connective tissue that surrounds the entire muscle. Perimysium surrounds fascicles (bundle) of muscle cells (Figure 13). Endomysium surrounds individual muscle fibres and it is composed of reticular filaments and an outer lamina (Junqueira *et al.*, 1998).

The cytoplasm of skeletal muscle is called the sarcoplasm. The plasmalemma is referred to as the sarcolemma, which forms deep tubular invaginations called the T-tubules. The T-tubular network extends into the cells. Myofibrils are bundles of filaments 1-2 µm in diameter and they extend the entire length of the muscle cell (Junqueira *et al.*, 1998).
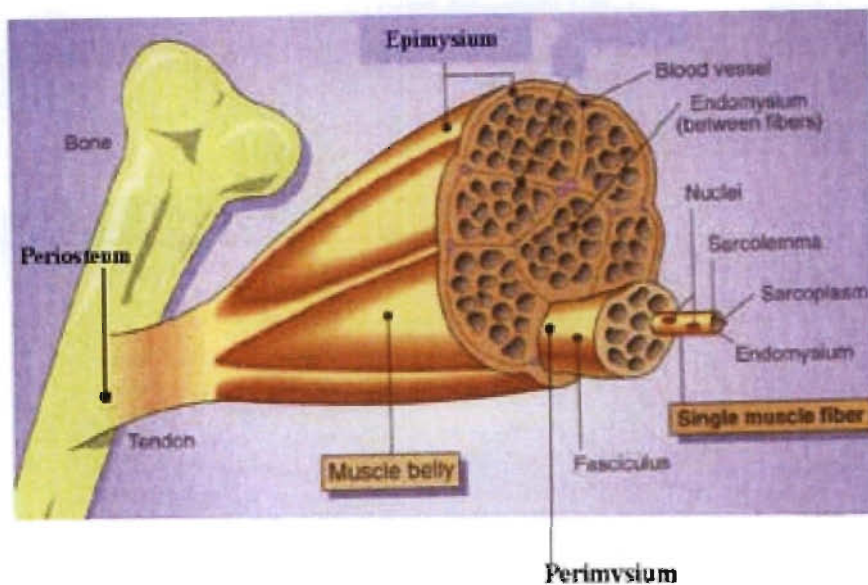


**Figure 13: Diagram illustrating the gross sub-cellular organisation of skeletal muscle.**
www.unm.edu/.../musclesarcomere.html

There are three types of muscle fibres. These include the red (slow), white (fast) and intermediate muscle fibres. All three types may occur in a particular muscle. These muscle fibres differ primarily on account of their myoglobin content however other differences include mitochondria presence, enzyme concentration and the rate of contraction. A change in innervation can change the fibre type of a muscle. For example, if a red fibre is denervated and it is re-innervated by an axon determining a white fibre, the red fibre will become a white fibre. The red or slow twitch fibres possess a large number of mitochondria and engage in predominantly aerobic metabolism and store oxygen in myoglobin. Endurance athletes have more red fibres. White or fast twitch fibres have fewer

44

mitochondria and are capable of metabolising ATP at a rapid rate. Sprint athletes have more white fibres (Junqueira *et al.*, 1998).

A multitude of genes are involved in producing the skeletal muscle phenotypes we are familiar with. Functional differences exist between the adult fast and slow twitch muscle fibres owing to varying degrees of expression from muscle proteins. Several signalling pathways regulate this process in both animals and humans. Such pathways include the Ras/mitogen-activated protein kinase (MAPK) signalling pathway, calcineurin, calcium/calmodulin-dependent protein kinase IV, and the peroxisome proliferator γ-coactivator 1 (PGC-1) (Widegren *et al.*, 2001).

Both cytoplasmic and nuclear proteins are phosphorylated by MAPK, thus revealing the essential role played by MAPK in transcriptional regulation (Chen *et al.*, 1992). Transcriptional factors activated by the MAPK family of proteins and other signalling partners include cyclic AMP response element binding protein (CREB), myocyte enhance factor 2 (MEF2) A and C, activating transcription factor (ATF) 1 and 2 and others (Han *et al.*, 1997, Xing *et al.*, 1996, Widegren *et al.*, 2006).

Calcineurin is a $Ca2^+$ sensitive phosphatase that has been found to play an integral role in contributing to fast to slow fibre type transformation. It has been implicated in the translocation of dephosphorylated NFATc (nuclear factor of activated T-cells) from the cytoplasm to the nucleus where NFATc brings about slow fibre type gene expression. Myocyte enhancer factor 2 (MEF2), a transcription factor has also been shown to cause fast-slow fibre type transformation with the help of nuclear calmodulin dependent kinase (CaMK) (Lui *et al.*, 2005). By extrapolation, it can be deduced from the data obtained thus

far (Lui *et al.*, 2005) that calcineurin plays an important role in initiation and maintenance of slow muscle fibre gene expression (Stewart & Rittweger, 2006).

## 3.1.2 Sarcomere

This is the single, basic unit of striated muscle's myofibril. Each striated myofibril is composed on alternating dark bands called "A-bands" and light bands called "I-bands". In the middle of each "A-band" is a lighter area referred to as the "H-zone" or "H-band", whereas the centre of each "I-band" houses a dark, thin line which is given the term, "Z-line". The segment of a myofibril between two "Z-lines" makes up a single sarcomere. The "Z-line" is also sometimes referred to as "Z-discs" or "Z-bodies". Inside the "H-zone" is located the "M-line".

Sarcomeres are made up of a complex of proteins, which are divided into three types of filament systems. The first is the thick, myosin protein containing filaments possessing a globular head and a long centre portion. It is located in the "A-band". The second are the thin actin filaments, which is the major constituent of the "I-band" but they also extend into the "A-band". The third is an elastic filament system that is made up of the giant protein titin, which extends from the "Z-line" of the sarcomere where it binds to the thin filament system to the "M-band" where is interacts with the thick filaments (Figure 14). Titin or connectin is the largest protein found in nature to date, spanning 4,200 kDa and it is thought to play a essential role in the assembly and functioning of the sarcomere (Tskhovrebova & Trinick, 2003). The dark colour that signifies the presence of the "A-bands" is due to the overlap between actin and myosin filaments. In much the same way,

the lighter "H-zone" occurs as a result of the absence of actin from the centre of the "A-band".

The process of muscle contraction occurs when an action potential is directed from the CNS to myosin which is thus stimulated. During the process of stimulation, neurotransmitter acetylcholine is released by the motor neuron and it travels along the neuromuscular junction. The nerve impulse then travels along the T (transverse) tubules until it reaches the sarcoplasmic reticulum where calcium release channels are activated. The myosin head then binds to actin and forms actomyosin, which results in the release of energy by breaking up ATP into ADP and $P_i$. This energy expenditure enables the myosin head to draw actin towards the centre of the sarcomere. The myosin head becomes liberated from actin and the entire process is repeated as more nerve impulses are received. This repeated motion causes the filaments to slide past one another. This process of muscle contraction was first proposed by Huxley (Cooke, 2004).

### 3.1.3 Muscles biopsied in dystrophinopathies

#### 3.1.3.1 Biceps muscle

This is the prominent muscle on each side of the upper arm and since it can be flexed easily it is associated with upper body strength. The biceps (Figure 15) is a muscle that is commonly biopsied in Duchenne muscular dystrophy as it is usually affected as a consequence of the disease process. Marked wasting of this muscle is a regular feature of DMD. The primary genetic defect in DMD, the absence / reduction of the protein dystrophin is thought to play a role in bringing about wasting of this muscle (Figure 15).
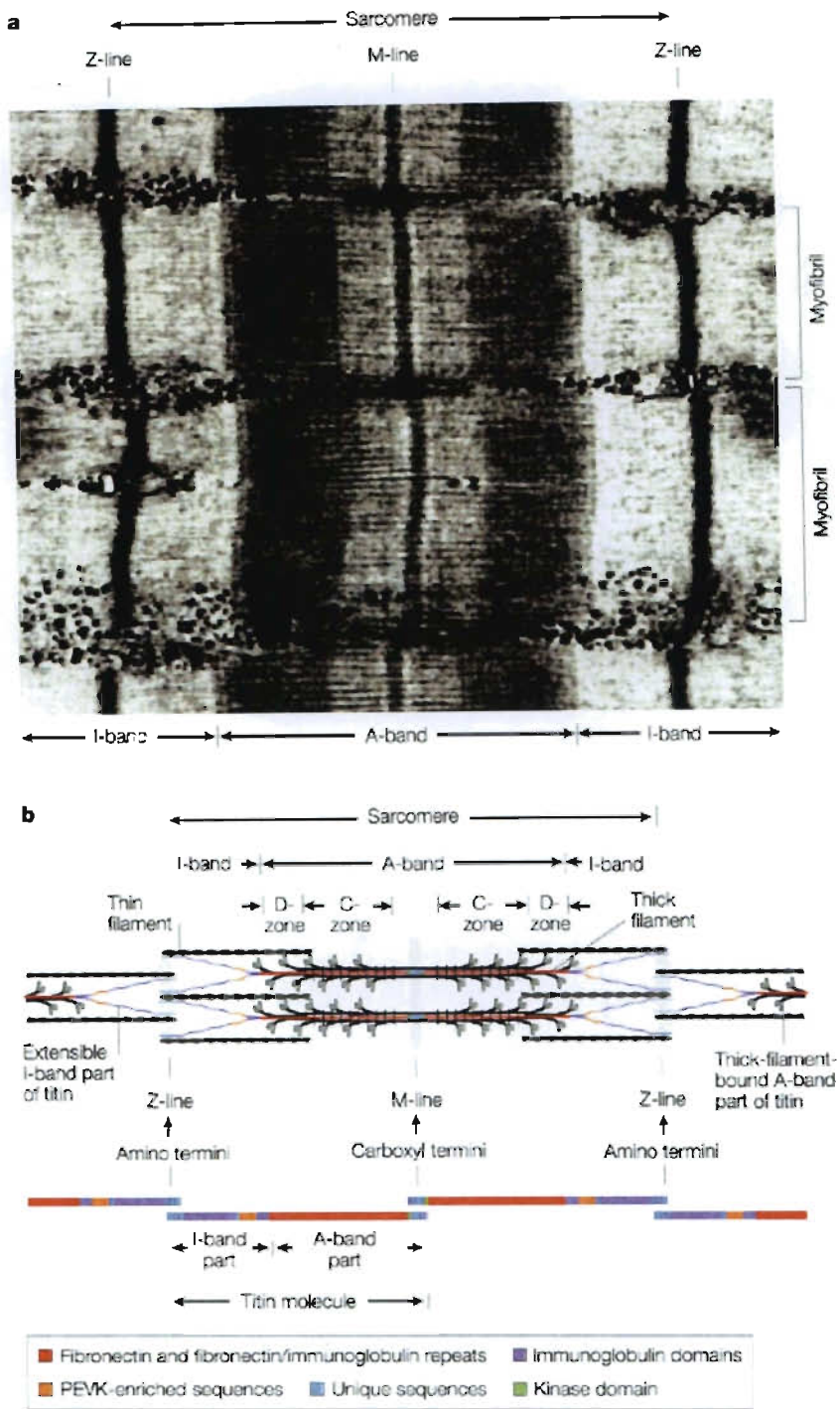
**Figure 14: Diagram illustrating the structural components that constitute striated skeletal muscle (Adapted from Tskhovrebova & Trinick, 2003).**
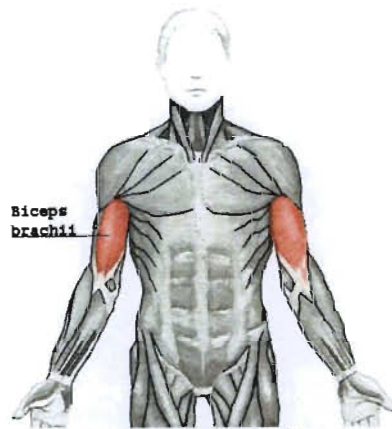
**Figure 15: Image showing the location of the biceps brachii muscle.**
http://en.wikipedia.org/wiki/Biceps_brachii_muscle

### 3.1.3.2 Quadriceps muscle

The quadriceps (Figure 16) includes the four muscles in the front of the thigh. It is referred

to as the extensor muscle of the thigh as it envelops the front and the sides of the femur.

Each of the four muscles has a distinctive name and role. The muscle that occupies the

middle of the thigh is called the rectus femoris, whereas the other three are connected to

the femur as their names suggest. They are called the vastus lateralis (lateral side), vastus

medialis (medial side), vastus intermedius (front of femur). All these muscles together

form powerful extensors of the knee joint. The quadriceps plays an important role in such

activities as walking, running, jumping and squatting. The rectus femoris is also involved

in hip flexion.

In DMD, these muscles are most often weak and wasted on clinical examination. For this

reason, it is a common muscle that is biopsied for histological and immunohistochemical

staining purposes. In Becker muscular dystrophy (BMD) too the quadriceps becomes weak

however not nearly to the extent that is seen in DMD. Absence of dystrophin staining is

common on immunohistochemical analysis of DMD biopsies. In BMD patients there is

49

either a mosaic pattern of staining or one of the three dystrophin antibodies shows absence of staining.
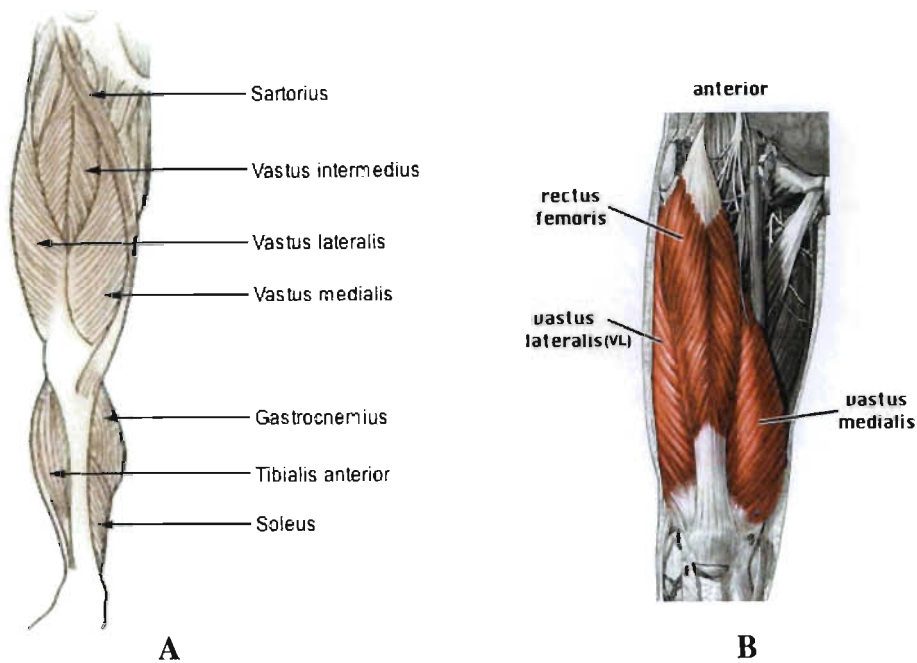


**Figure 16: Image of the muscles found in the lower extremities. (A) These include the quadriceps and gastrocnemius muscles. The rectis femoris, which forms part of the quadriceps is not included to show the vastus intermedius.**

http://en.wikipedia.org/wiki/Image:Illu_lower_extremity_muscles.jpg

**(B) Image revealing the location of the rectus femoris.** www.harkema.ucla.edu/muscles.html

### 3.1.3.3 Gastrocnemius muscle

This is a powerful muscle found at the back of the lower leg and together with the soleus it makes up the calf muscle (Figure 17). Its major action involves standing and walking, where it is responsible for increasing the angle between the foot and the leg (plantarflex the foot). The muscle starts from the back (posterior) area of the femur and its other end forms the Archilles tendon with the soleus muscle. This muscle is often hypertrophied in DMD patients (Bakker & van Ommen, 1998). Even though immunohistochemical staining of the muscle fibres from this muscle reveals absence of dystrophin, the muscle is found to be

strong on clinical examination of dystrophinopathy patients. There is currently no definitive reason as to why the calf muscle remains hypertrophied and strong whilst the other muscles become progressively weaker.
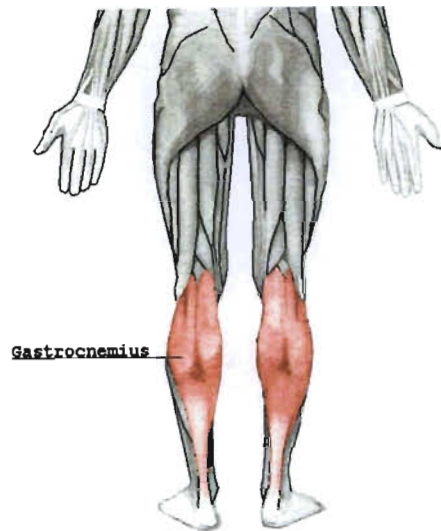


**Figure 17: Image showing the location of the gastrocnemius muscle.**
http://en.wikipedia.org/wiki/Image:Gastrocnemius.png

### 3.1.4  Histology of normal skeletal muscle

In normal skeletal muscle, the fibres are located in such close proximity to one another that they may appear to be in contact. This is due to the unobtrusive nature of the endomysium. The nuclei are located at the periphery of a muscle fibre. The mean diameter of muscle fibres in the neonate would be between 10-15 µm. In an adult, the mean diameter would usually be between 50-80 µm and this depends largely on various factors such as the muscle that was biopsied, gender and activity status of the individual.

The haematoxylin and eosin (H+E) stain is a commonly used histological stain to distinguish normal from myopathic muscle. Haematoxylin stains the nuclei blue whilst eosin stains the connective tissue and the cytoplasm pink. In longitudinal section, the cells run parallel to one another. In cross sectional view, the muscle fibres of an adult are

polygonal, whereas those of a child are almost round in appearance (See figure 18 A and B below). The skeletal muscle fibres from a child are much smaller than that of an adult as is shown in figure 18 (B and A) below. The same magnification was used to capture both the images (200 ×).

In longitudinal section, muscle fibres often show alternating light and dark banding patterns, thus giving it the striated appearance as shown in Figure 18 (C) below.



A                                   B



C
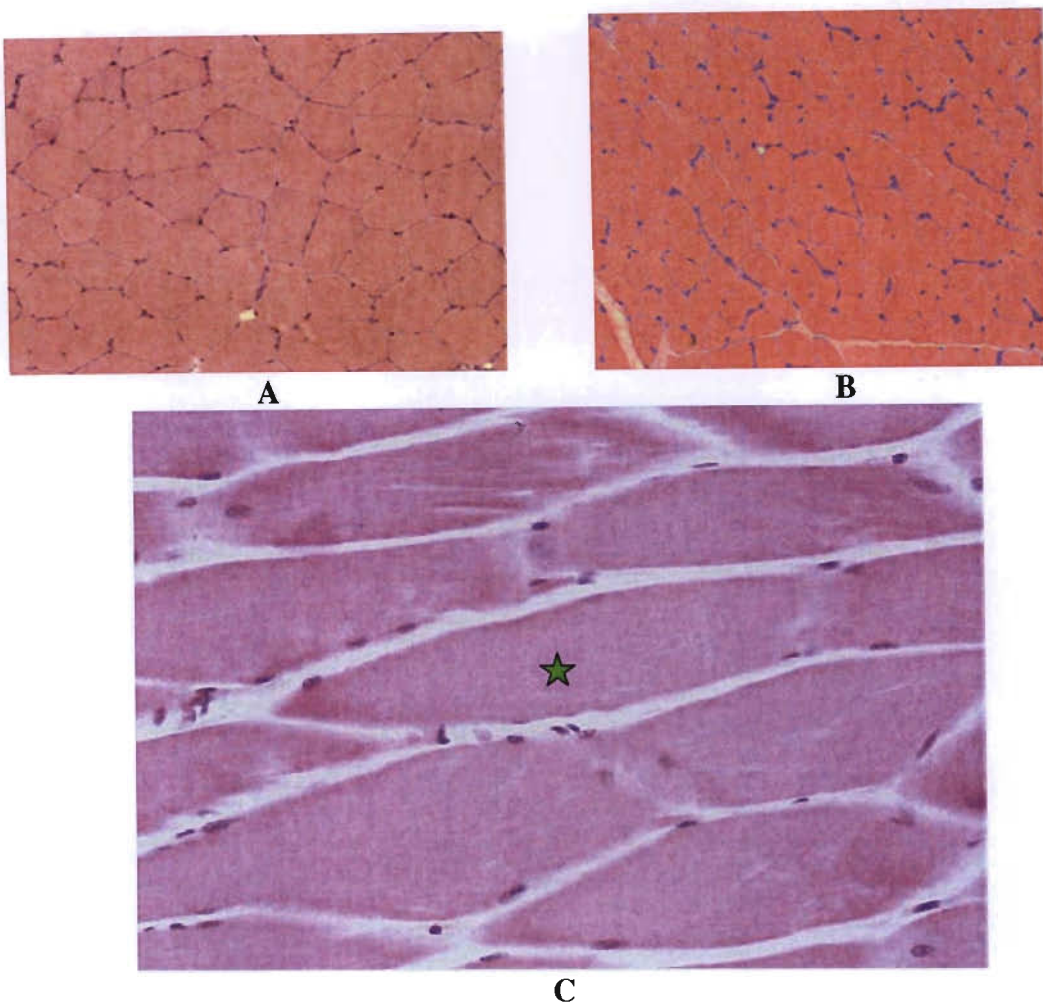
**Figure 18: Haematoxylin and eosin stained images of normal skeletal muscle fibres in cross sectional view at 200 × magnification and longitudinal section at 400 × magnification.**
**(A) Adult skeletal muscle fibres. (B) Skeletal muscle fibres from a 4 year old child.**
http://missinglink.ucsf.edu/lm/ids_104_musclenerve_path/student_musclenerve/normal.html.
**(C) Longitudinal muscle fibre sections show faint striations at high magnification (green star)**
http://www.usuhs.mil/pat/surg_path/nlhist/pictures/nl0004b.jpg&imgrefurl.
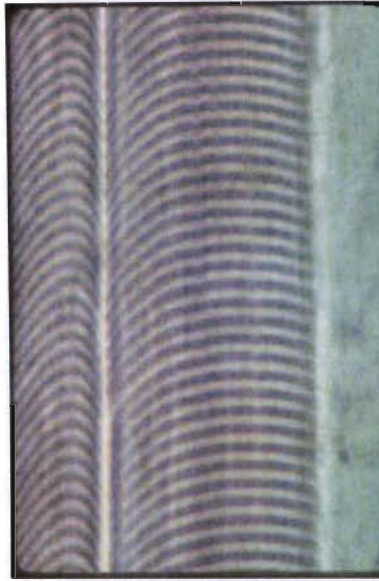
**Figure 19: Striated appearance of skeletal muscle in longitudinal section.**

http://users.rcn.com/jkimball.ma.ultranet/BiologyPages/M/Muscles.html

### 3.1.5 Pathology of dystrophic skeletal muscle
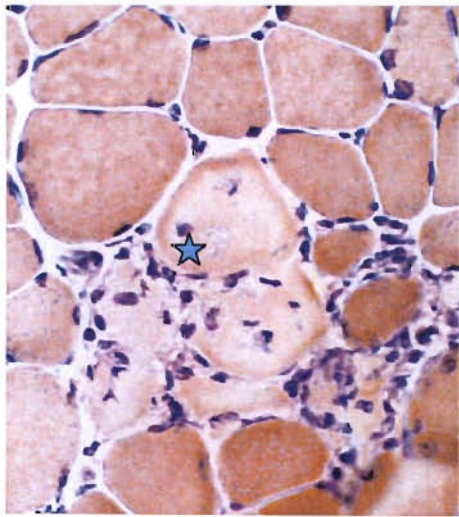


A
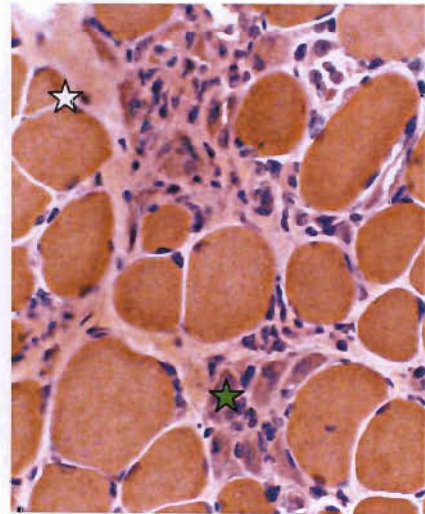
B
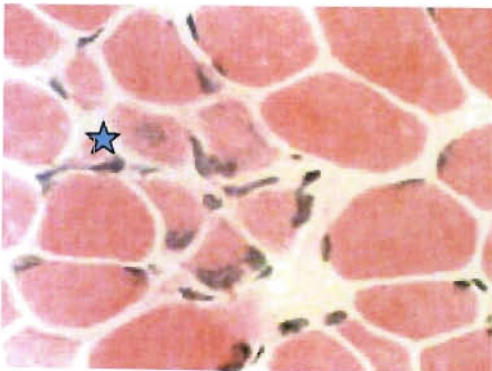
C
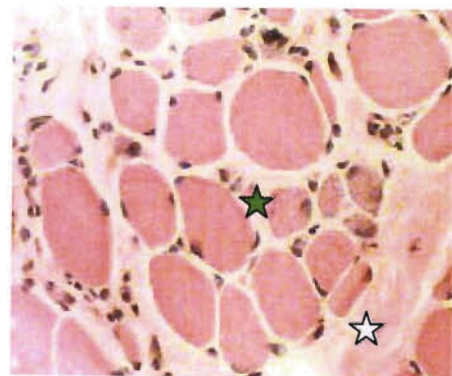
D

**Figure 20: Dystrophinopathy pathology illustrated by H+E staining.**

Images A, B and C reflect the early pathology seen on H+E staining of muscle biopsy samples in dystrophinopathy patients. (A) Presence of necrotic fibres (Blue star). (B) Regenerating muscle fibres are shown by the presence of many small fibres (white star) and increased nuclei (green star). (C) Immature basophilic muscle fibres (blue star). Image D reflects the later pathology seen in dystrophinopathy patients, where endomysial connective tissue infiltration (white star) is evident. Variable fibre size diameter (green star) is also shown.

http://www.neuro.wustl.edu/neuromuscular/pics/biopsy/dmd/dmdmyopthgreg.jpg

## 3.2 AIMS AND OBJECTIVES

i) To confirm dystrophinopathy status of clinically diagnosed patients using immunohistochemical antibody staining.

ii) Perform immunohistochemical staining on two biopsy samples from the same patient to detect the presence / absence of dystrophin.

Clinically diagnosed Duchenne and Becker muscular dystrophy patients underwent an open biopsy procedure with informed consent. Ethical approval was obtained for all muscle biopsies performed.

## 3.3 MATERIALS AND METHODS

The biopsy procedure in young children was performed under light general anaesthesia. In older children and in adults, the biopsy was performed under local anaesthetic.

### 3.3.1  Patient population

The biopsy database for this study contains muscle biopsy specimens from 55 DMD and BMD individuals. Eight of the muscle biopsy specimens were from Becker muscular dystrophy patients, one was from a female manifesting carrier and the rest of the patients exhibited symptoms of DMD.

### 3.3.2  Muscle biopsy cutting procedure for immunohistochemical analysis

The procedure was carried out as outlined in the Leica manual (Leica 1850 cryostat). The following aspects of the protocol related specifically to the type of muscle being sectioned:

- The sample was left in the microtome between four and six hours to allow it to equilibrate to the desired cutting temperature.
- The temperature at which the samples were cut varied owing to the state of the muscle tissue. If the tissue was found to contain adipose tissue infiltrates, the temperature was reduced to between -25°C and -30°C to allow for sections to be cut. If the temperature was too high, the sample would not be cold enough to obtain usable sections.
- The specimen was cut at an 8 μm diameter.

### 3.3.3  Muscle biopsy storage for RNA extraction

The remaining pieces of muscle tissue were stored in a tissue protectant called RNA*later* (Ambion). This solution was used to ensure that the quality and quantity of the RNA would not be compromised by degradation elements in downstream applications. The reagent

enters and saturates the tissue sample thereby stabilising and protecting cellular RNA in fresh tissue.

The muscle tissue sample was cut into pieces of not more than 0.5 cm in thickness. The tissue was placed into five volumes of the RNA*later* solution. The tissue in RNA*later* solution was incubated at 4°C overnight. Following incubation, the pieces of tissue were placed into a sterile 0.5 ml micro-centrifuge tube for long term storage at -80°C or until required.

### 3.3.4    Haematoxylin and eosin staining

Standard haematoxylin and eosin staining was performed on all muscle biopsy samples (http://en.wikipedia.org/wiki/H&E_stain). The stain was used to perform histological analyses and thereby confirm the presence of the dystrophic process that was clinically apparent to the Neurologist. It is also used to give an indication of what stage the individual is at, with respect to disease progression.

All the steps were carried out using protective eye-wear and either double latex gloves or nitrile gloves when available. All solutions were housed in a fume hood. Forceps were used at all times to handle the slides.

### 3.3.5    Dystrophin staining

The dystrophin stain was performed to confirm the dystrophinopathy state of the clinically assessed patient. The dystrophin stain would show the presence, reduction or complete

absence of dystrophin in different regions of the protein. There are three commercially available monoclonal antibodies for the dystrophin protein (Novocastra laboratory, United Kingdom). Dystrophin 1 (Dys 1) targets the rod domain of the protein, dystrophin 2 (Dys 2) targets the C-terminal domain and dystrophin 3 (Dys 3) targets the N-terminal domain of dystrophin. The absence of the protein in a particular domain is usually suggestive of a deletion or other mutation in that particular region. The staining therefore serves as the ultimate confirmatory test for dystrophin absence. For each batch of dystrophin stains that were conducted, a control slide was included for comparison purposes. Sometimes it was found that the staining was markedly reduced and not absent. This could only be properly assessed by comparing the staining profile of the suspected dystrophinopathy patient's sample to that of a control sample.

The Histostain™ Plus kit (Zymed Laboratories Inc.) is used to visualise the protein. This commercial kit utilises the Streptavidin-biotin methodology to detect binding of the monoclonal antibodies to tissue dystrophin.

The procedure followed was as per manufacturer's instructions (Novocastra Laboratories, United Kingdom; Zymed Laboratories Inc.).

### 3.3.6   Spectrin and other protein immuno-staining

For each suspected dystrophinopathy patient, other proteins were also stained for. A spectrin antibody stain was done to determine the membrane integrity of the sample. Spectrin would stain normal in dystrophinopathy patients as the membrane is intact even though dystrophin is deficient. Staining for the sarcoglycans ($\alpha$, $\beta$, $\gamma$ and $\delta$) is often

reduced in dystrophinopathy patients as the sarcoglycans are also a part of the dystrophin-associated glycoprotein complex (DAGC). When there is a mutation in the dystrophin gene, it disrupts the entire DAGC hence the reduction in sarcoglycan staining. Further to this, $\alpha$-actinin is stained for. Laminin-$\alpha$-2 or merosin, which is the name it is given because it is expressed in skeletal muscle, is also stained for as it forms the structural part of the basement membrane. If merosin is intact in dystrophinopathy then one can exclude such disorders as congenital muscular dystrophy or merosinopathy. All these subsidiary stains are done to exclude any limb girdle muscular dystrophy as a mild dystrophinopathy phenotype may be confused with a limb girdle muscular dystrophy (Blake *et al.*, 2002).

## 3.4  RESULTS

All clinically manifesting Duchenne muscular dystrophy patients that agreed to have a muscle biopsy showed reduced or absent dystrophin staining on immunochemical analysis.

In addition to this, four patients agreed to have double biopsies by informed consent. These samples formed the basis of the microarray aspect of the study. A detailed description of the staining patterns will be outlined for the four patients who agreed to have a double biopsy taken from the calf muscle and either the quadriceps or biceps muscle.

**Table 3: Outline of immunohistochemical results obtained for the four dystrophinopathy patients who agreed to have double biopsies of their calf and biceps or quadriceps muscles.**

| Biopsy number | Surname, Initials | Muscle | Immunohistochemical stain | Result |
|---|---|---|---|---|
| 23B/2004 | S, N | Calf | Dystrophin 1 | Mixture of poorly & irregularly stained fibres. Pattern varies in different parts of the biopsy. |
| | | | Dystrophin 2 | negative, no staining |

| | | | Dystrophin 3 | Scattered poorly stained fibres and mosaic pattern of staining. |
|---|---|---|---|---|
| | | | Spectrin | Present, but low intensity staining. |
| | | | Sarcoglycans<br>α<br>β<br>γ<br>δ | +ve<br>+ve<br>weakly +ve<br>weakly +ve |
| 23A/2004 | S, N | Biceps | Dystrophin 1 | Mixed pattern of staining, some weak or absent with others normal. Irregular pattern. |
| | | | Dystrophin 2 | Areas of absent or diminished staining. |
| | | | Dystrophin 3 | Areas of absent or reduced staining. Mosaic staining pattern. |
| | | | Spectrin | +ve |
| | | | Sarcoglycans<br>α<br>β<br>γ<br>δ | +ve<br>+ve<br>weakly +ve<br>weakly +ve |
| 03A/2005 | S, V | Biceps | Dystrophin 1 | Absent |
| | | | Dystrophin 2 | Absent |
| | | | Dystrophin 3 | Absent |
| | | | Spectrin | Fatty tissue prevalent, tissue section unsuitable. Data uninterpretable. |
| | | | Sarcoglycans<br>α<br><br>β<br><br>γ<br>δ | Poor tissue sections<br>Poor tissue sections<br>+ve<br>+ve |
| 03B/2005 | S, V | Calf | Dystrophin 1 | Absent |
| | | | Dystrophin 2 | Absent, connective tissue infiltration prevalent |
| | | | Dystrophin 3 | Faint staining of small clusters of fibres |
| | | | Spectrin | +ve |
| | | | Sarcoglycans<br>α<br>β<br>γ<br>δ | Faint staining<br>Faint staining<br>+ve<br>+ve |
| 06A/2005 | M, R | Calf | Dystrophin 1 | Absent |
| | | | Dystrophin 2 | Few staining fibres. Rare pseudofibres show weak staining. |
| | | | Dystrophin 3 | Few clusters of staining fibres |
| | | | Spectrin | Poor staining. |
| | | | Sarcoglycans<br>α<br>β | +ve<br>Weak staining |

| | | | γ δ | +ve Weak |
|---|---|---|---|---|
| 06B/2005 | M, R | Biceps | Dystrophin 1 | Connective tissue staining. |
| | | | Dystrophin 2 | Negative |
| | | | Dystrophin 3 | Negative |
| | | | Spectrin | Poor staining. |
| | | | Sarcoglycans α β γ δ | Sections were poorly stained due to fatty tissue accumulation. Data not definitive. |
| 19A/2003 | Z, S | Quadriceps | Dystrophin 1 | +ve and -ve fibres. Mosaic pattern of staining |
| | | | Dystrophin 2 | +ve and few -ve fibres |
| | | | Dystrophin 3 | +ve and few -ve fibres |
| 19B/2003 | Z, S | Calf | Dystrophin 1 | +ve and -ve fibres. Mosaic pattern of staining |
| | | | Dystrophin 2 | +ve and few -ve fibres |
| | | | Dystrophin 3 | +ve and few -ve fibres |
| | | | Spectrin | +ve |

## 3.4.1 Haematoxylin and eosin (H+E) staining
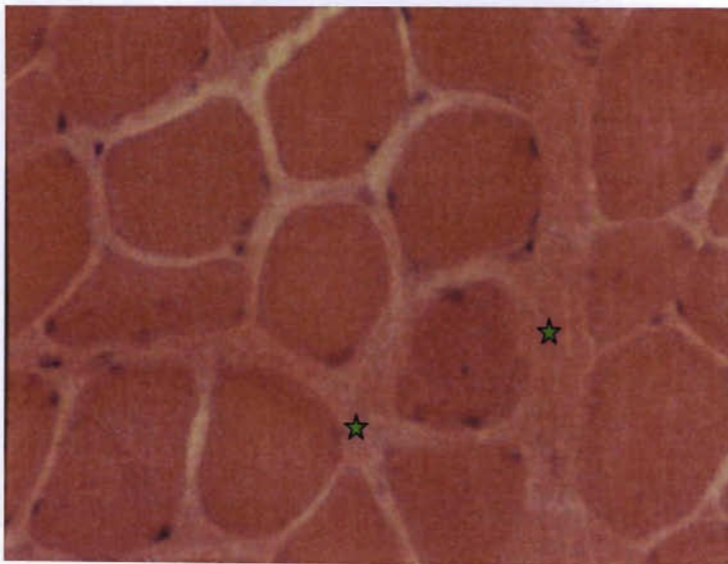


**Figure 21: Haematoxylin and eosin stain showing endomysial connective tissue infiltration illustrated by the green stars (magnification 200 ×).**
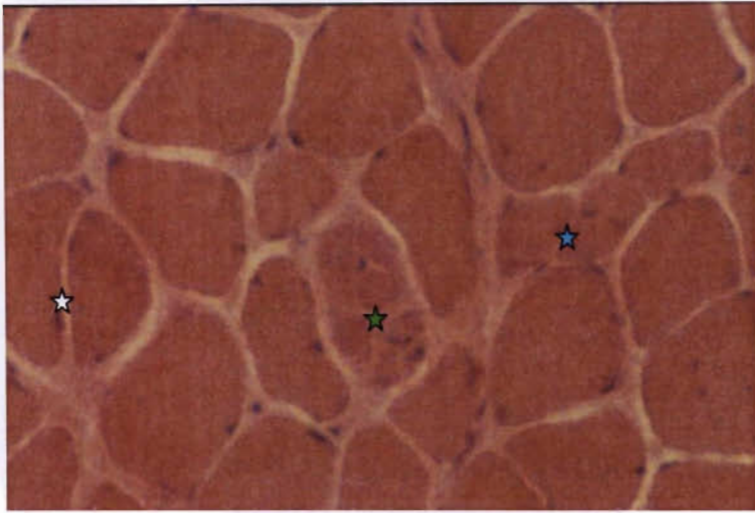
**Figure 22: Image showing regenerative muscle fibres at different stages of the regenerative process. The first reflects the early stage of the regenerative process (green star), whilst the second (cyan star) and third (white star) show the latter stages of the regenerative process (magnification 200 ×).**
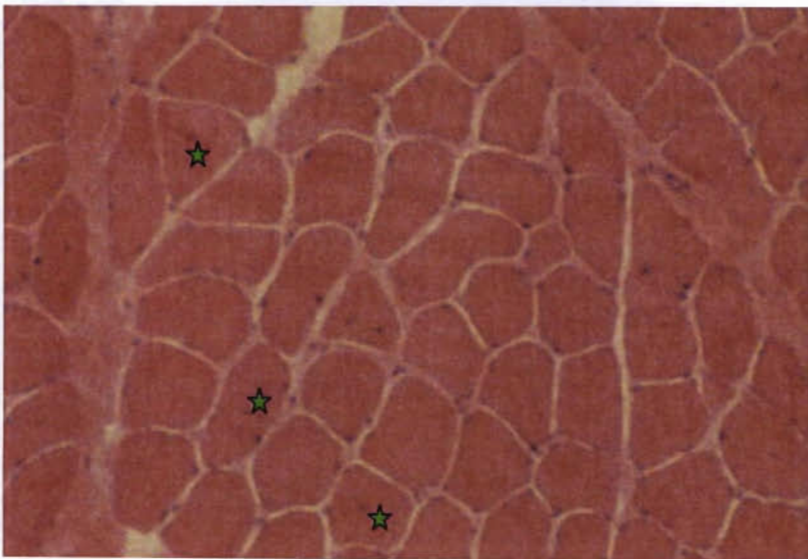


**Figure 23: Immunohistochemical stain showing the centralised nuclei (green star) that appear in muscle fibres of DMD patients (magnification 100 ×).**
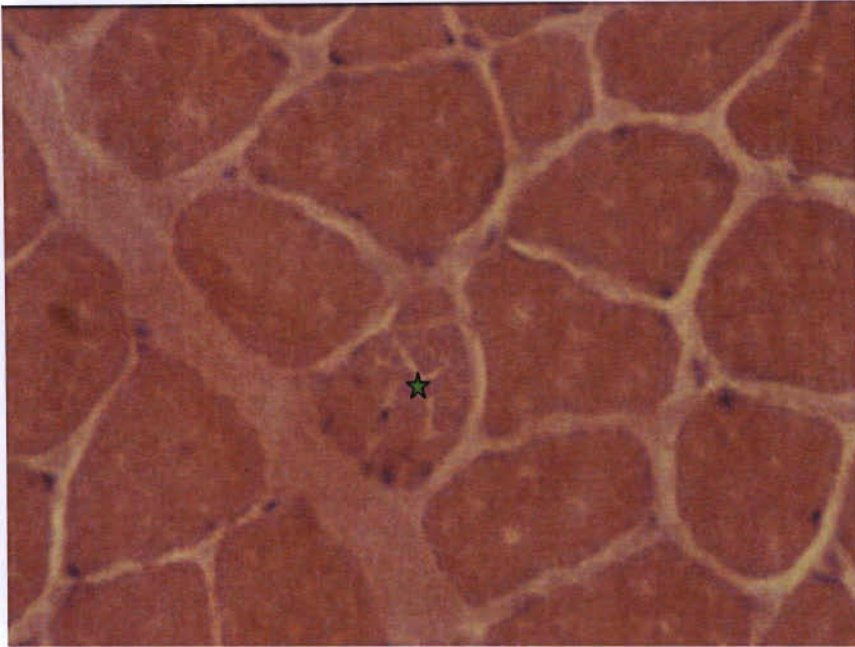
**Figure 24:** Image showing the invasion of muscle fibres by macrophages, which in effect bring about phagocytosis (green star) (magnification 200 ×).
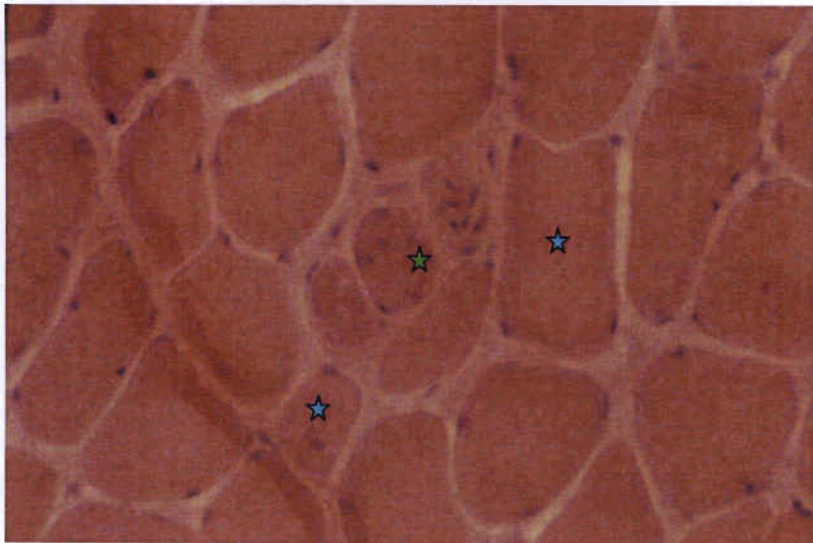


**Figure 25:** H+E stain showing muscle fibre degeneration (green star) and the variation in fibre size diameter that is often seen on muscle biopsy sample from DMD patients (cyan stars) (magnification 200 ×).
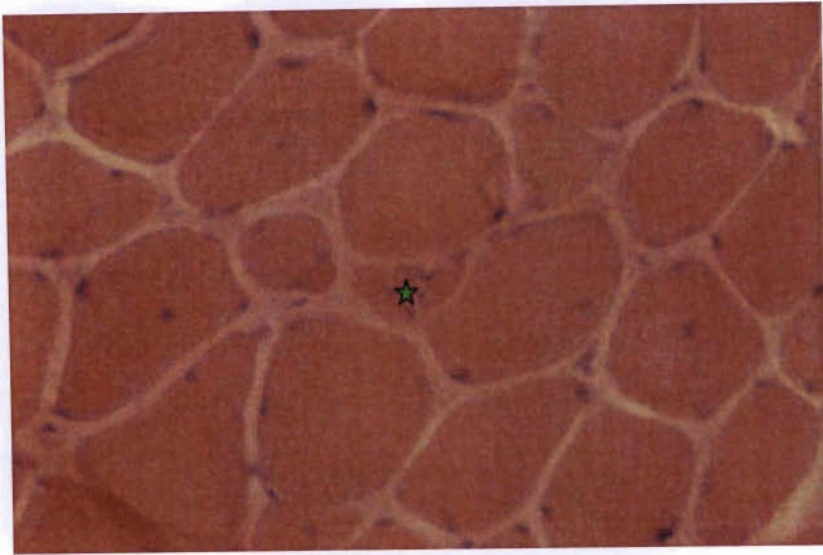
**Figure 26: Image showing muscle fibre degeneration or digestion that could be the result of lysosomal enzyme activity (magnification 200 ×).**

## 3.4.2 Dystrophin staining
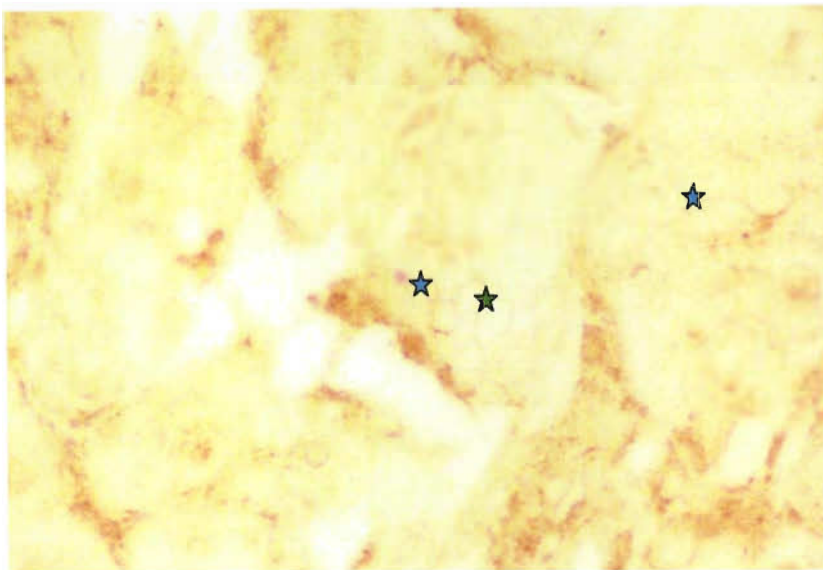


**Figure 27: Immunohistochemical stain of the dystrophin antibody (Dys3) that targets the amino-terminal domain of the protein. The DMD affected patient shows a mosaic pattern of staining (green star) in this region where a deletion was also found on multiplex PCR. Variable fibre size diameter is clearly evident (cyan stars). (Magnification 40 ×).**

The biopsy sample shown in figure 27 is from patient C, N, whose biopsy was taken in 1999 and stored at -80°. The patient could not be included in the molecular aspect of the project because there was not sufficient DNA left to perform multiple PCR assays for

deletion detection. On a previous occasion the multiplex PCR using 18 primer pairs was used and it detected deletions in exons 3, 6, 12, 45, 47, 48.



**Figure 28: Dystrophin stain using antibody Dys3, which targets the amino-terminal domain of the protein. The stain shows a mosaic pattern of staining in a DMD patient that was shown to have no deletions on multiplex PCR (magnification 100 ×).**

The biopsy was taken from patient M, S in 1999. There were two biopsy samples taken, one from the calf muscle and the other from the biceps muscle. The image above – figure 28 reflects the biceps muscle from the patient. The patient was shown to have no deletion when multiplex PCR using 18 exons was previously performed.

In figure 29 below, biopsies from the same dystrophinopathy patient were taken and subjected to dystrophin staining. Even though the calf muscle remains invariably strong compared to the biceps muscle, which becomes progressively weaker the pattern of dystrophin staining was similar in both muscles.

**Figure 29: Dystrophin 3 stain from patient 23A/ 2003 (A) and 23B/2003 (B). A mosaic pattern of staining is shown in both the biceps (23A) and calf (23B) muscles from the same patient (magnification 100 ×).**

## 3.5 DISCUSSION

Many of the patients' muscle samples were infiltrated by adipose tissue therefore the tissue was not of good and usable quality throughout the slide. The results were interpreted with caution when poor muscle sections were observed on a slide. The temperature of the cryostat was reduced significantly to between -28°C and -30°C in cases where the tissue was difficult to cut. This was an indication that the muscle tissue contained mostly connective tissue and adipose tissue as opposed to muscle tissue alone.

The DMD affected patients showed different muscle cell morphology to normal cells. The normal muscle cells were hexagonally shaped whereas the cells from DMD patients were irregular and round. There was often variation in fibre size diameter, with large and small fibres being present in the same region that was viewed under the microscope. An example of such an occurrence is shown in figure 25 above. In normal cells, the nuclei were present at the periphery compared to the centralised nuclei that were found in muscle cells from DMD affected patients, which is shown in figure 23 above. Fibre regeneration

and degeneration was also a common feature of dystrophic muscle. More regeneration appeared to occur in the muscle fibres of younger patients, where the muscle satellite cells actively proliferate. Satellite cells exhibit self-renewal and are capable of producing many progeny (Collins *et al.*, 2005; Wagers & Conboy, 2005). As time progresses, the regenerative capacity of the cells diminish owing to less muscle satellite cells being present. Owing to such an occurrence, the degeneration of muscle cells becomes more prevalent. More necrotic fibres are therefore seen in older DMD affected patients because the regeneration gives way to muscle cell necrosis. The degenerating fibres are often accompanied by inflammatory cells such as macrophages and CD4^{+} cells (Emery, 1993; Blake *et al.*, 2002).

Majority of the clinically affected dystrophinopathy patients had connective tissue infiltration, adipose tissue deposition and other histological patterns characteristic of their dystrophic phenotype. These signs become more apparent as the affected individual ages. Fibre type variation was another prominent feature in the DMD patients. Both small, rounded fibres as well as large, irregularly shaped fibres were evident as shown in the figures 25 above.

The biceps and quadriceps muscle tissues are those muscles that become weaker as the disease progresses. The calf muscle is the tissue that remains invariably strong in dystrophinopathy patients even when other muscle tissues become weaker leading to wheelchair confinement for the patient. The gastrocnemius, which forms part of the calf muscle, also lacks dystrophin when subjected to immunohistochemical analysis using a dystrophin antibody. This lack of staining for the dystrophin protein is expected as all muscles are affected when the dystrophin protein is lacking owing to a deletion or another

type of mutation in the gene. However, since the calf muscle is hypertrophied and appears stronger than the other muscles (biceps, quadriceps) when clinically assessed, the speculation is that there must be other regulatory mechanisms involved at the molecular level in producing the hypertrophied state often seen in dystrophinopathy patients.
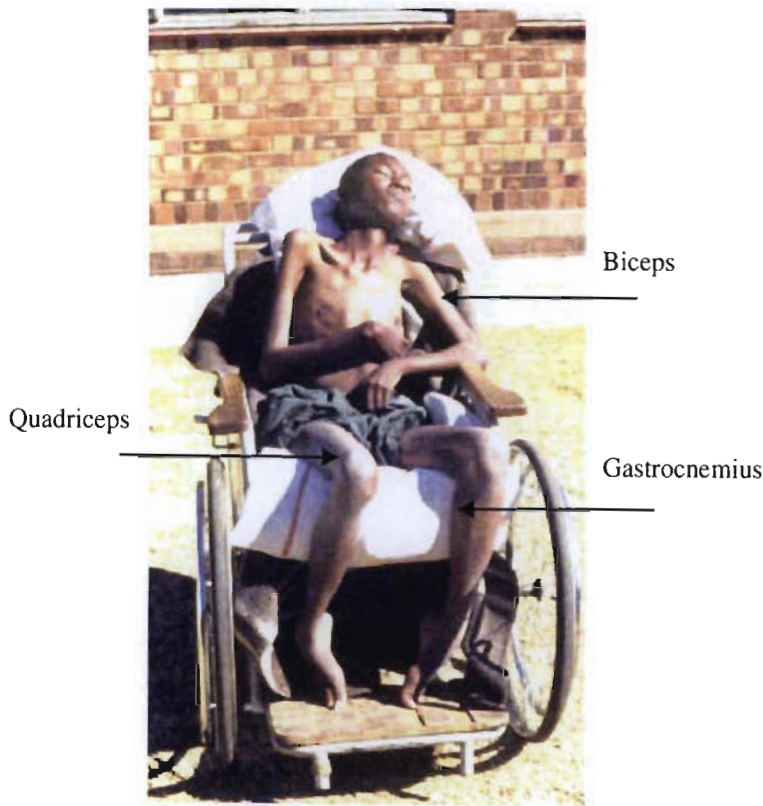


**Figure 30: Photograph showing a severely affected DMD patient who is wheelchair bound owing to generalised weakness of his muscles.**

The pattern of dystrophin staining varied between patients. In some DMD patients who showed advanced symptoms, the staining patterns correlated well with the clinical disease manifestation. In the case of the BMD patients, a mosaic pattern of staining was noted. The female manifesting carrier's immunohistochemistry revealed a mosaic staining pattern (Table 3 and figure 29).

Revertant fibres, which are thought to occur as a result of restoration of the reading frame through a splicing or exon-skipping mechanism, have been found in many patients (Thanh

*et al.*, 1995). During this time it was also shown that the number of revertant fibres increased with age however no correlation was found between number of dystrophin positive fibres and decreased disease severity (Fanin *et al.*, 1995). It was also thought that this phenomenon could open up possibilities for gene therapy however owing to the fibres being present in small numbers it turned out to not be feasible (Wilton *et al.*, 1997). A break-though did emerge from these findings and the anti-sense oligonucleotide approach was borne. In 2006, revertant fibres were induced in *mdx* using the anti-sense oligonucleotide method and functional dystrophin was detected using three independent methods (Fall *et al.*, 2006).

With respect to the patient that did not show any deletions on multiplex PCR yet a mosaic pattern of staining was found on immunohistochemical staining (figure 28), the absence of a deletion does not rule out the possibility of other mutations such as a duplication. In such an instance the next method of detection after the multiplex PCR would be the multiplex ligation-dependent probe amplification (MLPA) assay. At the time that this patient's sample was subjected to diagnostic testing, the MLPA assay had not been established in the Neuroscience laboratory.

# CHAPTER 4
# POINT MUTATION DETECTION IN NON-DELETION DYSTROPHINOPATHY PATIENTS

## SECTION A:
## EVALUATION OF THE SINGLE STRANDED CONFORMATION POLYMORPHISM (SSCP) ASSAY ON DNA SAMPLES

## 4.1    INTRODUCTION

The single stranded conformational polymorphism (SSCP) analysis method has been utilised to detect point mutations for over a decade in both research laboratories and in clinical diagnostic environments. Under non-denaturing conditions, nucleic acids comprising DNA, RNA or cDNA have different electrophoretic mobilities depending on their length and shape. DNA ranging from 40-500 bp, in a double stranded state, electrophoreses in a semi-rigid, rod-like manner. However denatured single stranded DNA and RNA in the range of 4-500 bp have the ability of forming "equilibrium-stable" conformations, which are stabilised by intra-molecular bonds and therein lies the advantage of the SSCP assay (Novex, 1996). Each single strand folds into a specific secondary structure that is determined by its primary nucleotide composition and temperature of the gel. The change in conformation allows for wildtype sequences to be distinguished from mutant sequences by virtue of their differing electrophoretic mobilities. Single strands even with one base pair differences can possess different conformations.

### 4.1.1    Conventional SSCP

One of the first papers that included SSCP as the primary method was published by Orita

*et al.* (1989) in Japan. At that stage it was referred to as a mobility shift assay, which was performed using a neutral polyacrylamide gel. The method involved restriction endonuclease digestion of genomic DNA, denaturation using NaOH and EDTA and electrophoresis on a neutral 5% polyacrylamide gel. The features of the mobility shift were termed single stranded conformation polymorphisms as it resulted from a conformational change in the single stranded DNA. This paper set the stage for some important technical criteria to be followed in successive laboratory experiments using SSCP. These included the use of an appropriate low temperature as higher temperatures were found to destroy "some semi-stable conformations" (Orita *et al.*, 1989). The other two factors that were shown to affect the mobility shifts included electrophoresis buffer concentration and the use of denaturing agents such as 10% glycerol.

Shortly after the publication by Orita *et al.* (1989), Poduslo *et al.* in 1991 described a similar methodology to detect high-resolution polymorphisms in human coding loci. These authors advanced the previous SSCP technique by combining it with PCR amplification of 3' untranslated regions. Two methods were subsequently employed to detect nucleotide substitutions. The PCR products were subjected to either restriction digestion or SSCP analysis. The bands from the SSCP assay were detected by autoradiography using radioactively labelled [32]P. The PCR-SSCP method was able to identify point mutations that could not be detected using restriction endonuclease digestion thereby proving the efficacy of the SSCP method.

In 1993, papers focussing on the optimisation and sensitivity of the SSCP method were published. These papers outlined the usefulness of this technique whilst revealing those parameters that adversely affected the detection rate of point mutations using this mobility

shift assay. Sheffield *et al.* (1993) performed an array of experiments to determine the optimum DNA fragment size for definitive point mutation detection. It was found that the sensitivity of the method was related to the fragment size, where the highest sensitivity was noted in fragments that were between 95 bp and 200 bp. Glavac and Dean (1993), in their optimisation paper were able to map out those factors that affected the detection efficiency of point mutations using SSCP. These included electrophoresis temperature, concentration of the buffer, gel concentration, the effect of compounds such as glycerol and urea. It was found that a lower temperature such as 4°C, higher acrlyamide concentrations with lower cross-linking and the addition of 10% sucrose provided optimum band separation and resolution.

There appeared to be some discrepancy in the papers that reported on the sensitivity of the PCR-SSCP technique. In a review by Hayashi & Yandell (1993) comparisons were made between published literature where SSCP was used with probability scores of the factors affecting sensitivity being provided. It was suggested that the starting point for the detection of most mutations would be to supplement the DNA fragments being electrophoresed at room temperature (22°C) with 5-10% glycerol, while those electrophoresed at 4°C required no glycerol addition. It was agreed that polyacrylamide gels were most efficient, provided the percentage of crosslinker was low such as 5%. With respect to detection rate, 90% of mutations were found when the DNA fragment size was <200 bp. The prediction was that approximately 80% of point mutations would be detected if the fragment sizes were between 300 and 350 bp. The number of bands per single strand was not definite as more than one stable conformation was possible. The findings were that shorter DNA fragments increased the sensitivity of the SSCP analysis and optimisation was the key factor in determining the success of the method (Hayashi & Yandell, 1993).

### 4.1.2 "Cold"-SSCP

The use of the "Cold"-SSCP technique was first documented by Hongyo *et al.* in 1993. It required a commercially available apparatus called the "Thermoflow electrophoresis temperature control system", which was designed for the purpose of maintaining the appropriate temperature. A "thermostatically controlled refrigerated circulator" (Hongyo *et al.*, 1993) was used to maintain the set temperature. The samples were loaded onto specially designed NOVEX pre-cast TBE gels. The technique was described as a "simple, rapid and non-radioactive method" for SSCP analysis (Hongyo *et al.*, 1993) The authors optimised a range of parameters, which included the voltage, gel concentration, buffer concentration, the use of denaturants and loading buffers. This method differed from the others by virtue of the short electrophoresis time of between 40 minutes and two hours as well as use of the intercalating dye ethidium bromide as the staining reagent. The PCR products screened were in the size range of 117 bp – 256 bp therefore this paper was unable to determine the size limits over which "Cold"-SSCP could resolve DNA fragments and detect polymorphisms.

Following the Hongyo *et al.* (1993) report, an extensive application manual was compiled by NOVEX, the company responsible for manufacturing the "Cold"-SSCP apparatus. This booklet outlined all the factors to consider when optimising the "Cold"-SSCP technique with detailed explanations of the method and interpretation of results obtained. The company suggested that a range of different detection methods could be used for visualisation of the single strands. These included ethidium bromide, SyBr Green II, silver staining, colorimetric, and fluorescent or chemi-illuminescent detection (Novex, 1996). Interestingly, the Novex review cited a paper by Michaud *et al.* (1992), where point

mutations were detected in DNA fragments that were 800 bp in length even though the maximum size for point mutation detection was previously documented as being 350 bp (Hayashi & Yandell, 1993). During the interpretation stage, it would be important to determine that the single strands are found above the double strands at "twice the molecular size of migration". The difference in electrophoretic mobility would be based on the differing charges of the single and double strands (Novex, 1996). Mutant bands would migrate at a different rate from the normal (wild-type) or there would be subtle changes such as increased thickness of a single band or very slight change in migration of the band.
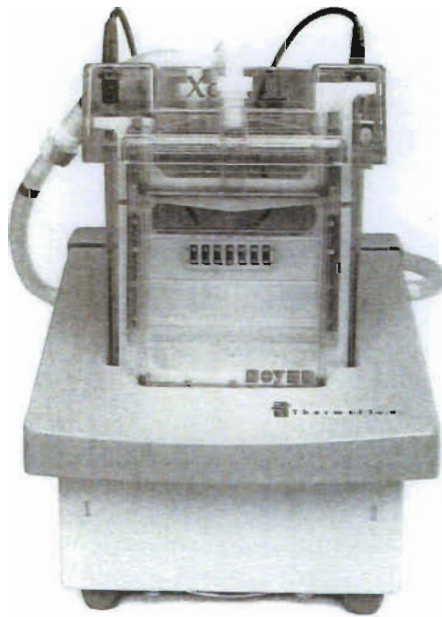


**Figure 31: Image showing the Novex Thermoflow™ SSCP mutation detection system that was used for separation and electrophoresis of single stranded PCR amplified DNA samples.**

### 4.1.3 PCR-SSCP and DNA sequencing using radioactive labelling

Shortly after the efficacy of the PCR-SSCP method was determined, the technique was combined with DNA sequencing analysis using radioactive labelling to definitively detect point mutations. The first paper to have used both methods was authored by Lenk *et al.* (1994), which focussed on the detection of carriers in Duchenne muscular dystrophy

(DMD). The patients' PCR products were electrophoresed on 5% non-denaturing polyacrylamide gels and the concentration of the carrier detection gels was 12%. Silver staining was used for detecting the SSCP fragments instead of radioactively labelling the primers.

### 4.1.4   Multiplex-SSCP

In a paper authored by Kneppers *et al.* (1995), a multiplex SSCP assay was developed, where 16 exons in the dystrophin gene were tested to detect point mutations. The automated Pharmacia PhastSystem was used to electrophorese and detect the point mutations. The exons tested were those included in the previously developed Chamberlain kit (Chamberlain *et al.*, 1988) and the Beggs kit (Beggs *et al.*, 1990). A 20% gel run at a single electrophoretic condition of 15°C was used and visualisation was performed with a silver stain. Band shifts were confirmed by DNA sequencing using the New England Biolabs Circumvent Sequencing kit. Interestingly, this was another report where the fragment size of >300 bp was not a limiting factor in detecting mutations. The detection rate was poor as only 6 band shifts were found in 70 patients tested. This report shows that the use of multiplex SSCP may not be sensitive enough to identify all point mutations.

The assumption that multiplex SSCP is not reliable enough to detect all point mutations was further emphasised in a paper by Larsen *et al.* (1999a). The SSCP analysis was performed using precast 10% polyacrylamide gels at 4°C and 20°C using a Multiphor apparatus from Pharmacia Biotech. Silver staining was used as the method of band visualisation and automated dye terminator cycle sequencing was performed using the ABI 373 DNA sequencer. This paper amplified 4 exons at a time in a single reaction tube. In

effect sixteen exons were amplified using this method. Even though multiplex SSCP was optimised in this paper, the authors do not recommend it as a reliable diagnostic test owing to the "theoretical possibility of decrease in sensitivity" (Larsen et al., 1999a).

In an attempt to revive the idea that multiplex SSCP was reliable and sensitive in detecting point mutations, Mendell et al. in 2001 using a "modification of SSCP analysis", screened 93 patients with DMD. A collection of ninety segments consisting of 21-23 amplicons were analysed, spanning the entire coding region of the dystrophin gene. The fragment sizes ranged from 128-346 bp. The fragments were radioactively labelled with α-33P-dATP and amplified using a robotic PCR instrument. A range of 5 different non-denaturing conditions was used for electrophoresis of the amplified products on a 6% acrylamide / 7 M urea denaturing gel. The bands were detected using autoradiography. Those bands with altered mobility or intensity patterns were sequenced using ABI 377 automated sequencer. The limitations of this SSCP modification method included the use of radioactivity and the small fragments sizes required for amplification and subsequent SSCP analysis.

### 4.1.5 Capillary electrophoresis SSCP

One of the earliest papers that focussed on the use of CE electrophoresis for SSCP was a Danish group (Larsen et al., 1999b). This group had previously performed SSCP using the conventional approach as reviewed earlier in this chapter. In this paper, the authors modified an ABI 310 instrument by attaching an in-house water cooling device within the chamber that houses the capillary array. The low temperatures increased the sensitivity of the SSCP assay and the results obtained were reproducible and of a higher resolution.
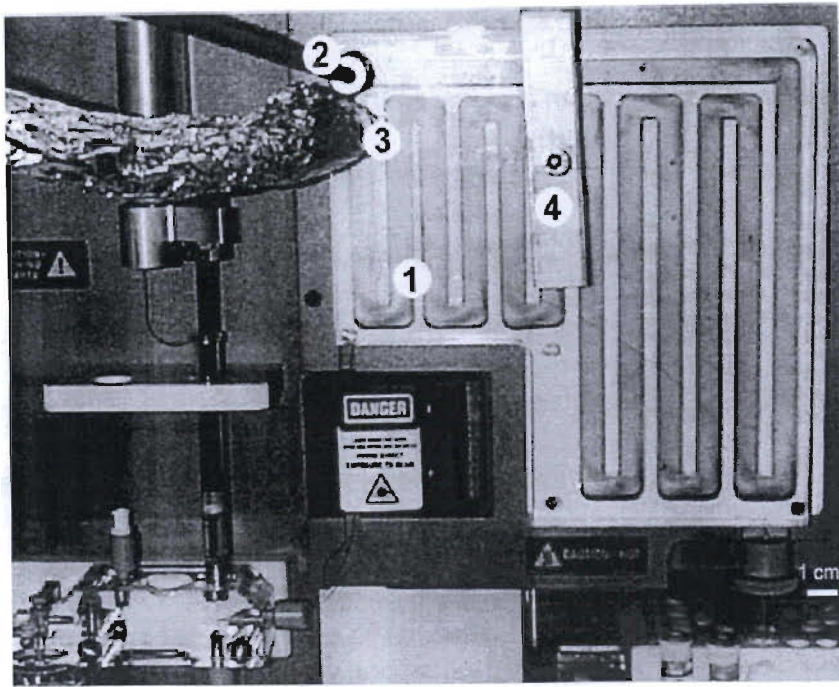
**Figure 32: Illustration showing the water cooling device installed into an ABI 310 instrument, to allow electrophoresis to be performed at lower temperatures for SSCP analysis (Adapted from Larsen *et al.*, 1999b).**

In a paper by Walz *et al.* (2000), the use of fluorescent based SSCP together with an ABI Prism 310 automated genetic analyser proved to be effective in detecting both known and unknown mutations in hemochromatosis and thrombogenetic diseases. The PCR amplification was performed using fluorescent labelled primers, with the forward primer being labelled with FAM (6-carboyx-fluorescein) and the reverse primer labelled with HEX (4,7,2', 4', 5', 7'-hexochloro-6-carboxy-fluorescein). Single PCR products were subjected to CE-SSCP, followed by multiplexed products, with only two PCR products being used in the multiplexed approach. Interestingly, the authors observed a change in the SSCP pattern in 59 of the 61 mutations studied. They were able to obtain a 100% mutation detection rate when the temperature was increased to above 40°C. It was shown that this method proved to be reproducible even when complex peak patterns were seen during the software analysis stage.

exons commonly involved in deletion mutations and those exons flanking the "hot-spots" for point mutations. A total of 28 primer pairs were subjected to PCR and subsequently SSCP analysis. A full list of primers is included in Appendix A.

Due to the limited resources in our laboratory a conventional gel apparatus, the Hoefer SE 600 was used for the electrophoresis. An externally attached re-circulating cold water-bath that was thermostatically controlled was attached to the gel apparatus using rubber tubing. The temperature in the room was kept constant at 18° using an air-conditioning unit that was electronically controlled. The temperature was regularly monitored using a mercury thermometer throughout the run as it was expected that there would be temperature fluctuations due to the electrical current passing through the apparatus during the run. The buffer inside the Hoefer SE 600 was re-circulated using a magnetic stirrer bar that ensured the temperature variation throughout the unit was negligible.

We do not have a radioactive facility at our laboratory therefore non-radioactive means was the preferred method. Those samples that showed a visual band shift were subjected to non-radioactive DNA sequencing, which was performed using the ABI 3100.

## 4.2    AIMS AND OBJECTIVES

i)      To use "Cold" PCR-SSCP to detect point mutations in patients found to have no deletions on conventional multiplex PCR.

ii)     To evaluate the efficiency and reproducibility of the technique in a resource-limited setting.

iii)    To assess the optimum temperature for best band resolution.

iv)    To assess different methods of SSCP fragment detection.

v)     To determine carrier status in the mothers of affected DMD patients.

## 4.3    MATERIALS AND METHODS

Blood samples were obtained through informed consent from clinically affected
dystrophinopathy patients and their mothers, who attended the Neuromuscular clinic at the
Department of Neurology, Inkosi Albert Luthuli Central Hospital, Durban, South Africa.
Prospective samples were collected in an EDTA tube and immediately transported to the
Neuroscience laboratory for processing. All 20 individuals included in this aspect of the
study formed part of the collective sample number comprising 68 individuals as previously
discussed in Chapter 3. The patients were found to have no deletions on multiplex PCR.
The DNA from mother and / or sister as well as child was subjected to SSCP analysis.

### 4.3.1.  Patient Population

**Table 4: Database of subjects included in the "Cold" PCR-SSCP aspect of the study.**

| DNA number | Surname, Initials | Age at diagnosis | Gender | Mother/child |
|---|---|---|---|---|
| 1 | S, R | 34 | F | Maternal Aunt of 2 |
| 2 | S, W | 8 | M | DMD |
| 3 | S, DK | 37 | F | Mother of 2 |
| 4 | M, M | N/K | F | Mother of 5 |
| 5 | M, B | N/K | M | DMD affected |
| 6 | H, S | 36 | F | Mother of 7 |
| 7 | H, J | 8 | M | DMD |
| 8 | S, T | 13 | M | DMD |
| 9 | S, NM | 17 | M | DMD |
| 10 | S, S | 53 | F | Mother of 8 and 9 |
| 11 | S, B | 29 | F | Sister of 8 and 9 |
| 12 | G, S | 16 | M | DMD |
| 13 | Mrs G | N/K | F | Mother of 12 |
| 14 | N, D | 9 | M | DMD |
| 15 | N, C | N/K | F | Mother of 14 |
| 16 | M, T | 14 | M | DMD |

| 17 | Mrs M | N/K | F | Mother of 16 |
|----|-------|-----|---|--------------|
| 65 | M, C  | N/K | F | Sister of 66 |
| 66 | M, R  | N/K | M | DMD          |
| 67 | M, P  | N/K | F | Mother of 66 |

**Legend: N/K – not known**

## 4.3.2 DNA Extractions

Two methods were employed in the isolation of DNA from the patients' blood samples. These included the QIAmp DNA blood mini kit (Qiagen) and the salting-out method.

### 4.3.2.1 QIAmp DNA blood mini kit

The QIAamp DNA blood mini kit would produce purified total DNA efficiently. Resulting DNA could be utilised in procedures ranging from conventional single PCR to the more sensitive multiplex PCR. The total DNA could be purified from whole blood, plasma, serum, buffy coat and lymphocytes. This straightforward spin column procedure would yield ultra-pure DNA in approximately 20 minutes. The main advantage was that purification would not require phenol-chloroform extraction or ethanol precipitation. A predominance of 20-30 kb sized purified DNA would be produced and a size range up to 50 kb has also been obtained using the QIAamp procedure.

The procedure followed was as per manufacturer's instructions (Qiagen Handbook, 2003).

### 4.3.2.2 Salting-out method

The salting out method was adapted from the protocol for the extraction of DNA from

white blood cells (leucocytes) by Miller *et al.* (1988).

### 4.3.3 DNA Quantification

Two methods of DNA quantitation were employed. These included: DNA quantitation using a DU800 UV/visible Spectrophotometer (Beckman Coulter) and the use of DNA quantitation standards (Invitrogen).

### 4.3.3.1 DNA quantitation using the Spectrophotometer

The DNA utilised in each PCR assay was quantitated using the DU800 Spectrophotometer by measuring the absorbance of the purified DNA at 260 nm. The DNA concentration was calculated by the spectrophotometer using the following parameters: cell pathlength (mm) of 10, dsDNA factor of 50. An OD of 1.0 corresponded to 50 µg/ml of dsDNA.

A 1 ml quartz cuvette was used to measure the absorbance. The transparent sides of the cuvette was not handled at this was the area through which the UV light would pass through and read the sample. The procedure followed was as outlined in the Beckman manual for the DU800 Spectrophotometer.

### 4.3.3.2 DNA quantitation using DNA quantitation standards

DNA quantitation standards (Invitrogen) were designed for the quantification of double stranded DNA on ethidium bromide stained gels. They consist of six standardised solutions of phage λ DNA of different concentrations. The DNA was supplied in storage buffer [10

mM Tris-HCl (pH 7.5), 20 mM EDTA, 10% (v/v) glycerol, 0.02% (w/v) bromophenol blue]. The concentration of each solution was as follows: 500 ng/6 μl (83 ng/μl), 250 ng/6 μl (42 ng/μl), 125 ng/6 μl (21 ng/μl), 63 ng/6 μl (10.5 ng/μl), 31 ng/6 μl (5.2 ng/μl) and 15 ng/6 μl (2.5 ng/μl).

The procedure followed was as per manufacturer's instructions (Invitrogen).

### 4.3.4   PCR Optimisation

All PCR steps were performed in separate rooms to avoid any PCR contamination. Prior to beginning the procedure, the Class II biohazard laminar flow unit in each room was wiped down first with 100% ethanol, then 70% ethanol. The "clean-room" was used to prepare the master mix reactions that contained all reagents except for DNA. The DNA was added in the room adjacent to the master mix room, designated the sample room. The amplification reactions were performed in the designated "PCR and real-time room". All materials such as pipette tips and micro-centrifuge tubes were autoclaved and placed into the designated rooms to prevent cross-contamination. Disposable gloves and laboratory coats, which were present in every room, were worn at all times. Freeze-thawing of reagents was avoided by making small aliquots of all reagents that were to be used in the PCR assay. After the first thaw cycle, most reagents (primers, buffers) were subsequently stored at 4°C until they were completely used.

As quality controls, a negative and positive control was included. The negative control tube contained all reagents except DNA, and distilled water was added instead of the DNA to ensure that the final volume and concentration of reagents were standardised. The

negative control was used to ensure that no contamination occurred during the PCR preparation stages. The positive control tube (normal individual) contained all reagents as well as the DNA from an individual that was not affected by Duchenne / Becker muscular dystrophy. A positive control was important as it could be used to show that the PCR assay had worked the way it was intended to and that the expected bands were produced.

With respect to the PCR assay, either duplex (2-plex) polymerase chain reaction assays using two primers pairs or triplex (3-plex) PCR assays using three primer pairs were performed. Thermocyclers with 96 well heated blocks from Applied Biosystems were used, which included a 2700 and 9700. PCR kits from different companies were used during the optimisation process. The procedures were followed according to the manufacturer's instructions as outlined in the respective handbooks.

The PCR kits and reagents used for the 2-plex PCR assays were as follows:

i)      the Roche taq system

ii)     the HotStarTaq system (Qiagen)

iii)    in-house *Taq* polymerase from Molecular Diagnostics Services

The PCR kit and reagents used for the 3-plex PCR assays were as follows:

i)      Amplitaq Gold™ DNA polymerase with buffer II and Gold buffer (Applied Biosystems)

ii)     in-house *Taq* polymerase from Molecular Diagnostics Services

A primer titration was carried out using 10 pMol and 25 pMol of primer respectively for the Roche taq system and the HotStarTaq system (Qiagen). A $MgCl_2$ titration was carried

out for the Roche taq system and the HotStarTaq system (Qiagen). The final $MgCl_2$ concentration varied from 1.5 mM to 6.0 mM. The only system that did not require primer or $MgCl_2$ titrations was the in-house *Taq* polymerase from Molecular Diagnostics Services as it produced defined and usable bands suitable for proceeding to SSCP analysis. This system was used in both the duplex and triplex amplification reactions.

**Table 5: Optimised procedure showing the PCR mix used for the 2-plex assay in a 50 µl reaction volume.**

| Reagent | Volume in µl | Final concentration |
|---|---|---|
| 10 × buffer IV containing 15 mM $MgCl_2$ | 5.0 | 1 × |
| dNTPs (Pharmacia) 2.5 mM | 4.0 | 200 µM |
| Forward primer (10 pMol/µl) | 1.0 | 0.2 µM |
| Reverse primer (10 pMol/µl) | 1.0 | 0.2 µM |
| Reverse primer (10 pMol/µl) | 1.0 | 0.2 µM |
| Forward primer (10 pMol/µl) | 1.0 | 0.2 µM |
| *Taq* 2 U/µl (in-house) | 1.0 | 2 U/reaction |
| 0.22 µm filter sterilised $dH_2O$ | 31.0 | - |
| DNA (50 ng/µl) | 5.0 | 250 ng/reaction |
| **Final volume** | 50.0 | - |

**Table 6: Optimised procedure showing the PCR mix used for the 3-plex assay in a 50 µl reaction volume.**

| Reagent | Volume in µl | Final concentration |
|---|---|---|
| 10 × buffer IV containing 15 mM $MgCl_2$ | 5.0 | 1 × |
| dNTPs (Pharmacia) 2.5 mM | 6.0 | 200 µM |
| Forward primer (10 pMol/µl) | 1.5 - 3.5 | 0.3 - 0.7 µM |
| Reverse primer (10 pMol/µl) | 1.5 - 3.5 | 0.3 - 0.7 µM |
| Forward primer (10 pMol/µl) | 1.5 - 3.5 | 0.3 - 0.7 µM |
| Reverse primer (10 pMol/µl) | 1.5 - 3.5 | 0.3 - 0.7 µM |
| Forward primer (10 pMol/µl) | 1.5 - 3.5 | 0.3 - 0.7 µM |
| Reverse primer (10 pMol/µl) | 1.5 - 3.5 | 0.3 - 0.7 µM |
| *Taq* 2 U/µl (in-house) | 1.0 | 2 U/reaction |
| 0.22 µm filter sterilised $dH_2O$ | 11- 23 | - |
| DNA (50 ng/µl) | 5.0 | 250 ng/reaction |
| **Final volume** | 50.0 | - |

The primer volumes varied depending on the primer pair that was used. The volume for the

forward and reverse Pm (muscle promoter) primers was 3.5 µl, exon 16 was 3.0 µl, exon 32 was 3.0 µl, Pb was 2.0 µl, exon 9 was 2.0 µl and exon 34 was 1.5 µl.

**Table 7: Amplification conditions for the duplex and triplex PCR reactions.**

|  | Temperature (°C) | Time | Cycle number |
|---|---|---|---|
| Initial denaturation | 94 | 4 minutes | 1 |
| Denaturation | 94 | 30 seconds | 35 |
| Annealing | 53 - 65 | 30 seconds | |
| Elongation | 72 | 30 seconds | |
| Final Extension | 72 | 4 minutes | 1 |
| Hold | 15 | ∞ | |

The annealing step was performed at different temperatures depending on the average $T_m$ of each primer pair.

### 4.3.5 Visualisation of PCR products

As with the other aspects to the PCR assay, the electrophoresis was carried out in a separate room that housed the amplicons. Tubes containing the amplification products were only opened in the electrophoresis room to avoid any aerosol amplicon contamination.

Different agarose gels were used to determine which provided the best resolution for the detection of PCR amplified products. Either a Hispan (Hispanlab) 2% agarose gel or a 2% SeaKem (BioWhittaker Molecular Applications) agarose gel was made using 0.5 × TBE buffer. The intercalating dye, ethidium bromide (10 mg/ml solution) was added to the agarose gel when it had cooled down to an appropriate temperature. For each set of reactions, a molecular weight marker (Gibco BRL or Roche, Germany) was loaded into a single well to allow for accurate size determination of the amplicons. The amplicons were

then electrophoresed with constant voltage at 100 V for 5 minutes. Thereafter the voltage was reduced to 80 V for 1 hour 30 minutes to allow for proper migration of the amplicons through the gel matrix and adequate resolution of the bands. The amplicons were visualised under UV transillumination using the BioRad 2000 gel documentation system.

### 4.3.6    SSCP electrophoresis of amplicons using the NOVEX™ Thermoflow System

This part of the procedure was performed at the University of California, Irvine under the supervision of Dr. William Byerley and his research assistant.

It was essential that a clear band was seen on the 2% agarose gel prior to running it on the SSCP polyacrylamide gel apparatus. No PCR product purification was performed before electrophoresis of the samples on the polyacrylamide gel system.

The procedure followed was as per manufacturer's instructions (NOVEX). The NOVEX™ Thermoflow SSCP system was used to electrophorese the PCR amplified products. An externally attached thermostatically controlled water bath with re-circulating ability was utilised to ensure that the temperature remained constant throughout the electrophoresis period. This procedure was referred to as cold-SSCP as the temperature at which the samples were run varied from 4-10°C. Pre-cast 20% TBE gels were purchased from NOVEX. A 1.25 ×concentration TBE buffer served as the tank buffer.

### 4.3.7    Electrophoresis using the Hoefer SE600 Ruby polyacrylamide gel system

The Hoefer vertical slab gel apparatus was prepared for casting. Initially 0.75 mm spacers

were used together with a 0.75 mm comb. Owing to sample drifting, a smaller volume and hence lower sample concentration was loaded into some wells. Following this, the 1.5 mm comb and spacers were found to be more practical for the SSCP application as they provided better band separation. Also, the problem of sample drifting into the adjacent well did not occur with the 1.5 mm comb. During the preparation of the casting apparatus, all equipment was fastened securely and the appropriate comb was placed such that a space was left between the comb and the glass plates. This was done to ensure that excess gel mixture could be added during the loading process as some shrinkage occurs during polymerisation. If this is not taken into account, each well would develop a distortion that resembles a "smiling" appearance, which prevents full use of the well for sample loading.

A 5%, 10% or 15% polyacrylamide gel was made during the optimisation stage of the SSCP assay. This was done to ensure that the resulting resolution was the best that could be obtained using a conventional slab gel apparatus. Either a liquid acrylamide: bis-acrylimide solution (Sigma-Aldrich) was used or the acrylamide:bis-acrylamide solution was made using the powders for each reagent. When the liquid acrylamide solution solidified due to a possible UV exposure, powders had to be used to make up the solution. The solution was made up in a laminar flow hood with gloves, a face mask and goggles to prevent accidental exposure by inhalation as acrylamide is neurotoxic and carcinogenic.

**Table 8: Table showing the different reagents that were added to produce specific concentrations of polyacrylamide (PA) gels.**

| STOCK reagent | 5% PA gel | 10% PA gel | 15% PA gel |
|---|---|---|---|
| 10X TBE | 4 ml | 4 ml | 4 ml |
| 40% Acryli-mix | 5 ml | 10 ml | 15 ml |
| Distilled water | 31 ml (21 ml) | 26 ml (16 ml) | 21 ml (11 ml) |
| Total | 40 ml (30 ml) | 40 ml (30 ml) | 40 ml (30 ml) |

### 4.3.7.1 Preparation of the PA gel

A 37.5:1 liquid acrylamide:bis-acrylamide (40%) mixture was used in the preparation of the PA gels. The initiator, ammonium persulphate (Sigma, 25% stock solution) was added at a volume of 2 μl per 1 ml of gel mix. The ammonium persulphate was made fresh each time a gel was prepared. The TEMED (Sigma), which served as the reaction catalyst was added at a volume of 2 μl per 1 ml of gel mix. Two gels were poured when a 40 ml solution was made. A 100 ml Buchner flask was used for the preparation of the gels. For the initial de-aeration, the TBE, acryli-mix and the distilled water were added to the Buchner flask. A stirrer bar was added to flask and placed onto a magnetic stirrer to mix the reagents. A stopper was placed into / on top of the Buchner flask with rubber tubing at the open end. The de-aeration was then performed using a vacuum. Following de-aeration, the TEMED and ammonium persulphate solutions were added simultaneously to initiate the polymerisation process. Immediately after adding the solutions, de-aeration was performed briefly.

### 4.3.7.2 Loading of PA gel and buffer preparation

The mixture was placed into a 50 ml syringe housing a needle. The solution was slowly placed between the glass plates with care taken to ensure no air bubbles were formed. The comb was then gently pushed down into the acrylamide mixture and the gel was left to polymerise for half hour prior to being used. It was important that no air bubbles were trapped beneath the wells, as this would inhibit polymerisation and prevent formation of a smooth gel matrix at the bottom of the wells. For the tank buffer, 1.25 × TBE buffer was prepared from a 10 × stock solution. To sufficiently cover the upper and lower reservoirs

of the tanks, at least 5 litres of buffer was prepared. The buffer was placed into the tank and incubated at 4°C overnight, prior to being subjected to electrophoresis, which was performed at between 4°C and 10°C. A stirrer bar was placed into the buffer tank of the Hoefer electrophoresis apparatus, which was then placed onto a magnetic stirrer. This ensured even distribution of the cooled buffer throughout the electrophoresis period that spanned 5-6 hours.

### 4.3.7.3 Sample preparation

A loading dye was prepared in a 50 ml tube, comprising, 47.5 ml formamide (Applied Biosystems), 40 mg NaOH (Merck), 125 mg bromophenol blue (Sigma), 125 mg xylene cyanol (Sigma). The loading dye was prepared in a fume hood owing to the toxic nature of formamide. The resulting mixture was vortexed and subsequently aliquoted into 1 ml vials that were stored at -20°C. For each SSCP run, a single fresh vial of loading dye was used and the remaining contents discarded. A 5 µl volume of amplicons was placed into a 0.5 ml centrifuge tube, with 25 µl formamide loading dye being added. Addition of 2-6 volumes of loading dye was necessary to facilitate optimum denaturation of the double stranded PCR products and maintenance of the single stranded state by formamide, prior to loading. The 50 µl mixture was then placed into the Hybaid PCR machine that was housed in the electrophoresis room and used as a heating block, for 10 minutes at 95°C. It was wise to not use the PCR machines in the amplification room as amplicons from the PCR products would be introduced into the room and result in contamination of other pre-PCR mixtures. Following denaturation, the samples were snap chilled on ice for 2 minutes. If a 0.75 mm comb was used, no more than 10 µl could be loaded comfortably into each well. When a 1.5 mm comb was used, the wells could accommodate up to 30 µl of sample.

Volumes ranging from 20-40µl were loaded onto the PA gel using the 1.5 mm combs. The lower volumes produced bands that were less intense than the higher volumes, which were expected. For each gel that was run, a non-denatured marker was included such as Marker VI (Roche) or Marker VIII (Roche). In some cases, undenatured double-stranded (ds) DNA was included to determine where single stranded conformers were running in relation to their double-stranded counterparts.

## 4.3.7.4 Electrophoresis of samples and staining of PA gel

Following the sample loading, the gel was electrophoresed at 100 V and 25 mA for 10%, 0.75 mm thick gels. These were run for 4-5 hours. For 10%, 1.5 mm thick gels, a maximum voltage (300 V) was used for 5-6 hours at approximately 50 mA. When dismantling the gel apparatus and removing the gel from between the glass plates, care was taken with the 5%, 0.75 mm thick gels as they were more fragile than the 1.5 mm thick gels. The gel was placed into a staining solution containing 5 µl ethidium bromide (10 mg/ml) in a 100 ml volume of 1.25 × buffer solution on an orbital shaker for 45 minutes. The gel was then de-stained in distilled water using an orbital shaker for 30 minutes. The ethidium bromide staining solution produced variable results therefore SyBr Gold (Molecular Probes, 10,000 × concentration) was used as the staining compound. SyBr Gold was reported to be more sensitive than ethidium bromide for detecting both double or single stranded DNA and RNA. All precautions were taken during the handling of SyBr Gold as the carcinogenic and other toxicity properties have not been determined as outlined in the MSDS (Material safety data sheet). A 1 µl volume of SyBr Gold dye was added to 30 ml of a 1.25 × TBE buffer. An orbital shaker was used for even distribution of the dye. De-staining could be omitted when SyBr Gold was used.

### 4.3.8 Analysis of SSCP bands

The abnormally migrating bands were detected on visual inspection. Each SSCP run was inspected for differences of either an additional band or a missing band. The abnormally migrating band was then compared to the normal control sample. Any difference indicated that the conformation of that product was not the same as the normal control. In such a case, the sample was subjected to DNA sequencing analysis using the ABI 3100 genetic analyser.

### 4.3.9 Purification of PCR reactions

The PCR products that were subjected to SSCP analysis and those bands found to be abnormally migrating were purified prior to being sequenced on the ABI 3100 for mutation confirmation. The High Pure PCR product Purification Kit (Roche) was used to remove contaminating substances such as unincoporated dNTPs, primers and salts from the PCR products. The technique utilises the chaotropic salt, guanidine thiocyanate, which is present within the binding buffer. The DNA from the PCR product binds selectively to special glass fibres housed within the High Pure filter tube.

The procedure followed was as per manufacturer's instructions (Roche).

### 4.3.10 DNA Sequencing of abnormally migrating bands using the Bigdye terminator cycle sequencing reaction kit (V. 3.1)

The sequencing assay was conducted using the Applied Biosystems (AB) 9700 PCR

machine. The reactions were performed in 0.2 ml PCR tubes.

The amount of sample used was dependent on the size of the PCR products being sequenced. Typically, a 200-500 bp product required 3-10 ng of amplified product. However the resultant sequences produced from such a template concentration was not as expected, thus the amount of product added was increased to about 50 ng. Each primer used in the sequencing reaction was diluted to 3.2 pmol/$\mu$l.

**A typical sequencing reaction was as follows:**

| | |
|---|---|
| Big Dye Reaction Mix | 4.0 $\mu$l |
| 3.2 pmoles /$\mu$l primer | 1.0 $\mu$l |
| Sample 10 ng/$\mu$l | 3.0 - 5.0 $\mu$l |
| ddH$_2$O | x $\mu$l (depending on the amount of DNA added) |
| **Total** | **20.0 $\mu$l** |

**Table 9: PCR program for the cycle sequencing reaction using the BigDye terminator sequencing chemistry.**

| | Time | Temperature (°C) | No. of cycles |
|---|---|---|---|
| Denaturation | 10 seconds | 96 | |
| Annealing | 5 seconds | 50 | 25 |
| Elongation | 4 minutes | 60 | |
| Hold | ∞ | 4 | 1 |

## 4.3.11 Purification of extension products

Two methods were employed in product purification. These included the sodium acetate method of purification and the Centri-sep column purification.

## 4.3.11.1    Sodium acetate purification method

The procedure followed was as per manufacturer's instructions (Big Dye Termination kit,

Applied Biosystems).

## 4.3.11.2   Centri-sep column purification

There were three parts to this procedure. The first involved column hydration, which was followed by removal of interstitial fluid and finally the sample processing step. The centri-sep columns were obtained from Applied Biosystems.

The procedure followed was as per manufacturer's instructions (Applied Biosystems).

## 4.3.12 Electrophoresis of samples on the ABI 3100

Prior to electrophoresis on the ABI 3100 of those samples that showed a visual band shift on slab gel electrophoresis, the genetic analyser had to be prepared. The POP-6 polymer, which is housed at 4°C, was left out at room temperature for 1 hour before it was inserted into the syringes on the instrument. The one hour incubation at room temperature was necessary to allow the crystals that form in the polymer matrix at low temperatures to dissolve before the polymer was injected into the instrument. A 36 cm capillary array or a 50 cm capillary array was placed onto the instrument. For shorter read lengths of <200 bp, the 36 cm capillary was used and for expected product lengths of >200 bp, the 50 cm capillary array was used. Initially a spacial and spectral calibration was performed on the ABI 3100, in preparation for the electrophoresis. The spacial calibration uses a water signal to ensure that the position of maximum fluorescence is mapped for each capillary. A spectral calibration had to be performed for dye set Z, which is used for sequencing. A "Q" or quality value of 0.95 or greater had to be obtained. The DNA sequencing was performed

using "Data collection V2.0". The preset module for DNA sequencing was chosen for the run.

After the sequencing run was completed, the raw data file was viewed to determine that the run had taken place as expected. The average signal of the raw data should be between 1000 and 2000 RFU. An analysis was automatically performed by the DNA sequencing software.

### 4.3.13  DNA sequencing analysis using the Bioinformatics software

A consensus sequence for the dystrophin gene was downloaded from NCBI (National Center for Biotechnology Information). A BLAST (basic local alignment search tool) search was performed to find consensus sequences for individual exons in the dystrophin gene. These fragments included the specified exon as well as the flanking intronic sequences. A new consensus sequence was made available for the dystrophin gene in 2003, namely NM 004006.1. This replaced the previous consensus sequence, M18533.

The author performed DNA sequencing data analyses using the Biotools software comprising Bioedit (Hall, 1999), Clustal X (Thompson *et al.*, 1997) and GeneDoc software programs (Nicholas & Nicholas, 1997). The electropherograms were viewed using FinchTV V 1.4.0 (Geospiza Inc, 2006 www.geospiza.com).

The Leiden muscular dystrophy website was used to obtain other relevant Genbank accession numbers for exons in the dystrophin gene. The mutation database housing all mutations found in the dystrophin gene was also consulted (http://www.dmd.nl).

## 4.4 RESULTS

Positive control samples were included in the study. These were normal control DNA from individuals such as staff members and nurses from Inkosi Albert Luthuli Central Hospital who showed no signs of muscular dystrophy. A negative control was a sample that contained all the reagents except for DNA. This was included to ensure that no PCR contamination occurred, which would confound the results.

### 4.4.1 PCR gels

The following image shows an example of a 2-plex PCR result.
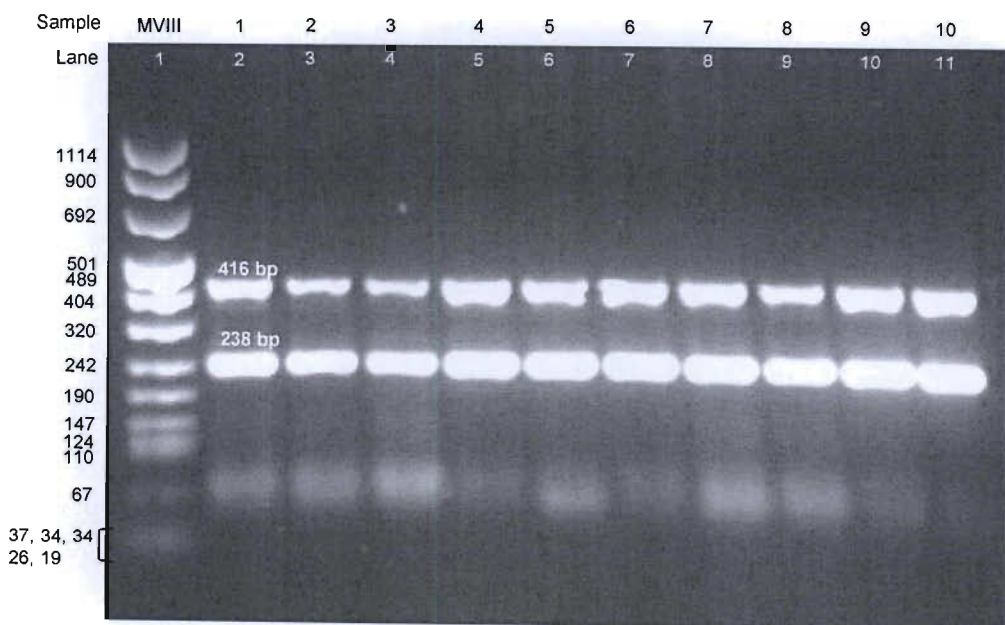


**Figure 33:** A representative image showing the PCR amplified products obtained when primer pairs for exons 13 and 17 were used in the same reaction. Molecular weight marker VIII from Roche was used to confirm the band sizes.

The following image shows an example of a 3-plex PCR result.
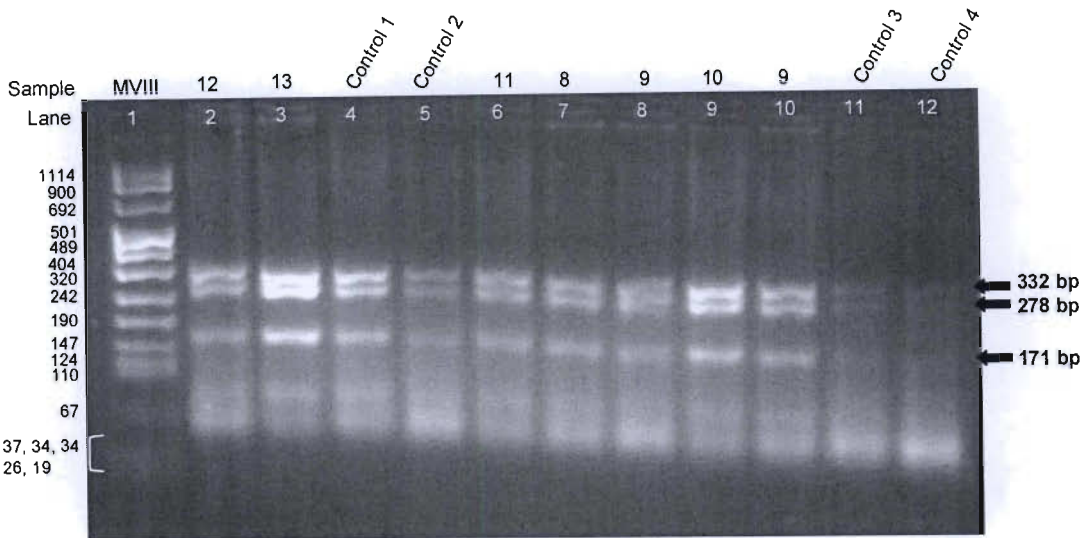
**Figure 34:** A representative image showing the PCR amplified products obtained when primer pairs for exons Pb, 9 and 34 were included in the same reaction. Molecular weight marker VIII from Roche was used to confirm the band sizes.

## 4.4.2 SSCP gels

The 5% polyacrylamide gel did not produce any bands. The gel was very thin and broke while being transferred to the de-staining solution. The 10% gel was found to produce the most usable data as the band resolution was best at this concentration for most exons. For some exons, a 10% gel did not produce bands that were well defined. In such an instance, a 15% polyacrylamide gel was used. A 20% gel was not made as this would have increased the length of electrophoresis significantly. The gels were electrophoresed at between 300-400 V, using 50-110 mA of current.

A molecular weight marker was included in most of the gels to confirm the sizes of the homoduplex or double stranded products. It was not heated as this would have resulted in denaturation. The single stranded products that were produced from denaturation were not size dependent as their migration reflects the conformation of the products and not the size. All the following controls were included if sufficient product was available:

i)      Denatured positive normal control which was compared to the patients' sample. It was denatured so that all parameters remained the same between sample and control.

ii)     Undenatured positive normal control to compare the denatured to an undenatured sample state.

iii)    Negative control containing no DNA to reveal any PCR contamination.

## 4.4.2.1 Optimisation of gel concentration
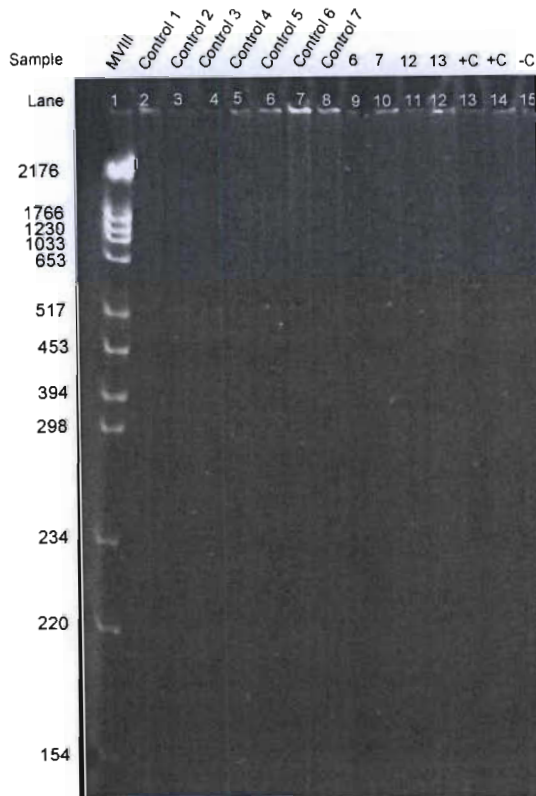


**Figure 35: An image showing the poorly defined bands and therefore unusable data produced on running a 10% gel at 4°C. These PCR products resulted from amplification of primer pairs for exons 45 and 47. Molecular weight marker VI from Roche was included in lane 1. Ethidium bromide was used as the agent of detection.**
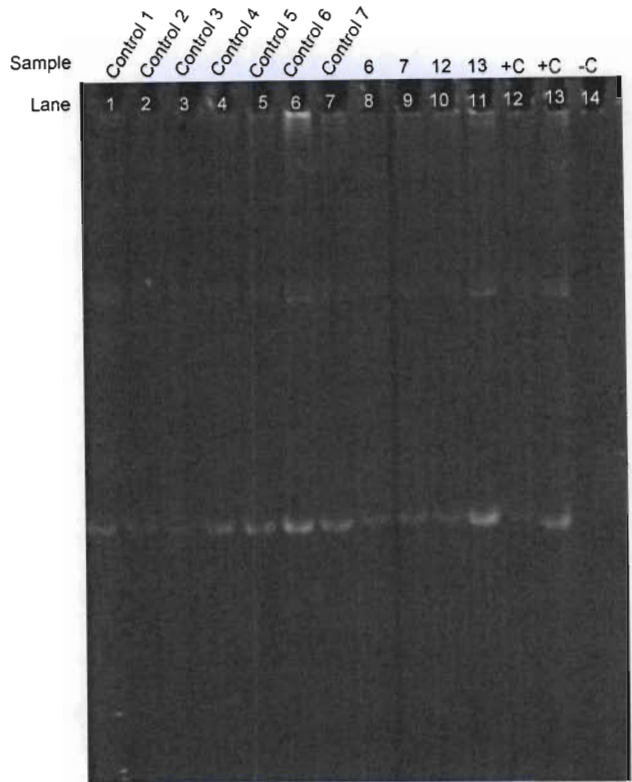
**Figure 36: Image showing a 15% polyacrylamide gel that was run using the same samples from figure 35 above. These were amplified products from primer pairs of exons 45 and 47, which were electrophoresed at 4°C. Ethidium bromide was used as the detection reagent.**

The bands were slightly better resolved using the 15% gel but not ideal. Even though low temperatures provided better band resolution, this was not always the case. The temperature at which the best resolution would be obtained depended very much on the primer composition and the amplified products that were generated. Using one specific temperature for the electrophoresis of all amplified products would not be possible (Larsen *et al.*, 1999a).

### 4.4.2.2 Band definition using different detection reagents and a comparison between the numbers of primer pairs used

The image below clearly indicates the benefit of using two primer pairs when performing
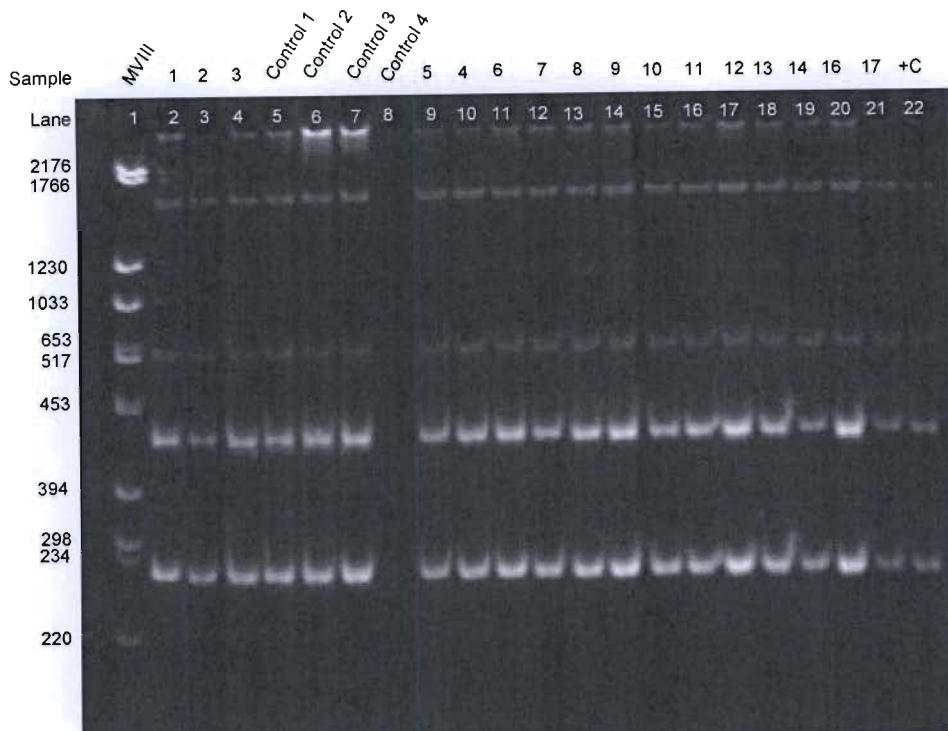
**Figure 37:** **A representative image illustrating the good band definition obtained when amplified products generated using two primer pairs for exons 6 and 8, were electrophoresed at 10°C on a 10% polyacrylamide gel.**

SSCP analysis. Even though it would take a lot longer to generate the PCR products to be subjected to point mutation analysis, the resolution obtained is of good quality. This allows the analyst to interpret the data correctly. Exons 6 and 8 appeared to produce the most well-defined bands at 10°C. When the same samples were electrophoresed at a lower temperature, 4°C, the bands were "fuzzy" and not sharp enough for accurate interpretation.

Ethidium bromide was used as the detection reagent in the above images (Figures 35, 36 and 37). It is evident that ethidium bromide is not a consistent agent of detection, since it produced poor bands in figures 35 and 36 however the band definition was of usable quality in figure 37.

The figure below shows the lack of definition produced when more than two amplified products were electrophoresed on a polyacrylamide gel. This made interpretation of the

data more difficult. These results were in keeping with a paper authored by (Larsen *et al.*, 1999a), where the recommendation was to use a single pair of primers per run. The use of SyBr Gold as a detection reagent is also more sensitive than ethidium bromide. The bands in the figure (amplicons from exons Pm, 16, 32) are more pronounced and brighter than in the previous figures 35, 36 and 37.
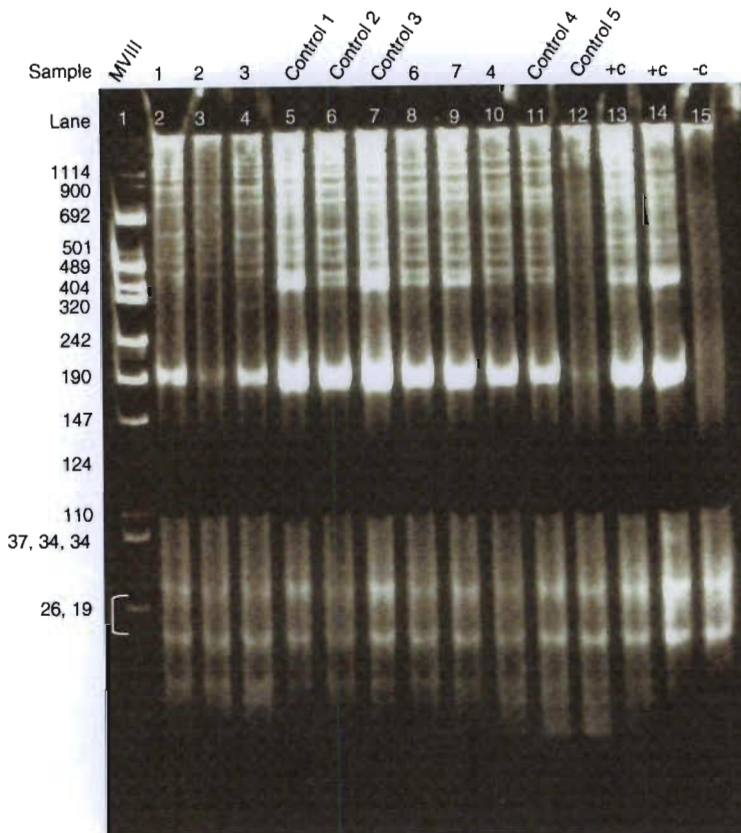


**Figure 38:** **Representation of the single stranded conformers that were produced when a 10% polyacrylamide gel was run with SyBr gold used as the detection agent. The amplified products were derived from the use of primer pairs Pm, 16 and 32. Marker VIII (Roche) was included in lane 1.**

### 4.4.2.3 Abnormally migrating bands

In figure 41, sample 3 shows an abnormally migrating band that is suggestive of a mutation. Ethidium bromide was used as the detection agent. Surprisingly sample 3, which is the mother's DNA sample of a DMD affected child, shows the mutant band only. The

mutant band does not appear to be present in the child's sample (sample 2).

Figure 42 shows an additional band as shown by the green arrows. Sample 2 belongs to a DMD affected patient that was previously shown to have no deletions on multiplex PCR. Sample 3 belongs to the mother of the DMD affected child. Ethidium bromide was used as the reagent for band detection.
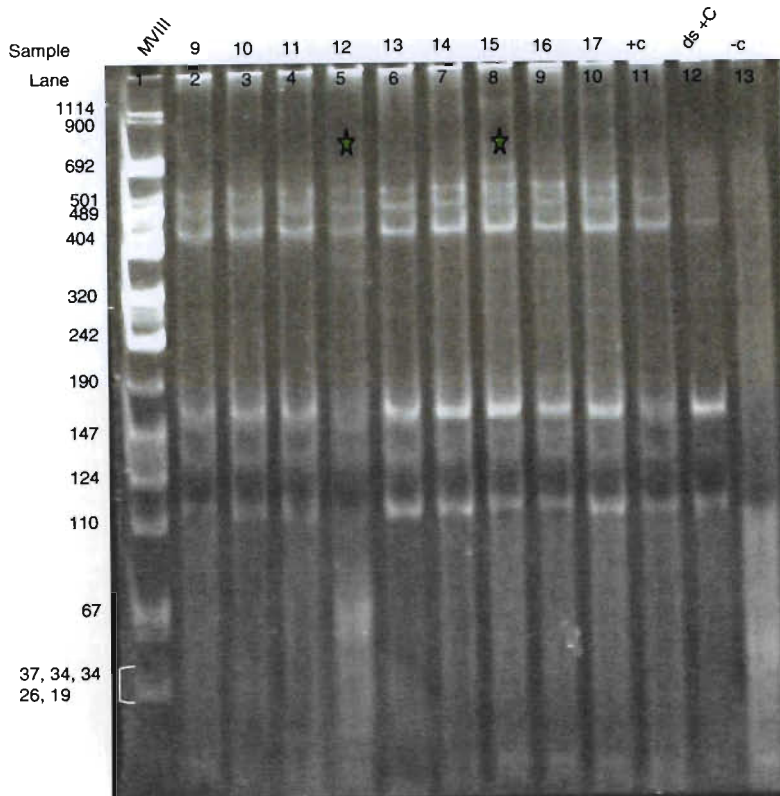


Figure 39: Image representing single stranded conformers resulting from denaturation of PCR amplified products derived from the use of primer pairs for exons 52 and 53. The gel was electrophoresed using a 10% gel at 10°C. SyBr Gold was used for detection. Abnormally migrating bands are indicated by the stars in lanes 5 and 8.
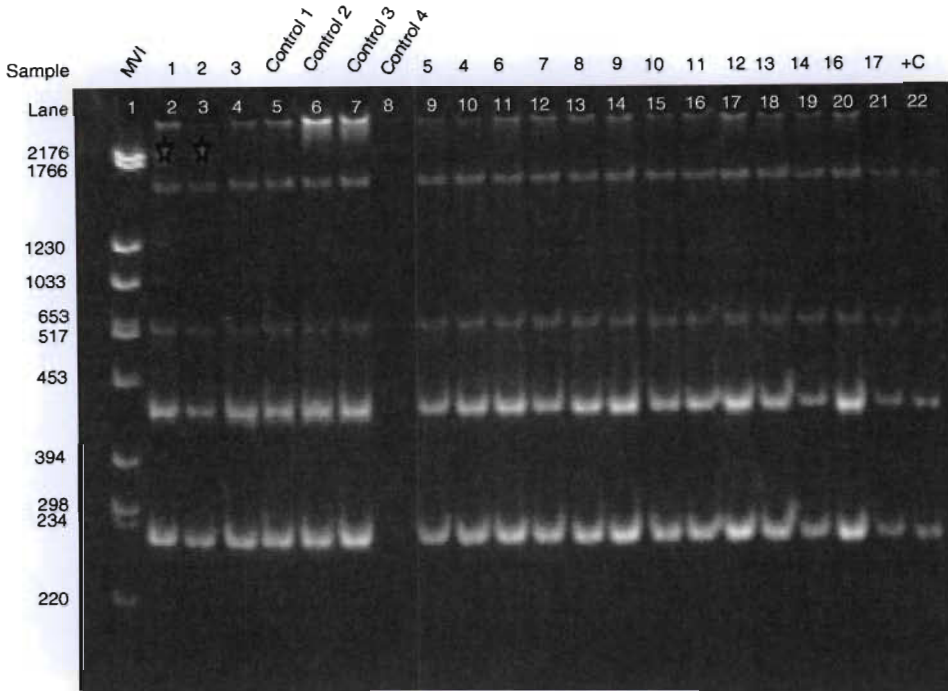
Figure 40: Image showing abnormally migrating conformers obtained when SSCP was performed on PCR products generated from primers pairs for exons 6 and 8. The samples were electrophoresed at 10°C using a 10% polyacrylamide gel. Abnormally migrating bands are indicated by the stars in lanes 2 and 3.
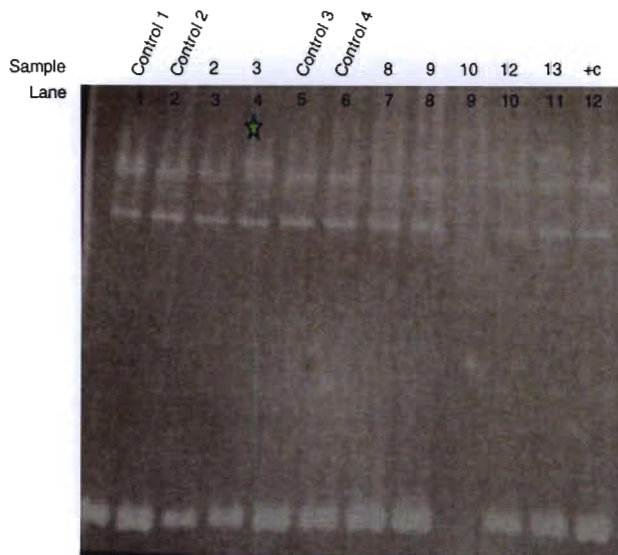


Figure 41: Image showing an abnormally migrating band (green star) when the PCR products were generated with primers for exon 53 which were electrophoresed at 4°C on a 20% Novex precast polyacrylamide gel. Abnormally migrating band are shown by the star in lane 3.
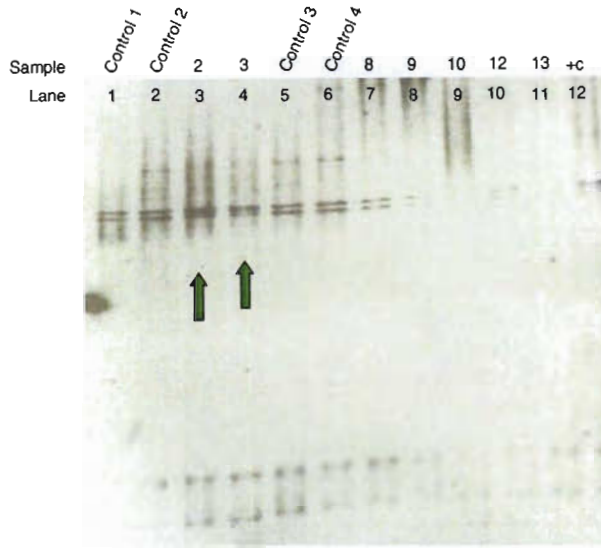
**Figure 42:** Image showing the presence of an additional band in samples 2 and 3, which would be suggestive of a mutation. The PCR products were generated by using primers for exon 60 and electrophoresis was carried out at 4°C with a 20% precast Novex gel.

**Table 10: Table showing those samples from subjects that were abnormally migrating on visual inspection following gel electrophoresis.**

| DNA number | Mutation / on visual inspection only | Dystrophinopathy /relative | Actual location of mutation after DNA sequencing |
|---|---|---|---|
| 1 | Exon 6 and / or 8 | Aunt of 2 | E6 |
| 2 | Exon 6 and / or 8 | DMD | E6 |
| 3 | Exon 6 and / or 8 | Mother of 2 | E6 |
| 1 | Exon 52/53 | Aunt of 2 | E52 |
| 2 | Exon 52/53 | DMD | E52 |
| 3 | Exon 53 | Mother of 2 | No mutation found |
| 12 | Exon 52, 53 | DMD | No mutation found |
| 15 | Exon 52, 53 | Mother of 14 | No mutation found |
| 6 | Exon 53 | Mother of 7 | No mutation found |
| 8 | Exon 53 | DMD | No mutation found |
| 9 | Exon 52 | DMD | E52 |
| 10 | Exon 52 | Mother of 8 and 9 | E52 |
| 11 | Exon 52 | Sister of 8 and 9 | E52 |
| 10 | Exon 20, 22 | Mother of 8 and 9 | No mutation found |
| 13 | Exon 20, 22 | Mother of 12 | No mutation found |
| 16 | Exon 20, 22 | DMD | No mutation found |
| 16 | Pb, 34, 9 | DMD | No mutation found |
| 17 | Pb, 34, 9 | Mother of 16 | No mutation found |
| 14 | Pm, 16, 32 | DMD | No mutation found |

| 2 | Exon 60 | DMD | No mutation found |
|---|---------|-----|-------------------|
| 3 | Exon 60 | Mother | No mutation found |
| 65 | Exon 41, 42 | Sister of 66 | X |
| 66 | Exon 41, 42 | DMD | X |
| 67 | Exon 41, 42 | Mother of 66 | X |

**Legend: X denotes unusable sequencing data, E denotes exon.**

## 4.4.3 DNA sequencing and analysis

Seventeen subjects showed abnormally migrating bands on visual inspection. These samples were then subjected to DNA sequence analysis. DNA sequencing was performed for exons 6, 8, 52, 53, 60, 41, 42 and flanking sequences. Of these exons tested, only exons 6 and 52 showed SNPs or point mutations. In exon 6 and flanking sequence of exon 5, three SNPs were found and in exon 52, two insertion mutations were found.

DNA sequencing was not performed for exons 20, 22, Pb, 34, 9, Pm, 16 and 32 on subjects 10, 13, 16, 17 and 14 because DNA was not available.

### 4.4.3.1 Exon 6 and flanking regions
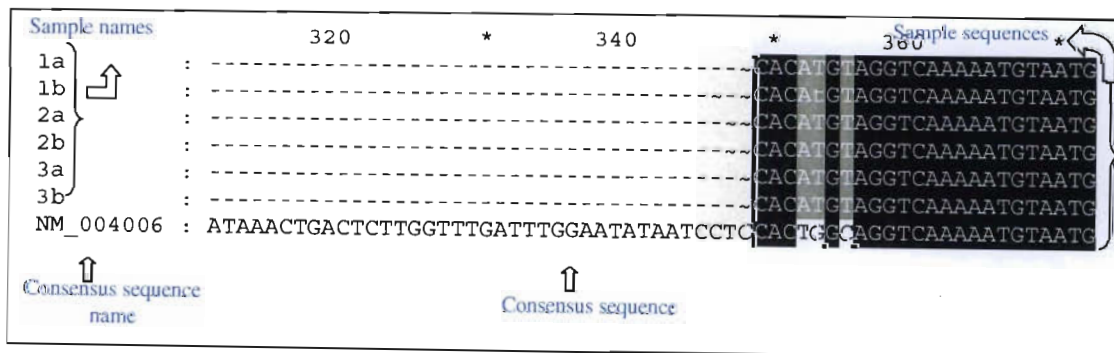


**Figure 43 : Alignment showing sequences in exon 6 and the flanking region in exon 5. A comparison is made to the cDNA consensus sequence of the dystrophin gene. Description of samples and consensus sequence is outlined.**
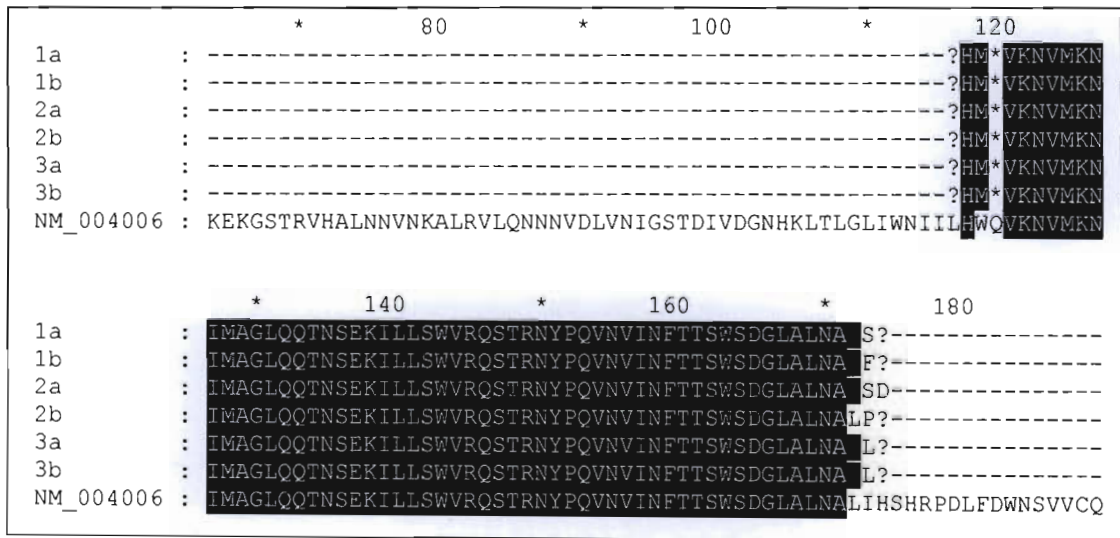
**Figure 44: Alignment showing the amino acid sequences of samples weighted against the consensus _c_DNA sequence of dystrophin.**

The samples 1, 2 and 3 for exon 6 were all subjected to DNA sequencing in duplicate for confirmation purposes hence the numbering 1a, 1b, 2a, 2b, 3a, 3b.

The SNP or mutation descriptions given below are taken from the official HGVS nomenclature (http://www.hgvs.org/mutnomen/recs-DNA.html, den Dunnen & Antonarakis, 2000). It is evident from the aligned sequences above that there are single nucleotide polymorphisms at position NM_004006.1: c.352T>A, c.353G>T and c.355C>T. The SNP at positions 352 and 353 are not listed on the Leiden pages. The c.355C>T SNP is listed on the Leiden website, where all known mutations are posted from throughout the world. This SNP has been previously reported three times with all patients being from the USA. The numbers on the _c_DNA consensus sequence correspond to exon 5.

In the case of the first SNP, NM_004006.1: c.352T>A with TGG being the amino acid and the second SNP, c.353G>T with ATG being the amino acid, they may be population specific changes. All the individuals were South African Black patients.

105

TGG on the consensus sequence codes for W or tryptophan whereas in the sample it codes for a methionine residue (NM_004006.1: c.352T>A). With respect to the third SNP, CAG on the consensus sequence encodes a Q or glutamine residue, whereas in the samples it codes for a stop sequence TAG denoted by X (NM_004006.1: c.355C>T). This is a pathogenic mutation that was also listed on the Leiden pages.

From these results, the carrier status in the mother of the DMD patient and his female relative could be determined. It was evident that the mother and female relative of the DMD patient showed the same nucleotide changes / mutations.

**4.4.3.2 Exon 52**
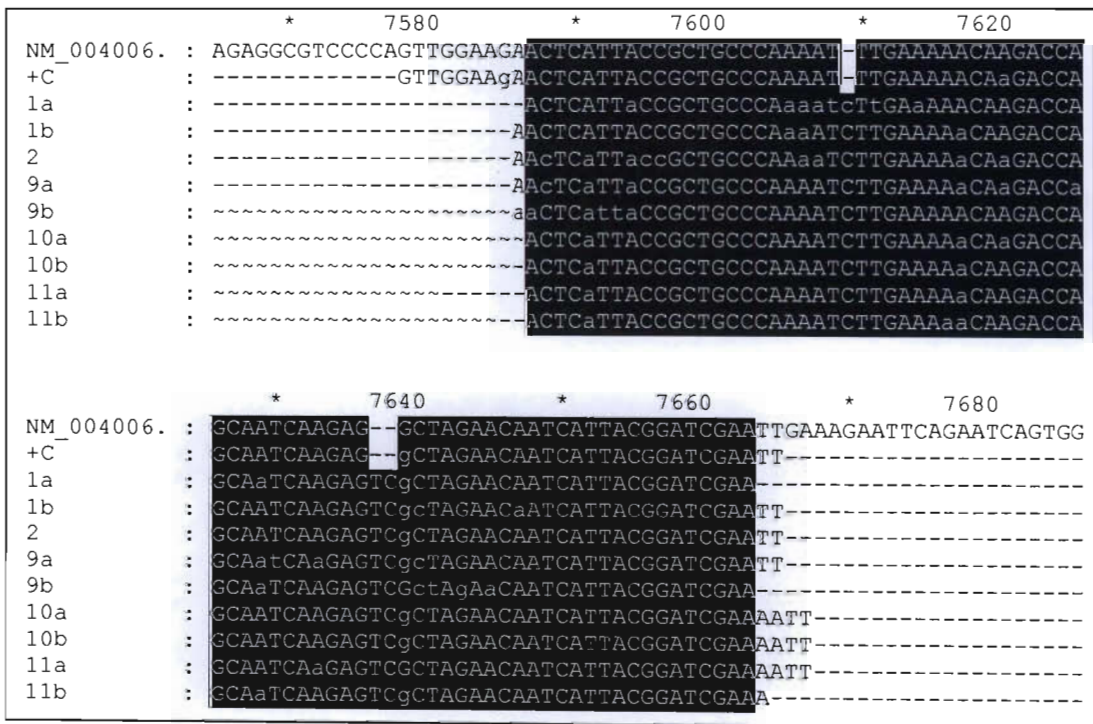


**Figure 45: Alignment of samples and positive control of exon 52 weighted against the cDNA consensus sequence of dystrophin.**

The samples were subjected to DNA sequencing in duplicate for confirmation purposes as is shown by "a" and "b" for exon 52 as was the case with exon 6. There was not enough

samples left from patient 2 therefore the DNA sequencing was only performed once in each direction ie. forward and reverse.

The figure shows two insertions found in the patients (2 and 9), a mother (10) and female relatives (1, 11). None of the insertions have been previously documented. The first occurred at NM_004006.1: c.7609insC and the second occurred at position NM_004006.1: c.7637_7638insTC. The first single base insertion brings about a lysine (K) to glutamic acid (E) change at amino acid position 2538. Owing to these insertions, the entire reading frame also changed.
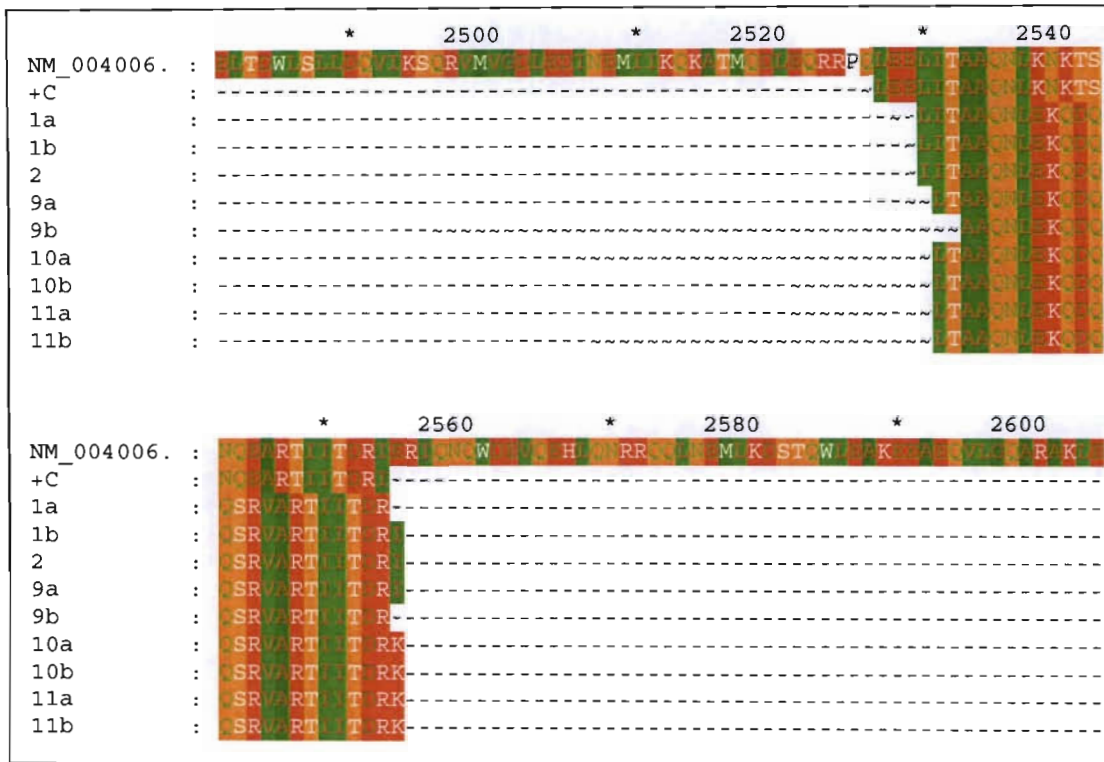


**Figure 46: Amino acid alignment of dystrophin *c*DNA consensus sequence and samples included in the study spanning exon 52.**

**Table 11: Outline of the mutations / SNPs that were found in the patients, their mothers and female relatives following DNA sequencing analysis.**

| DNA number | Surname, Initials | Actual mutation /SNP | Nucleotide change at the DNA level | Amino acid change |
|------------|-------------------|----------------------|------------------------------------|-------------------|
| 1 | S, R | c.352 T>A | TGG to ATG | |

| | | | | tryptophan to methionine |
|---|---|---|---|---|
| | | c.353 G>T | TGG to ATG | tryptophan to methionine |
| | | c.355 C>T | CAG to TAG | glutamine to stop codon |
| | | c.7609insC | Insertion C | lysine to glutamic acid |
| | | c.7637_7638 insTC | Insertion TC | changes the entire reading frame – no stop codons |
| 2 | S, W | c.352 T>A | TGG to ATG | tryptophan to methionine |
| | | c.353 G>T | TGG to ATG | tryptophan to methionine |
| | | c.355 C>T | CAG to TAG | glutamine to stop codon |
| | | c.7609insC | Insertion C | lysine to glutamic acid |
| | | c.7637_7638 insTC | Insertion TC | changes the entire reading frame – no stop codons |
| 3 | S, DK | c.352 T>A | TGG to ATG | tryptophan to methionine |
| | | c.353 G>T | TGG to ATG | tryptophan to methionine |
| | | c.355 C>T | CAG to TAG | glutamine to stop codon |
| 9 | S, NM | c.7609insC | Insertion C | lysine to glutamic acid |
| | | c.7637_7638 insTC | Insertion TC | changes the entire reading frame – no stop codons |
| 10 | S, S | c.7609insC | Insertion C | lysine to glutamic acid |
| | | c.7637_7638 insTC | Insertion TC | changes the entire reading frame – no stop codons |
| 11 | S, B | c.7609insC | Insertion C | lysine to glutamic acid |
| | | c.7637_7638 insTC | Insertion TC | changes the entire reading frame – no stop codons |

## 4.5 DISCUSSION

The use of SSCP as a method for detecting point mutations has been used by several groups. Even though it is time-consuming and laborious it is easy to set up in an

environment where infrastructure is limited. It was therefore an ideal technique to use in our laboratory. We already had the primers for the dystrophin gene and the equipment needed for electrophoresis and detection of the bands. Since dystrophin is such a large gene, encompassing 79 exons, literature consensus showed that the SSCP analysis was most efficient for products <300 bp. There were other reports (Michaud *et al.*,1992; Kneppers *et al.*, 1995) showing that SSCP produced good results for products greater than 300 bp and these reports motivated the undertaking of this study.

The study cohort was designed such that the dystrophinopathy patient and his mother and / or female relative were included to determine whether a carrier status assessment could be made by comparing results of the patient and his mother and / or female relative. It is unfortunate that the data did not yield positive carrier status results.

## 4.5.1 PCR optimisation

Several optimisation reactions were performed to obtain the best amplification products. This was essential as it would allow bands to be more easily visualised once they were electrophoresed on the PA gel. If bands were faint on PCR, then the resulting band after SSCP were even fainter thus preventing definitive conclusions to be made. One might assume that the band was absent however it may just have been very faint owing to the amplification reaction. A volume of 6 µl – 8 µl dNTP mix was tried for the 3-plex PCR assays and it was found that 6 µl was optimal for the reaction and the number of primers that were included. It was important to run the products on a conventional agarose gel to ensure that no ambiguous results were obtained once the SSCP gel was run (Hongyo *et al.*, 1993).

### 4.5.2 Two-plex and three-plex PCR

Prior to performing the PCR assays, a literature search was performed on the type of PCR assay that should be designed. There was much discrepancy between the papers with respect to developing a multiplex SSCP method. According to Kneppers *et al.*, (1995), the use of a multiplex SSCP was quite efficient. Larsen *et al.* (1999a), however suggested that a single SSCP reaction be performed encompassing a single exon because false-negatives would be common. This was due to the increasing number of single stranded conformers that would be produced as the number of amplified products increased (Larsen *et al.*, 1999a). Since a consensus in the literature could not be established, the author decided to try two and a three-plex PCR assays. Both assays produced well defined bands on PCR. However, when these amplified products were run on an SSCP gel the two-plex PCR produced conformers that could be distinguished from one another and the data was therefore easier to interpret than the three-plex SSCP bands.

### 4.5.3  "Cold" PCR-SSCP

The "Cold" PCR-SSCP method was chosen as it produced the most usable and well defined bands. When the author had first run precast 20% polyacrylamide gels on the ThermoFlow™ SSCP system at the University of California, Irvine (UCI) two temperatures were used to electrophorese the samples. The samples that were run at room temperature produced bands of very poor quality and most of the bands were not visible on UV trans-illumination. However, when the samples were run at 4°C, the bands were well defined and the data was interpretable, therefore all precast gels were run at this temperature. The data produced on using the precast gels were easily interpretable

therefore no other optimisation was required for those amplified products. However only a single pair of primers was electrophoresed during each run, since the author's time at the laboratory in Irvine was limited.

Literature consensus revealed that the "Cold"-SSCP method was quicker and more reproducible than the radioactive SSCP mobility shift assay, therefore it turned out to be the obvious choice. In addition to this, the molecular scientist did not have a radioactive facility at her disposal therefore the "Cold" PCR-SSCP was chosen. There were a few parameters that needed to be optimised before the technique was reproducible. These included using the optimal voltage, the correct pump or circulating device to maintain the temperature, TBE buffer concentrations, gel concentrations, the use of denaturants and the use of appropriate loading buffers (Hongyo *et al.*, 1993)

The author set-up the SSCP assay at the Neuroscience laboratory using conventional slab gel apparatus, with a cold water bath attached to the Hoefer SE600 polyacrylamide gel apparatus. The author had to improvise and use equipment that was available since the ThermoFlow™ SSCP apparatus and the Novex precast gel system that was utilised at UCI was not available at the Neuroscience laboratory. The equipment was also not obtainable from another laboratory at the Nelson R. Mandela School of Medicine, Durban, South Africa.

Samples were initially electrophoresed at room temperature and at 4°C to determine whether the same effect was achieved in that environment, compared to the University of California, Irvine. Once again the sample bands were poorly visible at room temperature and un-interpretable. Interestingly, the temperature at which best resolution was achieved

for most of the amplified products using conventional slab gels was 10°C as opposed to 4°C using the precast 20% gels. At 4°C some of the amplified products were "fuzzy" in appearance and the abnormally migrating conformers could not easily be distinguished from the normal conformers using the slab gels.

For slab gels, it was difficult to maintain the required temperature as there were factors that influenced the change in temperature. These included the temperature of the room at the time of running the samples and the ability of the thermostatically controlled re-circulating water bath to maintain the temperature precisely and at a constant temperature (Hongyo *et al.*, 1993). Owing to such factors, the room in which the electrophoresis was performed was maintained at a constant temperature of 16°C using an externally controlled electronic air-conditioning unit. The TBE buffer was incubated for a few hours at 4°C to maintain the low gel temperature that was required. A stirrer bar was inserted into the gel tank to ensure that cold buffer circulated throughout the buffer chamber.

Blurring of bands during some runs was also evident using the slab gel apparatus. This might have been due to temperature increases during the electrophoresis, which could be attributed to the increase in temperature from the power pack. According to Hongyo *et al.* (1993), the temperature during the electrophoresis would have to be adjusted if there was a single band or more than two bands being produced in the control sample for a single set of primers. It was important for the temperature as well as the ionic conditions to be constant as the DNA fragments move through the gel. According to Hongyo *et al.* (1993), as the denatured DNA is placed into a non-denaturing environment such as the gel, a conformation is reached and for this conformation to be maintained the temperature and ionic concentrations must remain constant throughout the electrophoresis. If there are

fluctuations in the thermal conditions, the shape of the band and the rate of band migration changes. Once this occurs, the sharpness and reproducibility of the band from a particular strand would be inconsistent. (Hongyo *et al.*, 1993). This might have resulted in "fuzzy" and blurred bands.

For slab gels, different gel concentrations were used to determine the optimum concentration at which the abnormally migrating conformers were most apparent. A 10% gel concentration was found to be optimum for most amplified products. When a 15% gel was made, the products were electrophoresed for approximately 8 hours; however a good separation was not achieved. This suggested that the length of time be increased to 9-10 hours for future runs using a 15% gel. A 20% polyacrylamide gel could not be used as it would have taken >12 hours to run a single gel. Using a 10% polyacrylamide gel the samples were run for approximately 5-6 hours to obtain optimum migration.

### 4.5.4 Reagents for maintaining the single stranded state of denatured DNA

Formamide was chosen since it has been proven to be efficient in maintaining denatured strands in a single stranded state. It is commonly used during DNA sequencing and fragment analysis procedures.

Another agent of denaturation, methyl-mercury hydroxide was also researched to determine whether it would better than using formamide. According to Weghorst and Buzard (1993), methyl-mercury hydroxide increased single stranded conformation detection. However, the MSDS for methyl-mercury hydroxide showed it to be highly carcinogenic and has many proven systemic effects. It also has been shown to have many

environmental effects. Owing to the severe effects of methyl-mercury hydroxide,

formamide was chosen as the reagent for maintaining the strands in a single stranded state.

### 4.5.5   Methods of detection

Two different reagents were used to detect the bands. For the samples electrophoresed at

UCI using the precast gels, ethidium bromide was the method of detection. Initially

ethidium bromide was used as the method of detection for the slab gels at the Neuroscience

laboratory as this was the only reagent available. There was evidence of high background

staining in a few gels stained with ethidium bromide. The recommendation was to de-stain

longer and use less ethidium bromide which was thereafter done. The background

decreased but so too did the resolution of the bands.

SyBr Gold was utilised for the remaining amplified products that were subjected to SSCP

analysis. According to the Molecular probes product insert sheet, SyBr Gold was found to

be more sensitive than SyBr Green II at staining single stranded DNA and detecting single

stranded conformers in SSCP derived products. In practice, SyBr Gold was so sensitive

that even at a 1:5,000 dilution the bands were significantly brighter than ethidium bromide.

Owing to the brightness of the resulting bands different concentrations of SyBr Gold,

ranging from 1:10,000 to 1:50,000 had to be tested. The optimum concentration was found

to be 1:30,000.

### 4.5.6   DNA sequencing and use of centri-sep columns

The centri-sep columns purification method resulted in better sequence data than the

conventional sodium acetate method. It was recommended that the sample not be heated at the end of procedure however the author tried the heating step as there was no vacuum centrifuge at the Neuroscience facility. The heating step did not prove to be a problem, and the resulting data was of good quality. It is therefore recommended that the heating step be included for those labs that lack a vacuum centrifuge.

### 4.5.7 Point mutation detection

DNA sequencing could not be performed on the DNA of all patients that showed abnormal band migration. There was no DNA available from these patients and since the patients were from rural areas they could not be reached for additional blood samples.

### 4.5.7.1 Exon 6 and flanking regions of exon 5

Three SNPs were found when exon 6 and flanking regions of exon 5 were analysed. The SNP located at NM_004006.1: c.355 C>T has been previously documented. The other two SNPs namely NM_004006.1: c.352 T>A, NM_004006.1: c.353 G>T have not been documented previously. It is likely that these SNPs are population specific. The carrier status of the mother and female relatives could be determined as they all shared the same polymorphisms / point mutations.

### 4.5.7.2 Exon 52

Two insertion mutations were found in exon 52 of two patients, a mother and two female relatives. They appear to be unique as they have not previously been reported. The

insertions changed the reading frame without introducing a stop codon.

### 4.5.7.3 Exon 41 and 42

The samples that appeared to have abnormally migrating bands in exons 41 and / or 42 were subjected to DNA sequencing to confirm the visual result. The DNA sequencing data produced was unusable. This may be attributed to the age of the samples as they were from 1996.

### 4.5.8 Usefulness of the technique

With respect to the aims that were initially proposed, the following statements provide insight into the usefulness of the SSCP analysis technique as a mutation detection tool. When the efficacy and reproducibility of the technique was evaluated by looking at the results obtained, it was concluded that SSCP should not be used as the primary method to detect point mutations. This is true as the abnormally migrating bands are not always easily detectable on visual inspection.

On assessment of the conventional slab gel SSCP analysis technique, the "cold" PCR SSCP method appeared to produce the best results when room temperature results were compared to results obtained at 4-10°C. The best temperature was 10°C for the majority of the PCR products being tested. The best method of detection was SyBr Gold compared to ethidium bromide as a very small amount (1:30,000) was sufficient to produce the desired band intensity. Where ethidium bromide is highly carcinogenic, SyBr Gold has not been fully assessed however its danger level is on a significantly lower scale.

The Novex precast gels and ThermoFlow™ SSCP system has several advantages over conventional slab gels. Firstly, the gel concentration would be consistent and reliable as a precast, commercially produced gel was being used and it would not be subject to the technical errors that could occur when a gel was being poured in the conventional way. Secondly, the thermal conditions set on the water-bath would be unchanging and consistent as a specifically designed water bath for SSCP was being used as opposed to an externally attached water-bath used with slab gels. It is also subject to temperature fluctuations.

Thirdly, the electrophoresis could be performed in 2-3 hours, thus ensuring the least amount of temperature fluctuations and quicker data generation. From the author's experience, the precast gels produced better band resolution and product separation than the slab gels. However in our resource limited setting this was not a feasible option as the equipment to run precast gels was not available.

# SECTION B:

# ASSESSING THE USEFULNESS OF REVERSE-TRANSCRIPTION PCR USING RNA FROM MUSCLE TISSUE

## 4.6    INTRODUCTION

Reverse-transcription PCR is a method where cDNA is synthesised using random hexamer primers or sequence specific primers to analyse a gene at the RNA level. Following cDNA production, the resulting fragment is amplified using conventional PCR or nested PCR. Nested PCR is an attractive way to improve sensitivity and specificity of a fragment that would otherwise not produce a definitive amplification product using a single PCR reaction.

Total RNA or Poly(A)$^+$ selected messenger RNA may serve as the RNA template for RT-PCR. The RNA can be extracted from tissue samples, blood samples or peripheral blood lymphocytes. The quantity and integrity of the RNA species are usually the key determinants in generating good quality RT-PCR products that are well resolved on gel electrophoresis. RNA degradation is one of the factors that reduce the probability of obtaining the highest "sequence information that can be converted into cDNA" (Invitrogen RT-PCR manual, http://www.invitrogen.com/content.cfm?pageid=4082).

RT-PCR can be performed using a one-step or two-step system of amplification. The conventional method of cDNA production follows the two-step format where all reactions are performed under optimal conditions. During the first step of the RT-PCR assay, a "first strand reaction" is performed where cDNA is manufactured from a RNA template within

RT-buffer. This reaction takes place in the presence of a reverse-transcriptase enzyme. The "second strand reaction" involves the amplification of the product from the "first-strand reaction" using PCR. The two-step system is the method of choice when difficult templates with little starting amount of RNA are being reverse transcribed and amplified.

In the one-step RT-PCR format both reverse-transcription and the PCR take place in a single tube. These reactions are performed under conditions that have been optimised for both RT and PCR assays thus making it quicker than its two-step counterpart especially in cases where large samples numbers are being processed. The one-step method also offers the advantage of no carry-over contamination as the tubes are not opened between reactions.

Good quality cDNA results when several criteria are met. These include the use of robust enzymes, appropriate buffers and additives when required and the establishment of suitable cycling parameters. Another important factor is the use of high quality templates lacking inhibitors that may interfere with downstream applications of the cDNA and that have been synthesised using efficient kits or reagents. Additives such as DMSO or glycerol can be added to the first-strand reaction to "destabilise nucleic acid duplexes and melt RNA secondary structure: (Invitrogen RT-PCR manual). Care should be taken to ensure that the appropriate amounts of each additive are included so as not to interfere with the RT enzyme efficiency. For those templates that have small starting amounts of RNA, the addition of a RNase inhibitor can enhance the level of detection.

When isolating RNA, the use of high grade reagents and RNase-free equipment are crucial in ensuring that degradation elements do not affect the quality of the RNA. One potential

problem often encountered involves the presence of contaminating DNA. The use of Trizol reagent significantly reduces the amount of contaminating DNA. Treatment with DNase I usually removes DNA such that no DNA generated products can result.

Primers should be desalted and preferably purified by HPLC. Lyophilised primers should be either reconstituted in nuclease-free water or TE buffer. Once the primer has been reconstituted in water, it should be stored in aliquots at -80°C to prevent acid hydrolysis during freeze-thaw cycles. For some GC-rich templates PCR additives such as Enhancer solutions that are available from commercial companies such as HotStar Taq system (Qiagen) can be included in the reaction.

RT-PCR is a method that has gained popularity in detecting mutations in the dystrophin gene owing to its large size of 427 kDa and exon number of 79. DNA based techniques such as conventional multiplex PCR have only been able to detect deletions in the "hot-spot" of the gene in 65% of cases or 72% of cases according to Aartsma-Rus et al. (2006). Many groups have found that DNA based strategies fail to detect splice-site mutations as the primers are designed within the exon (Tuffery-Giraud et al., 1999; Tuffery-Giraud et al., 2004). By using an RNA-based technique, such mutations can be identified and characterised at the RNA level. Alternative splicing and exon-skipping that occurs as a result of the rearrangement in the dystrophin gene can also be recognised by using RT-PCR (Roberts et al., 1991; Roberts et al., 1992). In these cases more than one fragment would appear on the gel following electrophoresis.

In 1999, Tuffery-Giraud et al. used RT-PCR and the protein truncation test (PTT) to identify translational termination mutations and splice-site mutations. PTT is a technique

that identifies mutations that lead to "premature termination of protein synthesis". The drawback of this technique is that an experienced scientist who has gained knowledge in the area is required to perform the assays and expensive reagents are needed. According to Tuffery-Giraud et al. (2004) the RT-PCR and PTT assays should be an essential part of the diagnostic work-up done on dystrophinopathy patients provided the technical expertise is available. In the report by Tuffery-Giraud et al. (2004), the authors utilised the experience as a DMD national referral centre for France and devised a protocol for the detection of mutations in the dystrophin gene. The RT-PCR methodology coupled with the protein-truncation test (PTT) employed by this group, allowed the detection of abnormal sized products in the dystrophin gene. Another advantage of using RT-PCR assays to detect aberrant fragments in the dystrophin gene would be the production of a template for use in DNA sequencing assays. The DNA sequencing will be able to detect small insertions and deletions or even nonsense mutations. Tuffery-Giraud et al. (2004) focussed primarily on point mutations as the detection of deletions and duplications have received much attention with the advent of the multiplex ligation-dependent probe amplification (MLPA) assay. This technique was also utilised by the author for deletion and duplication detection and will be discussed in a later chapter (Chapter 6) of this thesis.

The author attempted to set-up and optimise the RT-PCR assay; however she did not have the technical expertise to perform the PTT assay. In developing and implementing the RT-PCR assay in our laboratory we aimed to reduce the mutation-detection gap by being able to detect splice site mutations. By using RT-PCR we would be able to detect the changes at the RNA level and correlate these with the phenotype of the individual, which is difficult to achieve using DNA based methods.

## 4.7    AIMS AND OBJECTIVES

(i)    Set up and optimise reverse-transcription PCR.

(ii)    Detect splice site mutations using the RT-PCR assay.

## 4.8    MATERIALS AND METHODS

### 4.8.1    Patient database

**Table 12: Table showing the details of all patients that were included in the reverse-transcriptase PCR aspect of the study.**

| DNA number | Surname, Initials | Dystrophinopathy status / disease |
|---|---|---|
| 19 | M, S | DMD |
| 22 | N, N | DMD |
| 64 | M, S | Mother of 19 |
| Control 15 | P, MP | Polymyositis |
| Control 16 | V, A | Polymyositis |
| Control 17 | T, VA | Dermatomyositis |
| Control 18 | M, N | Dermatomyositis |
| Control 19 | M, TT | Polymyositis + Lupus |

### 4.8.2    Homogenisation of skeletal muscle using the Polytron Kinematica AG PT 1200

- The instrument used for the homogenisation procedure was the Polytron Kinematica AG PT 1200.

- The Polytron Kinematica AG PT 1200 was placed into a 0.1 M NaOH solution for 30 minutes to clean the probe prior to use. The instrument was further cleaned in 100% ethanol using the 6th speed setting. This was followed by 3 × 20 second bursts at full speed in autoclaved DEPC-treated water.

- All samples to be homogenised were placed in dry ice prior to undertaking the procedure.

- Each tissue sample to be homogenised was placed into a pre-weighed 1.5 ml micro-centrifuge tube and the weight of the sample was determined before use, and in between different samples, clean by agitating 3 x 20 sec using the 6$^{th}$ speed setting in ethanol and subsequently 3 x 20 sec in DEPC-treated water

- The tissue was transferred to a round bottom tubes (Lasec) instead of the 15 ml conical tubes (Corning) as the round bottomed tubes provided a larger area thereby providing more efficient homogenisation.

- A 1,000 μl volume of Trizol LS (Invitrogen) was added to the sample per 50 mg of tissue. A minimum volume of 2,000 μl was required for the homogenisation to work optimally.

- In some cases, to each tube containing the Trizol LS reagent and biopsy tissue sample was added 10 μl yeast tRNA (10 μg/μl, Sigma). The yeast tRNA was added to increase the amount of RNA in the tube thereby reducing the degradation that would occur during the homogenisation process.

- The fourth speed was used during the homogenisation procedure. The samples were homogenised 6-7 times for 5-6 seconds. On completion of this stage of the process, the samples were placed on ice.

- The homogenate was transferred to 1.5 ml micro-centrifuge tubes in 1000 μl volumes.

## 4.8.3   RNA extractions

### 4.8.3.1 Using Trizol LS

RNA was extracted from homogenised samples using the Trizol LS reagent and the procedure followed was as per manufacturer's instructions (Invitrogen).

### 4.8.3.2 Fibrous tissue mini kit (Qiagen)

The procedure followed was as per manufacturer's instructions.

### 4.8.3.3 Nucleospin® RNA II (Machery-Nagel)

The procedure followed was as per manufacturer's instructions.

### 4.8.4 Electrophoresis of RNA samples

The RNA samples were electrophoresed on 1% TBE buffer containing SeaKem agarose (BioWhittaker Molecular Applications) gels for 1.5 hours at 100 V. The procedure used is outlined in 4.3.5 above.

### 4.8.5 Reverse-transcription (RT) PCR using Superscript II

The procedure followed was as per manufacturer's instructions (Invitrogen). Amendments to the protocol were as follows:

- A master mix for the RT-reaction was prepared as follows:

**Table 13: Components included in the master mix for the first strand reaction of the reverse transcription.**

| Reagent | Volume in μl | Final concentration |
|---|---|---|
| 5 × First strand buffer (Invitrogen) | 4.0 | 1 × |
| 100 mM Dithiothreitol (DTT, Invitrogen) | 2.0 | 10 mM |
| 40 U/μl RNasin RNase inhibitor (Promega) | 1.0 | 40 U |
| Master mix total | 7.0 | - |
| RT-reaction | 13.0 | - |
| Final volume | 20.0 | - |

- Listed below are the primers that were included in either the 1ˢᵗ or 2ⁿᵈ round PCR assays.

**Table 14: Primers used in the RT-PCR assays. Primers are taken from the Leiden and Whittock sets. Primers from the Leiden set are AH and GB and where the Whittock set was utilised the letter "w" is shown.**

| 1ˢᵗ Round PCR | | 2ⁿᵈ Round PCR | | Exons included | Fragment length on gel |
|---|---|---|---|---|---|
| Forward Primer | Reverse primer | Forward primer | Reverse primer | | |
| Exon2F1 (1A) | Exon12R1 (1H) | Exon2F2 (1C) | Exon11R2 (1D) | 2-11 | 1217 |
| Exon9F1 (1G) | Exon18R2 (1B) | Exon10F 1(1E) | Exon18R1 (1F) | 10-18 | 1135 |
| Exon17F1 (2A) | Exon25R2 (2H) | Exon17F 2(2C) | Exon25R1 (2D) | 17-25 | 1203 |
| Exon23F2 (2G) | Exon35R1 (2Bw) | Exon23F 1(2E) | Exon35R2 (2Dw) | 23-35 | 1794 |
| Exon30F2 (3A) | Exon40R1 (3H) | Exon31f 1(3C) | Exon38F1 (3D) | 31-38 | 1052 |
| Exon36F3 (3G) | Exon46R1 (3B) | Exon36F 2(3E) | Exon45R3 (3Dw) | 36-45 | 1514 |
| Exon43F1 (4A) | Exon54R1 (4Bw) | Exon44F 2(4C) | Exon 53R1(4Dw) | 44-53 | 1488 |
| Exon50F1 (4G) | Exon59R4 (4B) | Exon51F 1(4E) | Exon59R3 (4F) | 51-59 | 1389 |
| Exon56/5 7F1 (5A) | Exon73R1 (5H) | Exon58F 1(5C) | Exon68R2 (5D) | 58-68 | 1342 |
| Exon63F1 (5G) | Exon79R2 (5B) | Exon67F 2(5E) | Exon79R1 (5F) | 67-79 | 1340 |

**Table 15: Reagents included in the master mix for the first round PCR reaction.**

| Reagent | Volume in µl | Final concentration |
|---|---|---|
| Sterile nuclease free water | 17.90 | - |
| 10 × In-house buffer | 2.5 | 1 × |
| 10 mM dNTPs | 0.5 | 10 Mm |
| Amplitaq polymerase (5U/µl, Applied Biosystems) | 0.3 | 1.5 |
| Final volume | 21.2 | - |

- To each master mix tube was added 1 µl of forward primer and 1 µl reverse primer, both at a concentration of 10 pMol/µl (See table 14 for primer pairs included in the 1ˢᵗ round PCR). The volume would be 23.3 µl.

- The appropriate *c*DNA was added at a volume of 1.8 µl to the reaction tube, and

the final PCR reaction volume was 25 µl. The following PCR conditions were employed.

**Table 16: Amplification conditions for the RT-PCR assay.**

|  | Temperature (°C) | Time | Cycle number |
|---|---|---|---|
| Initial denaturation | 94 | 5 minutes | 1 |
| Denaturation | 94 | 40 seconds |  |
| Annealing | 57 | 40 seconds | 32 |
| Elongation | 72 | 2 minutes |  |
| Final Extension | 72 | 5 minutes |  |
| Hold | 15 | ∞ | 1 |

Subsequent to the RNA extraction using Trizol LS reagent, the protocol from the clean-up section of the RNeasy fibrous tissue mini kit (Qiagen) was followed.

## 4.9 RESULTS

### 4.9.1 RNA extractions

Various methods were used in extraction of RNA from the tissue samples. The trizol method was found to be most efficient at producing a good RNA yield, with intact RNA. The two kits used in the extraction procedure did not produce consistent results as is shown below.

The images below (Figure 47) clearly show that the Fibrous tissue mini kit from Qiagen is not consistent with respect to the RNA that it produces. Even though the starting material was the same in all samples subjected to RNA extraction using the Qiagen kit, the final yield of RNA differed considerably. One of the reasons for reduced yield may be due to inconsistency in the Qiagen kit itself. Other reasons for such an occurrence may relate to
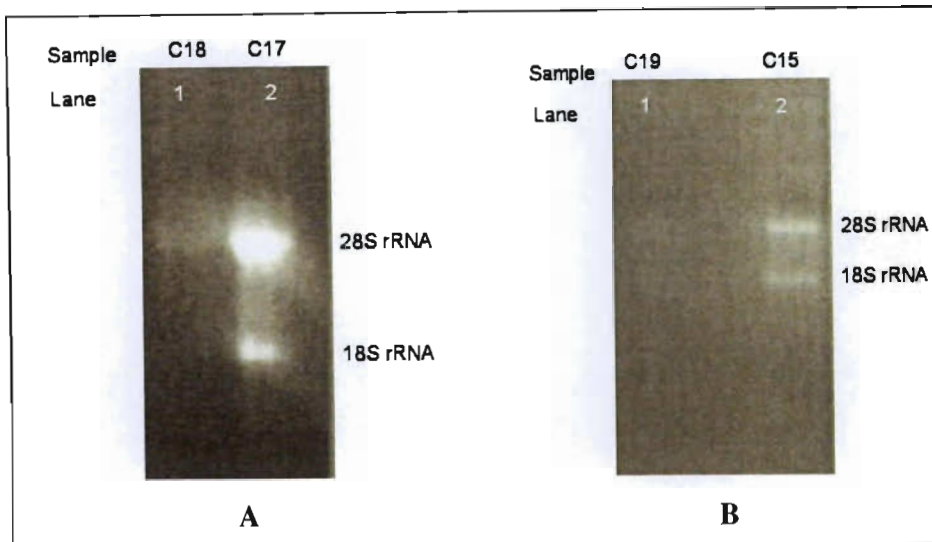
**Figure 47 : Images showing the 28S and 18S rRNA bands from control samples that were subjected to RNA extraction using the Qiagen fibrous tissue mini kit.**

the state of the tissue at the time of RNA extraction with respect to tissue integrity and tissue age of the sample. The biopsy taken from different patients may differ with respect to their muscle and adipose tissue content, especially in the case of those patients with neuromuscular abnormalities. The control samples used in many cases were from polymyositis and dermatomyositis patients, whom invariably possessed adipose tissue and decreased amounts of muscle tissue from which RNA would be obtained.

In figure 47, C17 (A) and C15 (B) showed that the RNA was intact after RNA extraction and the samples did not undergo RNA degradation. The two other samples C18 (A) and C19 (B) are in stark contrast to these results as the bands are barely visible. It is therefore difficult to conclude that the samples C18 (A) and C19 (B) are degraded.

Figure 48 clearly illustrates the difference in the amount of RNA that resulted from using the Machery-Nagel tissue kit and the Qiagen fibrous tissue kit. The same sample was used in both kits to ensure that there was no sample bias when performing the comparison.
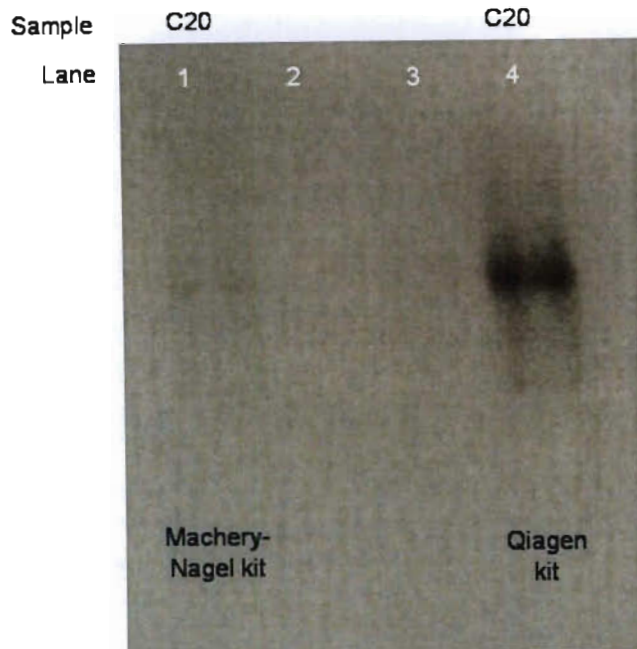
**Figure 48: Image showing the RNA that was produced following isolation using the Machery-Nagel tissue kit and the Qiagen kit as outlined.**

The 18S rRNA band is not visible when the Machery-Nagel kit was used as shown in lane 1 and the band is faintly visible when the Qiagen tissue kit was used in the RNA extraction procedure as shown in lane 4. The 28S rRNA band is faintly visible in lane 1 and is intense in lane 4. The loss (lane 1) and faint visibility (lane 4) of the 18S rRNA band may be due to sample degradation.

### 4.9.2   RT-PCR assays

In the images below, 1-10 represent the RT-PCR fragments. Expected sizes were as follows: fragment 1 was 1217 bp, fragment 2 was 1135 bp, fragment 3 was 1203 bp, fragment 4 was 1794 bp, fragment 5 was 1052 bp, fragment 6 was 1514 bp, fragment 7 was 1488 bp, fragment 8 was 1389 bp, fragment 9 was 1342 and fragment 10 was 1340 bp in length. The fragments for molecular weight marker VI (Roche) was as follows: 2176 bp, 1766 bp, 1230 bp, 1033 bp, 653 bp, 517 bp, 453 bp, 394 bp, 298  bp, 234 bp and 220 bp.
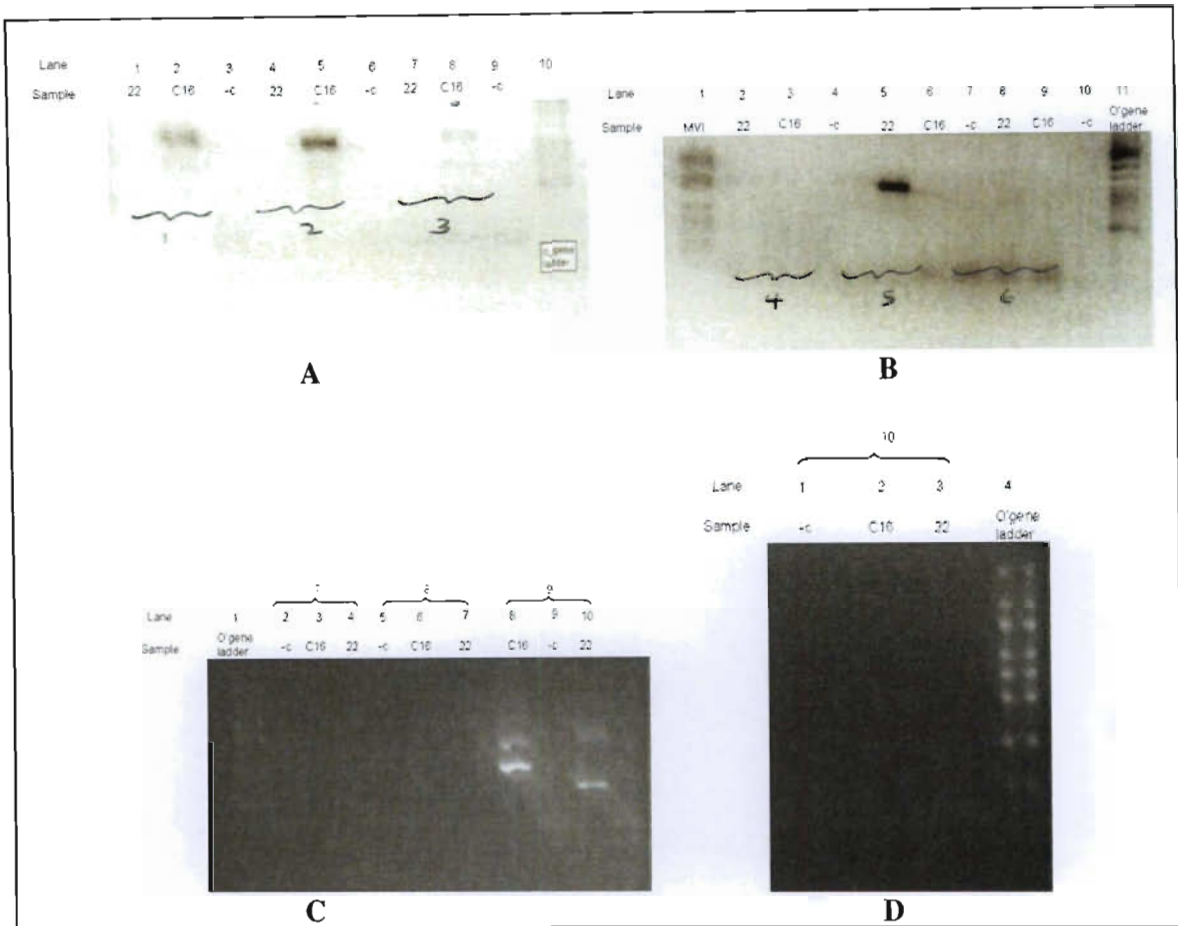
**Figure 49: Images showing the results obtained when all 10 fragments were electrophoresed on 1% NuSieve agarose gels.**

The O'gene ladder 100 bp marker was composed of the following fragments, 100 bp, 200 bp, 300 bp, 400 bp, 500 bp, 600 bp, 700 bp, 800 bp, 900 bp, 1000 bp, 1200 bp, 1500, 2000 bp and 3000 bp.

In this set, several products were not visible on the gel. This may have occurred as only 5 µl of sample was run or to unsuccessful amplification.

In fragments 8 and 9 of patient 22 in the figure above (B), the results obtained were interesting as it showed two fragments of different length, which suggests deletions, duplications or splice site mutations. In this case, since the patient's sample was subjected

to multiplex PCR and no deletions were found in the region of exon 51-59 (fragment 8, 1389 bp), a splice site mutations is the most likely possibility. There were also two fragments obtained for exons 58-68 (fragment size 1342 bp), which had not been checked for deletions using the multiplex PCR therefore in this case any of the three mutations (deletions, duplications, splice site mutations) could be present. The resulting higher band could have been the result of primer carry-over from the first / primary PCR reaction.

In the figures below, a 100 bp ladder (Fermentas) was used in this and previous RT-PCR experiments. The fragments ranged from 100 bp to 3000 bp as was previously mentioned (Figure 49). From the images below (figure 50) it is evident that the control samples showed more than one band. The expected result would have been a single band for each set. At that stage, several changes were made to the protocol. New primers were ordered with HPLC grade purification being performed as opposed to normal desalting purification, for those sets where more than one band resulted. The new primers produced the same outcome. The amplification protocol was then changed, with the cycle number being varied. This too did not produce the desired outcome.

The other reason for obtaining two bands in control samples, where it would be expected that one band should be produced may have been due to degraded RNA samples. The problem of degraded samples could not be overcome because it would not have been ethical for us to ask the patient to consent to another biopsy sample.

As this stage, RNA was extracted from blood samples by first performing a peripheral blood lymphocyte extraction. The resulting RNA was then included in the RT-PCR assays. However, no bands were obtained when reverse transcribed RNA samples extracted from

blood were subjected to RT-PCR. No conclusive data could be obtained from the RT-PCRs that were performed.
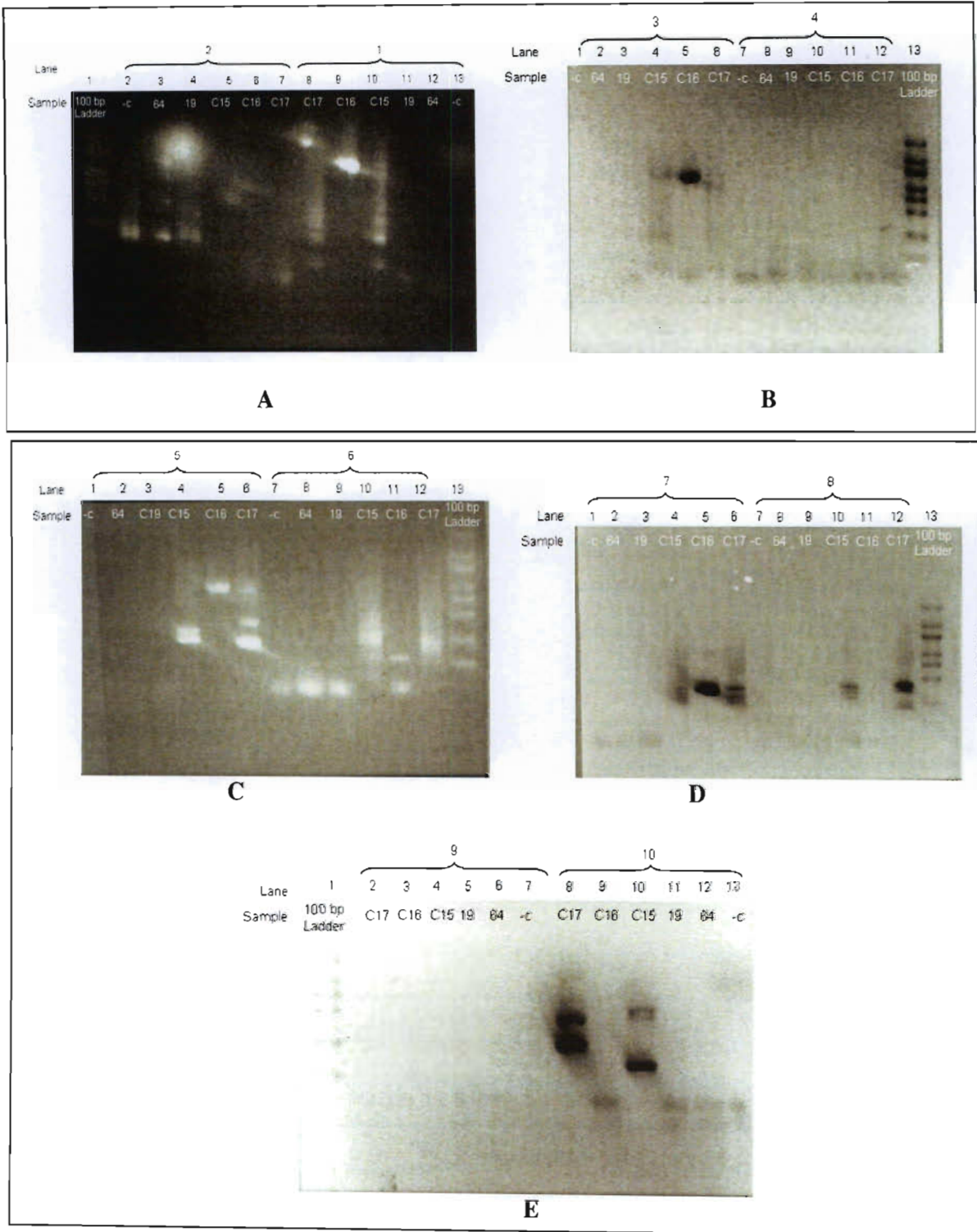


Figure 50: Images showing RT-PCR assays where amplification was successful for only some samples.

## 4.10    DISCUSSION

The RT-PCR results would have been initially useful in identifying re-arrangements in dystrophin negative patients, who have been shown to have no deletions on multiplex PCR. The data could have been used to categorise these patients as having a deletion / duplication. In so doing, further studies would not have had to be undertaken. The other reason for setting up the RT-PCR assay related to finding splice-site mutations that are usually not detected using DNA based techniques.

The author changed many parameters during the optimisation process in an attempt to produce usable data. New primer dilutions were initially made. When this did not change the results, new primers were ordered. The cycling conditions such as the annealing temperature was also varied. After implementing these changes, the results still did not match published data (Tuffery-Giraud *et al.*, 1999; Tuffery-Giraud *et al.*, 2004). RNA extracted from lymphocytes has previously been reported to contain fewer dystrophin transcripts. This may have been the reason for no bands being produced when RT-PCR was performed (Roberts *et al.*, 1991; Tuffery-Giraud *et al.*, 2004).

It therefore became evident that the RNA was not of high-quality. The starting material is of grave importance in producing usable data (Invitrogen RT-PCR manual). If the RNA is in any way degraded, false deductions and conclusions could be drawn from the outcome. In our study, the control samples that were included also became degraded. The degradation did not show up when a gel was run to show the presence of the 18S and 28S rRNA bands.

The control results had revealed two bands instead of the one expected band. The only time two bands would be expected is if a carrier's sample were being tested or rearrangements were present in the patient's sample. The patients included as controls were not DMD affected individuals and showed no clinical manifestations of DMD. The other explanation would be for the patient to have exhibited exon-skipping. Once again this could not have been possible as they were not dystrophinopathy patients. A more likely explanation would be primer carry-over from the primary PCR reaction. The reading frame hypothesis holds true for greater than 90% of cases. There are of course exceptions to this rule, and secondary mechanisms could account for these discrepancies.

The recommendation would be to ensure that the biopsy samples are immediately preserved in RNA*later* solution and stored at -80°C. All precautions should be taken to ensure that no degradation of the RNA occurs even during the extraction procedure. The cDNA should be synthesised and the RT-PCR performed soon after the RNA was isolated.

# CHAPTER 5

## MULTIPLEX PCR USING 30 EXONS TO IMPROVE THE DIAGNOSTIC EFFICACY FOR DELETION SCREENING IN DYSTROPHINOPATHIES

### 5.1    INTRODUCTION

The use of multiplex PCR to detect deletions in the dystrophin gene was considered an important step in diagnosing this debilitating disease. Chamberlain *et al.* (1988) and Beggs *et al.* (1990) were the first to develop multiplex PCR assays for the detection of 18 hot-spot exons throughout the dystrophin gene in two multiplex PCR sets. The use of molecular genetic approach together with an extensive clinical work-up and immunohistochemical analysis proved to be beneficial in diagnosing Duchenne muscular dystrophy.

Initially, the Southern blotting technique was used to detect deletions and / or duplications in the dystrophin gene. However, this technique was gradually replaced by the multiplex PCR assay owing to the high sensitivity and specificity of the technique. The molecular approach to detect deletions was preferred as it did not require *c*DNA probes (Koenig *et al.*, 1987; Forrest *et al.*, 1987) to be produced prior to undertaking the procedure. Even though the production of *c*DNA probes are time consuming and labour intensive, the results from such analyses provided much insight into the dystrophin gene. There were instances where the Southern blotting technique failed to detect fragments using the appropriate restriction endonuclease. According to Patria *et al.* (1999) this inability to detect the correct fragment led to an in-frame deletion being falsely detected, which was later shown to be an out-of-frame deletion using a molecular assay.

In 1987, Forrest *et al.* was able to conclude that the deletion / duplication spectrum in DMD is heterogeneous, an important finding that set the stage for further analyses to be conducted that supported the suggestion that the deletion spectrum was complex and difficult to characterise. Later studies confirmed that the deletions were clustered in two hot-spots, namely the 5' domain region comprising exons 3-7 and the 3' rod domain comprising exons 45-52. The term "high frequency deletion region" (HFDR) was subsequently coined (Baumbach *et al.*, 1989). The Southern hybridisation technique provided much data on the types of deletions and duplications that were present in the dystrophin gene of different patients. Further molecular and Southern analyses revealed that Duchenne and Becker muscular dystrophy (BMD) patients could be identified by virtue of the reading frame theory. The theory states that a Duchenne muscular dystrophy patient would possess an out-of-frame deletion that produces a conjectured transcript that prevents the production of a functional protein. Comparatively, a BMD patient would have an in-frame deletion allowing the production of a smaller, truncated yet functional protein, hence the milder phenotype that is associated with this form of the disease (Monaco *et al.*, 1988).

The reading frame theory does not hold true for all cases as was shown by many groups owing to the presence of multiple types of deletions in the dystrophin gene (Malhotra *et al.*, 1988; Monaco *et al.*, 1988; Baumbach *et al.*, 1989). According to Malhotra *et al.*, 1988 the theory does hold true for 92% of cases. Different groups working on DMD have noted the inconsistent relation between the detected deletion and the clinical phenotype (Chelly *et al.*, 1990; Gillard *et al.*, 1989).

As more data became available on the deletion and duplication spectrum in Duchenne and Becker muscular dystrophy, other groups set out to determine the deletion breakpoints in dystrophinopathies since this was not possible using the 18 exon multiplex PCR. In 1991, Kunkel *et al.*, expanded on the 18 exon multiplex PCR assay by including a further six exons to the assay in a third set. This third set was improved on by Covone *et al.* in 1992, where a 30-plex PCR was developed. The assay utilised four exons 20, 21, 22 and 29 from the central part of the rod domain to determine whether deletions were clustered in specific hot-spots or whether there were multiple deletions. The authors revealed that such an improvement in the multiplex PCR screening would improve the deletion detection rate from 98% to 99%.

In 1998, Haider *et al.* utilised 25 primer pairs to detect deletions in hot-spot exons by combining the Chamberlain *et al.* (1990), Beggs *et al.*, (1990) and Kunkel *et al.*, (1991) sets. The authors found it was not necessary to include the four exons in the rod domain, 20, 21, 22 and 29 as it was previously reported by Beggs *et al.* (1991) that such internal deletions in that region of the rod domain have minimal effects on protein function and clinical phenotype of the individual. Different phenotypes (severe cramps, increased serum creatine kinase and typical BMD) have been observed in patients with deletions in the three regions of the rod domain (proximal, central, distal) respectively. Such differences in phenotype may occur on account of the functional associations between dystrophin and other proteins that it binds to and interacts with at the rod domain (Beggs et al., 1991; Chamberlain *et al.*, 1997).

When all this data was collated it was found that approximately 65% of mutations in the dystrophin gene were made up of intragenic deletions (Koenig *et al.*, 1989; Baumbach *et*

*al.*, 1989; Muntoni *et al.*, 2003). In 2006, Aartsma-Rus *et al.* reviewed all the mutations that were posted on the Leiden Muscular dystrophy (MD) website and concluded that the deletion rate was slightly higher at 72% than was previously reported. The authors suggested that the reason for the higher rate may be attributed to the fact that those patients in whom no mutations are found are not included in the database however they are included in the analysis steps when "percentages are calculated for general patient screenings". The Leiden MD website contains over 4700 mutations in the dystrophin gene. This review differs from all other publications in that it provides a detailed overview of the different mutations and particularly those that do not follow the reading-frame rule. The most commonly deleted exon is exon 45 and exons 45-47. Previous literature consensus revealed one of the high frequency deletion regions (HFDR) or deletion "hot-spots" clusters around exon 45-53 and the data collated from the review is in keeping with this (Beggs *et al.*, 1990, Aartsma-Rus *et al.*, 2006).

In this aspect of the study, we assessed the 30-plex PCR in our South African patients to determine whether the deletion spectrum changed if additional exons were added to the conventional 18-exon multiplex PCR assays. From the author's previous Master's study where she focussed on a cohort of 68 dystrophinopathy patients, 43% were found to have no deletions. The author set out to determine whether the percentage of non deletion patients still remained the same using the 30-plex PCR, or whether they had deletions in those exons that were not tested using the 18 exon conventional multiplex PCR sets. The 30-plex PCR used in our study varied slightly from those exons that were tested in the Covone *et al.* (1992) and Haider *et al.* (1998) studies.

## 5.2 AIMS AND OBJECTIVES

i)     To evaluate the multiplex PCR using 30 primer pairs as a screening tool for

deletion detection.

ii)    To improve the diagnostic efficacy of deletion screening in

dystrophinopathies.


## 5.3 MATERIALS AND METHODS


### 5.3.1 Patient population


**Table 17: Database showing the details of those patients that were included in the 30-plex PCR aspect of the study.**

| DNA number | Surname, Initials | Age | DMD/BMD |
|---|---|---|---|
| 2 | S, W | 16 | DMD |
| 8 | S, T | 13 | DMD |
| 9 | S, NM | 17 | DMD |
| 12 | G, S | 16 | DMD |
| 14 | N, D | 9 | DMD |
| 16 | M, T | 14 | DMD |
| 18 | R, J | 34 | BMD |
| 19 | M, S | 6 | DMD |
| 20 | M, S | N/A | DMD |
| 21 | R, S | 8 | DMD |
| 22 | N, N | 10 | DMD |
| 23 | H, ZM | 13 | DMD |
| 24 | P, D | 8 | DMD |
| 25 | R, D | 35 | BMD |
| 26 | Z, S | 18 | BMD |
| 27 | L, L | N/A | DMD |
| 28 | M, MB | 10 | DMD |
| 29 | N, C | N/A | DMD |
| 30 | W, R | N/A | DMD |
| 31 | C, L | 12 | DMD |
| 32 | M, NL | 6 | DMD |
| 33 | G, P | N/A | DMD |
| 34 | N, M | N/A | BMD |
| 35 | S, G | N/A | BMD |

| | | | |
|---|---|---|---|
| 36 | H, XV | 22 | BMD |
| 37 | G, M | 8 | DMD |
| 38 | N, M | 14 | DMD |
| 39 | S, T | 14 | DMD |
| 40 | S, C | 12 | DMD |
| 41 | M, S | 10 | DMD |
| 42 | M, R | 12 | DMD |
| 43 | S, V | 14 | DMD |
| 44 | C, L | N/A | DMD |
| 45 | M, T | 13 | DMD |
| 46 | M, S | N/A | DMD |
| 47 | M, ST | N/A | DMD |
| 48 | M, S | N/A | DMD |
| 49 | M, W | 7 | DMD |
| 50 | N, T | 14 | DMD |
| 51 | H, N | 19 | BMD |
| 52 | K, TP | 18 | DMD |
| 53 | V, S | 10 | DMD |
| 54 | B, N | N/A | DMD |
| 55 | F, S | N/A | BMD |
| 56 | S, T | 12 | DMD |
| 68 | N, S | N/A | DMD |

**Legend:N/A - Not available**

### 5.3.2   DNA extractions

The methods that were performed in the isolation of DNA from the patients' blood samples included the QIAmp DNA blood mini kit (Qiagen) and the salting-out method. The detailed methodology has been outlined in Chapter 4 (Point mutation detection in non-deletion dystrophinopathy patients) of this thesis.

### 5.3.3   DNA quantification

The DNA was quantitated using the spectrophotometric method as outlined in the Beckman manual for the DU800 spectrophotometer.

## 5.3.4   PCR reactions and conditions

Three separate PCR reactions were performed to collectively form the multiplex PCR assay. These reactions were adapted by the author from the original Chamberlain (Chamberlain *et al.*, 1988, Chamberlain *et al.*, 1990), Beggs (Beggs *et al.*, 1990) and Kunkel (Kunkel *et al.*, 1991) sets to suit our laboratory conditions and environment. These sets were improved on by Covone (Covone *et al.*, 1992).

The original Chamberlain and Beggs sets were optimised for the Neuroscience laboratory during the author's Master's project and this formed a chapter in the Master's thesis. The Kunkel set was not optimised or included at that time. In this aspect of the present study, the author improved on the diagnostic efficacy of the Chamberlain, Beggs and Kunkel multiplex PCR sets by following the recommendations of Covone *et al.* (1992).

The previous optimisation procedures that were successfully performed during the author's Master's study were duplicated for the Chamberlain and Beggs sets using the Platinum *Taq* reagents (Invitrogen). However, as an addition to the Chamberlain set of nine exons, another three primer pairs were included in the reaction to make a total of 12 primer pairs in the single reaction tube (Covone *et al.*, 1992). For the Beggs set, the nine primer pairs were increased to 10 primer pairs (Covone *et al.* 1992). In our optimisations, 10 primer pairs were still used in the Beggs set however two different primer pairs for exon 50 were included in reaction to determine which primer pair produced the most visible band for detection purposes. The Kunkel set was increased to nine primer pairs. In our optimisation of the Kunkel set, 13 primer pairs were used to determine the most appropriate fragment

combination. Two different primer pairs were tested for exon 42 to determine which primer pair produced the most visible band.

**Table 18: PCR mix used in the first multiplex PCR set composed of 12 primer pairs, in a 60 μl reaction volume.**

| Reagent | Volume (μl) | Final concentration |
|---|---|---|
| 10X Platinum PCR buffer | 6.0 | 1 × |
| 50mM $Mg_2Cl$ | 6.0 | 5 mM |
| dNTPs 25mM (Pharmacia) | 3.0 | 1.25 mM |
| Forward primer (25 pMol/μl) exons 30, 22, 29 | 2.0 | 0.8 μM |
| Reverse primer (25 pMol/μl) exons 30, 22, 29 | 2.0 | 0.8 μM |
| Forward primer (25 pMol/μl) exons 45,48,19,17,51,8,12,44,4 | 1.5 | 0.625 μM |
| Reverse primer (25 pMol/μl) exons 45,48,19,17,51,8,12,44,4 | 1.5 | 0.625 μM |
| Filter sterilised (fs)d$H_2O$ | 0.5 | - |
| Platinum Taq 5U/μl | 0.5 | 2.5 U/ reaction |
| DNA(50ng/μl) | 5.0 | 250 ng/ reaction |
| Final volume | 60.0 | - |

The primers included in the above table include all the possible primers that have been used to produce a 12-plex PCR. During the optimisation process, the fragment sizes of the primer pairs differed, owing to different primer pairs being used as was the case with exon 44. Exon 44 was either 426 bp or 268 bp in length. All the primers and their corresponding fragment sizes as observed on an agarose gel are outlined in Appendix A.

**Table 19: Amplification conditions for the 12-plex PCR reaction adapted from Chamberlain et al. (1990).**

| | Temperature (°C) | Time | Cycle number |
|---|---|---|---|
| Initial denaturation | 94 | 6 minutes | 1 |
| Denaturation | 94 | 30 seconds | |
| Annealing | 53 | 30 seconds | 35 |
| Elongation | 65 | 4 minutes | |
| Final Extension | 65 | 7 minutes | |
| Hold | 15 | ∞ | 1 |

**Table 20: PCR mix used in the second multiplex PCR set composed of 10 primer pairs, in a 60 µl reaction volume.**

| Reagent | Volume (µl) | Final concentration |
|---|---|---|
| 10 × Platinum PCR buffer | 6.0 | 1 × |
| 50 mM Mg$_2$Cl | 6.0 | 5 mM |
| dNTPs 25 mM (Pharmacia) | 3.0 | 1.25 mM |
| Forward primer (25 pMol/µl) exons 3, 43, Pm, 21 | 2.0 | 0.8 µM |
| Reverse primer (25 pMol/µl) exons 3, 43, Pm, 21 | 2.0 | 0.8 µM |
| Forward primer (25 pMol/µl) exons 50,13,6,47,60,52 | 1.5 | 0.625 µM |
| Reverse primer (25 pMol/µl) exons 50,13,6,47,60,52 | 1.5 | 0.625 µM |
| Filter sterilised (fs)dH$_2$O | 5.5 | - |
| Platinum Taq 5U/µl | 0.5 | 2.5 U/ reaction |
| DNA(50 ng/µl) | 5.0 | 250 ng/ reaction |
| **Final volume** | **60.0** | - |

The fragment sizes for exon 50 were either 337 bp or 271 bp, depending on the primer pairs that were included in the reaction mix. Different primers were used during the optimisation process to determine which primer pairs produced the most usable and well resolved bands. The primers and their fragment lengths are outlined in appendix A.

**Table 21: PCR mix used in the third multiplex PCR set composed of 9 primer pairs, in a 50 µl reaction volume.**

| Reagent | Volume (µl) | Final concentration |
|---|---|---|
| 10 × Platinum PCR buffer | 5.0 | 1 × |
| 50 mM Mg$_2$Cl | 5.0 | 5 mM |
| dNTPs 25 mM (Pharmacia) | 3.0 | 1.5 mM |
| Forward primer (25 pMol/µl) exons Pb,49,(20 or 2 or 5) | 2.0 | 1.0 µM |
| Reverse primer (25 pMol/µl) exons Pb,49,(20 or 2 or 5) | 2.0 | 1.0 µM |
| Forward primer (25 pMol/µl) exons 16,41,32,42,34,46 | 1.5 | 0.75 µM |
| Reverse primer (25 pMol/µl) exons 16,41,32,42,34,46 | 1.5 | 0.75 µM |
| Filter sterilised (fs)dH$_2$O | 1.5 | - |
| Platinum Taq 5U/µl | 0.5 | 2.5 U/ reaction |
| DNA(50 ng/µl) | 5.0 | 250 ng/ reaction |
| **Final volume** | **50.0** | - |

Exons 20, 2, or 5 could be included as an optional extra once the other 8 primer pairs have been tested for compatibility. During the optimisation process, other primer pairs (exons 1 and 62) were also included in the set to determine whether the data produced would be usable. The additional primers that were included and their fragment sizes are outlined in Appendix A.

**Table 22: Amplification conditions for the 10-plex and 9-plex PCR reaction adapted from Beggs *et al.*, (1990) and Kunkel *et al.* (1991) respectively.**

| | Temperature (°C) | Time | Cycle number |
|---|---|---|---|
| Initial denaturation | 94 | 7 minutes | 1 |
| Denaturation | 94 | 30 seconds | 35 |
| Annealing/ Elongation | 65 | 4 minutes | |
| Final Extension | 65 | 10 minutes | |
| Hold | 15 | ∞ | 1 |

### 5.3.5 Gel electrophoresis

Various standard melt and low melt agarose gels were used to separate the multiplex PCR fragments. The first agarose gel used was the MetaPhor (Cambrex) gel, which is able to separate products in the range of 20 bp to 800 bp with high resolution.

The next agarose gel used was the NuSieve 3:1 (FMC/ Cambrex), a standard melting temperature gel used to resolve products 20 bp to 2,000 bp in length. In order to increase the strength of the gel, a 0.5% concentration of conventional SeaKem agarose (FMC) was added to the 2.5% NuSieve agarose and TBE buffer. SeaKem agarose is used for general separation of PCR products by electrophoresis. By adding both agarose powders to the buffer of choice we were able to separate the products using a high strength gel and still benefited from the increased resolution that the gel offered.

Another gel used was the NuSieve GTG, which is a low melt agarose gel used for the electrophoresis of products in the range of 10 bp to 1,000 bp. Other gels used include the low melt MS-4 and standard melt MS-8 high resolution gels from Hispanlab. The MS-4 size range is between 9 bp and 600 bp and the MS-8 size range is between 50 bp and 1,000 bp. The percentages of all gels used varied from 2.5 to 4.0%. The lower the gel percentage, the more fragile the gel became.

## 5.4 RESULTS

The DNA samples from 46 dystrophinopathy patients were subjected to multiplex PCR using 30 primer pairs, in three different sets.

With respect to agarose gel electrophoresis, the MetaPhor gel produced well resolved bands, however in many instances the gel broke owing to its non-sturdy nature and care had to be taken with the gel at all times. Also, during the heating step, numerous tiny air bubbles were produced, which could not be adequately removed.

In comparison, the NuSieve 3:1 agarose gel was an easy gel to work with and produced well resolved bands at a low percentage (2.5% - 3.0%).

The NuSieve GTG and the low melt agarose gel also produced air bubbles during the preparation as did the MetaPhor gel. The bubbles were removed by placing the bottle with the gel into a water-bath set to 60°C. The gel was left in there for half hour to equilibrate to the temperature of the water-bath. Following the water-bath treatment, all air bubbles had

disappeared and a smooth gel with no air bubbles could be poured. The incubation step was subsequently undertaken for the MetaPhor gel with the desired effect.

The recommendation for an inexperienced laboratory scientist or research assistant would be to use the NuSieve 3:1 agarose gel at first until one gets acquainted with the preparation and handling of such gels. Thereafter one can progress to using the NuSieve GTG and MetaPhor gels as these are not as sturdy, some experience in handling such gels is required. The MS-4 and MS-8 gels were found to be less resilient to handling pressure than the NuSieve agarose gels and would therefore not be a first choice. A 3% NuSieve agarose + 0.5% SeaKem agarose would produce a high resolution gel with increased strength.

### 5.4.1  Optimisation of the multiplex PCR sets

These sets were optimised for our laboratory environment using PCR reagents different from those recommended in the original papers. In some instances, the sizes of the exons originally used (Chamberlain *et al.*, 1990; Beggs *et al.*, 1990, Kunkel *et al.*, 1991) differ as other primer sequences were used. All primer sequences are outlined in Appendix A. The polymerase enzyme used in the three sets was Platinum taq and reagents (Invitrogen).

The first multiplex PCR set was adapted from the original Chamberlain set (Chamberlain *et al.*, 1990) and improved on by Covone *et al.* (1992). Instead of including exon 20 as was suggested by Covone *et al.* (1992), exon 30 was included in set 1 during this optimisation run. For the second set, which was adapted from the original Beggs set (Beggs *et al.*, 1991) and improved on by Covone *et al.* (1992), the primer for exon 21 was changed. The size of
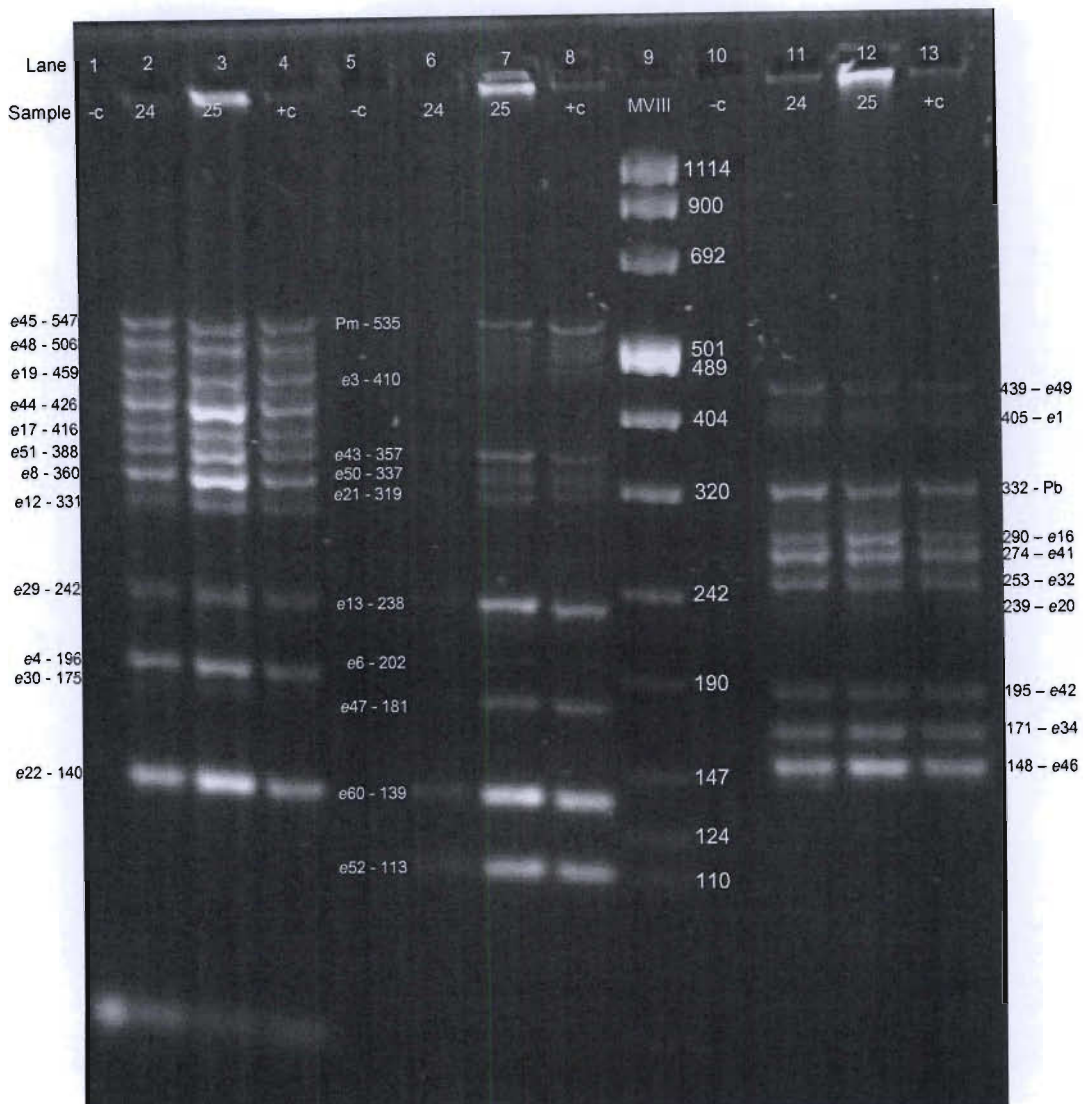
**Figure 51: Image showing all three sets of multiplex PCRs that were optimised using the Platinum taq reagents at the Neuroscience laboratory, Durban, South Africa.**

the fragments for exon 47 was 181 bp and exon 21 was 175 bp respectively, according to Covone *et al*. (1992). This meant that there was a very small difference in size between the two fragments thus making interpretation on a gel more difficult. The resulting product size for exon 21 was changed from 175 bp to 319 bp. In the third and last multiplex PCR set, which was originally described by Kunkel *et al*. (1991) and improved on by Covone *et al*. (1992), the author made the following changes. The primers for exons 16 and Pb were changed to produce different sizes fragments from the published papers. Additions to this set were exons 1 and 20 (figure 51).

146

In some instances, owing to primer competition the bands were very faint. Those bands that were not easily visible on the NuSieve gel used to run the multiplex PCR assay were re-amplified in a single PCR reaction to confirm the presence or absence of the band. The annealing temperatures of those primers were calculated and used in the single primer pair, PCR assay. For each single primer pair PCR assay that was performed, a positive and negative control was included.

The gel had to be run for several hours to obtain a good enough separation of the products so that an informed decision could be made with respect to the presence or absence of a band. A number of the products run close to one another therefore a high resolution gel was used.
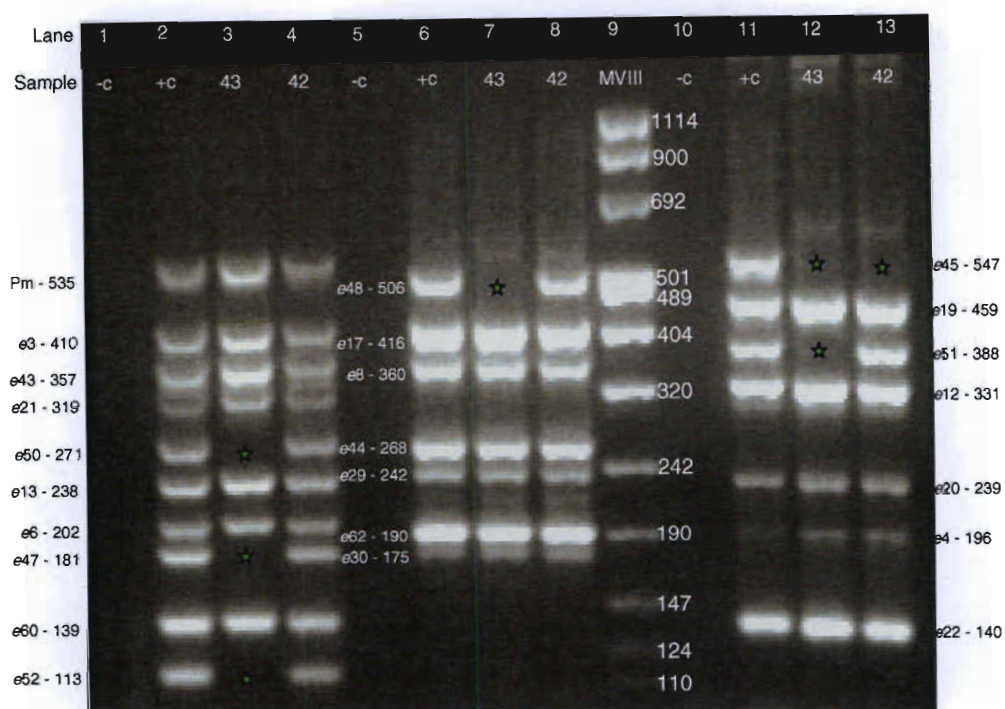


**Figure 52: Representative image of amplified products from set 1 and set 2 showing deletions in two clinically affected dystrophinopathy patients (patients 42 and 43) from the Neuromuscular clinic at Inkosi Albert Luthuli Central Hospital, Durban, South Africa.**

In these sets of multiplex PCRs, set 1, which was adapted from the original Chamberlain set was divided into two sets, with seven primer pairs being used in each set. This reaction

was performed because a previous multiplex PCR using 12 primer pairs produced poor results, with some bands being faint and undefined. Therefore the results were not definitive. When the multiplex PCR was done using seven primer pairs in a reaction, intense bands were obtained as is clearly evident in the figure above (Figure 52). Non- specific bands were obtained due to the cycle number being the same as that used in the reaction with 12 primer pairs. This could have been avoided by reducing the cycle number.

Using different primer pair combinations in the 7 primer pair reaction a better spread of amplified products was obtained compared to the 12 primer pair reaction amplification products which were close together. On comparison with the previous image (figure 51) showing 12 primer pairs the multiplex PCR with seven primer pairs per reaction produced more clearly defined bands (figure 52). The band for exon 30, which was not easily visible in the 12 primer pair reaction, was more defined in the seven primer pair reaction. Exon 62 and exon 20 were included in one of the two PCR reactions and a different primer pair was used for the amplification of exon 44. All primer sequences are outlined in Appendix A.

In the above image (figure 52), patient 42 was shown to have a single exon 45 deletion, which might not be a deletion but a single nucleotide polymorphism, pathogenic point mutation or a primer site polymorphism.
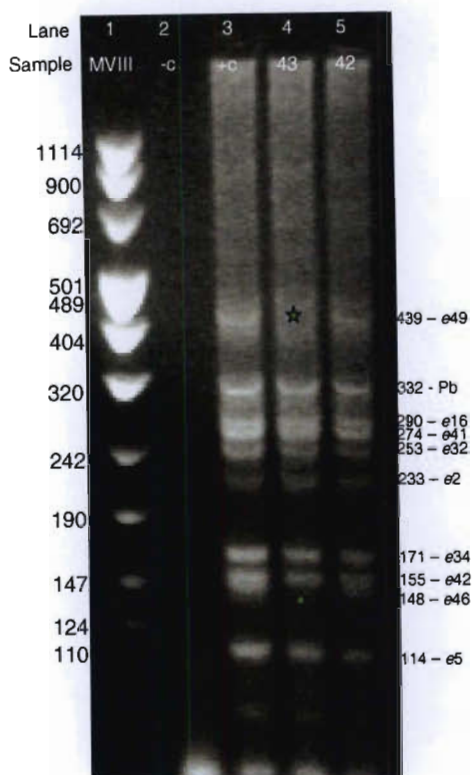
**Figure 53: Representative image of the third multiplex PCR set adapted from Kunkel *et al.*(1991) showing deletions of exons 49 and 46 in patient 43.**

In the above multiplex PCR reaction, 10 primer pairs were included. This reaction was performed on the DNA sample from the patient during the optimisation procedure, hence the increase in the number of primers used. In this patient, the results fit together neatly to provide an overall representation of the actual deletion in the patient.

Collating the data from all three multiplex PCR sets, the patient (as shown in the figure below) was shown to have a deletion from exons 47-52.
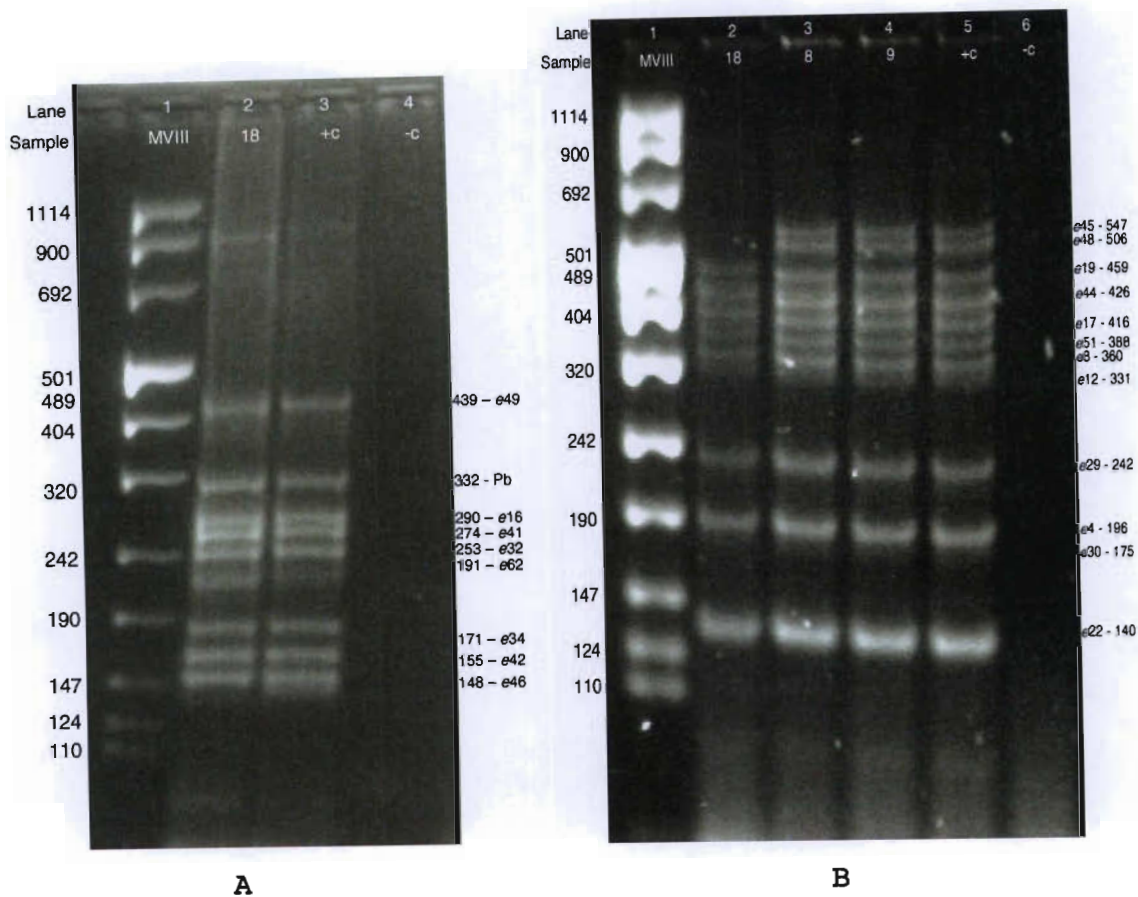
**Figure 54: Image of set 3 (A) and set 1 (B) multiplex PCRs for patient 18, showing exons 45 and 48 deletion.**

## 5.4.2 Deletion confirmation using duplex PCR
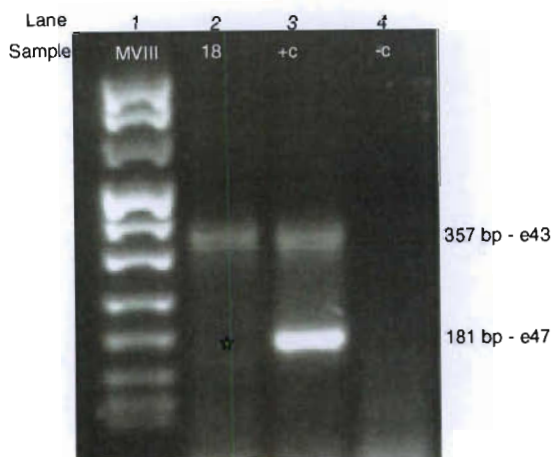


**Figure 55: Image of a single exon PCR showing an exon 47 deletion in patient 18.**

Initially it was assumed that the patient had a deletion from exon 45-52, however exon 46 was present as is shown by the band in figure 54 (A). It was therefore concluded that the
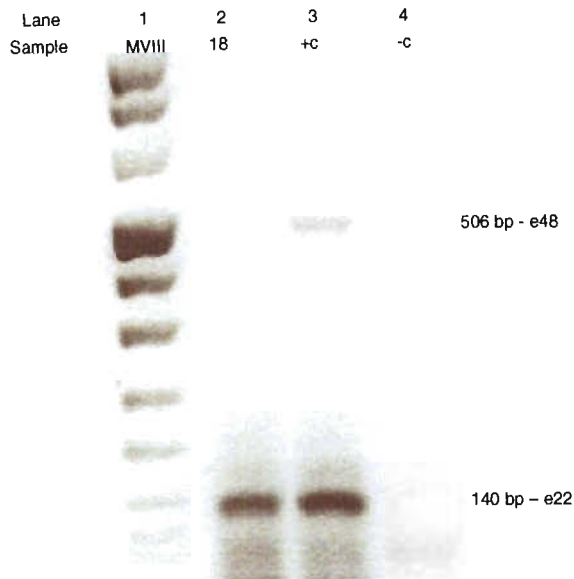
**Figure 56: Image of a single exon PCR showing an exon 48 deletion in patient 18.**

exon 45 deletion may have resulted from a primer site polymorphism hence the appearance

of a deletion when multiplex PCR was performed.

**Table 23: Deletion data obtained for the patients that were included in the study. This was assessed by analysing the multiplex PCR results when 30 exons in the dystrophin gene were tested for deletions.**

| Sample number | Surname, Initials | Deletion | Frame of deletion |
|---|---|---|---|
| 2 | S, W | No deletions | |
| 8 | S, T | No deletions | |
| 9 | S, NM | No deletions | |
| 12 | G, S | 20-29 and 52-60 (20,29,52,60) | |
| 14 | N, D | No deletions | |
| 16 | M, T | No deletions | |
| 18 | R, J | 47-48 | In-frame |
| 19 | M, S | 8-16 (8,12,13,16) | Out-of-frame |
| 20 | M, S | 45-60 (45,48,49,50,52,60) | In-frame |
| 21 | R, S | 45-60 (45,48,49,51,52,60) | In-frame |
| 22 | N, N | No deletions | |
| 23 | H, ZM | 50-52 (50,51,52) | Out-of-frame |
| 24 | P, D | No deletions | |
| 25 | R, D | No deletions | |
| 26 | Z, S | 45-47 (46,45,47) | In-frame |

| | | | |
|---|---|---|---|
| 27 | L, L | No deletions | |
| 28 | M, MB | No deletions | |
| 29 | N, C | 48-50 (48,49,50) | Out-of-frame |
| 30 | W, R | No deletions | |
| 31 | C, L | No deletions | |
| 32 | M, NL | 46-50 (46,47,48,49,50) | Out-of-frame |
| 33 | G, P | No deletions | |
| 34 | N, M | No deletions | |
| 35 | S, G | No deletions | |
| 36 | H, XV | No deletions | |
| 37 | G, M | 51 | |
| 38 | N, M | 45-52 (45,46,47,48,49,50,51,52) | Out-of-frame |
| 39 | S, T | No deletions | |
| 40 | S, C | No deletions | |
| 41 | M, S | No deletions | |
| 42 | M, R | 45 | |
| 43 | S, V | 45-52 (45,46,47,48,49,50,51,52) | Out-of-frame |
| 44 | C, L | No deletions | |
| 45 | M, T | No deletions | |
| 46 | M, S | No deletions | |
| 47 | M, ST | No deletions | |
| 48 | M, S | No deletions | |
| 49 | M, W | 45-52 (45,46,47,48,49,50,51,52) | Out-of-frame |
| 50 | N, T | No deletions | |
| 51 | H, N | No deletions | |
| 52 | K, TP | No deletions | |
| 53 | V, S | 45-52 (45,46,47,48,49,50,51,52) | Out-of-frame |
| 54 | B, N | No deletions | |
| 55 | F, S | No deletions | |
| 56 | S, T | No deletions | |
| 68 | N, S | Deletions 47-52 | Out-of-frame |

## 5.5 DISCUSSION

### 5.5.1   Multiplex PCR sets

The multiplex PCR set that was adapted from the Beggs *et al.* (1990) set was the most

reproducible in comparison to the other two multiplex PCR sets. All 10 primers pairs

always produced defined and high resolution bands. This suggests that the 10 primers used in this set work best together with the least amount of competition between primers noted. There is also a wider separation between the fragment sizes, therefore making interpretation easier and more definite. Such a consideration would be important in a diagnostic setting.

The overall recommendation for a diagnostic laboratory that already has the primers for multiplex PCR would be to separate set 1 (adapted from Chamberlain *et al.*, 1988) into two reactions, with six or seven primer pairs per reaction, leave the 10 primer pairs in set 2 (adapted from Beggs *et al.*, 1990) and include either 8 or 9 primer pairs in set 3 (adapted from Kunkel *et al.*, 1991). The researcher should also use the Platinum (Invitrogen) set of reagents as our multiplex PCRs were optimised using these reagents and amplification was relatively high. Various other *taq* polymerases were tested and none produced fragments of comparable quality to those obtained with Platinum reagents.

Single PCRs should generally be included as confirmation of a deletion found using multiplex PCR. In some instances, competition between primers makes it difficult to visually detect a band for an exon, which may be interpreted as a deletion, when in effect it was faint and not visible to the naked eye.

### 5.5.2 Comparison between 12 and 7 primer pair reaction in set 1 (adapted from Chamberlain *et al.*, 1988; Chamberlain *et al.*, 1990).

When the seven primer pair reactions were compared to the 12 primer pair reactions more defined bands were evident in the seven primer pair reactions. Even though it is more

expensive to run two reactions instead of one, finding ill-defined bands in a 12 primer pair reaction would make it necessary to perform single PCR reactions. If the bands are easy to view, the researcher would not have to perform single PCR reactions to confirm the results. Running single PCR reactions may prove to be even more expensive than performing two multiplex PCR reactions.

### 5.5.3 Gel electrophoresis

Several different types of agarose gels were tested and compared to determine which produced the highest resolution bands with the least effort during the preparation. By using a product that is not fragile, results could be obtained immediately and without the need to repeat the electrophoresis on account of broken gels, which is a common occurrence with multiplex PCR electrophoresis.

When the different agarose gels were compared, the NuSieve gel (FMC, Cambrex) was found to be the most robust gel that was easier to use than other products such as the MetaPhor gel. The NuSieve gels did not produce as many air bubbles as the MetaPhor gels therefore ensuring that tight and good quality bands were obtained. The final recommendation would be to incubate the gel for half hour in a 60°C water bath, which has been shown to remove all air bubbles.

### 5.5.4 Efficacy of deletion detection

In the hope of improving the diagnostic efficacy, this 30-plex PCR was optimised for our laboratory.

By collating all the data, we conclude that the 30-exon multiplex PCR did not increase the number of patients that were shown to have deletions using the conventional Chamberlain and Beggs 18 exon multiplex PCR assays. The 30-plex PCR that was implemented in our laboratory improved the diagnostic efficacy by determining the deletion breakpoints in patients where there appeared to be more than one deletion. We were able to detect the start and end exons of the deletion using this screening method. Such a method is important to confirm the clinical diagnosis of DMD or BMD. If the exons involved in the deletion are known, the frame of the deletion can be determined using the frame-checker software from Leiden University Medical Center, Leiden, The Netherlands (www.dmd.nl). Both clinical and molecular data can be collated and the progression of the patient can be determined. This may be especially useful in children. If the patient had an out-of-frame deletion, the clinician may be able to predict that the progression of the disease would be more rapid than a patient found to have an in-frame deletion. This might also influence the decision to adopt more aggressive management of an out-of-frame deletion using other available options such as exon-skipping therapy. The exon skipping therapy may be able to convert the out-of-frame deletion into an in-frame deletion and in so doing this may reduce the severity of the clinical outcome (Aartsma-Rus et al., 2003).

Patient 42 was found to have a single exon 45 deletion, which is unusual. The exon may have appeared to be deleted owing to a primer site polymorphism, creating the false impression of a deletion by virtue of non amplification. The other possibility is that there could be a single nucleotide polymorphism (SNP) in that exon that once again appears as a deletion on multiplex PCR. The last possibility is that there could be a pathogenic point mutation that is disease causing. To confirm the presence or absence of a SNP or point mutation one would have to perform DNA sequencing on the exon using other primers that

extend further out into the intron to obtain a complete exon fragment. DNA sequencing was not performed on the DNA of this patient.

Genotype-phenotype correlations have been a topic of debate since the dystrophin gene was first discovered and characterised. Many groups have attempted to correlate disease severity with deletions that were found (Beggs *et al.*, 1991; Baumbach et al., 1989). As more sophisticated techniques and technology was developed so to did the ability to predict genotype-phenotype correlations.

There appears to be a few patients that have a single exon deletion. This might not be a true deletion as the exon may appear to be deleted on multiplex PCR on account of a single nucleotide polymorphism in the exon itself or there could be a SNP in one of the primers. Such exonic "deletions" should be tested using a new set of primers to confirm that the exon is in fact deleted. Once a PCR product has been obtained it could then be subjected to DNA sequencing.

# CHAPTER 6

## THE MULTIPLEX LIGATION-DEPENDENT PROBE AMPLIFICATION (MLPA) ASSAY AS A METHOD TO DETECT DELETIONS AND / DUPLICATIONS THROUGHOUT THE 79 EXONS OF DYSTROPHIN

### 6.1 INTRODUCTION

MLPA or the multiplex ligation-dependent probe amplification assay is a technique that utilises the power of PCR by simultaneously quantitating and detecting up to 40 different target sequences. The technique was first described by Schouten *et al.* (2002) and used the related technique MAPH (multiplex amplifiable probe hybridisation) as the foundation on which it was built. The two techniques are similar in that oligonucleotide probes added to the reaction are amplified instead of the actual target sequences being subjected to the PCR procedure. In this way, one ensures that cross-contamination between targets is minimised.

The MAPH technique involves hybridisation of probes to immobilised samples, followed by a series of stringent wash steps to remove unbound probes, which are potentially amplifiable. In comparison the MLPA assay does not require immobilisation of sample nucleic acids and the excessive washing steps necessary in the MAPH procedure.

The MAPH procedure, which was developed in 2000, preceded the MLPA procedure. The probes for the MAPH procedure were initially created from cloning fragments into a vector of choice (Armour *et al.*, 2000). Probe preparation involved amplification of the target

sequence from the vector using specific primers, which is a laborious task (White, 2005).

In 2003, the method of probe design was changed from cloning to a procedure using

BLAST (Altschul *et al.*, 1990) and primer design software such as Primer 3

([http://frodo.wi.mit.edu/](http://frodo.wi.mit.edu/)) where specific sequences for the gene of interest were created

and each was flanked with M13 synthetic primer sites (Reid *et al.*, 2003). This

methodology also incorporated FAM-labelled M13 primers, which allowed the amplicons

to be electrophoresed on the ABI 377. Even though the MAPH procedure is efficient and

useful for detecting deletions and duplications in large genes, there still exists the problem

of additional products being amplified in the original PCR reaction from genomic DNA

(White, 2005). Other reasons for MLPA now being the method of choice in many mutation

detection laboratories around the world is the small of amount of DNA (100 ng) required

for amplification as opposed to 1 µg for MAPH (White, 2005).
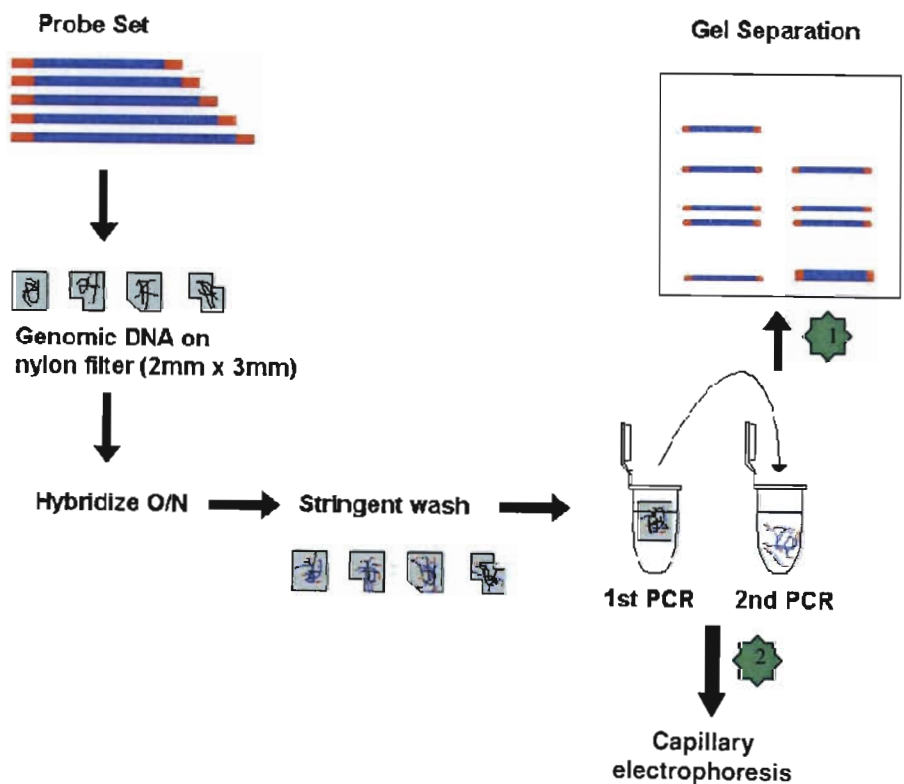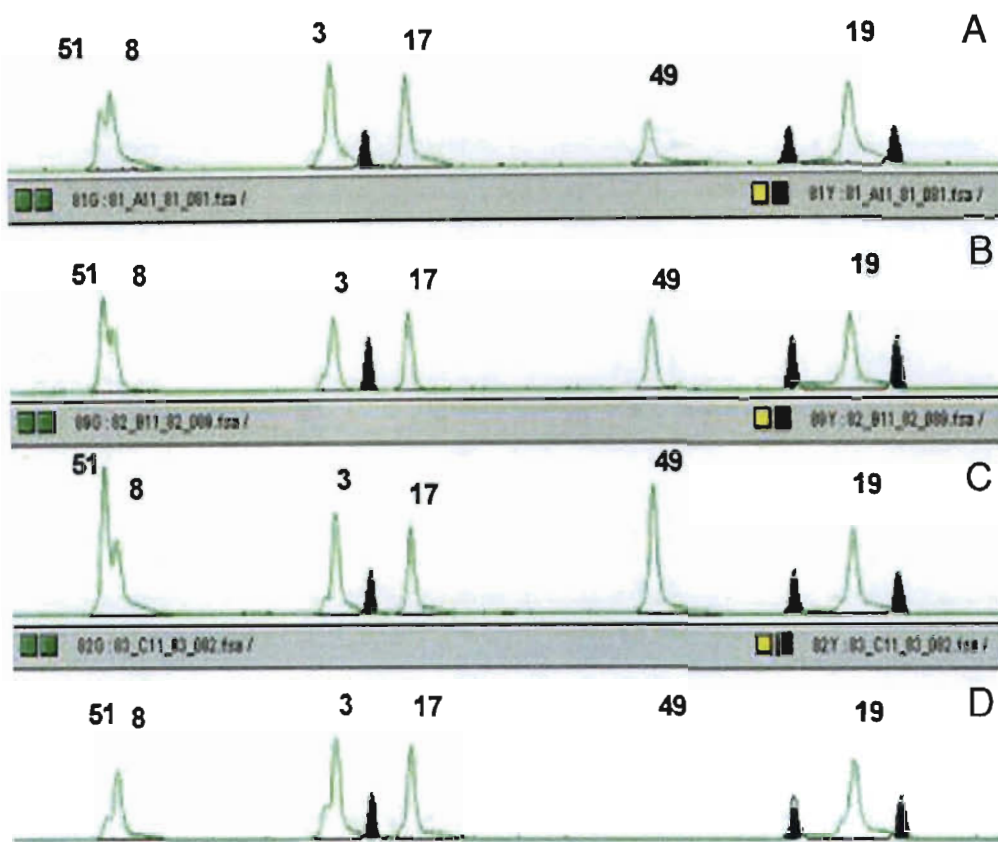
**Figure 57: Image representing the multiplex amplifiable probe amplification assay as adapted from www.dmd.nl and Armour *et al*. (2000). The products can either be separated using polyacrylamide gel electrophoresis (1) or capillary electrophoresis (2) using an ABI genetic analyser.**

The MLPA assay is based on the hybridisation of commercially designed and available probes to target sequences, which are subsequently ligated and quantitatively amplified to produce a copy of the target sequence. The simultaneous amplification of the reactions results in a useful multiplex set of fragments being produced, which can then be analysed for exonic deletions and duplications in the gene being studied. Since all fragments are created in the same reaction, analysis is simplified and no normalisation of any sort needs to be undertaken to account for thermocycler or PCR reaction differences. The MLPA probe itself consists of two parts, which includes a "short synthetic oligonucleotide" containing a "target specific sequence at the 3' end" composed of 21 to 30 nucleotides and a "common 19 nucleotide (nt) sequence that is identical to the labelled PCR primer at the

5' end" whilst the other part of the probe consists of a "M13 derived long" oligonucleotide probe (as shown in the figure below). The long probes are produced by inserting a target specific sequence of between 25 and 40 nucleotides into M13 derived "SALSA" vectors, containing a "stuffer" sequence of different lengths (Schouten *et al.*, 2002). A detailed description of the MLPA procedure and probe production is outlined in Schouten *et al.* (2002).
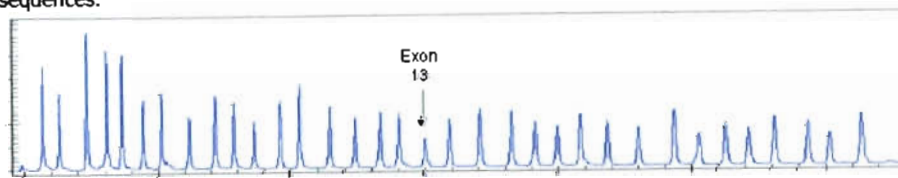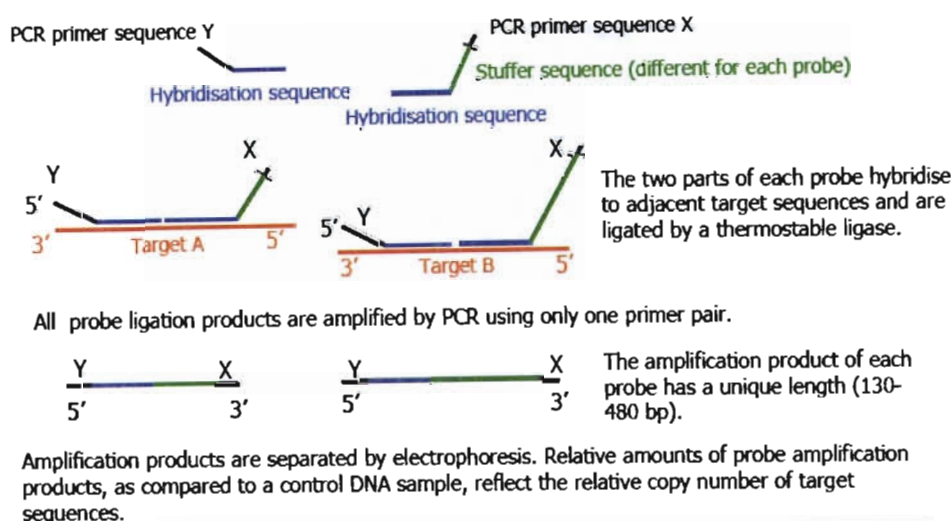


**Figure 58: Outline of the multiplex ligation dependent probe amplification assay as adapted from Schouten *et al.* (2002) and http://www.mlpa.com.**

According to Schouten *et al.* (2002), the MLPA procedure required that the genomic DNA be diluted with buffer TE (Tris-EDTA) and heated for 5 minutes at 98°C. This was followed by the inclusion of a salt solution together with the probe mixture, each of which was 1.5 µl volumes. The samples were re-heated for 1 minute at 95°C and incubated at 60°C for 16 hours. Even though this 16 hour incubation would be optimal for obtaining all fragments especially longer products, a reduction in the incubation period has been tested and found to produce the same results as those samples incubated for the 16 hour duration

by the Molecular diagnostics laboratory headed by Professor E. Bakker. The reduced incubation time was adopted by the author and implemented at the Neuroscience laboratory. According to White (2005), the PCR volume could be reduced to 25 µl from the original 50 µl reaction volume that was proposed by Schouten *et al.* (2002). The original protocol suggests that the ligation reaction be performed in a total volume of 50 µl, whereas only 10 µl of the ligation mixture would be included in the amplification reaction. By reducing the hybridisation and ligation reaction to a volume sufficient to achieve one PCR reaction per sample, minimal wastage of sample and probe mixes is assured.

Separation of the amplifications products from the MLPA reaction is performed using a capillary electrophoresis apparatus, such as the ABI genetic analysers (Applied Biosystems). Once the samples have been separated using a genetic analyser, the results are viewed using the Genemapper software program (Applied Biosystems). Even though exonic deletions can be detected visually as there would be the absence of a peak, detection of duplications is be more complicated. The data extracted from the software, which could either be the peak areas or the peak heights, are exported into an Excel spreadsheet for further analysis by the researcher. The peak areas or peak heights from patient samples are compared to the results from the samples of normal individuals using the student's T-test as the statistical method to produce a dosage quotient analysis. According to White *et al.* (2003), sample analysis can be performed using the Agilent lab-on-a-chip Bioanalyser 2100, where 12 samples could be analysed using a single chip. Such an option may suit many laboratories as fluorescently labelled primers are not required and the results are obtained in under an hour.

Aartsma-Rus *et al.* (2006) performed an evaluation of all the mutation data that was present on the Leiden muscular dystrophy pages (http://www.dmd.nl) that amounted to >4700 mutations. Intragenic deletions were found to be most common totally approximately 72%, which is slightly higher than the literature consensus of 65%. Majority of these deletions appear to cluster in a hot-spot region of the dystrophin gene spanning exons 45-53. In the case of duplications, there may be either single exon or multi-exon duplications and these are found in 7% of cases. As was reported by White *et al.* (2006) the most commonly duplicated exon is exon 2, which collectively made up 6% of the duplications in the database. Duplications are located in the minor mutation hot-spot spanning exons 2-20, which is in contrast to the location of deletion mutations (Aartsma-Rus *et al.*, 2006).

The MLPA assay was observed, learned and performed at the research laboratory in the Department of Human and Clinical Genetics, Leiden University Medical Center, The Netherlands under the supervision of Dr. Stefan White.

During the author's visit to the research laboratory in the Department of Human and Clinical Genetics, Leiden University Medical Center, The Netherlands she met and liaised with her scientific supervisor, Professor E. Bakker who is the head of the Molecular Genetics Laboratory where the MLPA assay was being implemented as a diagnostics assay. It was at this time that the author obtained feedback on the manner in which the diagnostics laboratory had implemented the assay in their setting, which was different from the approach used by the research laboratory in the Netherlands.

The MLPA assay was set-up at the Neuroscience laboratory, Durban, South Africa using

the knowledge gained from both the research and diagnostics laboratories at the Center for

Human and Clinical Genetics in the Netherlands. The DNA samples were electrophoresed

using the ABI 3100, on the author's return to South Africa. The subjects were chosen by

virtue of DNA availability and non-deletion status in the case of DMD/BMD patients.


## 6.2    AIMS AND OBJECTIVES


i)    To detect deletions and duplications throughout the dystrophin gene in
      Duchenne and Becker muscular dystrophy patients.

ii)   To determine the carrier status in mothers and female relatives of
      dystrophinopathy patients and thereby implement genetic counselling.


## 6.3    MATERIALS AND METHODS

### 6.3.1    Patient population


**Table 24: Database showing details of all individuals included in the multiplex ligation-
dependent probe amplification assay aspect of the project.**

| DNA number | Surname, Initials | Age | DMD/BMD/RELATIVE |
|---|---|---|---|
| 6 | H, S | N/A | Mother of 7 |
| 7 | H, J | 8 | DMD |
| 9 | S, NM | 17 | DMD |
| 14 | N, D | 9 | DMD |
| 15 | N, C | N/A | Mother of 14 |
| 19 | M, S | 6 | DMD |
| 21 | R, S | 8 | DMD |
| 24 | P, D | 6 | DMD |
| 26 | Z, S | 18 | BMD |
| 30 | W, R | N/A | DMD |
| 31 | C, L | 12 | DMD |
| 32 | M, NL | 6 | DMD |
| 37 | G, M | 8 | DMD |

| 38 | N, M | 14 | DMD |
|----|------|-----|-----|
| 42 | M, R | 12 | DMD |
| 43 | S, V | 14 | DMD |
| 57 | M, T | N/A | F mother of 28 |
| 58 | M, M | 14 | DMD |
| 59 | B, X | 10 | DMD |
| 60 | N, S | 12 | DMD |
| 61 | L, M | 8 | DMD |
| 62 | S, S | N/A | DMD |
| 63 | S, N | 25 | BMD Carrier F |

**Legend: N/A – not available**

## 6.3.2 DNA extractions

The DNA blood mini kit (Qiagen) was used to isolate DNA from the blood samples of patients. The procedure followed was as per manufacturer's instructions (Qiagen, 2003).

## 6.3.3 DNA quantification

Two methods of quantification were employed. The first used the Nanodrop 1000, which was housed at the Department of Human and Clinical Genetics, Leiden University Medical Center, the Netherlands.

The second method made use of commercially available DNA quantification standards (Invitrogen) that were quantitated against the DNA from patients' samples. This method was employed as the Neuroscience laboratory did not have a Nanodrop instrument. The samples were electrophoresed on a 1% agarose gel (Seakem) at the Neuroscience laboratory, University of KwaZulu-Natal, Durban, South Africa. The same procedure was followed as was previously outlined in Chapter 4 of this thesis.

### 6.3.3.1 Quantification using the Nanodrop-1000

The procedure followed was as outlined in the Nanodrop manual.

### 6.3.4 Vacuum centrifugation of DNA samples

The procedure was carried out as per manufacturer's instructions (Eppendorf).

### 6.3.5 DNA denaturation

The procedure was carried out as per manufacturer's instructions (MRC-Holland).

### 6.3.6 Hybridisation of the SALSA-probes (MRC-Holland)

The procedure was carried out as per manufacturer's instructions (MRC-Holland). Amendments to the protocol were as follows:

- The recommended volume of the SALSA probe mix by MRC-Holland was 1.5 μl per sample and 0.375 μl at the diagnostics laboratory. On the author's return to South Africa both volumes (1.5 μl and 0.375 μl) were compared.
- A master mix was prepared for all sample reactions as shown in table 25.
- The mixture was incubated in a thermal cycler at 95°C for one minute. This was followed by incubation at 60°C for three hours. The recommended length of time for the 60°C incubation was 16 hours by MRC-Holland, and three hours at the diagnostics laboratory in the Netherlands. The author therefore utilised this optimised time period when the procedure was implemented in South Africa.

**Table 25: Table showing the master mix reaction volumes for the SALSA-probes hybridisation to the sample DNA.**

| Reagent | Volume per reaction (μl) Diagnostics laboratory | Volume per reaction (μl) Research laboratory |
|---|---|---|
| SALSA-probe mix | 0.375 | 1.5 |
| SALSA MLPA buffer | 0.375 | 1.5 |
| Nuclease free water | 0.25 | 0 |

### 6.3.7 Ligation reaction

- During the hybridisation procedure at 60°C, a master mix was prepared for the ligation reaction less than one hour prior to use and stored on ice to prevent degradation of the ligase enzyme.

- Prior to the end of the three hour incubation at 60°C, the temperature in the thermal cycler was reduced to 54°C.

**Table 26:      Ligation reaction master mix that was added to the hybridised sample mix whilst at 54°C.**

| Reagent | Volume per reaction (μl) Diagnostic laboratory | Volume per reaction (μl) Research laboratory |
|---|---|---|
| Ligase-65 buffer A | 0.75 | 3.0 |
| Ligase-65 buffer B | 0.75 | 3.0 |
| Nuclease free water | 6.25 | 25.0 |
| Ligase-65 | 0.25 | 1.0 |

- Whilst the thermal cycler was at 54°C, either a 32 μl volume (MRC-Holland and research laboratory protocol) or an 8 μl volume (diagnostics laboratory protocol) of ligation mix was added to the hybridised mixture. The ligation mixture was incubated at 54°C for 15 minutes. This was followed by a five minute incubation at 98°C. This incubation served to inactivate the ligase enzyme.

- At this point, the samples could be stored at 4°C for 48 hours awaiting the PCR reaction or it could be stored at -20°C for a longer time period. However the

166

recommendation was to start the PCR reaction immediately as this would ensure that the best results were obtained.

## 6.3.8 PCR reaction and conditions

- A master mix was prepared as shown in the table below for the PCR reaction less than one hour prior to being used.

**Table 27: Table showing the PCR reaction volumes of each reagent that was added to the ligation mixture.**

| Reagent | Volume per reaction ($\mu$l) Diagnostic laboratory | Volume per reaction ($\mu$l) Research laboratory |
|---|---|---|
| 10 × SALSA PCR buffer | 2.0 | 4.0 |
| Nuclease free water | 15.75 | 31.5 |
| SALSA PCR primers | 1.0 | 2.0 |
| SALSA enzyme dilution buffer | 1.0 | 2.0 |
| SALSA polymerase | 0.25 | 0.5 |

- The SALSA polymerase enzyme was added to each master mix whilst on ice. The contents were mixed well by pipetting but no vortexing was performed. It was important that the contents be thoroughly mixed as incomplete mixing of the 50% glycerol enzyme solutions with the dilution buffers is usually a major source of error.

- The PCR conditions that were employed varied depending on the protocol that was used. The table below show the conditions used in the diagnostic laboratory protocol. The MRC-Holland protocol differed in that the denaturation time was 30 seconds as opposed to 20 seconds and the cycle number was increased to 35 cycles.

- The PCR apparatus was placed on "hold" at 60°C whilst the 10 µl volume of ligation product was added to the PCR master mix. Thereafter the PCR program

with the conditions listed below was implemented.

**Table 28: Table illustrating the PCR conditions used in the optimised diagnostic laboratory multiplex ligation-dependent probe amplification assay.**

| | Temperature | Time | Cycle number |
|---|---|---|---|
| Denaturation | 95°C | 20 seconds | 33 |
| Annealing | 60°C | 30 seconds | |
| Elongation | 72°C | 60 seconds | |
| Final Extension | 72°C | 20 minutes | 1 |
| Hold | 4°C | ∞ | |

- The PCR products were now referred to as amplicons, which is potentially a source of contamination. The PCR tubes were therefore not opened in the amplification room in the vicinity of other thermal cyclers. Instead they were transferred to the electrophoresis room where they were stored at 4°C for 48 hours, -20°C for longer periods of time or used immediately for the electrophoresis procedure.

### 6.3.9 Performing spacial calibration on the ABI 3100

The procedure followed was as outlined in the Applied Biosystems manual.

### 6.3.10 Setting up spectral dyes on the ABI 3100

The procedure followed was as outlined in the Applied Biosystems manual.

### 6.3.11 Electrophoresis of samples on the ABI 3100

- A heating block that could house a 96-well plate was adjusted to 95°C in the electrophoresis room. If this was not present, a heating block that could house

168

0.5 ml centrifuge tubes was used. All reactions were performed in the electrophoresis room as the amplicons are a source of contamination and should not be carried into other rooms.

- The number of samples to be electrophoresed was determined. A master mix of the ROX-500 (Applied Biosystems) internal standard and deionised formamide (HiDi formamide, Applied Biosystems) was prepared depending on the number of samples that were to be run on the ABI 3100. A 0.5 µl volume of ROX-500 was added to 7.5 µl HiDi formamide. To each master mix was added 2.0 µl sample.

- The mixture was heated for five minutes at 95°C and immediately cooled on ice for two minutes. The samples were pulsed centrifuged to collect the contents at the bottom of the tube. A 10 µl volume of samples were then placed into a specific pattern using a 96-well plate as this plate was to be placed into the autosampler of the ABI 3100 for electrophoresis.

### 6.3.12 Run conditions for DMD samples on the ABI 3100

The procedure followed was as outlined in the Applied Biosystems manuals and the handout provided by MRC-Holland. Amendments to the protocol were as follows:

### 6.3.13 Data analysis and creation of bins for each exon using Genemapper software

The procedure followed was as outlined in the Applied Biosystems Genemapper software manual and the handout provided by MRC-Holland.:

### 6.3.14 Further analysis using the Excel spreadsheet

For further analysis to be undertaken the peak heights or peak areas can be exported from the Genemapper software into an Excel spreadsheet by copying the values and transferring it across to the Excel program.

On visual inspection, an exonic deletion can be seen once the sample is viewed in the Genemapper software program. An exonic duplication however cannot be definitively detected using the visual method. The values therefore need to be exported into Excel and using the student's T-test methodology a duplication can be confirmed. In all cases, the values of two control samples are compared to the values obtained for each DMD sample. Using the dosage quotient analysis method, a duplication is defined as a mutation where the value obtained is >1.5 however in reality the value is usually closer to >1.65. The cut-off values for duplications vary from one lab to another and care should be taken to repeat the sample when a duplication is thought to be present.

If there is a deletion present and confirmation is required by inserting the values into the Excel spreadsheet in addition to visual inspection, the value obtained would be <0.5 in an ideal situation. In reality the value would be closer to <0.65.

### 6.4    RESULTS

### 6.4.1    DNA quantitation using quantification standards
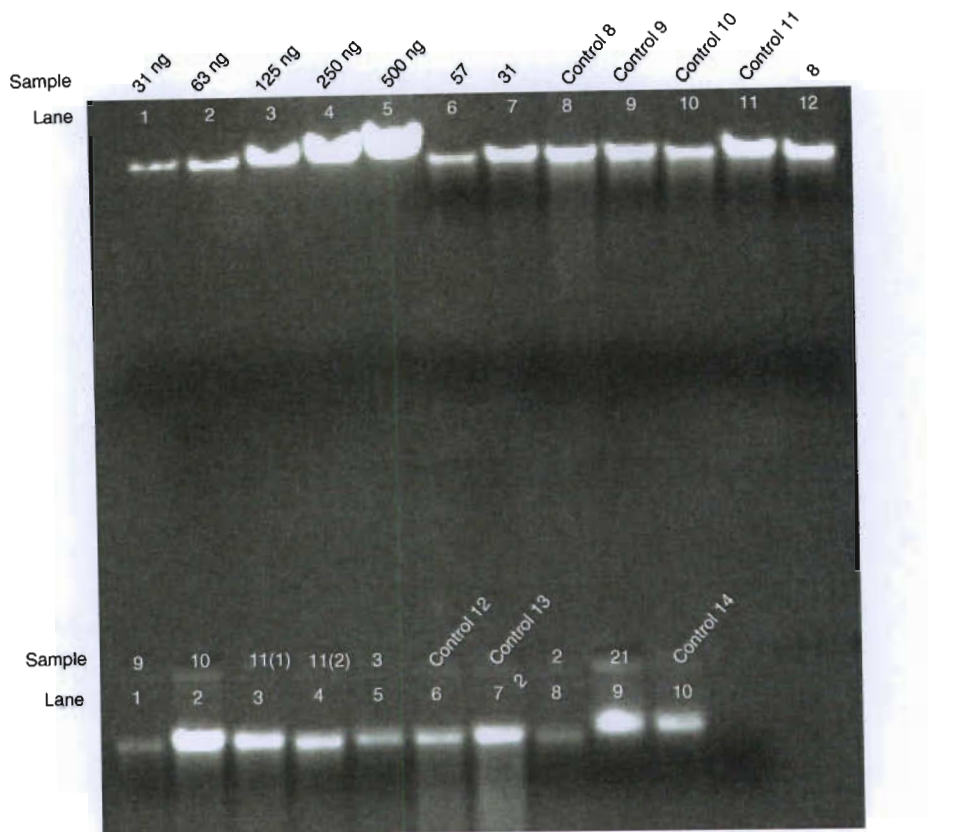
**Figure 59: Representative image showing DNA samples that were electrophoresed on a 1% agarose gel together with DNA quantification standards (Invitrogen).**

## 6.4.2 Spacial calibration
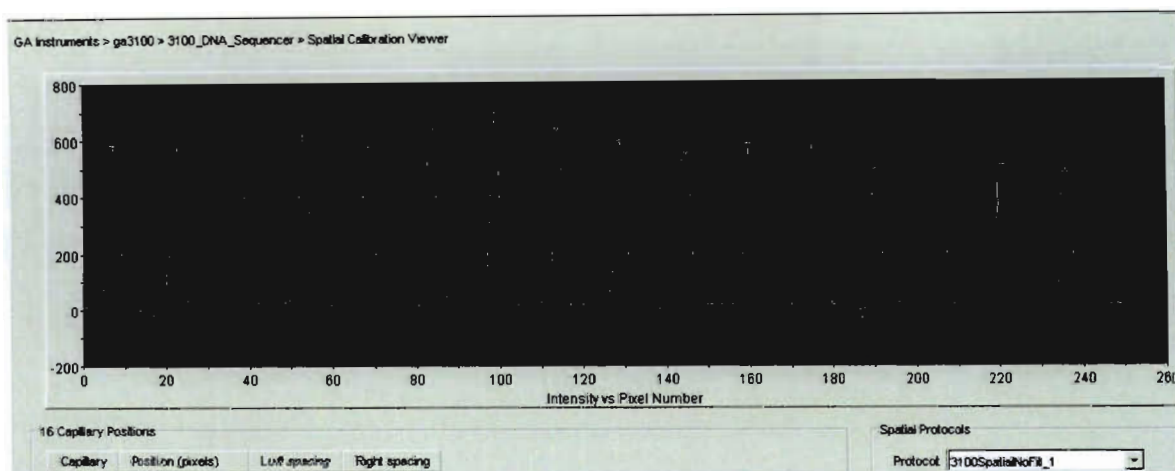


**Figure 60: Graphical representation of a poor spacial that was obtained when the calibration was performed on the ABI 3100.**

The poor spacial resulted from a condensation on the detection window that prevented

clear data from being obtained. The condensation occurred as a result of the humid

environment of the Durban climate as well as the assembly of the capillary array in a cold state. The cold state of the detection window caused droplets to be present on the window thereby preventing a clear spacial from being obtained. The detection window was cleaned several times with 100% HPLC grade methanol and still the poor spacial was produced. Several applied biosystems applications specialists tried to solve the problem over a period of 6-8 weeks during which time several capillary arrays were tried and none of them worked. The problem was finally solved by removing the capillary array from the 4°C fridge and leaving it at room temperature for at least one hour to allow it to equilibrate to room temperature before it was assembled onto the instrument.

All further spacial runs produced good quality peaks that were all in the recommended range. The heights of all capillaries were similar and no shoulders were obtained.

### 6.4.3    Spectral calibration run

Under normal circumstances the spectral run would give a fluorescence intensity of approximately 4000, however in the above representative image the value is only 100. The fluorescence intensity is extremely low as is shown above. Such a value is indicative of a spectral data that is unusable. Prior to the spectral being re-run all steps were taken to ensure that the calibration would work such as cleaning the detection window on the capillary array with methanol. It turned out that the detection window was moist from condensation owing to it being left in the refrigerator. Once the problem was solved, all the spectral runs were of high quality and the intensity values were in the range of 3000-4000. The Q-values were acceptably high being in the range of >0.98 and the condition number was within range for fragment analysis (4-7).
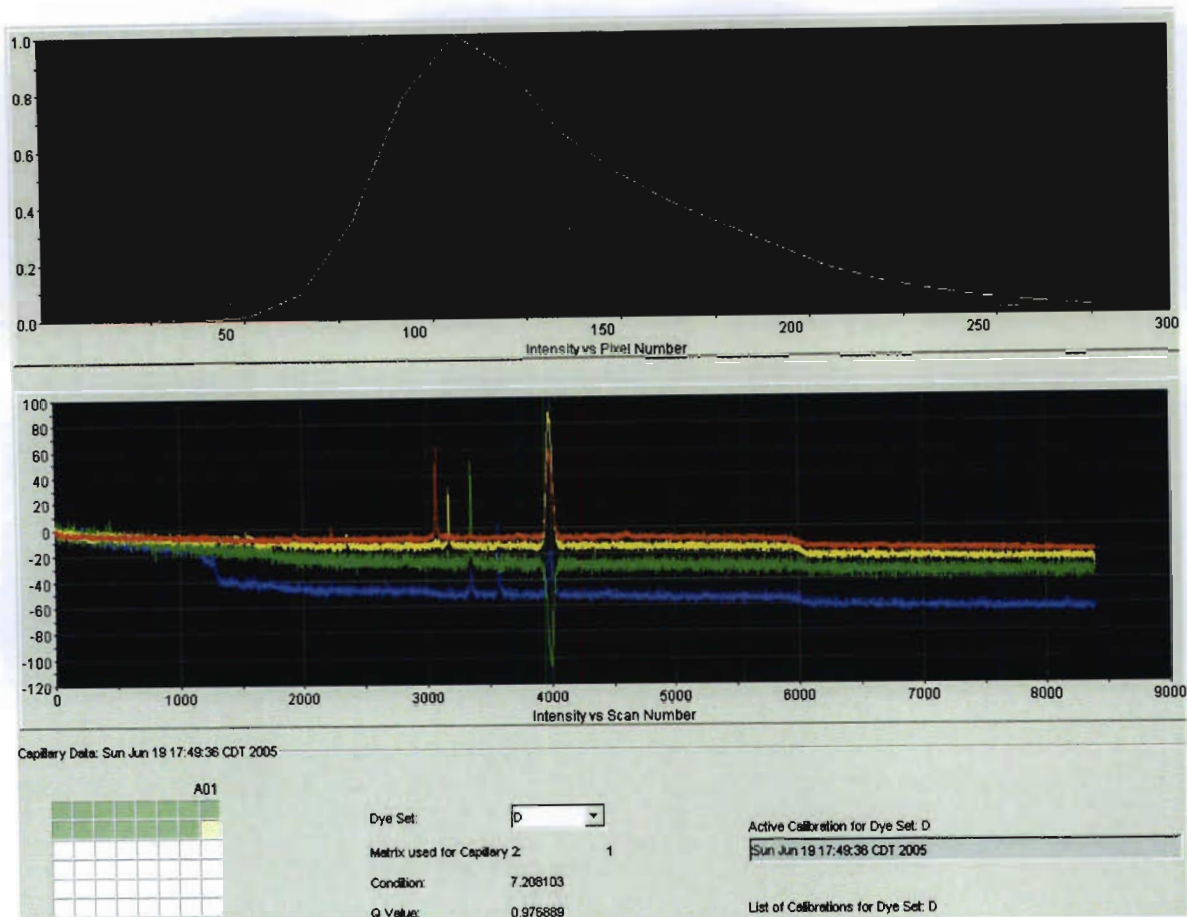
**Figure 61:** Image showing a poor spectral calibration that was obtained on the ABI 3100 using Dye set D for fragment analysis.

### 6.4.4 Electropherogram of all exons present in control

In the electropherograms below, each peak represents an exon. The signal intensity is shown on the right (oval shape). The ideal peak heights should be in the dynamic range of 1000-4000 RFU (relative fluorescence units), which is necessary for data validation and usability. For those that are <1000, one should manually view them in order to determine whether other characteristics are met, such as evenness and sharpness of the peak. The baseline should also be relatively flat. Signal strength is an essential factor when results are being confirmed. If the signal is below average or low the process of electrophoresis would first need to be repeated. If the signal still turns out to be lower than the normal cut-off value, the amplification step would be repeated and the amount of starting material would

be reassessed and usually increased thereby ensuring an increase in the peak signal
intensity.
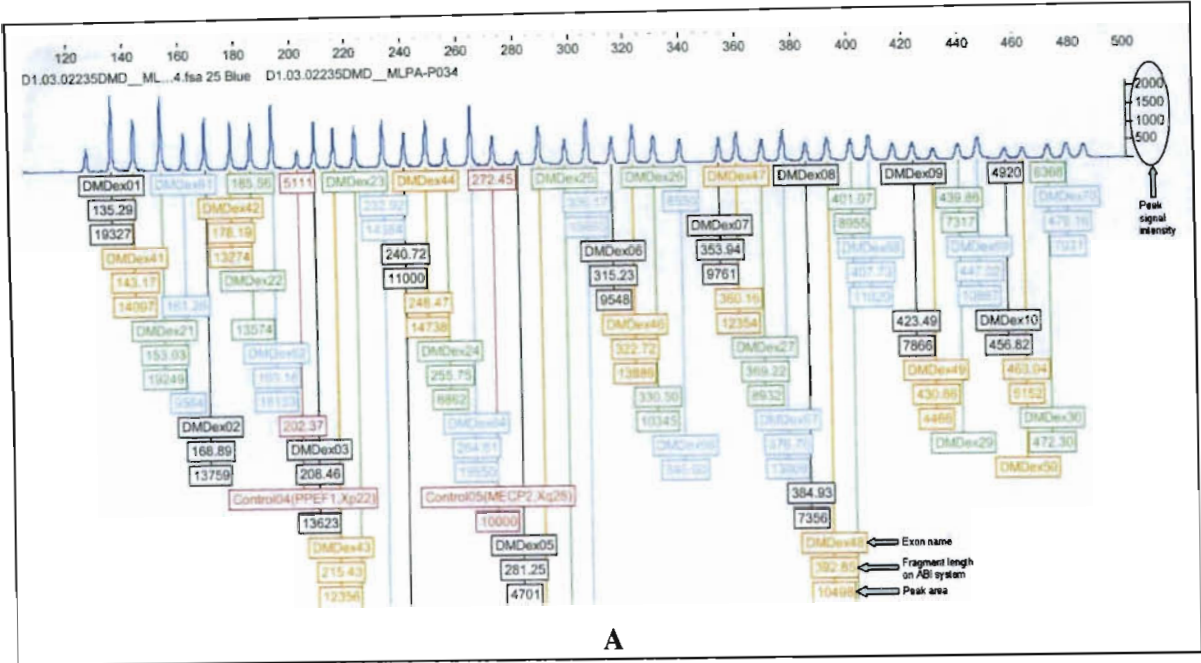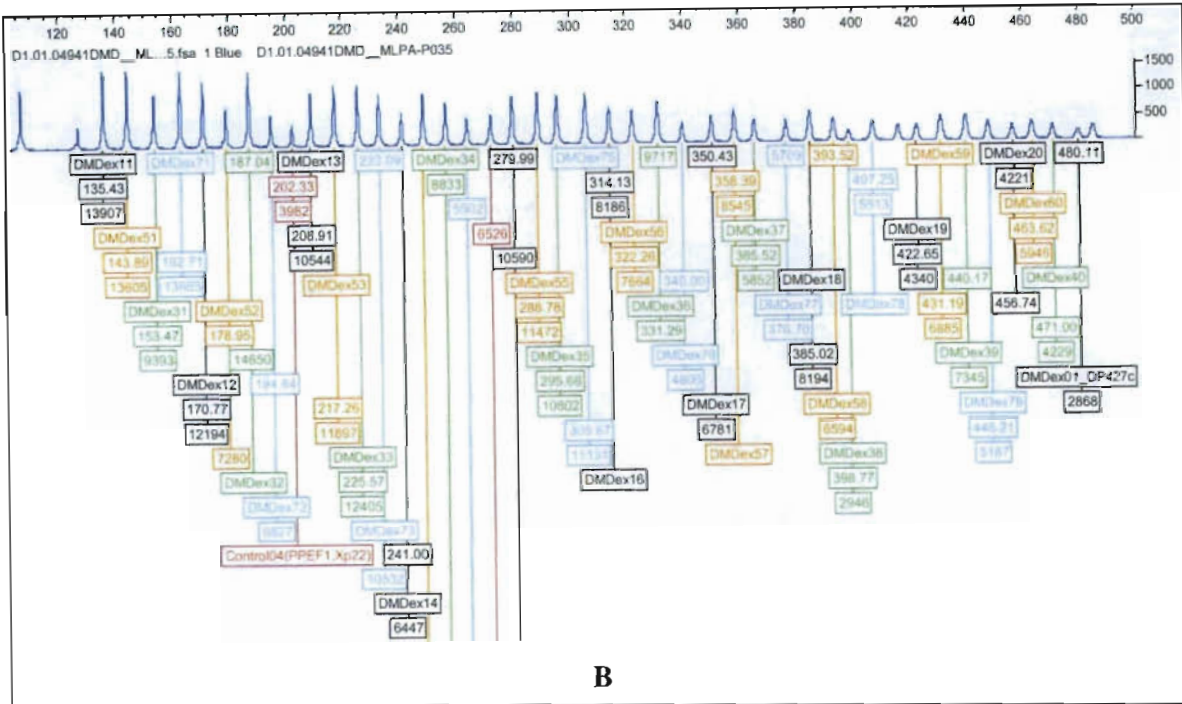


**Figure 62: Representative electropherograms showing the peaks that resulted when the P034 (A) and P035 (B) probe mixtures were amplified and analysed on the ABI genetic analyser.**

In some instances a split peak can be obtained for a particular exon. In such cases, two values would be obtained for the exon.

These values should be added and the sum of the values needed to be included in the

dosage quotient analysis step.

It was found that using approximately 50 ng of DNA was adequate to produce an optimum

peak intensity signal.

### 6.4.5   Binning



| Dye/Sample Peak | Sample File Name | Marker | Allele | Size | Height | Area | Data Point |
|---|---|---|---|---|---|---|---|
| B,69 | frag_002_A08.fs | | | 194.25 | 2356 | 25543 | 3696 |
| B,70 | frag_002_A08.fs | | | 196.26 | 63 | 382 | 3725 |
| B,71 | frag_002_A08.fs | | | 202.02 | 1792 | 21310 | 3806 |
| B,72 | frag_002_A08.fs | | | 209.34 | 6537 | 79025 | 3904 |
| B,73 | frag_002_A08.fs | | | 218.46 | 5023 | 59505 | 4026 |
| B,74 | frag_002_A08.fs | | | 227.22 | 5208 | 64861 | 4143 |
| B,75 | frag_002_A08.fs | | | 235.1 | 4343 | 53497 | 4248 |
| B,76 | frag_002_A08.fs | | | 243.6 | 4116 | 51805 | 4361 |
| B,77 | frag_002_A08.fs | | | 251.45 | 4133 | 51494 | 4467 |
| B,78 | frag_002_A08.fs | | | 259.04 | 3589 | 45605 | 4577 |
| B,79 | frag_002_A08.fs | | | 266.86 | 2276 | 28079 | 4690 |
| B,80 | frag_002_A08.fs | | | 274.51 | 2512 | 32983 | 4800 |
| B,81 | frag_002_A08.fs | | | 281.2 | 5792 | 74423 | 4896 |
| B,82 | frag_002_A08.fs | | | 289.59 | 4196 | 54934 | 5016 |
| B,83 | frag_002_A08.fs | | | 295.84 | 4293 | 56544 | 5105 |
| B,84 | frag_002_A08.fs | | | 305.2 | 4049 | 52802 | 5230 |

**Figure 63: Image showing the binning mode where each peak is assigned a name and a size.**

The figure above (Figure 63) shows a peak highlighted in the binning mode. In this mode,

the user would be able to change the size assigned to each peak and the area over which it

is recognized by the software. The peak location varies between runs, hence the need to

broaden the area over which the peak is recognised.

## 6.4.6 Name assignment to peak

In the figure below (figure 64), details of the highlighted peak are shown in the table. Important details include the peak height, peak area and exon name.



**A**

| | | | | | | | |
|---|---|---|---|---|---|---|---|
| ■ | B,60 | frag_004_B08.fsi | | 139.3 | 64 | 357 | 2896 |
| ■ | B,61 | frag_004_B08.fsr | | 143.07 | 66 | 410 | 2946 |
| ■ | B,62 | frag_004_B08.fsi | | 147.44 | 65 | 391 | 3004 |
| ■ | B,63 | frag_004_B08.fsi | | 151.95 | 356 | 2458 | 3065 |
| ■ | B,64 | frag_004_B08.fsi PO35 | Exon31 | 153.03 | 6823 | 74560 | 3080 |
| ■ | B,65 | frag_004_B08.fsi PO35 | Exon71 | 161.79 | 7464 | 92453 | 3204 |
| ■ | B,66 | frag_004_B08.fsi PO35 | Exon12 | 169.85 | 7272 | 81690 | 3321 |
| ■ | B,67 | frag_004_B08.fsi | | 174.95 | 138 | 1317 | 3395 |
| ■ | B,68 | frag_004_B08.fsi PO35 | Exon52 | 177.86 | 3751 | 41427 | 3437 |
| ■ | B,69 | frag_004_B08.fsi PO35 | Exon32 | 186.1 | 7492 | 96899 | 3556 |
| ■ | B,70 | frag_004_B08.fsi PO35 | Exon72 | 194.22 | 3727 | 40915 | 3673 |
| ■ | B,71 | frag_004_B08.fsi PO35 | Xp22 | 202.03 | 2329 | 25559 | 3783 |
| ■ | B,72 | frag_004_B08.fsi | | 204.91 | 74 | 446 | 3820 |
| ■ | B,73 | frag_004_B08.fsi PO35 | Exon13 | 209.32 | 6528 | 74702 | 3880 |

**B**

**Figure 64: Genemapper image showing a highlighted peak and the names assigned to each peak.**

## 6.4.7 Visual interpretation of a duplication

In (A) below, the electropherogram is that of a patient's sample. On visual inspection, the peak heights of exons 49 (green line) and 50 (red line) are higher than that of the control sample as shown in (B). The peak area of exon 49 for the patient (A) is 6344 whereas the

176

peak area for the control (B) is 4466. The peak area of exon 50 for the patient (A) is 7646 and the peak area of exon 50 for the control (B) is 5152. Even though the peak areas differ considerably it is still wise to confirm the presence of a duplication using the dosage quotient analysis method by placing the peak area or peak height data into an Excel spreadsheet and subjecting it to the student's T-test statistical analysis method.
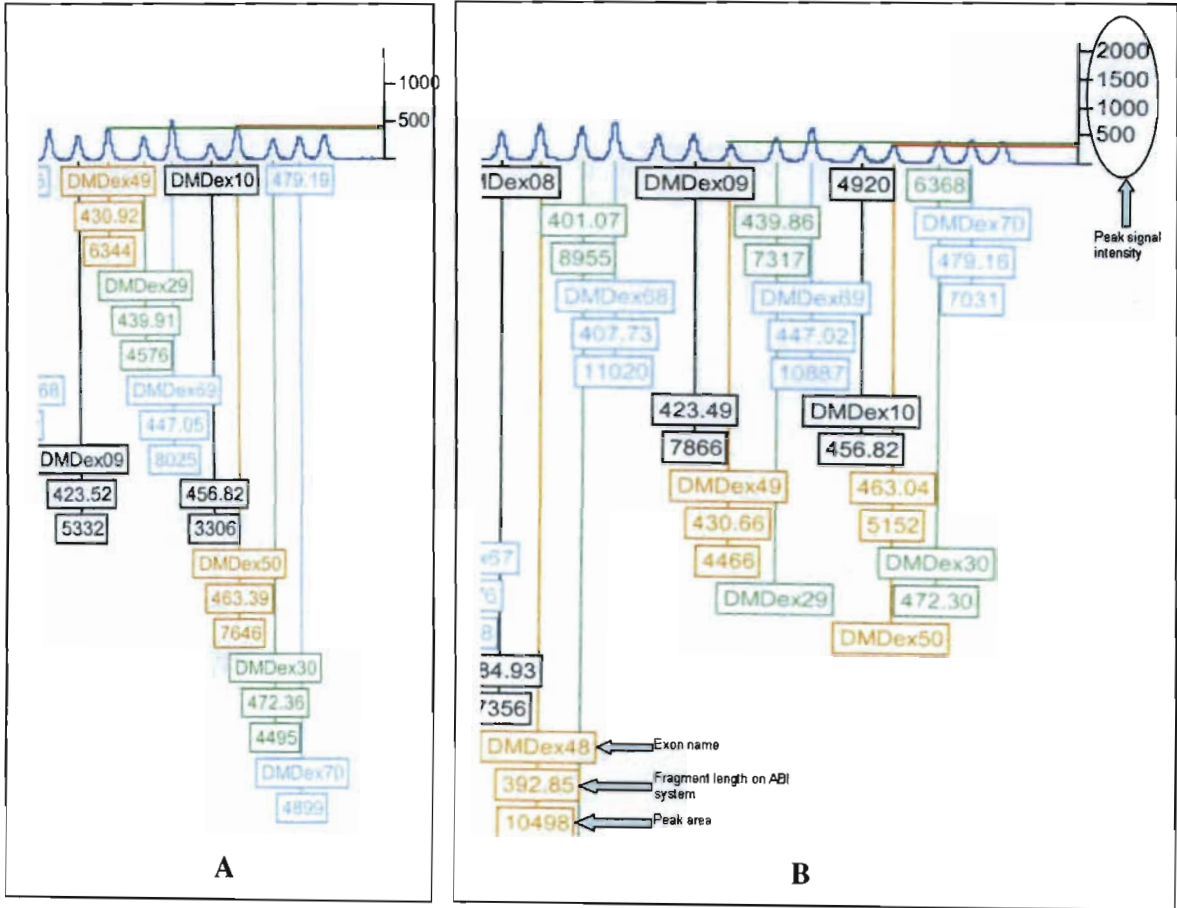


**Figure 65:** **Electropherograms comparing results from a patient sample 62 (A) with an exon 49 and exon 50 duplication, to that of a control sample (B).**

In figure 66 (A), the peak area for exon 51 is 26062 whereas the peak area for the control (B) is 16512. The peak area for exon 52 is 12452 and control is 8298. The peak area for exon 53 is 24949 and control is 13968. The peak area for exon 54 is 23280 whereas the peak control is 13122.

As is clearly shown on visual inspection the peak heights and peak areas provide a good

way of determining whether a duplication is present or not. When the peak heights between the patient's sample and control are compared, as shown in the profiles above (A and B) the peak heights in those exons that are highlighted in the patient's sample are higher than those of the control sample. Patient 62 therefore has a duplication from 49-54.
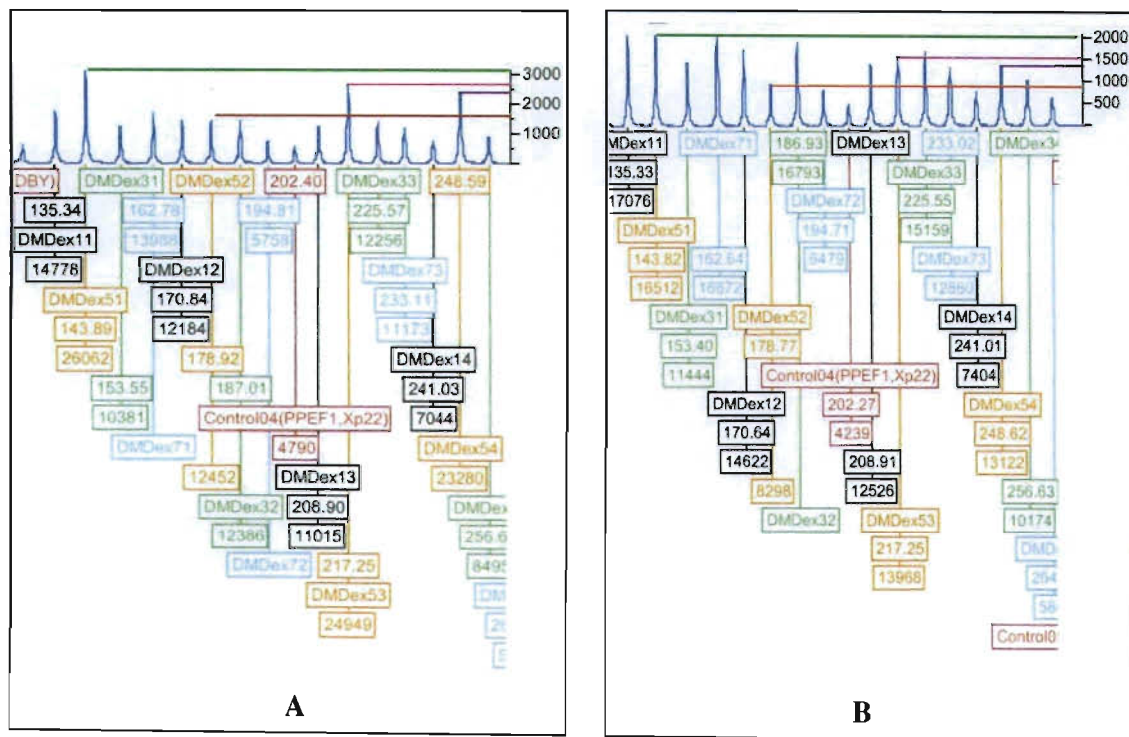


Figure 66: Electropherograms showing the peak heights and peak areas from patient sample 62 (A) with exons 51, 52, 53 and 54 being duplicated and a control sample (B).

### 6.4.8 Confirmation of duplication using dosage quotient analysis

The peak areas from the patient who was shown to have a duplication from exons 49-54 by visual inspection was then imported into Excel. The student's T-test was used to compare the results obtained from the patient to those from two control samples. The exons are compared to each and between samples to achieve confirmation of the mutation. In the above figure, the duplication is shown by values being in a range >2.0 in the vertical columns as shown by the blue highlights. These indicate that a particular exon is

**A**

| EXONS | DMDex48 | DMDex49 | DMDex50 | DMDex61 | DMDex62 | DMDex63 | DMDex64 | DMDex65 | DMDex56 | DMDex57 | DMDex68 | DMDex69 | DMDex70 |
|---|---|---|---|---|---|---|---|---|---|---|---|---|---|
| C2(DBY) | 0.00 | 0.00 | 0.00 | 0.00 | 0.00 | 0.00 | 0.00 | 0.00 | 0.00 | 0.00 | 0.00 | 0.00 | 0.00 |
| C4(PPEF1,Xp22) | 0.84 | 1.91 | 1.82 | 0.92 | 0.82 | 0.82 | 0.85 | 0.89 | 1.01 | 0.99 | 0.80 | 0.90 | 0.84 |
| C5(MECP2,Xq28) | 0.82 | 1.86 | 1.77 | 0.89 | 0.80 | 0.80 | 0.83 | 0.86 | 0.98 | 0.97 | 0.78 | 0.88 | 0.82 |
| DMDex01 | 1.11 | 2.53 | 2.41 | 1.22 | 1.09 | 1.06 | 1.13 | 1.17 | 1.33 | 1.31 | 1.06 | 1.20 | 1.11 |
| DMDex02 | 1.02 | 2.32 | 2.21 | 1.11 | 1.00 | 0.99 | 1.03 | 1.07 | 1.22 | 1.20 | 0.97 | 1.10 | 1.02 |
| DMDex03 | 0.92 | 2.11 | 2.01 | 1.01 | 0.91 | 0.90 | 0.94 | 0.98 | 1.11 | 1.09 | 0.88 | 1.00 | 0.93 |
| DMDex04 | 0.88 | 2.01 | 1.91 | 0.96 | 0.86 | 0.86 | 0.89 | 0.93 | 1.06 | 1.04 | 0.84 | 0.95 | 0.88 |
| DMDex05 | 0.94 | 2.13 | 2.03 | 1.03 | 0.92 | 0.91 | 0.95 | 0.99 | 1.12 | 1.11 | 0.89 | 1.01 | 0.94 |
| DMDex06 | 1.00 | 2.28 | 2.18 | 1.10 | 0.98 | 0.98 | 1.02 | 1.06 | 1.20 | 1.19 | 0.95 | 1.08 | 1.00 |
| DMDex07 | 0.86 | 1.97 | 1.87 | 0.95 | 0.85 | 0.84 | 0.88 | 0.81 | 1.04 | 1.02 | 0.82 | 0.93 | 0.87 |
| DMDex08 | 0.92 | 2.10 | 2.00 | 1.01 | 0.91 | 0.90 | 0.94 | 0.98 | 1.11 | 1.09 | 0.88 | 1.00 | 0.92 |
| DMDex09 | 1.00 | 2.28 | 2.17 | 1.10 | 0.98 | 0.98 | 1.02 | 1.06 | 1.20 | 1.19 | 0.95 | 1.08 | 1.00 |
| DMDex10 | 0.96 | 2.18 | 2.07 | 1.05 | 0.94 | 0.93 | 0.97 | 1.01 | 1.15 | 1.13 | 0.91 | 1.03 | 0.96 |
| DMDex21 | 1.05 | 2.38 | 2.27 | 1.15 | 1.03 | 1.02 | 1.06 | 1.11 | 1.26 | 1.24 | 0.99 | 1.13 | 1.05 |
| DMDex22 | 1.02 | 2.32 | 2.21 | 1.11 | 1.00 | 0.99 | 1.03 | 1.08 | 1.22 | 1.20 | 0.97 | 1.09 | 1.02 |
| DMDex23 | 1.01 | 2.31 | 2.20 | 1.11 | 0.99 | 0.99 | 1.03 | 1.07 | 1.22 | 1.20 | 0.96 | 1.09 | 1.01 |
| DMDex24 | 1.01 | 2.30 | 2.19 | 1.11 | 0.99 | 0.98 | 1.02 | 1.07 | 1.21 | 1.19 | 0.96 | 1.09 | 1.01 |
| DMDex25 | 0.97 | 2.22 | 2.11 | 1.07 | 0.95 | 0.95 | 0.99 | 1.03 | 1.17 | 1.15 | 0.92 | 1.05 | 0.97 |
| DMDex26 | 1.02 | 2.33 | 2.22 | 1.12 | 1.00 | 0.99 | 1.04 | 1.08 | 1.23 | 1.21 | 0.97 | 1.10 | 1.02 |
| DMDex27 | 0.94 | 2.13 | 2.03 | 1.02 | 0.92 | 0.91 | 0.95 | 0.99 | 1.12 | 1.11 | 0.89 | 1.01 | 0.94 |
| DMDex28 | 0.96 | 2.18 | 2.08 | 1.05 | 0.94 | 0.93 | 0.97 | 1.01 | 1.15 | 1.13 | 0.91 | 1.04 | 0.96 |
| DMDex29 | 1.03 | 2.35 | 2.24 | 1.13 | 1.01 | 1.01 | 1.05 | 1.09 | 1.24 | 1.22 | 0.98 | 1.11 | 1.03 |
| DMDex30 | 0.91 | 2.06 | 1.97 | 0.99 | 0.89 | 0.88 | 0.92 | 0.96 | 1.09 | 1.07 | 0.86 | 0.98 | 0.91 |
| DMDex41 | 1.03 | 2.35 | 2.23 | 1.13 | 1.01 | 1.00 | 1.04 | 1.09 | 1.24 | 1.22 | 0.98 | 1.11 | 1.03 |
| DMDex42 | 1.02 | 2.32 | 2.21 | 1.11 | 1.00 | 0.99 | 1.03 | 1.07 | 1.22 | 1.20 | 0.97 | 1.10 | 1.02 |
| DMDex43 | 1.07 | 2.43 | 2.31 | 1.17 | 1.05 | 1.04 | 1.08 | 1.13 | 1.28 | 1.26 | 1.01 | 1.15 | 1.07 |
| DMDex44 | 0.99 | 2.26 | 2.15 | 1.08 | 0.97 | 0.96 | 1.00 | 1.05 | 1.19 | 1.17 | 0.94 | 1.07 | 0.99 |
| DMDex45 | 1.02 | 2.33 | 2.22 | 1.12 | 1.00 | 1.00 | 1.04 | 1.08 | 1.23 | 1.21 | 0.97 | 1.10 | 1.02 |
| DMDex46 | 1.13 | 2.58 | 2.46 | 1.24 | 1.11 | 1.10 | 1.15 | 1.20 | 1.36 | 1.34 | 1.08 | 1.22 | 1.13 |
| DMDex47 | 0.91 | 2.06 | 1.99 | 1.00 | 0.90 | 0.89 | 0.93 | 0.97 | 1.10 | 1.08 | 0.87 | 0.99 | 0.92 |
| DMDex48 | | | 2.28 | 2.17 | 1.10 | 0.98 | 0.97 | 1.01 | 1.06 | 1.20 | 1.18 | 0.95 | 1.08 | 1.00 |
| DMDex49 | | | 0.95 | 0.48 | 0.43 | 0.43 | 0.45 | 0.46 | 0.53 | 0.52 | 0.42 | 0.47 | 0.44 |
| DMDex50 | | | | 0.50 | 0.45 | 0.45 | 0.47 | 0.49 | 0.55 | 0.55 | 0.44 | 0.50 | 0.46 |
| DMDex51 | | | | | 0.90 | 0.89 | 0.93 | 0.96 | 1.10 | 1.08 | 0.87 | 0.99 | 0.91 |
| DMDex62 | | | | | | 0.99 | 1.03 | 1.08 | 1.22 | 1.21 | 0.97 | 1.10 | 1.02 |
| DMDex63 | | | | | | | 1.04 | 1.08 | 1.23 | 1.21 | 0.98 | 1.11 | 1.03 |
| DMDex64 | | | | | | | | 1.04 | 1.18 | 1.17 | 0.94 | 1.07 | 0.99 |
| DMDex65 | | | | | | | | | 1.14 | 1.12 | 0.90 | 1.02 | 0.95 |

**B**

| EXONS | DMDex51 | DMDex52 | DMDex53 | DMDex54 | DMDex55 | DMDex56 | DMDex57 | DMDex58 | DMDex59 | DMDex60 | DMDex71 | DMDex72 |
|---|---|---|---|---|---|---|---|---|---|---|---|---|
| C2(DBY) | 0.00 | 0.00 | 0.00 | 0.00 | 0.00 | 0.00 | 0.00 | 0.00 | 0.00 | 0.00 | 0.00 | 0.00 |
| C4(PPEF1,Xp22) | 1.70 | 1.61 | 1.82 | 1.93 | 0.90 | 1.06 | 1.08 | 1.10 | 1.07 | 1.12 | 0.90 | 1.00 |
| C5(MECP2,Xq28) | 1.44 | 1.36 | 1.55 | 1.64 | 0.77 | 0.90 | 0.92 | 0.94 | 0.91 | 0.95 | 0.76 | 0.85 |
| DMDex01_DP427c | 1.43 | 1.35 | 1.54 | 1.63 | 0.76 | 0.89 | 0.91 | 0.93 | 0.90 | 0.95 | 0.76 | 0.84 |
| DMDex11 | 1.84 | 1.74 | 1.98 | 2.10 | 0.98 | 1.14 | 1.17 | 1.20 | 1.16 | 1.22 | 0.97 | 1.08 |
| DMDex12 | 1.87 | 1.77 | 2.01 | 2.14 | 1.00 | 1.17 | 1.19 | 1.22 | 1.18 | 1.24 | 0.99 | 1.10 |
| DMDex13 | 1.78 | 1.68 | 1.91 | 2.03 | 0.95 | 1.11 | 1.13 | 1.16 | 1.12 | 1.18 | 0.94 | 1.04 |
| DMDex14 | 1.78 | 1.68 | 1.91 | 2.03 | 0.85 | 1.11 | 1.13 | 1.16 | 1.12 | 1.17 | 0.94 | 1.04 |
| DMDex15 | 1.63 | 1.54 | 1.75 | 1.86 | 0.87 | 1.01 | 1.04 | 1.06 | 1.03 | 1.08 | 0.86 | 0.96 |
| DMDex16 | 1.86 | 1.76 | 2.00 | 2.12 | 0.99 | 1.16 | 1.18 | 1.21 | 1.17 | 1.23 | 0.98 | 1.09 |
| DMDex17 | 1.81 | 1.71 | 1.95 | 2.06 | 0.96 | 1.13 | 1.15 | 1.18 | 1.15 | 1.20 | 0.96 | 1.06 |
| DMDex18 | 1.96 | 1.86 | 2.11 | 2.23 | 1.04 | 1.22 | 1.25 | 1.28 | 1.24 | 1.30 | 1.04 | 1.15 |
| DMDex19 | 1.75 | 1.65 | 1.88 | 1.99 | 0.93 | 1.09 | 1.11 | 1.14 | 1.11 | 1.16 | 0.92 | 1.03 |
| DMDex20 | 1.65 | 1.56 | 1.77 | 1.88 | 0.88 | 1.02 | 1.05 | 1.07 | 1.04 | 1.09 | 0.87 | 0.97 |
| DMDex31 | 1.84 | 1.74 | 1.98 | 2.10 | 0.98 | 1.14 | 1.17 | 1.20 | 1.16 | 1.22 | 0.97 | 1.08 |
| DMDex32 | 2.28 | 2.16 | 2.45 | 2.60 | 1.21 | 1.42 | 1.45 | 1.49 | 1.44 | 1.51 | 1.21 | 1.34 |
| DMDex33 | 2.02 | 1.91 | 2.17 | 2.30 | 1.08 | 1.26 | 1.29 | 1.32 | 1.28 | 1.34 | 1.07 | 1.19 |
| DMDex34 | 1.95 | 1.84 | 2.09 | 2.22 | 1.03 | 1.21 | 1.24 | 1.27 | 1.23 | 1.29 | 1.03 | 1.14 |
| DMDex35 | 1.84 | 1.74 | 1.98 | 2.10 | 0.98 | 1.15 | 1.17 | 1.20 | 1.16 | 1.22 | 0.97 | 1.08 |
| DMDex36 | 1.77 | 1.68 | 1.90 | 2.02 | 0.94 | 1.10 | 1.13 | 1.15 | 1.12 | 1.17 | 0.94 | 1.04 |
| DMDex37 | 2.09 | 1.98 | 2.25 | 2.38 | 1.11 | 1.30 | 1.33 | 1.36 | 1.32 | 1.38 | 1.11 | 1.23 |
| DMDex38 | 1.85 | 1.75 | 1.99 | 2.11 | 0.98 | 1.15 | 1.18 | 1.21 | 1.17 | 1.22 | 0.98 | 1.09 |
| DMDex39 | 1.91 | 1.81 | 2.06 | 2.18 | 1.02 | 1.19 | 1.22 | 1.25 | 1.21 | 1.26 | 1.01 | 1.12 |
| DMDex40 | 1.88 | 1.78 | 2.02 | 2.14 | 1.00 | 1.17 | 1.19 | 1.22 | 1.19 | 1.24 | 0.99 | 1.10 |
| DMDex51 | | 0.95 | 1.07 | 1.14 | 0.53 | 0.62 | 0.64 | 0.65 | 0.63 | 0.66 | 0.53 | 0.59 |
| DMDex52 | | | 1.14 | 1.20 | 0.56 | 0.66 | 0.67 | 0.69 | 0.67 | 0.70 | 0.56 | 0.62 |
| DMDex53 | | | | 1.06 | 0.50 | 0.58 | 0.59 | 0.61 | 0.59 | 0.62 | 0.49 | 0.55 |
| DMDex54 | | | | | 0.47 | 0.55 | 0.56 | 0.57 | 0.55 | 0.58 | 0.46 | 0.52 |
| DMDex55 | | | | | | 1.17 | 1.20 | 1.22 | 1.19 | 1.24 | 0.99 | 1.10 |
| DMDex56 | | | | | | | 1.02 | 1.05 | 1.02 | 1.06 | 0.85 | 0.94 |
| DMDex57 | | | | | | | | 1.02 | 0.99 | 1.04 | 0.83 | 0.92 |
| DMDex58 | | | | | | | | | 0.97 | 1.01 | 0.81 | 0.90 |

**Figure 67: Graphical representations (A and B) of the duplication from exons 49-54 found in patient 62 using dosage quotient analysis in the Excel spreadsheet.**

179

duplicated. The corresponding horizontal rows are in a range <0.6 as shown by the yellow

highlights.

### 6.4.9 Visual identification of a deletion
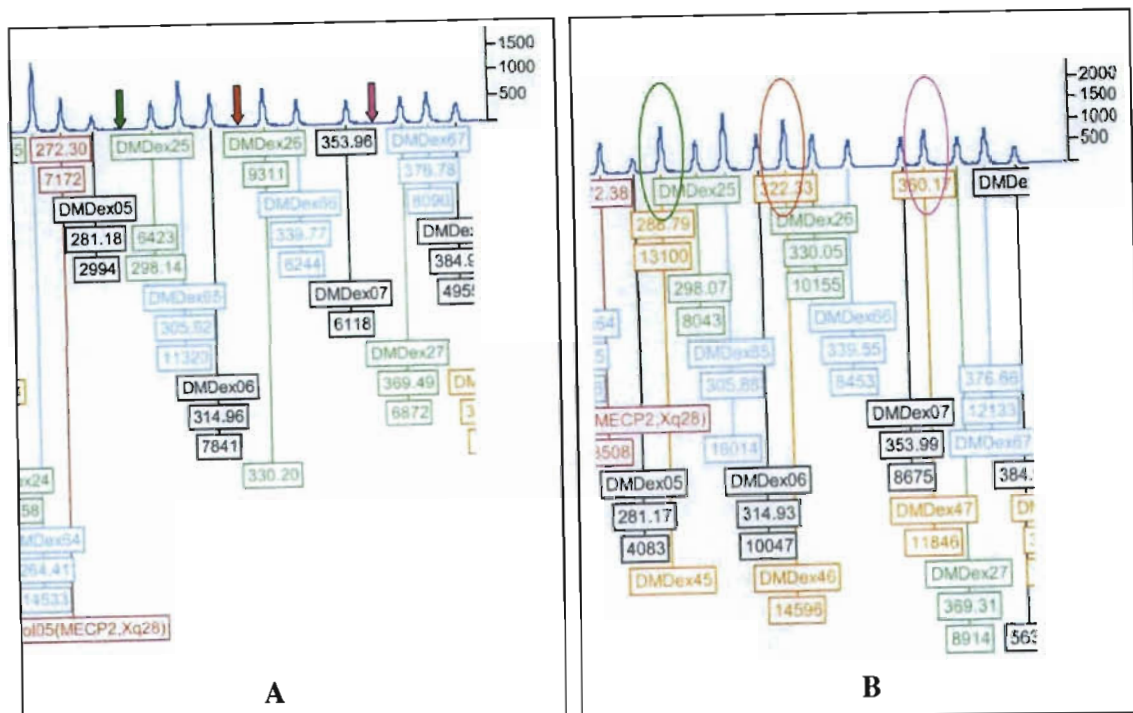


**Figure 68:** Fluorescent profiles showing patient sample 26 (A) with deletions as shown by the arrows and a control sample indicating the exon locations and the peaks, which are highlighted by the oval shapes (B).

### 6.4.10 Mutation confirmation using DNA sequence analysis

In the above figure, exons 45, 46 and 47 are shown to be deleted in patient sample 26. It is easily visible by the absence of a peak. By comparing the patient's electropherogram with that of a control sample one can conclude that a deletion is present without having to perform dosage quotient analyses using the Excel spreadsheet and the T-test statistical analysis. In the case of the above patient, exon 13 had appeared to be deleted. The DNA from the patient was subjected to PCR amplification and subsequent DNA sequencing for exon 13. The results are shown below.
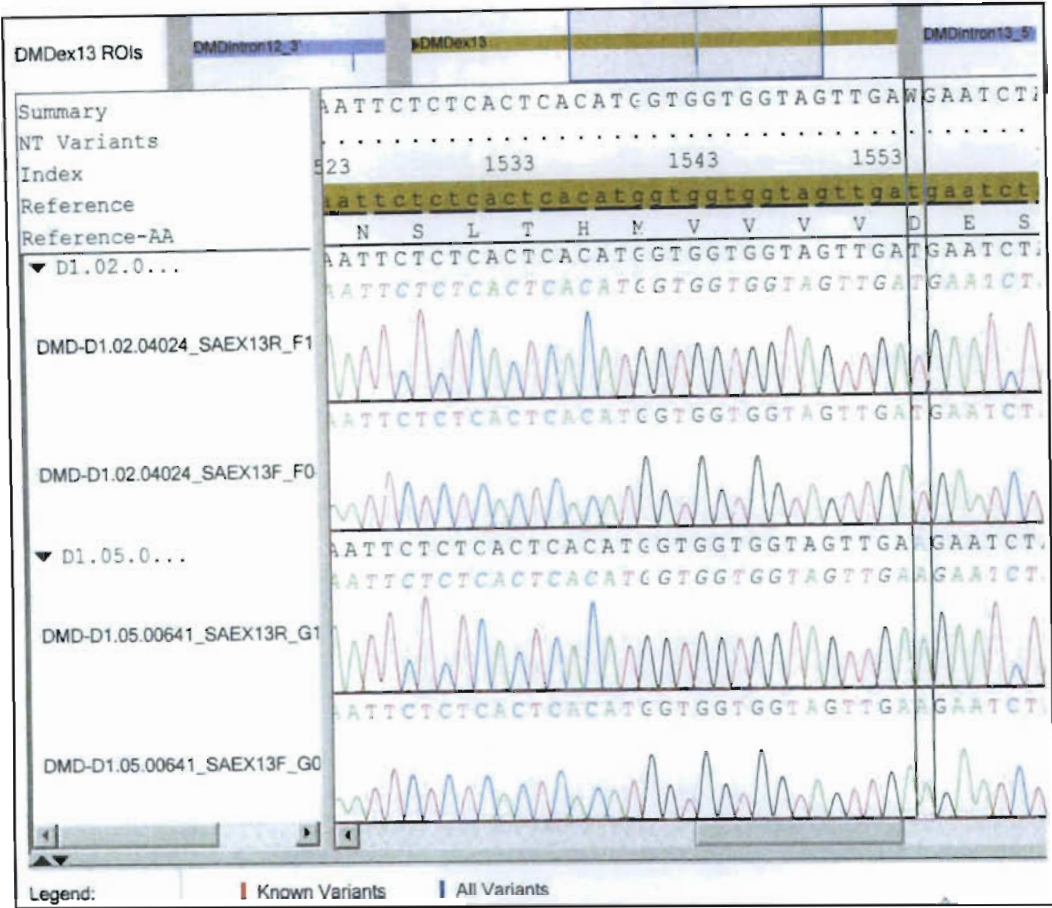
**Figure 69: Sequence data showing a polymorphism found on exon 13 in patient sample 26.**

In the above sequence data the C>T polymorphism was located at *c*DNA position 1554.

This polymorphism resulted in an aspartic acid residue being replaced with a glutamic acid

residue at position 518. This is a known polymorphism that has also been listed on the

Leiden muscular dystrophy pages where it was found in a BMD patient's sample in the

Netherlands. Our patient in whom the polymorphism was found also manifests a Becker

muscular dystrophy phenotype.
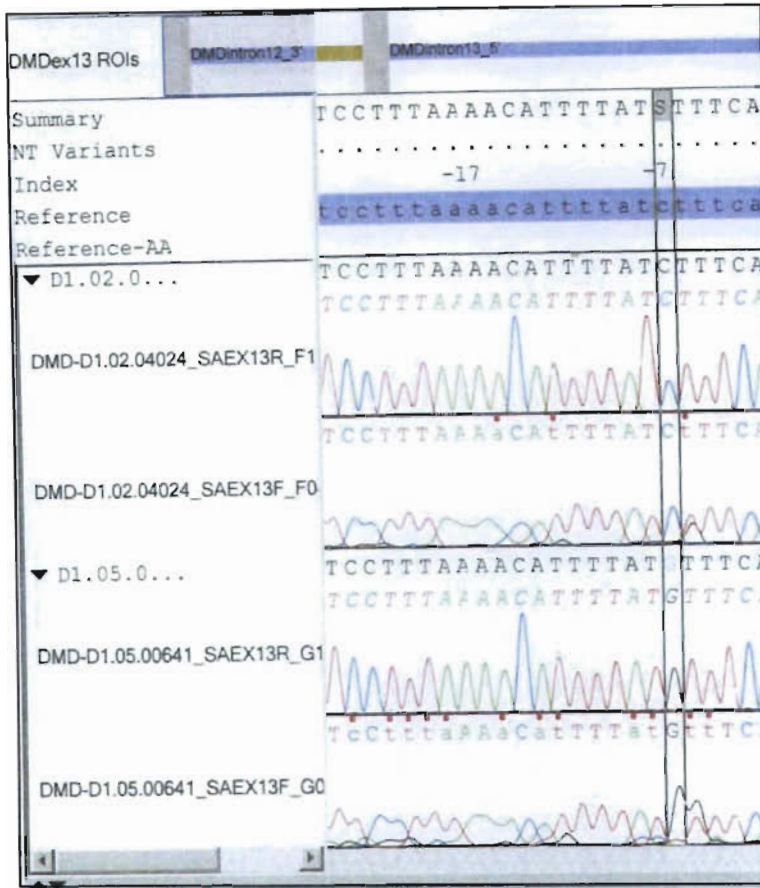
**Figure 70: DNA sequence data showing an intronic substitution in exon 13 of sample 26.**

In the DNA sequence data shown above the actual intronic change was a c1483 -7C>G intronic change. The location of the change on the cDNA is shown first followed by the actual nucleotide substitution. This change occurred close to a splice site, which required that splice site predictions be made. When donor site predictions were made for the -7 C>G exon 13 substitution, the score was found o be 0.51, suggesting that a splice site mutation is a possibility. The donor site prediction for the wild type sequence was 0.59. When the acceptor site prediction was made for this substitution mutation -7C>G the score was 0.85 therefore suggesting a strong match to the consensus sequence. The acceptor site prediction for the wild type sequence was 0.94. A strong match to the consensus indicates that the splice site is likely to be recognised by the snRNP (small nuclear ribonucleoproteins) in the spliceosomal complex. In so doing the exon is not spliced out

**Table 29: Deletion and duplication data obtained after Genemapper analysis on the ABI 3100 for the patients that were included in the multiplex ligation-dependent probe amplification assay.**

| DNA number | Surname, Initials | Age | DMD/BMD | Deletion / Duplication | Frame |
|---|---|---|---|---|---|
| 6 | H, S | N/A | Mother of 7 | Duplication 68-78 | In-frame |
| 7 | H, J | 8 | DMD | Duplication 68-78 | In-frame |
| 9 | S, NM | 17 | DMD | Deletion of exon 56 | Out-of-frame |
| 14 | N, D | 9 | DMD | Complex re-arrangement (Duplication of exon 1 and 46-63) | Out-of-frame |
| 15 | N, C | N/A | Mother of 14 | Complex re-arrangement (Duplication of exon 1 and 46-63) | Out-of-frame |
| 19 | M, S | 6 | DMD | Del 8-16 | Out-of-frame |
| 21 | R, S | 8 | DMD | Del 45-54 | In-frame |
| 24 | P, D | 6 | DMD | Dup 6-18 | In-frame |
| 26 | Z, S | 18 | BMD | Del 45-47 | In-frame |
| 30 | W, R | | DMD | No del/dup | |
| 31 | C, L | 12 | DMD | No del/dup | |
| 32 | M, NL | 6 | DMD | Del 45-50 | Out-of-frame |
| 37 | G, M | 8 | DMD | Del 51 | Out-of-frame |
| 38 | N, M | 14 | DMD | Del 45-46,51-52 | In-frame, in-frame |
| 42 | M, R | 12 | DMD | Del 45 | Out-of-frame |
| 43 | S, V | 14 | DMD | Del 45-56 | Out-of-frame |
| 57 | M, T | | F mother N/A | No del/dup | |
| 58 | M, M | 14 | DMD | No del/dup | |
| 59 | B, X | 10 | DMD | No del/dup | |
| 60 | N, S | 12 | | Del 45 | Out-of-frame |
| 61 | L, M | 8 | DMD | No del/dup | |
| 62 | S, S | | DMD | Dup 49-54 | Out-of-frame |
| 63 | S, N | 25 | Carrier F | No del/dup | |

## 6.5    DISCUSSION

The MLPA procedure was optimised by the Molecular Genetics Laboratory, headed by Professor E. Bakker, the scientific supervisor of the author. All volumes were reduced with no difference being noted in the final result. Both the recommended procedure by MRC-Holland and the revised procedure implemented by the diagnostics laboratory in the Netherlands are included in the thesis, as both were performed. The recommended procedure was followed by Dr. Stefan White at the research laboratory, Center for Human and Clinical Genetics in the Netherlands and the procedure was first taught to the author by Dr. White. Whilst liaising with the diagnostics laboratory and Professor E. Bakker, the author was introduced to the optimised procedure, where reduced volumes of each reagent were used. The author therefore obtained training on both methodologies and compared them on her return to South Africa.

### 6.5.1    Hybridisation reaction

When the technique was learned under the supervision of Dr. Stefan White at the research laboratory at the Center for Human and Clinical Genetics, Leiden University Medical Center in the Netherlands, a volume of 1.5 µl probe mix was used per DNA sample as per recommendation by MRC-Holland . However, the probe concentration and volume was optimised at the Molecular Genetics laboratory, Leiden University Medical Center in the Netherlands, where Professor Bakker, the author's scientific supervisor is based. The author therefore compared both 1.5 µl probe mix per sample as well as 0.375 µl probe mix per sample on her return to South Africa where the technique was implemented at the Neuroscience laboratory, Department of Neurology, University of KwaZulu-Natal,

Durban. The results obtained following electrophoresis on the ABI 3100 were the same therefore in all subsequent reactions the 0.375 μl volume of probe mix was used per DNA sample. The 16 hour incubation period and the three hour incubation period at 60°C were performed using the same samples and electrophoresed using the same conditions on the ABI 3100 in South Africa. The author therefore opted to use the three hour incubation period for all subsequent reaction as this was being implemented as a diagnostic test and the time saving was tremendous. There was no difference noted if the DNA sample was added to the master mix in the presence or absence of buffer TE.

## 6.5.2 PCR reaction

The PCR reaction for the MRC-Holland procedure was different from the diagnostics lab procedure. Using the MRC-Holland procedure, the research laboratory used only 10 μl of the ligation mixture in the PCR reaction. The remaining ligation mixture was stored at 4°C and could be used to perform subsequent PCR reactions if the PCR reaction failed for some reason without having to go through the entire process hybridisation process again as it takes 16 hours for the hybridisation reaction. However, the diagnostic laboratory utilised a quarter of the reagents throughout the procedure. There would be no need to repeat the PCR reaction unless the PCR failed and if a repeat was required, reagents would not be wasted and the time taken would not be as significant since the hybridisation reaction required a three-hour incubation as opposed to a 16 hour incubation.

The PCR conditions that were used differed slightly in the two protocols. The diagnostic laboratory protocol was only changed because the MRC-Holland handout indicated that those changes could be made with no loss of product if the concentration of the DNA was optimal (50 ng/μl) in a given reaction.

### 6.5.3 Spacial and spectral calibration

At one point both the spacial and spectral calibrations failed as the detection window was moist. This resulted from a capillary array that was not equilibrated to room temperature. After this experience, the author removed any arrays that were in short-term storage at 4°C in the fridge to the bench-top. The array was left to equilibrate to room temperature for half hour to one hour before being installed onto the genetic analyser. Prior to being installed the detection window of the array was wiped clean with lint-free paper and further cleaned with a drop of HPLC grade methanol to ensure no dust residue remained. It is important that the environment in which the genetic analyser is housed is taken into account when troubleshooting problems that are encountered. We initially did not taken into account that we housed the ABI 3100 in the humid climate of Durban, which had an effect on the cooling capacity of the refrigerator that was used to store the array for a short time.

### 6.5.4 Data analysis using peak area or peak height

When the MLPA analysis was performed, the author was introduced to both the peak height and peak area methods. Dr. Stefan White, based at the Department of Human and Clinical genetics supervised the author in the MLPA assay and he preferred to use the peak height method in analysing the sample data. In comparison, staff at the Molecular diagnostics laboratory headed by Professor E. Bakker used the peak area method to analyse the MLPA assay results. Reports have shown that both methods are comparable in the results that they produce (White *et al.*, 2004; Janssen *et al.*, 2005). Owing to the fact that the PCR methodology is not quantitative by nature, the amplicon produced would alter the peak height and in so doing the results obtained on dosage quotient analysis would not be

definitive. The author therefore chose to use the peak area method in analysing the data produced at the Neuroscience laboratory.

### 6.5.5  Deletion and duplication results

Definitive results are shown for a small number of the actual patients' samples that were subjected to MLPA analysis. In some instances, the Genemapper analysed results produced poor peak quality. Such samples were repeated. We encountered other problems with the samples as well such as non amplification of the samples. All these samples were repeated until appropriate results were obtained. The last stumbling block encountered related to an inability to obtain a dosage quotient value of 1.0 when peak areas or peak heights were exported from Genemapper into an Excel spreadsheet. The values that were being obtained were in excess of 6.0 and this did not match previous Excel results.

When visually inspecting the data using the Genemapper software it became clear that deletions can easily be detected by the absence of a peak. Duplications too can be detected when one compares the peak areas or peak heights between sample and control. It is however advisable to confirm the results using the dosage quotient analysis method and the Excel spreadsheet program, especially for duplications.

With respect to the fragment analysis data that produced usable results, in some instances a single exon deletion was found. Such a deletion should be confirmed using another set of probes or by sequencing the exon of interest. The probes used are generally chosen within the exon and hybridisation failure could be caused by the presence of a SNP or mutation under the hybridisation site (Bakker, personal communication). There could also have been

a point mutation present that was pathogenic and that once sequenced may show the presence of a premature stop codon. The company that manufacturers the probes also has a list of those exons that can sometimes produce higher than normal values for the dosage quotient analysis. An example of such an exon is exon 37 however they have recently changed the probe for this exon. During the analysis evaluation one has to take all of this into account before stating that a patient has a single exon deletion, which is a rare occurrence.

The table above shows those patients that had deletions or duplications. Four of the 21 patients had duplications, with two mothers being confirmed as duplication carriers. These patients were previously shown to have no deletions, which placed him into the query point mutation category. With the advent of this new technique finding a duplication at the screening stage prevents any further diagnostic tests such as multiplex PCR or SSCP analysis from being performed. This is also helpful with respect to genetic counselling as the Neurologist can provide information on the type of mutation that the child has to parents and they can make informed decisions as to the type of therapy they would like to include in the treatment regimen. Specific deletions or duplications may allow the patient to be included in certain clinical trials, for examples those that convert an out-of-frame deletion into an in-frame deletion by the exon-skipping approach (Aartsma-Rus et al., 2003; Zhou et al., 2006).
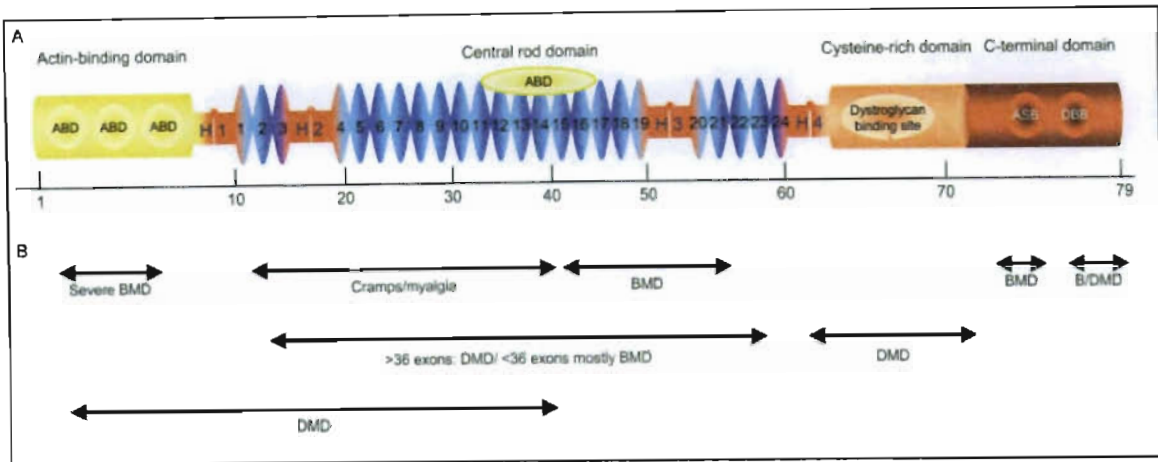
**Figure 71: Image showing the domains of the dystrophin protein (A) together with the genotype-phenotype correlations (B) postulated and based on data from Beggs *et al.* (1991) as adapted from Aartsma-Rus *et al.* (2006). ABD represents the actin-binding domain, ASB represents the α-syntrophin binding and DBB represents the dystrobrevin binding site.**

When one attempts to correlate the mutation with physical symptoms there isn't always a steadfast rule to disease progression. A guideline to determining the phenotype once a deletion has been found is outlined in the figure above that is based on data obtained from Beggs *et al.* (1991). One child may progress much faster than the other and yet they may both have the same type of deletion. Such an effect may occur on account of the location of the deletion or duplication. If the mutation is in a region of the gene that is responsible for binding other proteins for example, a more severe outcome may be present. In patient 62 who has a duplication from exons 49-54, the phenotype was that of toe walking and inability to stand from the sitting position, extreme weakness and resulting lack of co-ordination. The 9-year old male was still ambulant even though he was progressing rapidly. Even though the duplication was in-frame, which implies the presence of some of the protein, his disease severity was moderate to severe. His duplication is located in the rod domain. Another duplication (dup 6-18) patient was a 6-year old male with Gowers sign, a waddling gait and calf hypertrophy. He was also having much difficulty walking. The progressive nature of the disease may be explained by the location of the mutation. This mutation starts in the amino terminal domain where many protein interactions

between dystrophin and other components of DAGC occur and in the central part of the rod domain, which is thought to be less important for protein interactions. The severity of disease in both these patients may cause one to speculate that duplication mutations are more complex and produce different effects in comparison to deletion mutations and disease progression can be mapped out more readily for deletions than duplications. According to White *et al.*, (2006) the mechanisms by which duplications result are different from those that produce deletions and this may account for the difference in severity of duplication patients with in-frame duplications compared to deletion patients with in-frame deletions.

In the case of deletions, visual inspection would be sufficient to determine that a deletion exists as there would be the absence of a peak. There is no need to take the analysis a step further by performing dosage quotient analysis using the Excel spreadsheet and the t-test. A single deletion of exon 45 was confirmed in patient 42.

Performing genotype-phenotype correlations for deletions is more possible compared to duplications. One can generally assume that an in-frame deletion would result in a shorter yet functional protein being produced and therefore the patient presents with a milder phenotype. In contrast an out-of-frame deletion would result in a truncated, non-functional protein being produced and therefore a more severe phenotype would be expected (Beggs *et al.*, 1991; Comi *et al.*, 1994). There are exceptions to this "reading-frame rule", which was first proposed by Monaco *et al.*, 1988 (Aartsma-Rus *et al.*, 2006). According to Aarstma-Rus *et al.* (2006), 9% of the mutations listed on the Leiden MD site did not follow the reading-frame rule. Even though this may seem like a high percentage, the authors suggest that the mutation which is thought to not agree with the reading frame rule should

be confirmed using RNA because the discordance may only appear to be true at the DNA level. Once RNA is used to determine the mutation and the reading-frame >99.5% of mutations fit the conventional reading-frame rule (Aartsma-Rus et al., 2006).

In some cases patients will have polymorphisms in addition to deletions and / or duplications in different parts of the dystrophin gene. One such example is patient 26, where an in-frame deletion spanning exons 45-47 was confirmed. In addition to this, the BMD patient showed dosage quotient values that were not in keeping with the normal expected value of 1.0 or close to that value. The exon was sequenced and he was shown to have a polymorphism as well as an intronic substitution close to a splice site, which suggested the possibility of a splice site mutation. Such results relay the importance of performing DNA sequencing on those exons that show abnormal values during dosage quotient analysis.

The most interesting case was the complex re-arrangement found in patient 14. The mother was also confirmed as having he same re-arrangement, thus also providing her carrier status.

# CHAPTER 7

## GENE EXPRESSION PROFILING OF DOUBLE MUSCLE BIOPSIES FROM DYSTROPHINOPATHY PATIENTS USING MICROARRAY ANALYSIS

### 7.1    INTRODUCTION

The use of microarray analysis in revealing and understanding the simultaneous interactions between various genes has become the latest new trend in biological research. The data produced from exploiting microarray technology was rapidly advanced by the draft mapping of the human genome where the "complete sequence of the euchromatin portion of the genome" was published in 2001 (Lander *et al.*, 2002; Venter *et al.*, 2001). This milestone in life science history was further extended to include the "complete sequencing and characterisation of 21,243 full-length *c*DNAs" (Ota *et al.*, 2004) as well as the annotation of 21,037 human genes (Imanishi *et al.*, 2004). These remarkable achievements set the course for extensive gene profiling experimentation and analyses to be performed on normal and diseased human tissue as well as blood. In order to unravel the mechanisms that regulate gene expression both normal and diseased states are being studied using microarrays and the bioinformatics tools that accompany this revolutionary technique.

The advent of microarray technology may be thought of as a profound development of previous molecular biology hybridisation methodology and fluorescence based techniques that had grown remarkably over the past few decades. The classical methods used to determine simultaneous expression of various genes were time-consuming, required

radioactive labelling and were only able to provide a limited amount of data. These methods gave rise to the macroarray technology that preceded the microarray revolution, where the principle of Northern blotting was reversed and the outcome was one where the expression of thousands of genes could be determined in a single experiment (Amersham Biosciences, 2002). In 1996, Southern published an article on high-density gridding, which set the scene for undertaking large scale gene expression analysis (Southern, 1996). In 1999, Baldwin *et al.* provided a three-tiered comparison of the most popular techniques in gene expression analysis in plants, which could easily be adapted to *Arabidopsis* and organisms such as yeast.

Macroarrays differ from microarrays by virtue of their spot size, with macroarrays being 300 microns or larger, which could easily be viewed using available laboratory gel blotters and scanners. Comparatively, microarray spots are <200 microns in diameter and require specialised apparatus that include robotic equipment for spotting and imaging as the gene expression of several thousands of spots are identified simultaneously (Amersham Biosciences, 2002).

### 7.1.1. What is a microarray?

In broad terms, a microarray may be defined as a highly dense and compact arrangement of oligonucleotides or *c*DNA probes that are immobilised onto a solid support, which is usually glass. Each of these nucleic acid sequences in effect forms a tiny "spot". The spot may either be referred to as a "probe" or a "target". These two names vary by virtue of their function however they are also used interchangeably since at present there is no defined nomenclature to discriminate between the two.
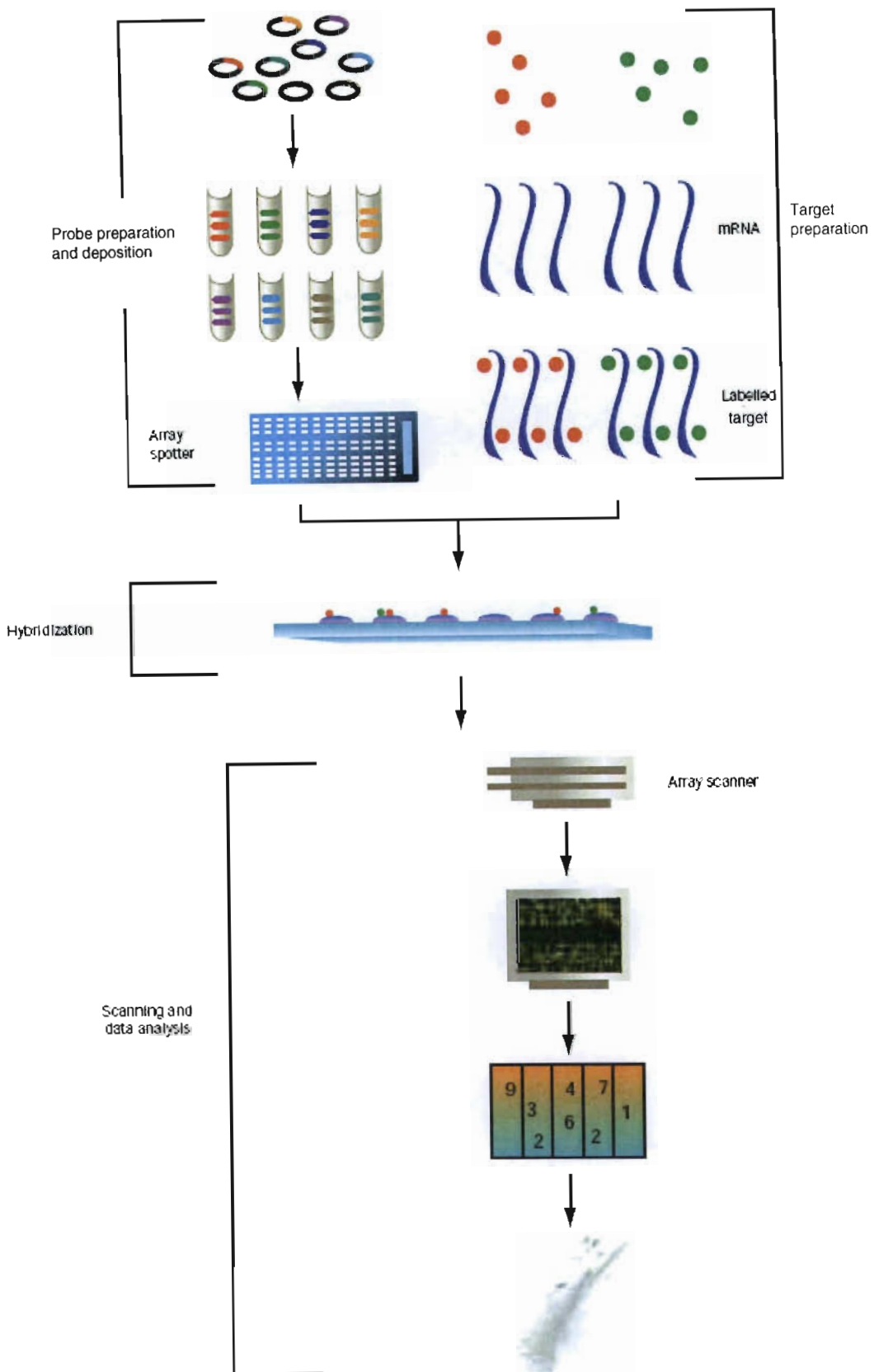
**Figure 72: Graphical representation of a generalised microarray scheme (Amersham Biosciences., 2002).**

There exists a recommended nomenclature proposed by Phimister in 1999, where the immobilised oligonucleotides are referred to as the probe and the labelled sample represents the target.

## 7.1.2. Designing a microarray system

A successful microarray experiment requires the utilisation and / or development of several tools. These include, the probe selection and synthesis thereof, type of array platform and spot production, labelling of the target or mRNA, a well designed assay including hybridisation method, scanning and image analysis and data mining using bioinformatics tools to provide biological as well as statistical significance of the gene expression data.

There are three types of microarray platforms currently being used. These include i) spotted cDNA arrays, ii) spotted oligonucleotide arrays and iii) *in-situ* oligonucleotide arrays such as the Affymetrix GeneChip arrays.

cDNA probes are double-stranded and generally created from a cDNA library containing plasmid vectors with inserted mRNA segments that are harboured in bacterial clones, which can effortlessly be amplified up using PCR. Spotted oligonucleotide arrays are similar to cDNA arrays except that 20-80 mer synthetic oligonucleotide probes are designed and immobilised onto glass slides by a robotic spotter. The last array system that was developed by Affymetrix is referred to as the in-situ hybridisation platform where photolithography (Lee, 2004) is used to synthesise and immobilise directly onto a solid support base.

The spotting procedure can be undertaken using either contact or non-contact arraying of the cDNA or oligonucleotides onto the solid support base. The non-contact spotting method was adapted from the ink-jet industry where minute drops of solution are deposited onto the glass surface (Amersham Biosciences, 2002).
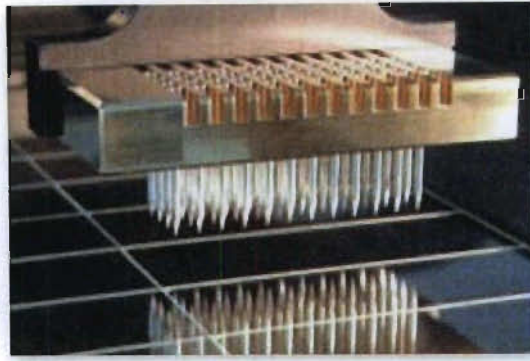


**Figure 73: Image showing the spotting of cDNA or oligonucleotides arrays into a glass support base (http://www.genetechhk.com/image/ser_spotting.jpg).**

The next aspect in the design process relates to target preparation, where target refers to the RNA or mRNA that was extracted using conventional methods and that was subsequently amplified and labelled using in-house or kit based methods. The purity of sample is of paramount importance when performing a microarray experiment as the data produced would only be as good as the RNA quality.

Following on from this is the process of target labelling. The use of fluorescent labelling in microarray analysis is favoured over other labelling options since fluorescence provides more sensitive detection and they are not chemically or biologically hazardous. The use of Cy dyes in microarray experiments is popular owing to their robust nature and resistance to photobleaching, as opposed to the fluorescein dyes. The Cy3 and Cy5 dyes complement each other well in experiments owing to minimal overlap between the two spectra.
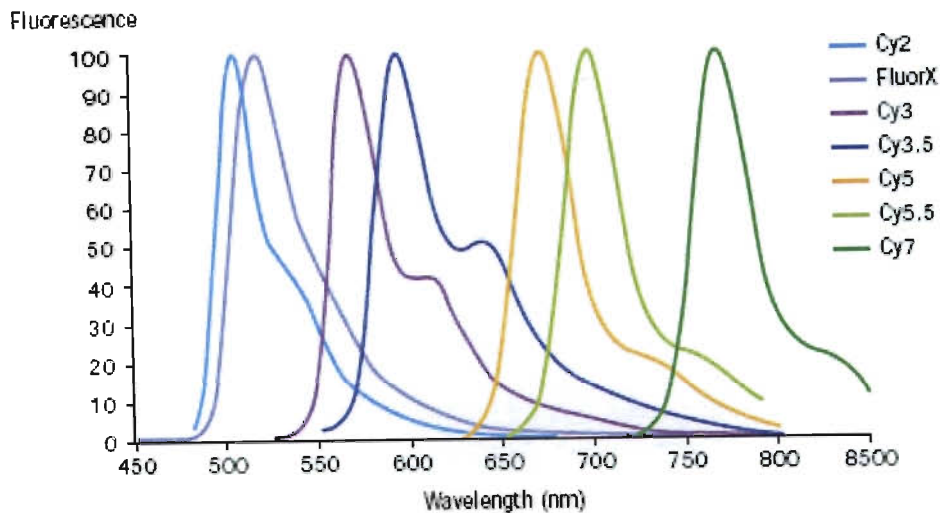
**Figure 74: Image representing the emission spectra and spectral overlaps between different Cy fluorophores (Amersham Biosciences., 2002).**

The Cy3 dye is detected at 532 nm and the Cy5 dye at 635 nm. (Amersham Biosciences, 2002).

Implementing the assay is the next step in the process where all necessary precautions need to be undertaken in order to produce the best quality data. After hybridisation, the slides are scanned and images are extracted.

The data resulting from microarray experiments have a biological significance once the statistical analyses have been performed by a bioinformatician. The two are closely intertwined as the one gives meaning to the other. Genepix is a software program that was designed to assist the researcher in assessing the microarray data. The software has several useful functions that make manual evaluation less demanding. There are numerous algorithms present within GenePix that allows one to quantify the changes in activity levels between test and reference. Before any further analysis is performed the user would have to manually detect all spots on the array and flag them as useable or not. This is a very important part of the process of analysis because it allows one to assess the quality of

the experiment based on the visual inspection of each spot. Spots can be manually flagged with quality flags such as good, bad, absent or not found.



| A | B |
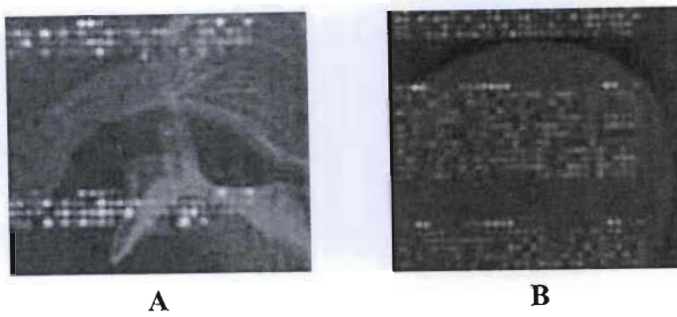
**Figure 75: Images showing some of the problems that can be encountered after completion of a microarray experiment. A: fluorescent background from hybridisation or pre-hybridisation mixture; B: air was trapped under the coverslip (Amersham Biosciences., 2002).**

### 7.1.3. Confirmation of microarray results

The high cost of microarray experiments makes it difficult for a biological researcher to include many replicates into an experiment in order to test the reliability of the data. One of the ways to confirm the results would be to use different microarray systems and compare the results obtained between platforms. That way the same samples would be included in both array systems and the need to confirm the data using other means would fall away.

Many laboratories only have a single microarray system at their disposal. Owing to this, other methods for confirmation of microarray data is employed. Such methods include the use of immunohistochemical analyses coupled to fluorescent imaging on a confocal microscope to detect the presence of immune response infiltrates in a muscle tissue for example that are over-expressed using microarray analysis. Other methods include Northern blotting and real-time PCR detection. The main concern with using Northern blotting is the large amount of RNA that would be required to obtain a definitive result.

This method has lost support as biopsy samples are difficult to obtain in abundant supply. Quantitative real-time PCR has gained much popularity owing to the short time over which the assays is run, the high accuracy of results obtained since fluorescence is used to monitor the amplification and most importantly small amounts of RNA is required.

### 7.1.4. Applications and importance of microarrays

There are numerous applications in the use of microarray technology, which includes both DNA and protein arrays. The first and most important application in DNA microarrays is that of gene discovery. The next area to benefit from microarray technology is the field of drug discovery. The buzzword in this burgeoning field is pharmacogenomics (Relling & Hoffman, 2007). For a long time it has been known that drugs affect individuals differently based on genetic background, ethnicity and other factors and the analysis thereof is given the term pharmacogenetics. The essential role of pharmacogenetics has already been documented in virological and oncology research scenarios (Mayor, 2007). Another related area is that of toxicological research where the changes in the genetic profiles of individuals can be monitored on exposure to the toxic elements under investigation. The terms toxicogenomics and systems toxicology have been coined to draw attention to this new field. There has been such a flood of data in the field of expression profiling that a specially designed database has been set-up by the FDA (Food and Drug Administration National Center for Toxicological Research, USA) to manage the data generation (Tong *et al.*, 2003).

A new aspect that is being developed in the field of expression profiling is protein microarray technology. One of he advantages of utilising protein microarrays is that one can study protein-protein interactions. (Hall *et al.*, 2007).

### 7.1.5. Literature survey

The molecular mechanisms underlying the pathogenesis of Duchenne muscular dystrophy (DMD) and the milder allelic form, Becker muscular dystrophy (BMD) have become the focus of attention. Internationally there has been a move towards finding clues to elucidate the molecular signatures that make DMD unique from other muscular dystrophies. Much time and effort have been invested in trying to find those genes that are differentially expressed in dystrophic tissue instead of maintaining their inactivated form as is the case in normal individuals. It is anticipated that gene profiling using microarray analysis will unveil the regulatory mechanisms that play a key role in effecting the differential expression of specific genes in dystrophic tissues. Once these genes have been identified their functional attributes in different tissues can be assessed.

The first paper to have provided an in-depth profile of the pathophysiological cascade of events that take place in two types of muscular dystrophies using the Affymetrix HuGeneFL high-density oligonucleotide array system (~6,000 full-length genes) was undertaken by Chen *et al.* (2000).

In an attempt to reduce the parameters that are affected in a study of this nature, the author declared that they limited the number of variables in the study to ensure that the outcome could be accepted. This was done by pooling RNA samples from different patients that

were approximately age matched from each of the three cohorts, which included an α-sarcoglycan group, a dystrophinopathy group and a control group. By implementing such a strategy they ensured that the primary biochemical defect remained constant. This is an original approach that has proven to be successful in providing data in an area where it was lacking, however there is still the problem of different patients having their own genetic background which is a bias that is difficult to remove completely when performing data analyses.

From 2001 to the present time, many studies have focussed on mapping the molecular signatures that underlie the disease processes in dystrophinopathies. In 2001, Tkatchenko et al. provided the first gene expression report using a cDNA microarray. Apart from those genes that were previously reported to be dysregulated in DMD muscle (Chen et al. 2000), of interest was the unexpected result of finding a downregulation of titin expression in DMD patients that confirmed using Northern blotting. The authors speculated that specific alterations may occur in DMD muscle with respect to the expression status of titin.

In 2002, Haslett et al. embarked on a study to compare 12 quadriceps samples from DMD patients and 12 normal control skeletal muscle tissue samples using the Affymetrix HG-U95Av2 arrays containing 12,500 known genes and full-length expressed sequence tags (ESTs). This study claimed to be different from the Chen et al. (2000) study as there was no pooling of the RNA samples and it was noted that a more elaborate and statistical analysis was included with two methods being employed. An important finding in this study was that more genes were up-regulated than down-regulated in DMD, which has been a consistent finding in those groups that worked on the mdx mouse model (Tseng et al., 2002; Porter et al. 2002). The mdx mouse model is not an ideal one for DMD since the

molecular circuitry involved in producing muscle pathology and clinical disease manifestations varies between the two species. Rouger *et al.*, (2002) also found that alterations to other genes on account of dystrophin deficiency are dissimilar between human and mouse (Rouger *et al.*, 2002), however *mdx* still provides important data relating to muscle fibre regeneration pathways. A caveat in the Haslett study (Haslett *et al.*, 2002a, Haslett *et al.*, 2002b) was the lack of clinical details for DMD affected males and the control individuals. Owing to this, it would be difficult to assess whether the data was in any way skewed by the varying ages of the individuals at the time of biopsy.

In 2002, Bakay *et al.* conducted a study aimed to provide a transcriptome for DMD and non-dystrophic, normal muscle. The four study categories included two dystrophinopathy groups comprising 10 samples and two non-dystrophic groups consisting of 8 samples which were subsequently pooled. This extensive study utilised the Affymetrix arrays together with a custom designed "MuscleChip" specific for human skeletal muscle (Bakay *et al.*, 2002), which collectively incorporated six different types of microarrays. The usefulness of the study was further augmented by the data being made publicly available on the following website http://microarray.cnmcresearch.org. This study served to improve on the expression status data of DMD patients that was previously reported (Chen *et al.*, 2000) by increasing the dataset to ~65,000 as opposed to the 5,600 microarray resource. On comparison of DMD affected to unaffected tissue using stringent statistical analyses, three times more genes were found to be over-expressed in DMD affected muscle than normals, in keeping with mdx mouse model findings (Tseng *et al.*, 2002; Porter *et al.* 2002). A new finding using cluster analysis revealed that there were genes specifically expressed in males that were not detected in the female group of patients. Even though the data is impressive owing to the amount of RNA samples required for Affymetrix analysis,

the samples had to once again be pooled as was the case in a previous paper by the same group (Chen *et al.*, 2000).

In 2003 Noguchi *et al.* designed a *c*DNA microarray composed of >4,000 genes and ESTs that were exclusively expressed in skeletal muscle. The study was considered unique as tissue samples were not pooled and the pathophysiological changes in each patient was mapped and compared to one another. The authors succeeded in correlating histological changes with the molecular alterations observed on gene expression analysis bringing us a step further in unravelling the mechanisms involved in pathogenesis.

To date, there have been no studies comparing different muscle groups in the same DMD affected patient. There has been one study by Kang *et al.* (2005), where four different muscle groups were compared using autopsy samples from individuals that had no signs of muscular dystrophy at the time of death. The study showed that individuality, age and muscle type significantly influenced gene expression differences suggesting that gene expression is very much influenced by a person's health at a given time. The age of an individual also reflected the state of the muscle and other tissues, which was confirmed by the adipose tissue that was observed in the muscle of geriatric group of patients. Even though the authors have highlighted some interesting and important findings, these results cannot be directly compared to biopsy samples as the samples were taken from autopsy patients.

In an attempt to understand why the regenerative process in DMD patients is so inefficient even though satellite cells are present, Sterrenburg *et al.* (2006) conducted cell culture studies on normal and DMD myoblasts at the activation and differentiation stages. One of

the key findings related to the over-expression of aquaporin 1 that signifies the active regenerative state in DMD and bone morphogenetic protein 4 (BMP4), which is known to inhibit differentiation of myoblasts into myotubes. Another significant finding was the reduction of sarcomeric proteins following the expression of dystrophin, which is thought to contribute to the instability of the DAGC. The other reduction noted was that of fibroblast growth factor 1, which is responsible for recruiting satellite cells for proliferation. Such a finding is significant as it explains the reduced proliferative capacity of myoblasts and why the regenerative process in DMD is flawed even though satellite cells are in the vicinity.

### 7.1.6. Reason for embarking on the study

At the time that this study was undertaken there was a gap in the literature with respect to gene profiling experiments on Duchenne muscular dystrophy where the same patient has been used to study and elucidate the pathogenesis in different tissues. Previous studies that focussed on generating pathogenesis data for DMD used either pooled samples from different dystrophinopathy patients (Chen *et al.* 2000) or a comparison was made between DMD affected and normal patients (Haslett *et al.*, 2002b).

We had a pool of DMD biopsy samples at the Neuroscience laboratory at IALCH, Durban, South Africa and we therefore attempted to answer some questions that would assist in the current understanding of DMD pathogenesis. An area of particular interest was the difference in size and strength seen in two muscle groups, the calf and either the biceps or the quadriceps muscles in the same dystrophinopathy affected patient. As is often seen in dystrophinopathy patients, the calf muscle remains invariably strong whereas the biceps /

quadriceps muscles become progressively weaker even though immunohistochemical analyses have revealed no dystrophin protein in either muscle group.

The use of two biopsy samples from the same patient as a comparison is unique as no other study of this nature has been performed using microarray analysis. It ensures no genetic variability therefore an unbiased study could be performed. Therefore using the same patient is a useful strategy as the genetic variability is completely removed, which is not the case when comparative studies are done between normal and diseased tissue. The approach of using the same patient and comparing different tissue groups had not been explored at the time of the study and it is bound to yield promising and definitive results as more large scale analyses are undertaken.

In 2006, there was a study conducted by Zhang *et al.*, where the same limb girdle muscular dystrophy patient was used to show differential expression between different muscles. However the authors utilised differential display RT-PCR, which was a completely different approach from microarray analysis. Further to this, the study was performed on muscle tissues of a different disease (LGMD) from Duchenne muscular dystrophy thus no comparisons could be made with other studies where normal and diseased tissues in DMD patients were compared. The authors (Zhang *et al.*, 2006) did however attempt to compare their results with previous DMD related studies and found no correlation with the two sets of data. This clearly emphasises the need for disease specific studies to be performed as the molecular mechanisms that regulate the pathogenesis in different diseases varies.

Our study initially utilised spotted oligonucleotide arrays to detect differential expression between different muscle groups in the same dystrophinopathy patient. Thereafter the

Illumina beadchips were incorporated into the study so that a comparison could be made between the spotted oligonucleotide arrays and the Illumina beadchips. The data was then compared to data obtained from a previous study performed at Professor Eric Hoffman's laboratory (Chen *et al.*, 2000). In this study pooled samples from DMD patients were compared to normal patients' biopsy samples (See "literature survey" above for more details).

The quantitative real-time PCR in our study focussed on a gene that is as yet not well characterised. The gene, adlican was found to be dysregulated during the microarray analysis therefore the author thought it would be interesting to try and unravel some of the properties of this gene by performing gene expression analysis on dystrophinopathy and polymyositis patients. In so doing, one could speculate about the role that adlican plays in diseased cells / tissues in different neuromuscular diseases.

## 7.2    AIMS AND OBJECTIVES.

(i)     To perform gene profiling analysis on double skeletal muscle biopsy samples from the same dystrophinopathy affected patient using spotted oligonucleotide arrays.

(ii)    Determine whether there were differences in the dysregulated genes between the two muscle groups using microarrays.

(iii)   Compare data between spotted oligonucleotide arrays and the Illumina beadchips.

(iv)    Unravel the properties of adlican and attempt to understand the gene's role in the disease process with real-time PCR using the LightCycler 2.

## 7.3 MATERIALS AND METHODS

Muscle tissue samples were stored in RNA*later* (Ambion) immediately after the biopsies were taken. This RNA protectant preserved the biopsies for future use and when they were needed.

### 7.3.1    Patient database

**Table 30: Database of patients included in the gene profiling analysis part of the study.**

| DNA number | Biopsy number | Surname, Initials | Gender | Age |
|---|---|---|---|---|
| 26 | 19/2003 | Z, S | M | 18 |
| 42 | 06/2006 | M, R | M | 12 |
| 43 | 03/2006 | S, V | M | 14 |
| 63 | 23/2004 | S, N | F | 25 |

Three males and a female manifesting carrier agreed to have double biopsies performed.

### 7.3.2    Tissue homogenisation

Two methods were assessed for optimal tissue homogenisation. The first used the MagnaLyser tissue homogenising instrument from Roche. The second included the use of the Ultra-Thurrax T25 homogenising tool. All muscle tissue samples were always stored on dry ice and minimally handled to prevent protease degradation.

### 7.3.2.1  MagNA Lyser (Roche)

The procedure followed was as per manufacturer's instructions (Roche).

### 7.3.2.2 Ultra-Thurrax T25 (Janke & Kunkel IKA-Labortechnik)

- The procedure used in the homogenisation was the same as detailed in 4.8.2, of Chapter 4. Amendments to the protocol are indicated below.

- The instrument used for the homogenisation procedure was the Ultra-Thurrax (Janke & Kunkel IKA-Labortechnik).

- The instrument was placed into a 0.1 M NaOH solution for 30 minutes to clean the probe prior to use. It was further cleaned in 100% ethanol using $3 \times 20$ second bursts at full speed (black setting). This was followed by $3 \times 20$ second bursts at full speed in autoclaved DEPC-treated water.

- A 1,000 µl volume of RNA-Bee (Tel-Test, USA) was added to the sample per 50 mg of tissue, instead of Trizol LS reagent.

- Each sample was homogenised for 2 x 30 seconds at low speed (yellow) using the homogenising tool.

- This step was repeated if tissue remnants were visible.

### 7.3.3    RNA isolation using RNA-Bee

The reagent used in the RNA extraction procedure was called RNA-Bee (Tel-test, USA). This reagent is similar to Trizol (Invitrogen) reagent. The active ingredient guanidinium isothiocyanate is used by both companies. The same procedure was undertaken as outlined in 4.8.3 of Chapter 4. Amendments to the protocol are presented below.

- All centrifugation were performed at 13,000 rpm (Biofuge A, Heraeus Sepatech) for at 4°C.

**Note.** Those samples that were homogenised using the MagnaLyser took much longer to resuspend in DEPC treated water than those that were homogenised using the Ultra-Thurrax.

### 7.3.4 RNA purification using the RNeasy mini clean-up kit (Qiagen)

The procedure was undertaken as shown in the manufacturer's handbook. The actual steps undertaken are also outlined in 4.8.3.2 of Chapter 4.

### 7.3.5 RNA quantification using the Nanodrop ND-1000

The same procedure was followed as was outlined in Chapter 6 (MLPA) of this thesis. The only amendment to the protocol was as follows:

- The spectrophotometer was initialised by placing a one microlitre volume of nuclease free water onto the lower measurement pedestal of the instrument.
- The "RNA" dialog box was chosen from the software.
- A 1.2 µl volume of RNA sample was placed onto the lower measurement pedestal of the Nanodrop.

All other aspects of the protocol remained the same.

### 7.3.6 Bioanalyser Lab-on-a-chip detection of total RNA quality and quantity

The RNA Nano kit was used to measure the quality and quantity of RNA samples prior to amplification and hybidisation reactions. The quality and quantity is measured to ensure that no degraded samples are used in the microarray experiments as this would confound

the results. Further to this, there has to be sufficient RNA sample for the experiments to yield useful results. Prior to undertaking the procedure, a new chips for 12 samples was removed from the storage cupboard. An aliquot of the RNA ladder was removed from -80°C and denatured at 72°C for two minutes using a PCR machine. The machine electrodes must be decontaminated prior to each run.

### 7.3.6.1 Decontaminating electrodes

The procedure followed was as outlined in the manufacturer's handbook (Agilent).

### 7.3.6.2 Preparation and measurement of samples

The procedure followed was as outlined in the manufacturer's handbook (Agilent). The aim was to work quickly and efficiently as it was important that the chip be electrophoresed on the bioanalyser within five minutes of being prepared and vortexed. If the procedure was not performed during this time, the reagents might evaporate thus leading to poor results since the volumes are very small to start with. Therefore all instrument preparations were completed before the chip preparation was undertaken. This included starting up the instrument as well as initiating the Agilent 2100 biosizing software. Following the software initialisation, the RNA-eukaryotic total RNA Nano assay was chosen.

### 7.3.6.3 RNA 6000 Nano assay expected results

- After the run has been completed, the results should be checked and verified. A run

takes approximately 30 minutes for 12 samples.

- The ladder should have six well resolved RNA peaks and one marker peak. The location of the peaks is important so as to correctly detect the ribosomal RNA bands from each sample.

- Each sample should have two ribosomal peaks (18 S rRNA and 28 S rRNA) and one marker peak.

- The reproducibility of the samples should be tested at the beginning of a sample batch. If the reproducibility is poor or if the ladder is not properly resolved and produces fewer peaks, it might be due to the use of a degraded ladder or the dye gel matrix being too old and unusable.

- An electropherogram, a gel image and a tabulated format was provided for each sample run.

### 7.3.7 RNA amplification using the MessageAmp™ aRNA kit (Ambion) for spotted oligonucleotide arrays

This kit was designed especially for the amplification of RNA that would be used in microarray analysis.

The procedure followed was as per manufacturer's instructions.
Amendments to the protocol are shown below:

- A spike mix (AA3 or AA4) was added at a 1:10 dilution to the samples. For each quadriceps or biceps muscle sample, a 1.0 µl volume of AA3 was added. This served as the muscle that was severely affected. For each calf muscle sample, a 1µl volume of AA4 was added. This muscle served as the less affected muscle.

### 7.3.8 *In-vitro* transcription in the presence of aminoallyl UTP for spotted oligonucleotide arrays

- Following the *c*DNA synthesis using the MessageAmp™ kit (Ambion), to the 15.2 μl double stranded *c*DNA was added 4 μl T7 ATP, 4 μl T7 CTP, 4 μl T7 GTP 2.4 μl T7 UTP, 2.4 μl T7 aminoallyl UTP (Ambion), 4 μl T7 10 × RT buffer and 4 μl T7 enzyme mix. The 10 × RT buffer was left at room temperature prior to use as it precipitates on ice.

- The above mixture was incubated at 37°C for nine hours in a thermal cycler block.

- Following the incubation, the samples were placed on ice. To each sample was added 2 μl of DNase I and it was incubated at 37°C for 30 minutes.

### 7.3.9 Amplified RNA (aRNA) purification using the MessageAmp™ kit for spotted oligonucleotide arrays

The procedure followed was as per manufacturer's instructions.

### 7.3.10 Hybridisation scheme for spotted oligonucleotide microarrays

For the two-colour spotted oligonucleotide arrays, two arrays per patient were included as is shown in the table below. The array utilised was taken from the "Sigma-Compugen human 19K 60-mer oligonucleotide collection". A single spotting approach was adopted by the LGTC (Leiden Genome Technology Center) and poly-L-lysine coated slides were used.

**Table 31: Table showing the dye-swap experimental scheme that was followed with the relationship between the biopsy number, muscle type and the fluorescent label outlined.**

| Sample number | Biopsy number | | Muscle type | | Microarray slide number |
|---|---|---|---|---|---|
| | Cy3 | Cy5 | Cy3 | Cy5 | |
| 1 | 06A/2005 | 06B/2005 | Calf | biceps | KD_human#17 |
| 2 | 06B/2005 | 06A/2005 | Biceps | calf | KD_human#18 |
| 3 | 23A/2004 | 23B/2004 | Biceps | calf | KD_human#19 |
| 4 | 23B/2004 | 23A/2004 | Calf | biceps | KD_human#16 |
| 5 | 19A/2003 | 19B/2003 | Quad | calf | KD_human#12 |
| 6 | 19B/2003 | 19A/2003 | Calf | quad | KD_human#13 |
| 7 | 03A/2005 | 03B/2005 | Biceps | calf | KD_human#07 |
| 8 | 03B/2005 | 03A/2005 | Calf | biceps | KD_human#85 |

## 7.3.11 Labelling cDNA with amine-reactive reagent for spotted oligonucleotide arrays

The procedure was carried out as outlined in the Amersham handbook (Amersham Biosciences, 2002).

## 7.3.12 Slide pre-hybridisation for spotted oligonucleotide arrays

The procedure was carried out as outlined in the Amersham handbook (Amersham Biosciences, 2002).

## 7.3.13 Hybridisation of sample mixture to expression array in the hybridisation station

The procedure was carried out as outlined in the handbook (Amersham Biosciences, 2002).

### 7.3.14 Post-hybridisation washing for spotted oligonucleotide arrays

The procedure was carried out as outlined in the Amersham handbook (Amersham Biosciences, 2002).

### 7.3.15 Cleaning apparatus, module, rubber "O" rings and white screws

The procedure followed was as outlined in the instrument manual (GeneTAC hybridisation station, Genomic Solutions).

### 7.3.16 Scanning spotted oligonucleotide slides and data extraction on the Agilent system

The procedure was carried out as outlined in the Agilent handbook.

### 7.3.17 Manual visualisation of spotted oligonucleotide array data and analysis using GenePix 5.1

The procedure was carried out as outlined in the GenePix 5.1 manual.

### 7.3.18 Rosetta resolver

The methodology followed was as per manufacturer's instructions.

**Table 32: Table showing the sample number and sample type used for analysis in Rosetta resolver.**

| Sample number | Patient's name | Biopsy number | Muscle type |
| --- | --- | --- | --- |

| 1 | M, R | 06A/2005 | Calf |
|---|---|---|---|
| 2 | M, R | 06B/2005 | Biceps |
| 3 | S, N | 23A/2004 | Biceps |
| 4 | S, N | 23B/2004 | Calf |
| 5 | Z, S | 19A/2003 | Quadriceps |
| 6 | Z, S | 19B/2003 | Calf |
| 7 | S, V | 03A/2005 | Biceps |
| 8 | S, V | 03B/2005 | Calf |

## 7.3.19 Analysis using "R"

- "R" is a microarray analysis program where macros and other algorithms are written to achieve the desired analysis for a data set.

- "R" version 2.0.1 was downloaded and installed from the website www.bioconductor.org. This is the website of the developers. To download the software, click on "base" and download "rwz001.exe. Choose setup 1 from the executable file.

- Drop down menus can be used to perform a few tasks.

- The package contains algorithms that people have designed and these contain signettes, such as QC scripts and normalis.

- Instructions for the use of "R" are explained in the website. Such features as "GoTools", "limma", "multitest" and "respos tool" are included.

- A series of exercises are set up for first time users.

- For practical course go to http://dial.liacs.nl.courses/. This would take one to the QC practical, which is a quality control exercise for 2 colour microarrays in "R".

- The first task would be to create a directory where all files are housed as "R" can only read and write to one directory.

- An example of what can be done is as follows: on the "R' console type

  > library(marray)     [to load]

215

- The directory should be changed to the data file being used, which is also called the working directory, I:/>everyone/Kumari/microarray/R.

- All previous commands that are included are still available to the user by means of the arrow keys.

- To read the gal. file, type

  galinfo ← read galfile

  sigmahuman.layout ← galinfolayout sigmahuman.gnomes, where gnomes will be the gene identifiers. In this case the accession numbers.

- Background correction can also be done using "R'. Normalisation is done by determining the quality control by using "limma". One can do both pre-normalisation and post-normalisation plots to get a idea of the data quality.

### 7.3.20 Spotted oligonucleotides: analysis of differential expression for each patient

The samples were processed and normalised with Rosetta's error models. A dye-swap was performed therefore two arrays per patient were combined. P-values were calculated using Rosetta's error model. A P-value of <1E-6 was significant, which is equivalent to the Bonferroni method for multiple testing. The Bonferroni method is highly stringent, however owing to the small replicate size of two per group, it is essential that stringency be high.

### 7.3.21 Illumina bead arrays

This part of the work was performed by the laboratory technician at the Leiden genome technology centre under the supervision of Dr. P.'t Hoen. The RNA that was previously

extracted and purified by the author (see 7.3.2, 7.3.3, 7.3.4, 7.3.5 above) was used in these experiments. Amplification reactions and subsequent biotin-labelling for each sample was performed using the Illumina RNA amplification kit (Ambion) according to the manufacturer's instructions as outlined in the handbook.

**7.3.21.1    Arrays used**

These were one-colour chips, where one sample was used per array. Many arrays per sample were therefore obtained. The "Illumina Human Sentrix-6 Beadchip" arrays were used. These were 45K 50-mer oligonucleotides that are attached to beads. For each gene being represented, an average of 30-50 beads is used. Since a single chip was made up of 6 separate but identical arrays it was possible to load 6 samples from positions A-F.

**7.3.21.2    Hybridisation scheme**

**Table 33: Table outlining the hybridisation profile for each sample on the Illumina Sentrix human-6 expression bead chip system.**

| Chip Barcode | Position | Array Batch | Hyb Day | Patient | Severity | Muscle | Sample |
|---|---|---|---|---|---|---|---|
| 1412091107_D | 1412091107 | D1 | 1 | 6 | Low | 6A | Calf |
| 1412091107_E | 1412091107 | E1 | 1 | 6 | High | 6B | Biceps |
| 1412091107_F | 1412091107 | F1 | 1 | 3 | High | 3A | Biceps |
| 1412091105_D | 1412091105 | D1 | 1 | 3 | Low | 3B | Calf |
| 1508893088_A | 1508893088 | A2 | 2 | 6 | Low | 6A | Calf |
| 1508893088_B | 1508893088 | B2 | 2 | 6 | High | 6B | Biceps |
| 1508893088_C | 1508893088 | C2 | 2 | 6 | Low | 6A | Calf |
| 1508893088_D | 1508893088 | D2 | 2 | 23 | High | 23A | Biceps |
| 1508893088_E | 1508893088 | E2 | 2 | 6 | Low | 6A | Calf |
| 1508893089_A | 1508893089 | A2 | 2 | 23 | High | 23A | Biceps |
| 1508893089_B | 1508893089 | B2 | 2 | 23 | Low | 23B | Calf |
| 1508893089_C | 1508893089 | C2 | 2 | 19 | High | 19A | Quad |
| 1508893089_D | 1508893089 | D2 | 2 | 19 | Low | 19B | Calf |
| 1508893089_E | 1508893089 | E2 | 2 | 3 | High | 3A | Biceps |
| 1508893089_F | 1508893089 | F2 | 2 | 3 | Low | 3B | Calf |
| 1508893080_A | 1508893080 | A2 | 3 | 3 | High | 3A | Biceps |

| 1508893080_B | 1508893080 | B2 | 3 | 3 | Low | 3B | Calf |
|---|---|---|---|---|---|---|---|
| 1508893080_C | 1508893080 | C2 | 3 | 23 | High | 23A | Biceps |
| 1508893080_D | 1508893080 | D2 | 3 | 23 | Low | 23B | Calf |
| 1508893080_E | 1508893080 | E2 | 3 | 19 | High | 19A | Quad |
| 1508893080_F | 1508893080 | F2 | 3 | 19 | Low | 19B | Calf |
| 1508893086_A | 1508893086 | A2 | 3 | 19 | High | 19A | Quad |
| 1508893086_B | 1508893086 | B2 | 3 | 19 | Low | 19B | Calf |
| 1508893086_C | 1508893086 | C2 | 3 | 23 | Low | 23B | Calf |
| 1508893086_D | 1508893086 | D2 | 3 | 23 | High | 23A | Biceps |
| 1508893086_E | 1508893086 | E2 | 3 | 23 | High | 23A | Biceps |
| 1508893086_F | 1508893086 | F2 | 3 | 23 | Low | 23B | Calf |
| 1412091107_D | 1412091107 | D1 | 1 | 6 | Low | 6A | Calf |

### 7.3.21.3 Analysis of differential expression

Sample data was subjected to quantile normalisation using "R", with no background correction being performed. Even though a different wash protocol was performed on day one hybridisation samples compared to days two and three, the data from day one was included in the analysis in order to ensure an adequate number of sample replicates were included. The Benjamin-Hochberg multiple testing was used, which creates adjusted P-values. These are interpreted as the "lowest false discovery rate (FDR) at which the gene is still significant". To establish differential gene expression, an FDR of 0.05 was used as the cut-off value. This equates to 5% false positives in a list of differentially expressed genes. An FDR of 0.1 was used to detect the overlap between biopsy samples 6, 19 and 23.

### 7.3.22 Confirmatory quantitative PCR

One of the genes, adlican or MXRA5, a matrix remodelling precursor protein was subjected to quantitative real-time PCR using the LightCycler 2. This protein appears to play a role in the pathological states of diseases such as muscular dystrophy and inflammatory conditions. Comparisons in gene expression were tested in dystrophinopathy

and the inflammatory condition, polymyositis. Probes obtained from the universal probe library were used to detect the product with gene specific primers. This gene expression was compared in the following ways:

1. Dystrophinopathy patients' double biopsy samples were compared.

2. Duchenne and Becker muscular dystrophy patients' samples were compared.

2. Polymyositis patients' biopsy samples were compared to the samples from dystrophinopathy patients both DMD and BMD patients.

### 7.3.22.1 Biopsy tissue homogenisation

Muscle biopsy samples that were cut into tiny pieces and preserved using RNA*later* were homogenised when required. The same procedure for homogenisation was followed as previously outlined in 4.8.2 of Chapter 4. The Polytron Kinematica AG PT 1200 with six speeds served as the homogenising tool.

### 7.3.22.2 RNA extractions using Trizol LS

RNA was extracted from homogenised samples using the Trizol LS reagent (Invitrogen). The same procedure was followed as outlined in 4.8.3.1 of Chapter 4. Subsequent to the RNA extraction using Trizol LS reagent the protocol from the clean-up section of the RNeasy fibrous tissue mini kit (Qiagen) was followed.

### 7.3.22.3 *c*DNA preparation and RT-PCR using ImProm-II™ RT (Promega)

- Sterile nuclease free tubes and reagents were used in the preparation of the *c*DNA.

- All master mix preparations were performed in a biohazard laminar flow bench that was wiped down with RNAZap prior to undertaking the procedure.

- The initial amount of RNA added to each reaction tube was diluted to 50 ng/µl and a 3 µl volume was included per reaction, therefore 150 ng was included per reaction.

- Two methods were used in the preparation of the RNA target and the production of the cDNA. These included the use of (i) random hexamers (Roche) and (ii) gene specific primers (Adlican primers).

- For the two types of reactions outlined in the tables below, the same samples were used so that a comparison could be made between the two types of reaction methods.

**Table 34: Table showing the inclusion of random hexamers in the initial reaction for the preparation of cDNA.**

| Reagent | Concentration | Volume (µl) |
|---|---|---|
| RNA template | Up to 1 µg | 3.0 |
| Random hexanucleotides | 20 pMol / 0.5 µg | 1.0 |
| Nuclease free water | | 1.0 |
| Final volume | | 5.0 |

**Table 35: Table showing the inclusion of gene specific primers in the initial cDNA preparation reaction.**

| Reagent | Concentration | Volume (µl) |
|---|---|---|
| RNA template | Up to 1 µg | 3.0 |
| Adlican forward primer | 20 pMol / 0.5 µg | 1.0 |
| Adlican reverse primer | | 1.0 |
| Nuclease free water | | 0 |
| Final volume | | 5.0 |

- Samples were incubated at 70°C using a thermocycler for 5 minutes.

- Following incubation, the samples were placed on a hold cycle at 4°C using the

220

thermocycler and subsequently chilled on ice until the master mix for the RT

reaction was ready.

**Table 36: Reagents included in the reverse transcriptase reaction mixture using the ImProm-II RT enzyme.**

| Reagent | Concentration | Volume (µl) |
|---|---|---|
| Nuclease free water | | 5.6 |
| ImProm-II 5 × reaction buffer | 1 × | 4.0 |
| MgCl$_2$ 25 mM | 3 mM | 2.4 |
| dNTPs (10 mM) | 0.5 mM | 1.0 |
| Recombinant RNAsin® ribonuclease inhibitor | 1 U/µl | 20.0 |
| RT enzyme (vortex mixture and add enzyme) | | 1.0 |
| Final volume | | 15.0 |

- The solution was gently vortexed to mix and 5 µl of RNA template was added to the reaction mixture. The final volume was 20 µl.

- Only one tube was opened at any given time to avoid any cross-contamination between samples.

- The universal probe library (Roche) was used to design probes that suited the gene specific primers for adlican. The adlican primers were designed using the Primer express software by a Roche applications specialist.

- The reverse transcription was performed as per manufacturer's instructions (Roche).

**Table 37: Master mix reagents used in the preparation of the amplification reaction for the LightCycler 2.**

| Reagent | Volume (µl) |
|---|---|
| Nuclease free water | 11.0 |
| Primers + Probe [10 ×] | 2.0 |
| 5 × Master mix | 4.0 |
| cDNA | 3.0 |
| Final volume | 20.0 |

- Following the master mix addition, the template was added to each glass capillary. Each capillary has a number and the template being added to each capillary was noted.

- Immediately following the addition of template to the master mix, a cap was securely fastened to each glass capillary using the capping tool. This device was used to place the stopper into the glass capillary to ensure no cross contamination occurred between samples. Once all samples were added, the adaptors containing the glass capillaries were centrifuged using a regular bench top centrifuge at $700 \times g$ for 5 seconds. The adaptors are made such that they fit securely into a regular bench top centrifuge.

- Each capillary was then placed into the LightCycler 2 carousel in the appropriate order.

**Table 38: Programs included in the amplification of the adlican gene using the UPL and TaqMan hydrolysis probe detection system on the LightCycler 2.**

| Program name : Pre-incubation | | | | | | |
|---|---|---|---|---|---|---|
| Cycles | 1 | Analysis mode | None | | | |
| Target (°C) | Hold (hh:mm:ss) | Slope (°C/s) | Sec target (°C) | step size (°C) | step delay (cycles) | Acquisition mode |
| 95 | 00:10:00 | 20 | 0 | 0 | 0 | None |
| Program name: Amplification | | | | | | |
| Cycles | 45 | Analysis mode | Quantification | | | |
| Target (°C) | Hold (hh:mm:ss) | Slope (°C/s) | Sec target (°C) | step size (°C) | step delay (cycles) | Acquisition mode |
| 95 | 00:00:10 | 20 | 0 | 0 | 0 | None |
| 60 | 00:00:20 | 20 | 0 | 0 | 0 | None |
| 72 | 00:00:20 | 20 | 0 | 0 | 0 | Single |
| Program name: Cooling | | | | | | |
| Cycles | 1 | Analysis mode | None | | | |
| Target (°C) | Hold (hh:mm:ss) | Slope (°C/s) | Sec target (°C) | step size (°C) | step delay (cycles) | Acquisition mode |
| 40 | 00:00:30 | 20 | 0 | 0 | 0 | None |

- The LightCycler software version used was LCS4.0.0.23.

- Following the amplification, absolute quantification was performed and the channel used was 530 nm.

**Note.** The primers/probe mixture was reduced to 1 µl per reaction in subsequent amplifications reactions.

### 7.3.22.4     RT-PCR using Transcriptor reverse transcriptase (Roche)

- The same procedure was followed as is outlined above in 7.3.21.3 for the preparation of the RNA target prior to reverse transcription. Random hexanucleotides were used in the RNA target preparation. The RNA + template mixture was incubated at 65°C for 10 minutes, which was the recommendation in the package insert to denature the RNA secondary structures. This step differed slightly from the procedure in 7.3.21.3 where the RNA + template mixture was incubated at 70°C for 5 minutes.

- The mixture was composed of template, water and random primers, which collectively produced a volume of 13 µl. A concentration of 300 ng per RNA samples was included, with 2 µl of random hexamers being added.

**Table 39: Description of the components that were included in the reverse transcription reaction using transcriptor reagents.**

| Reagent | Volume (µl) | Final concentration |
|---|---|---|
| 5 × Transcriptor RT reaction buffer | 4.0 | 1 × |
| RNase inhibitor | 0.5 | 20 U |
| dNTPs (10 mM) | 2.0 | 1 Mm |
| Transcriptor RT enzyme | 0.5 | 10 U |
| Final volume | 7.0 | |

- Following the denaturation step, the reverse transcription procedure was undertaken (Table 39).

- The contents were mixed well by vortexing. The tube was briefly spun down using a micro-centrifuge to collect the content at the bottom.

- The 7 µl master mix was added to the 13 µl template + random hexamer mixture. The 20 µl final volume was mixed well by pipetting.

- The solution was incubated for 10 minutes at 25°C using a thermocycler. This was followed by a 30 minute incubation at 55°C.

- The reverse transcriptase enzyme was inactivated by heating for 5 minutes at 85°C.

- The tubes were immediately placed on ice.

- The recommendation according to the package insert was that the reaction could be stored at 4°C for 1-2 hours or at -20°C for longer periods. We opted to use the cDNA immediately in a PCR reaction, which followed the same procedure as was outlined above in 7.3.21.3.

## 7.4 RESULTS

There were initially six samples that would have been included in the study. However, due to sample degradation the quality of the RNA was poor as was the purity in two pairs (calf and biceps muscle) of tissue samples. Sample degradation could have been attributed to the age of the samples as the biopsies were taken in 1996 and 1999 respectively. The samples were not preserved in a RNA protectant such as RNA*later*. They were merely stored at -80°C.

Initially the homogenisation was carried out without the addition of yeast tRNA. However,

on running those samples that did not contain yeast tRNA in the centrifuge tube, degradation of the sample was evident. This was shown by the 28 S rRNA band being less intense than the 18 S rRNA band as is revealed in the figure below. For the next batch of samples, a 10 µl volume of yeast tRNA (Sigma) at a concentration of 10 µg/µl was added to the sample tube prior to the homogenisation procedure. The yeast tRNA served as an additional substrate thereby reducing the amount of RNA degradation to the sample.

## 7.4.1 Gel image comparing the Magnalyser instrument (Roche) and the Ultra-Thurrax homogenising tool.

With respect to the images below, the RNA high range (Fermentas) molecular weight marker, comprising eight bands was included in lane 1 of each gel that was electrophoresed.



(A)                                        (B)
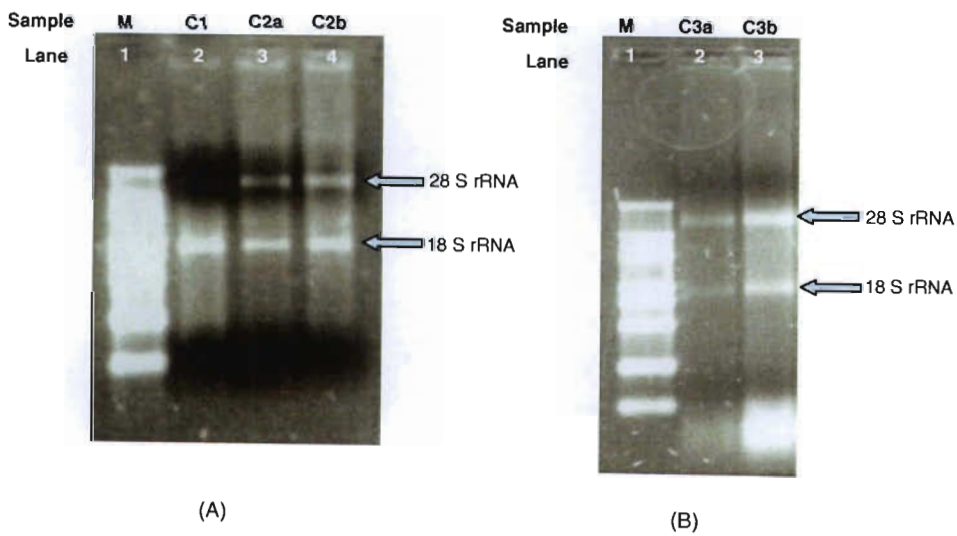
**Figure 76: Image showing the 28 S and 18 S rRNA bands from control muscle tissue when tissue homogenisation was compared using the MagnaLyser instrument (A) and the Ultra-Thurrax (B).**

The band sizes were as follows: 6,000; 4,000; 3,000; 2,000; 1,500; 1,000; 500; 200 bp. C1 = control sample 1, C2a, control sample 2a, C2b, control sample 2b, C3a = control sample

C3a, C3b = control sample C3b. Image (A) compares the rRNA bands that were obtained

when the MagnaLyser and the Ultra-Thurrax were used. Control sample C1, illustrates the

loss of the 28 S rRNA band when the Magnalyser (Roche) was used. Other individuals at

the Department of Human and Clinical genetics research laboratory, Leiden University

also had the same problem. Control samples C2a and C2b were homogenised using the

Ultra-Thurrax. No tRNA was added to centrifuge tubes containing either tissue sample C2a

or C2b. All other parameters remained the same as that of the samples that were subjected

to homogenisation using the MagnaLyser. As is evident from the above image, the 28 S

rRNA band in samples C2a and C2b were slightly degraded since the 28 S band is not

twice as intense as the 18 S band. The reason for this could be attributed to not adding

yeast tRNA to the sample tubes. The addition of the yeast tRNA served to provide another

substrate that would also be subjected to protease degradation thereby reducing the

degradation caused to the tissue sample. In effect this served to protect the tissue sample.

Image (B) shows the 28 S rRNA band being twice as intense as the 18 S rRNA band,

which suggests no sample degradation. In this case the Ultra-Thurrax was used to

homogenise the sample and 10 µl of yeast tRNA was added to the sample tube. This result

revealed the usefulness of adding yeast tRNA as an additional substrate to be digested by

degradation substances. For all subsequent tissue homogenisations, the Ultra-Thurrax was

used and 10 µl of yeast tRNA was added to the tube. The samples were kept on ice at all

times to minimise protease degradation.

## 7.4.2   RNA quantity and quality assessment using the Bioanalyser lab-on-a-chip.

All samples to be included in the gene profiling aspect of the study had to be of high

quality and purity to ensure that the results obtained could be utilised in further

bioinformatics and statistical analyses. This quality assessment was performed using the

RNA 6000 Nano kit. Each sample was electrophoresed twice on the Bioanalyser to test the

reproducibility of the instrument. For each batch of samples electrophoresed, the

instrument produced a gel image, a graphical representation of the bands and a tabulated

result. The area under the peak of the 28 S and 18 S rRNA bands was calculated.
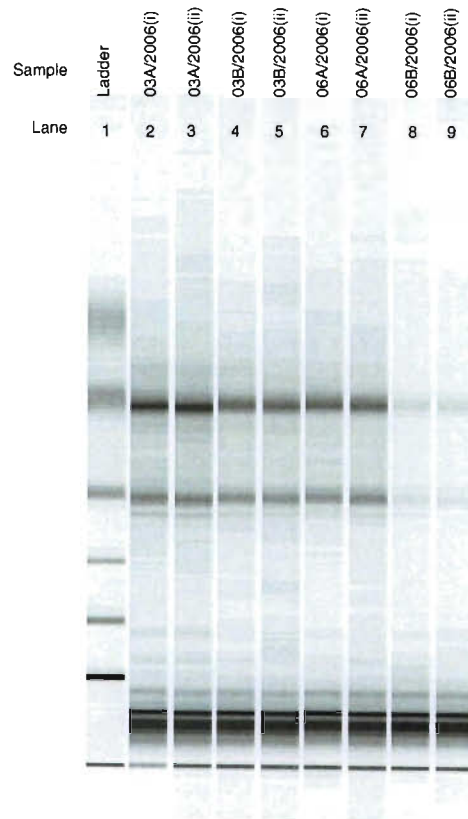


**Figure 77: Gel image generated by the Bioanalyser software to illustrate the intensity of the rRNA bands and their corresponding position in relation to a known ladder with defined sizes.**

The images and table 40 illustrates that the reproducibility of the bioanalyser was good

considering only 1 µl of sample was used. The 28 S rRNA band would normally need to be

twice that of the 18 S rRNA band. This is a sign of good quality and pure RNA that is not

degraded. Owing to this, we were confident of the results obtained and it would precisely

reflect the actual state of the genes as it would not be confounded by other factors such as

sample degradation.
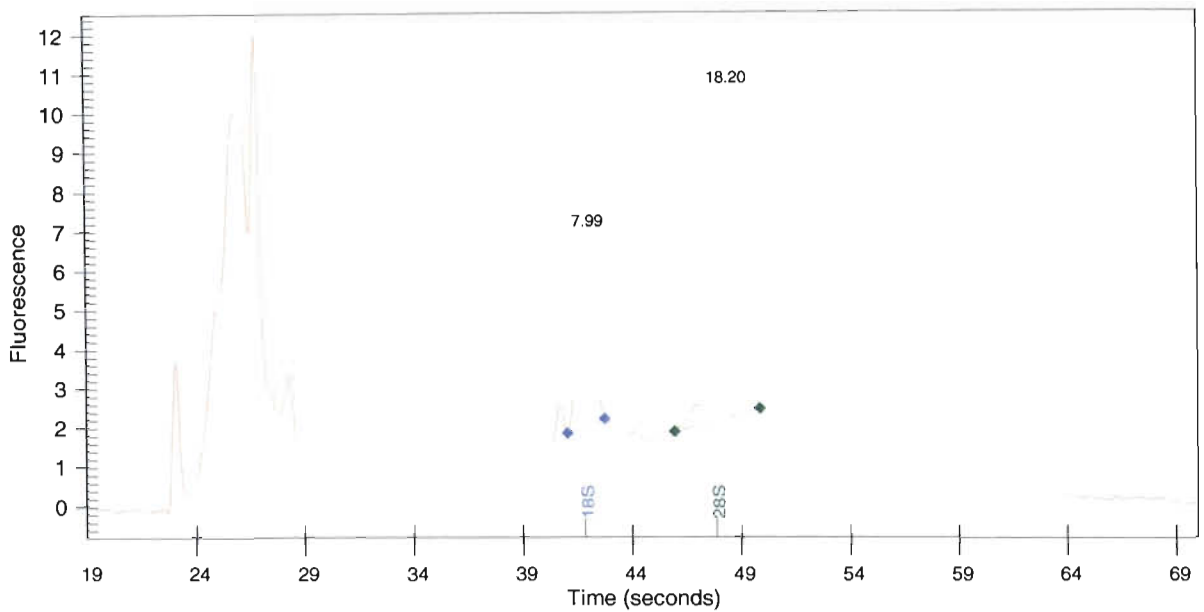


**Figure 78:** Graphical image showing peaks of the 18 S and 28 S rRNA species obtained using the biceps muscle sample 03A/2006(i) from patient S.V. as the representative sample.
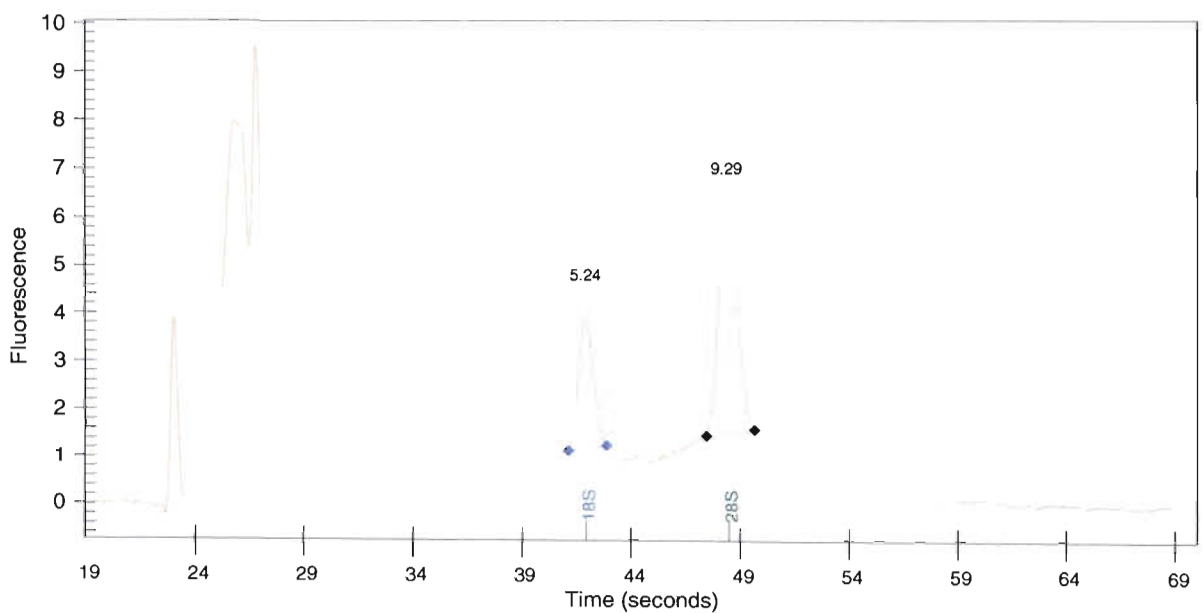


**Figure 79:** Representative graph showing peaks of the 18 S and 28 S rRNA species obtained using the calf muscle sample 03B/2006(i) from patient S.V.

Since the samples from patients 19/1999 (Figure 80) and 06/1996 (Figure 81) had very low concentrations of RNA, the samples were excluded from the study.

Data interpretation could not have been done with poor quality RNA, especially since we would be looking for subtle gene expression changes.

**Table 40: Table demonstrating the reproducibility of the Bioanalyser when the same sample subjected to electrophoresis and analysis.**

| Fragment 03A/2006(i) | Name | Start_Time(secs) | End_Time(secs) | Area | % of total _Area |
|---|---|---|---|---|---|
| 1 | 18S | 41.05 | 42.75 | 7.99 | 3.63 |
| 2 | 28S | 45.95 | 49.85 | 18.20 | 8.26 |
| RNA Area | 220.26 | | | | |
| RNA Concentration(ng/ul) | | 253.56 | | | |
| rRNA Ratio [28S / 18S] | | 2.28 | | | |

| Fragment 03A/2006 (ii) | Name | Start_Time(secs) | End_Time(secs) | Area | % of total_ Area |
|---|---|---|---|---|---|
| 1 | 18S | 41.00 | 42.65 | 7.60 | 3.55 |
| 2 | 28S | 46.20 | 49.75 | 17.90 | 8.37 |
| RNA Area | 213.80 | | | | |
| RNA Concentration(ng/ul) | | 246.12 | | | |
| rRNA Ratio [28S / 18S] | | 2.36 | | | |
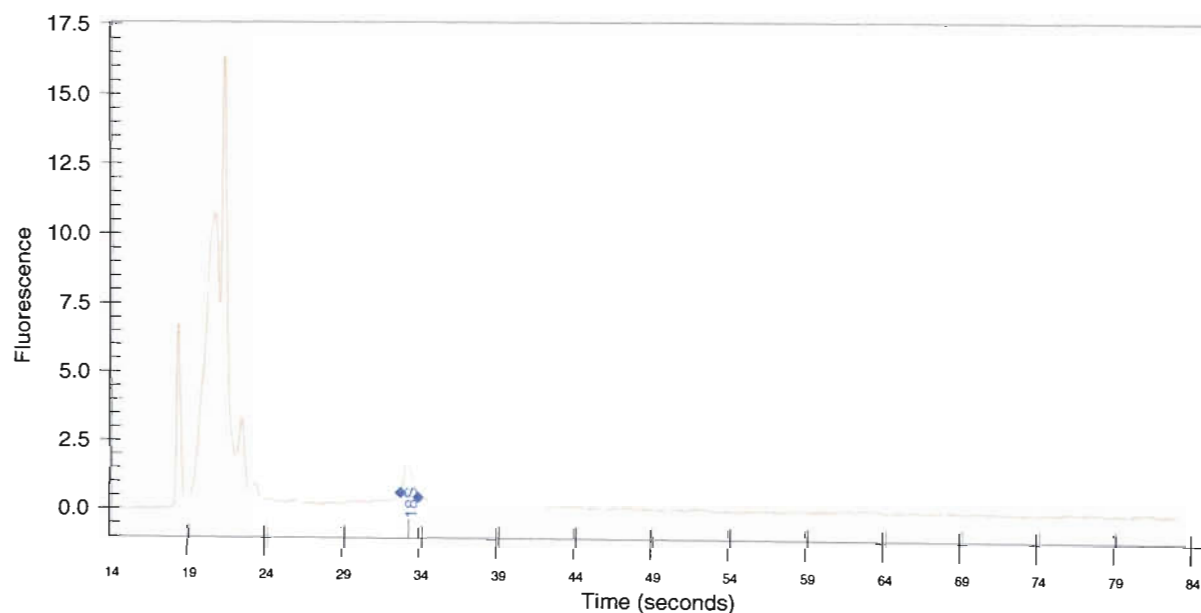


**Figure 80:** Image showing a poor quality sample with a low RNA concentration. The sample (19/1999) is also degraded as is shown by the 18 S rRNA peak being larger than the 28 S rRNA peak.
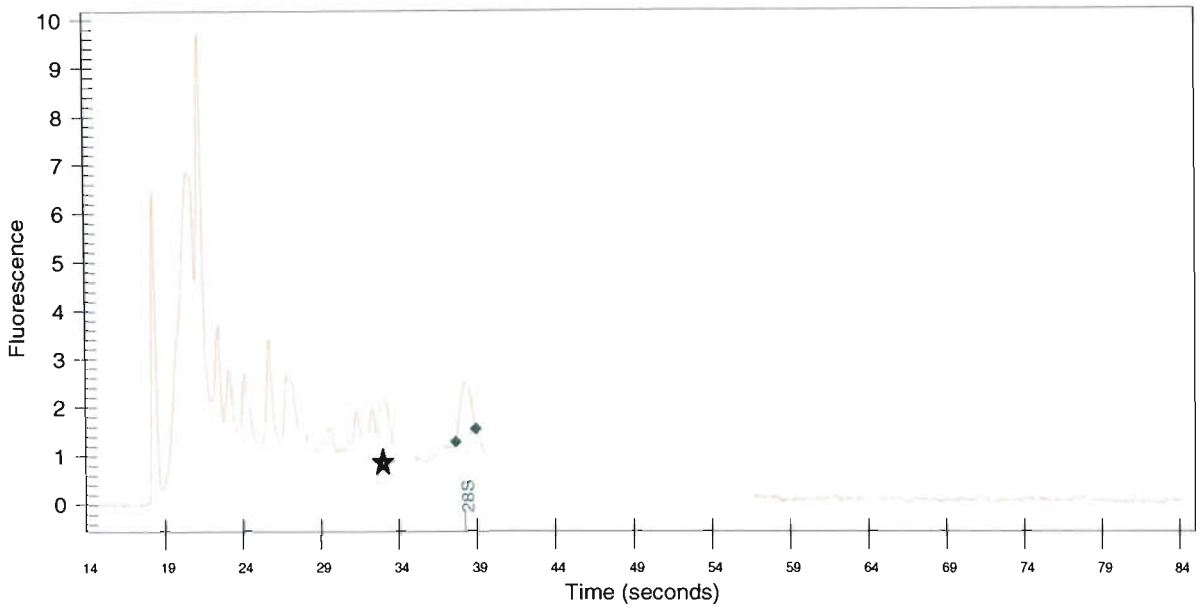
**Figure 81:** **Graphical representation of an impure sample. The sample (06/1996, biceps) also shows degradation products in the form of multiple peaks, in close proximity to where the 18 S rRNA band would normally be present (green star).**

### 7.4.3 GenePix image of a scanned slide

"A" shows the actual slide using the sample from patient 43 (Sibiya,V), "B" reveals the glyceraldehydes-3-phosphate dehydrogenase (GAPD-H)control spots, "C" shows a down-regulated gene visualised as a green spot and "D" shows an up-regulated gene which is viewed as a red spot.

The GAPD-H control region is easily visible as can be seen by the yellow spots at the top left of the slide. There are over 300 GAPD-H control spots on a single slide.

**A: Sibiya, V**

**B: GAPD-H spots**

**C: Downregulated: Cy3**

**D: Upregulated: Cy5**
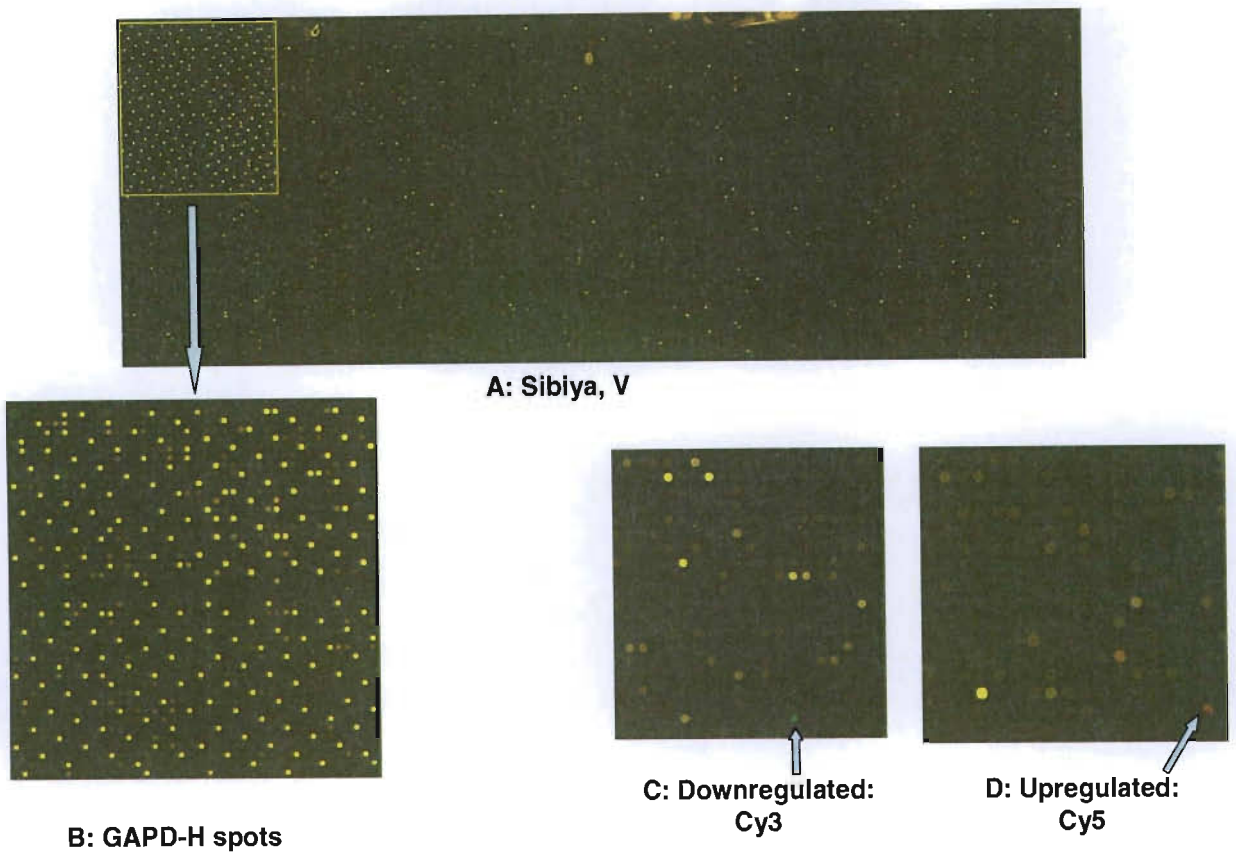
**Figure 82:** **Representative image of a microarray slide that was viewed using the GenePix 5.1 software.**

## 7.4.4 Normalised data from spotted oligonucleotide arrays

For each patient, biceps / quadriceps and a calf muscle sample were compared. The graphs below show those genes that were unchanged, represented by blue (+), the down-regulated genes represented by green (+), the up-regulated gene represented by red (+) and a combination of the dysregulated genes, which are represented by grey (+).

Interestingly, the data obtained for the patient with biopsy number 06/2005 showed many more dysregulated genes than the other patients. This is a 12 year old Indian South African patient. He had enlarged calf muscles and had much pain and weakness in his upper arms and his legs were becoming progressively weaker. Hypertrophy was also noted in his

231

forearm flexors. This child appears to be severely affected, which may be attributed to the exon 45 deletion that was found on multiplex PCR and MLPA analysis. A single exon deletion is usually not common and DNA sequencing of the exon would have to be performed using a PCR product that was amplified using different primers, to confirm whether it is a single exon deletion or a single nucleotide polymorphism that is pathogenic. If the deletion were genuine, this would indicate an out-of-frame deletion hence the severe clinical symptoms.
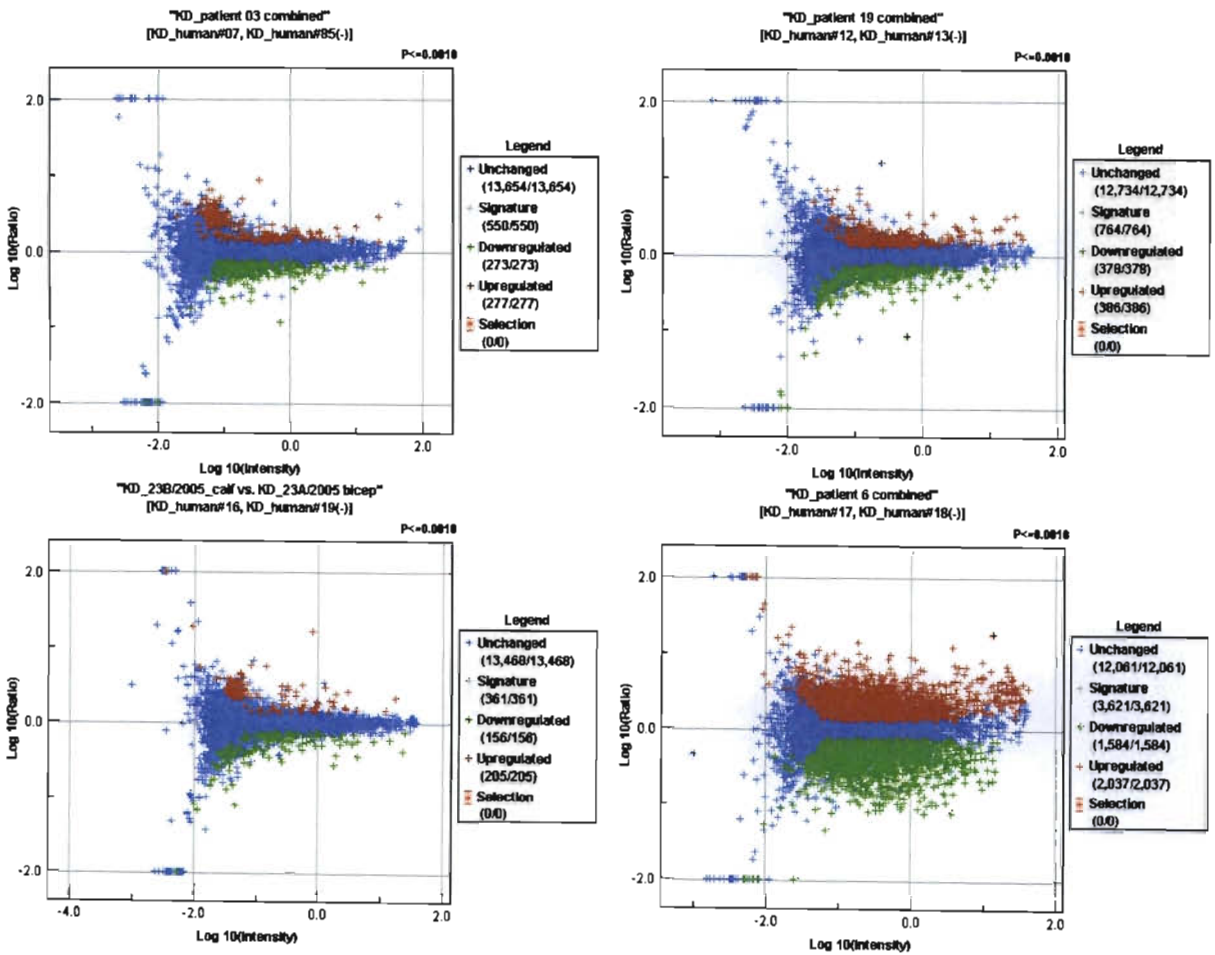


**Figure 83: Images showing scatter plots of normalised data for each patients' samples that were subjected to the spotted oligonucleotide array approach.**

The other three patients did not show as many dysregulated genes. This may be due to the less severe clinical manifestation of the disease. The DNA from patient 03/2005 showed a

deletion of exons 45-52 (out-of-frame) on multiplex PCR and deletion of exon 45-56 on MLPA analysis. The patient is a 14 year old Black South African. He showed marked wasting of proximal muscles and slight calf hypertrophy with normal strength in the calves being noted.

The other male patient, whose biopsy number was 19/2003 showed a Becker muscular dystrophy phenotype. He was an 18 year old Black South African patient. He showed marked calf hypertrophy and forearm hypertrophy. Multiplex PCR on the patient's DNA sample revealed a 45-47 in-frame deletion hence the milder disease severity seen in this patient. The quadriceps muscle for the dystrophin 1 stain showed a mosaic pattern of staining, dystrophin 2 showed positive and a few negative fibres and dystrophin 3 showed positive and a few negative fibres. The calf muscle showed a mosaic pattern of staining for dystrophin 1, dystrophin 2 showed positive and a few negative fibres and dystrophin 3 showed positive and a few negative fibres.

The last patient was a 25 year old female Black South African, biopsy number 23/2004. She showed marked calf hypertrophy. She revealed that she has cramps in her calves and they were sore at times. She was mentally retarded. Proximal muscle weakness in lower limbs and wasting of the rhomboids, deltoid, supraspinatus, infraspinatus (left > right) and vastus medialis was found. The multiplex ligation-dependent probe amplification assay was performed on the DNA of this patient and no deletions or duplications were found.

All patients appeared to have calf hypertrophy on clinical examination by the Neurologist at the Department of Neurology, Inkosi Albert Luthuli Central Hospital, Durban, South

Africa. They also showed very high serum creatine kinase values. The dystrophin stains of all the patients were abnormal.

### 7.4.5 Student's t-test on all patients for spotted oligonucleotide arrays

In the student's t-test statistical analysis method used, the calf muscle was compared to the biceps / quadriceps muscle for all patients. No multiple test correction was performed. The dysregulated genes are represented by blue (+) and those genes that remained unchanged are represented by grey (+). A P-value of <0.01 was considered significant.
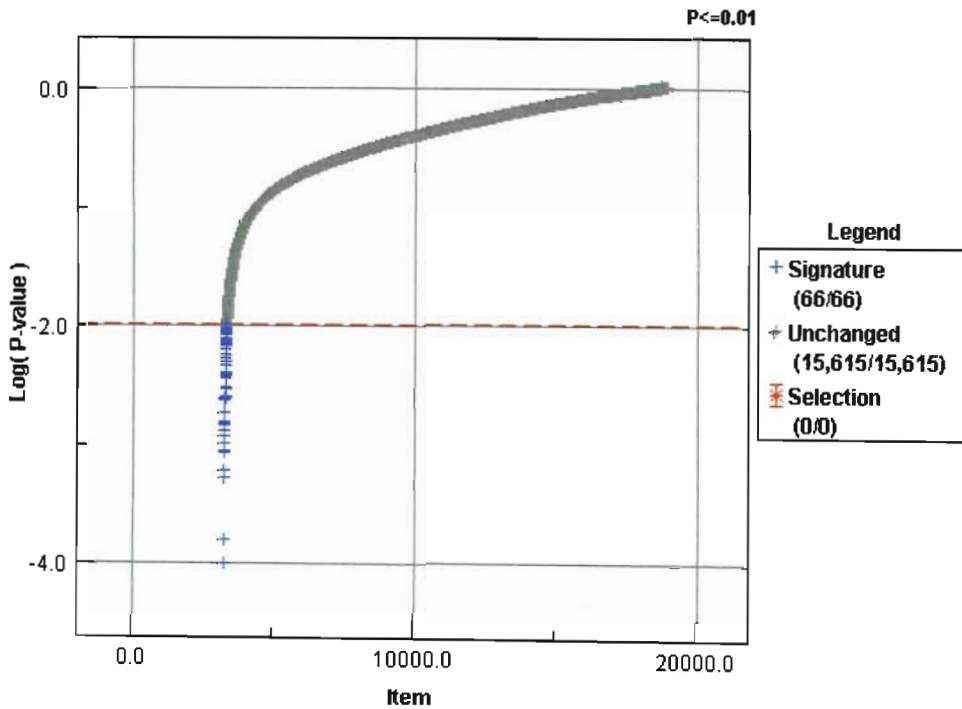


**Figure 84: Graphical representation of those genes that were dysregulated in all patients when the statistical analysis using the student's t-test was performed on all arrays.**

### 7.4.6 Trend plot of significant genes on all patients for spotted oligonucleotide arrays

The trend plot below showed consistency between patients 03/2005 and 06/2005 when the dysregulated genes were plotted. There was agreement with respect to the up or down

234
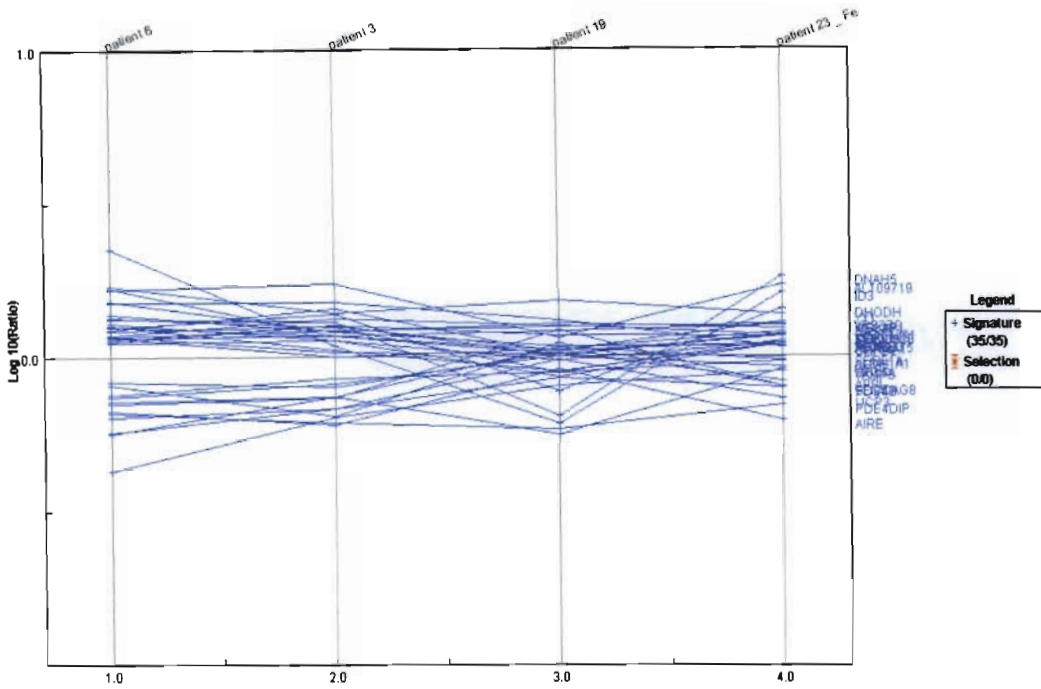
**Figure 85: Graph showing the trend for all those 66 significant genes for all patients when compared to another.**

regulation of the gene when the "log-intensity" values were viewed, for example if a gene

was over-expressed in patients 03/2005 it was also over-expressed in patient 06/2005.

However the results became more varied as the other two patients' samples (19/2003 and

23/2004) were incorporated into the comparison. The data used in the comparison were

generated using Rosetta resolver.

The similarity between the two DMD patients, 03/2005 and 06/2005 may have occurred

because the same molecular signatures and regulatory processes are being activated in

these two patients. The other two patients (19/2003 and 23/2004) have a more complex

disease process because they exhibit milder signs, thus from a pathogenesis angle, other

regulatory machinery may be activated. This implies that not just one but many signalling

cascades may be involved in bringing about the phenotypic characteristics and

pathophysiology seen in these patients.

### 7.4.7 Clustering of up and down regulated genes using Anova

When hierarchical clustering was performed in order to categorise the genes that were up and down regulated, a fingerprint was created for 142 genes from those that were up-regulated and for 106 for down-regulated genes. A literature based annotation of biological concepts was obtained (www.biosemantics.org).

The genes that are up-regulated are measured as those that are higher expressed in biceps / quadriceps than in calf muscle. The genes that are down-regulated are those that are lower expressed in biceps / quadriceps than in calf muscle.

**Table 41: Table showing hierarchical clustering data using Anova for up and down-regulated genes found in all four dystrophinopathy patients.**

| Up-regulated genes | Down-regulated genes |
|---|---|
| Transcription factors | NADH-dependent oxidoreductases |
| Actins - stress fibers | Transcription factors |
| Homeodomain proteins | Homeodomain proteins (HOXC6, HOXC10, Meis1) |
| Nucleolar proteins | Calcium release channels |
| Immediate-early proteins | Muscular dystrophies (CAPN3, DTNA, POMT1) |
| MAP kinases | Muscle-specific phosphotransferases |
| Collagens | |
| Proteoglycans/ECM | |
| Heat-shock proteins | |
| IGF binding | |

It was previously reported by Haslett *et al.* (2002b) that a significantly higher number of genes were up-regulated than down-regulated in DMD versus control samples. This also appeared to be the case in our study even though we were comparing the more affected biceps/ quadriceps muscle to the less affected hypertrophied calf muscle. On evaluation of the microarray data, it is evident that the molecular findings correlate positively with the

immunohistochemical observations on muscle biopsy. This association was also noted in the study by Haslett *et al.* (2002b).

Up-regulation of the proteoglycans / ECM (extra-cellular matrix) genes and collagens in our microarray study affirms the already well-documented observation of connective tissue infiltration in the muscle fibres of affected patients using immunohistochemistry. This result is further cemented by the observation that no ECM proteins are down-regulated, an indication of the inflammatory process being active in dystrophic muscle.

With respect to the muscular dystrophy related genes that were down-regulated in the biceps / quadriceps muscles, it is as yet unclear what the significance of this is. Calpains have been implicated in the pathophysiology of the muscular dystrophies and this may hold a clue to its down-regulation status.

### 7.4.8   Projected comparison between our study and data from Chen *et al.* (2000).

In 2000, Professor Eric Hoffman's laboratory published a gene profiling paper where normal and diseased tissue samples were pooled and a comparison between the two was performed using the Affymetrix array system. The data from the study was made available on a website. Even though the data produced were from pooled samples, the data was extensive and included many useful outcomes.

When the Benjamini-Hochberg adjustment for multiple testing was employed with $p(severity) < 0.0.5$, the following dysregulated gene values were obtained, 211 up-

regulated genes and 243 down-regulated genes were obtained. All four patients were included for biceps/quadriceps vs. calf.

Those genes that were concordant in both datasets amounted to 52 genes. The genes that were discordant amounted to 42 genes. Those that were up-regulated and significant in Anova in our study and up-regulated (>1.3 fold) in DMD vs. normal in the Chen *et al.* (2000) study are shown below.

In addition to this, several transcription factors (TAF15, USF2, CEBPA, RNPS1, SAFB, MEIS1, HOXC6) were down-regulated in biceps / quadriceps vs. calf but this was not so in DMD vs. healthy.

**Table 42: List of concordant and discordant genes obtained when a comparative analysis was performed between our study and that of Chen *et al.* (2000).**

| Concordant genes | Discordant genes |
| --- | --- |
| Immediate early factors | MAP kinase signalling (MAPK1, DUSP1, DUSP6, JAK1, GRB2, ILK) |
| Transcription factors | immediate early proteins (ZFP36, EGR1) |
| ECM | ubiquitin (UBE2D2, UBC) |
| IGF binding proteins | NF-Kb |
|  | Homeobox proteins (IRX5, MSX1, PRRX1), FZD1 |
|  | some extracelluar matrix proteins. |

In a study by Kang *et al.* (2005), HOXC10, also a transcription factor was found to be differentially expressed between quadriceps and gastrocnemius muscles. These comparisons were made between the muscles of autopsy patients who had no symptoms of muscular dystrophy at the time of death. Such a result may prove to be significant in unravelling the regulatory mechanisms and pathways involved in gene expression, which may differ between muscle groups.

The homeobox transcription factors that appear to be differentially expressed in our study but not in other studies (DMD vs. normal), may be responsible for sparing the gastrocnemius muscle in DMD patients when other muscles become progressively weaker.

Some of the important overlap data and two of those genes that were significant are outlined below.

Of those genes that were differentially expressed, 59 were up-regulated and 3 were down-regulated. Interestingly it was found that the one gene, Hsp70 or Hspa1B showed strong down-regulation in DMD versus healthy in the Chen *et al.* (2000) study however it was up-regulated in our study with biceps or quadriceps versus calf muscle. In a publication by Kim *et al.* (2006), it was reported that absence of Hsp70 (heat shock protein 70) is associated with induction of cardiac hypertrophy in as well increased signalling molecules such as MAPK (mitogen activated protein kinase). Our results show that Hsp70 is reduced in hypertrophied DMD calf muscle however it is also lower in DMD quadriceps muscle compared to healthy quadriceps. This shows that the MAPK/p38 pathways is increased in DMD and it is even more active in DMD calf muscle therefore contributing to the phenotypic hypertrophy seen in the patients.
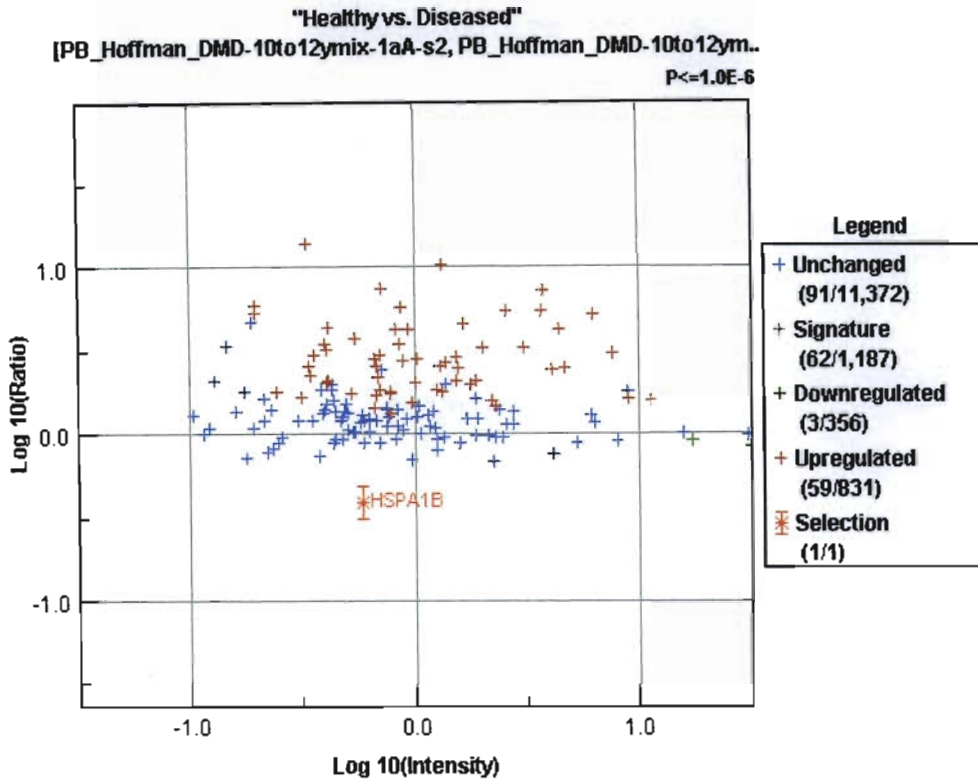
**Figure 86: Graph showing the overlap of differentially expressed genes and the dysregulation of Hsp70 (Hspa1B) when data of our study was weighted against that of Chen _et al._ (2000).**

Figure 87 shows that 134 genes were found on the DMD chip of the down-regulated genes, where 119 were unchanged, 14 were down-regulated and 1 was up-regulated. CYP2J2 is a P450 epoxygenase that synthesizes arachadonic acid. It has also been shown to activate the p42/p44 MAPK signalling cascade in cardiomyocytes, which in effects provides cardioprotection after ischaemia.
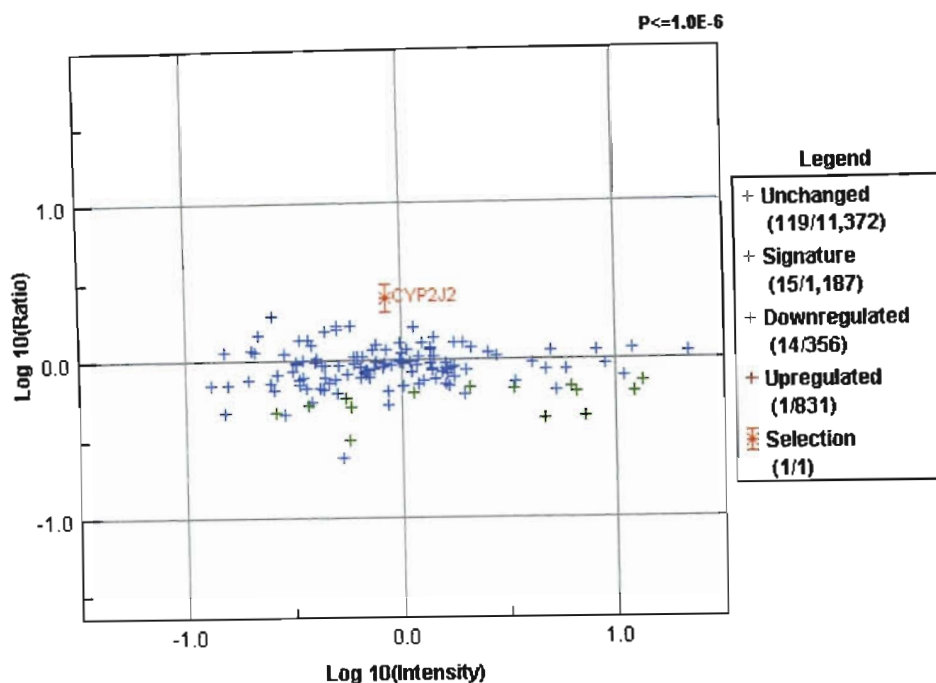
**Figure 87: Graphical representation showing the overlap of data and the dysregulation status of the Cyp2J2 gene, when our results were projected against the data from Chen *et al.* (2000).**

By extrapolation such results indicate that if the similar pathways were to be activated in skeletal muscle, the upregulation of CYP2J2 may confer a protective effect. This may prove to be the case seeing that CYP2J2 was recently found to be expressed in skeletal muscle using real-time reverse-transcription PCR assays (Bie`che *et al.*, 2007).

### 7.4.9    Real-time PCR using the LightCycler 2

### 7.4.9.1 Comparison between the random hexamer method and the gene specific primer method of *c*DNA production

The starting material was the same for both methods. The *c*DNA was obtained using the ImProm-II reverse transcriptase enzyme (Promega). The samples that were reverse transcribed using the gene specific primers are represented by (a), which includes 28/2003(a), 03/2004(a), 06A_2005(a) and 06B_2005(a).
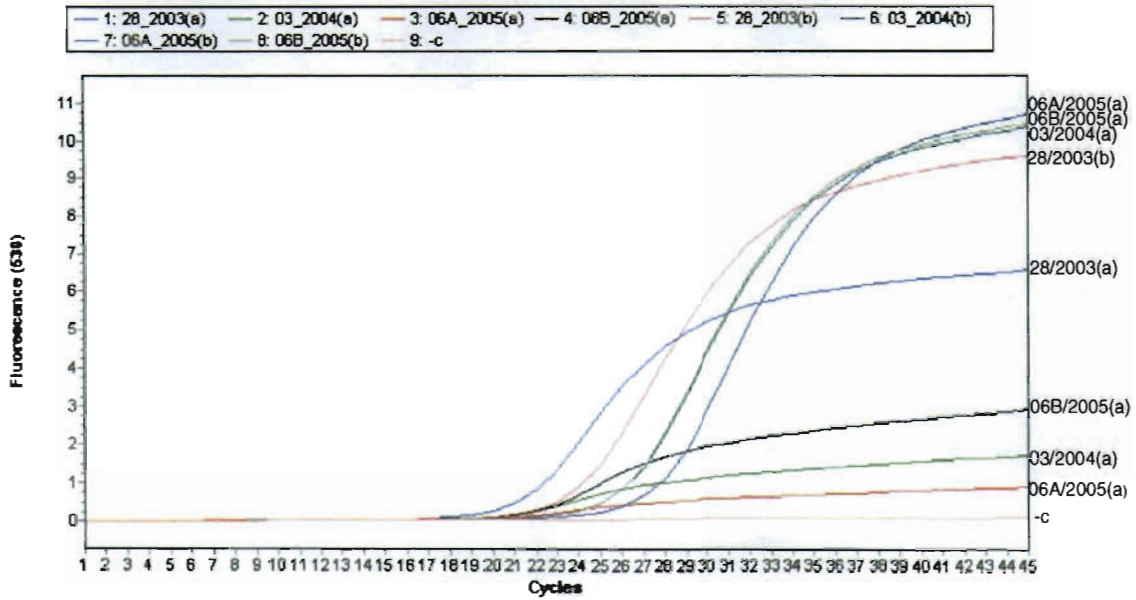
**Figure 88: Graph showing the amplification curves obtained for the adlican gene comparing the amplification when gene specific primers or random hexamers were used.**

The samples that were reverse transcribed using the random hexamer approach were 28/2003(b), 03/2004(b), 06A_2005(b) and 06B_2005(b).

The results from the above image clearly show that the random hexamer approach produced better amplification curves. The Ct or crossing point is the point at which the samples are first visible above background fluorescence. This is important as it represents the amplified product and is able to show that the random hexamer approach was more efficient at producing more product than the gene specific primer method when performing the reverse transcription. The crossing points for each sample were as follows:

06A_2005(a) = 19.49, 03/2004(2) = 19.63, 28/2003(a) = 20.16, 06B/2005(a) = 20.67, 28/2003(b) = 22.82, 06B/2005(b) = 25.05, 03/2004(b) = 25.11, 06A_2005(b) = 26.64.

In the graph below, the amplification curves are difficult to distinguish as the Ct values for many products were in the same vicinity. The slightest difference in Ct values between samples was important as it would be used to reveal gene expression changes.
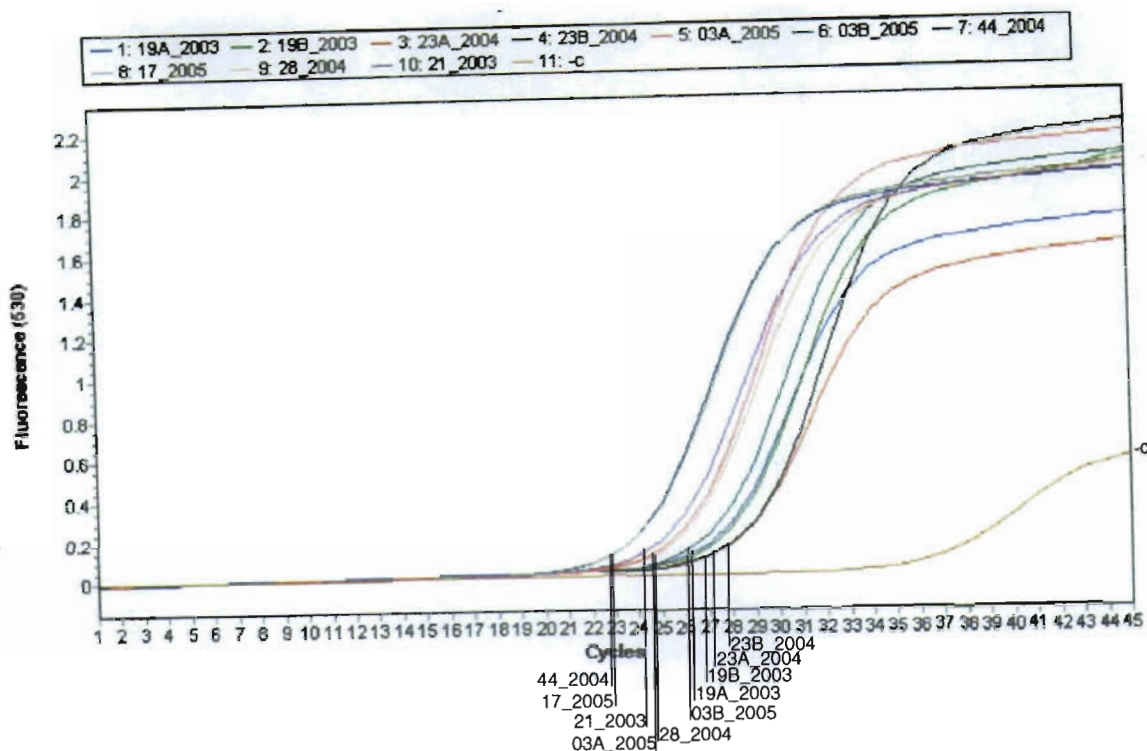
**Figure 89:** Graphical representation of the amplification curves obtained for the adlican gene using ImProm-II derived cDNA that was subjected to PCR with the LightCycler 2.

The amount of primer/probe mix added to these set of reactions was reduced to 1 µl compared to the 2 µl that was added in the previous batch of reactions (Figure 88).

**Table 43: Table showing the crossing point values obtained from amplification curves for the adlican gene in each patients' sample when subjected to PCR using the LightCycler 2.**

| Disease | Biopsy number | Crossing point |
|---------|---------------|----------------|
| Polymyositis | 44/2004 | 22.86 |
| Polymyositis | 17/2005 | 22.97 |
| Polymyositis | 21_2003 | 24.20 |
| DMD | 03A_2005 | 24.86 |
| Polymyositis | 28_200? | 24.87 |
| DMD | 03B_2005 | 26.09 |
| DMD | 19A_2003 | 26.28 |
| DMD | 19B_2003 | 26.72 |
| DMD | 23A_2003 | 27.13 |
| DMD | 23B_2003 | 27.73 |

When the Ct values of the above patients were compared, it was found that the gene expression values of the polymyositis patients were higher than the dystrophinopathy patients. Adlican is a matrix remodelling precursor protein, previously referred to as MXRA5. According to UniProt, the universal protein knowledgebase, MXRA5 (http://www.ebi.uniprot.org:80/index.shtml) is an "adhesion protein with leucine-rich repeats and immunoglobulin domains related to perlecan". The consensus is that not much is known about this precursor protein. When an NCBI search was performed on this molecule, only three hits come up in PubMed and seven in PubMedCentral. Most of these publications relate the adlican gene to diseased states such as cancers and / or senescence. One reason for why the dystrophinopathy patients had lower expression levels could be because the fibre regeneration is more active at this point than tissue remodelling and necrosis. It makes sense that the female patient (23/2003) would show the lowest gene expression for adlican as she is a carrier of the disease and would not exhibit extensive changes in the muscle machinery as a result of matrix remodelling. The 18 year old (19/2003) showed the next lowest gene expression value as he was diagnosed with Becker muscular dystrophy and was shown to have an in-frame deletion (exons 45-47). This deletion makes it possible for him to produce a smaller yet functional protein therefore tissue remodelling and necrosis is not at an advanced stage at this point. Patients 23/2004 and 19/2003 showed hypertrophied calf muscles and these enlarged calf muscles might serve a protective effect especially when the microarray results are taken into account. The calf muscle had reduced Hsp70 and increased CYP2J2, which could collectively confer protection to the calf muscle.

# 7.5 DISCUSSION

## 7.5.1 Muscle tissue storage prior to RNA isolation

All precautions were taken to ensure RNA quality was maintained. All surfaces, pipettes

and disposal items in the UV protected biohazard cabinet were treated with RNaseZap.

Nuclease free micro centrifuge tubes were utilised for all RNA related activities. The RNA

was processed immediately on receipt of the biopsy sample from the patient. The sample

was divided into several parts for immunohistochemical analyses, molecular analyses as

well as storage at -80°C. The samples were treated with RNA*later*, which served to

maintain the integrity and protect the RNA from further degradation. Tissue samples to be

stored at -80°C for microarray analysis were cut into tiny pieces and stored in single use

nuclease free 0.5 ml centrifuge tubes in RNA*later* to prevent freeze-thawing.

## 7.5.2 Tissue homogenisation and RNA isolations

During the homogenisation process, all samples were stored in liquid nitrogen until they

were placed into the RNA-Bee solution to prevent degradation. Two methods of

homogenisation were employed. The first method utilised the MagnaLyser instrument

from Roche. This instrument was expected to produce completely homogenised tissue

without having to manually perform the homogenisation for long periods of time. Also, the

actual homogenisation procedure takes a few minutes at the most therefore the sample

would be at room temperature for a minimal period of time. This would ensure that the

least amount of protease degradation occurred. However, disappointingly when control

samples were homogenised using this method, the sample did not survive the centrifugal

agitation produced by the instrument. This agitation appeared to fragment the 28 S rRNA sample as was evident by the loss of the band on 1% agarose gel electrophoresis. Such a result was also obtained by other individuals at the Department of Human and Clinical genetics research lab, Leiden University, when mouse tissue was subjected to homogenisation using the MagnaLyser.

When the Ultra-Thurrax homogenisation was compared to the MagnaLyser it was found that the 28 S rRNA band was intact and did not get fragmented. However, good quality, non-degraded RNA resulted only when yeast tRNA (Sigma) was added to the muscle tissue sample tube. The addition of the tRNA, which served as an additional substrate to be digested by proteases, minimised degradation to the muscle sample.

The RNA-Bee reagent served the same purpose as Trizol LS reagent. It is a potent reagent containing guanidinium thiocyanate used for extraction of RNA. In addition to the in-house method of isolation that was employed, other RNA extractions methods were also attempted. These included the use of specialised kits such as the fibrous tissue kit (Qiagen) and the tissue extraction kit from Machery Nagel. Both these methods had produced pure, good quality RN however the yield was much lower than that of the RNA-Bee method.

## 7.5.3   RNA quality and quantity

The RNA quality of each sample included in the study was maintained by always storing the samples one ice between steps. The procedure was performed as quickly as possible to avoid any RNA loss and at no point was the RNA left at room temperature unless it was for an incubation that was required in the protocol.

In order to avoid down stream microarray procedural problems, the RNA quality and quantity was determined using a fluorescence based system, the Bioanalyser. The Bioanalyser (Agilent) is an instrument that is based on microfluidic technology that couples miniaturisation with automation. The chips are composed of a "network of miniaturized, microfabricated channels" (http://www.chem.agilent.com/) through which fluids can pass thereby facilitating the qualitative and quantitative analysis of different substances. It served an important role in this microarray study as it is able to detect quantity and quality of RNA very precisely. This quality assessment ensured that the parameter of starting material was taken care of and if a problem was evident after data analysis, the author was assured that the RNA was not the cause. The reproducibility of the Bioanalyser was tested in this study and it was found to be high when the same sample was electrophoresed twice using two different channels on a micro-chip. The results are represented by sample 03/2006 in figures 78 and 79. No sample degradation was noted. Since the muscle biopsy samples were taken during 2003-2005, the samples were of good quality. Owing to the lack of degradation, we had confidence that the data obtained was of good and usable quality and the dysregulated genes were unambiguous and clear-cut. If the sample is of poor quality, there might be differential expression of genes that would not usually be dysregulated. The purity of the RNA was further tested when samples were left out at room temperature overnight. When the RNA samples were assayed using the Bioanalyser the next morning, the amount of sample was almost identical to the previous run the day before. This had demonstrated that our method of choice for RNA extraction and purification was suitable in producing high-quality RNA and it also confirmed the reproducibility of the Bioanalyser.

### 7.5.4 Comparison between the Affymetrix system and spotted oligonucleotide arrays

The drawback of using an Affymetrix system relates to the large amount of RNA (Haslett *et al.*, 2002, Haslett *et al.* 2003, Chen *et al.*, 2000) required as starting material. In most cases, biopsy samples are composed of adipose and connective tissue thus making it difficult to obtain large quantities of RNA. However the spotted oligonucleotide array system utilises a fraction of RNA compared to the Affymetrix system. Better still is the new Illumina beadchip arrays that only require approximately 100 ng of RNA for the procedure to be undertaken (Illumina Inc., 2007 www.illumina.com).

Regarding the array itself, various control measures were in place. The first was the addition of >300 GAPD-H spots on the microarray slide. The second control was the inclusion of genes from other species such as mouse genes that would not yield a result as no binding of the RNA to that oligonucleotide probe would occur.

All precautions were taken to prevent any loss of sample. For example, Cy dye incorporation into the labelled sample was measured using the Nanodrop spectrophotometer, which utilises 1ul sample.

In order to ensure that the ratio of Cy3/Cy5 was consistent and that equal amount of dye was loaded onto each slide, a self-hybridisation experiment was performed. All spots came up as yellow because the same RNA sample was used, however different dyes were included. Since differential expression is not expected in any gene, a graph of normalised signals for Cy3 plotted against normalised Cy5 signals should give a straight line. It is

important for a "yellow" or self-hybridisation experiment to be performed as all stages of the microarray experiment can be assessed using just the one RNA sample. If this is not done and experiments on different RNA samples are performed, one would not be able to determine which differentially expressed genes are there as a result of actual up or down regulation or whether there was a flaw in one part of the microarray experimental process.

The experiments that were performed on all four patients were repeated 3 times in order to obtain enough replicates to verify the data. To ensure that the data obtained was not due to a single slide, multiple slides were hybridised with each pair of labelled probes. This allowed us to ensure that the data obtained was true and real.

### 7.5.5 Evaluation of clustering data

Interestingly, other studies have previously shown that many more genes were up-regulated than down-regulated when DMD affected patient samples were compared to unaffected normal biopsy samples (Haslett *et al.*, 2002b; Porter *et al.*, 2002, Tseng *et al.*, 2002). The Haslett *et al.* (2002b) study used the Affymetrix system for gene profiling analysis in human patients and normal controls whereas the Tseng *et al.* (2002) and Porter *et al.* (200) studies focussed their attention on the *mdx* mouse model. All three authors allude to protein turnover being responsible for the discrepancy between the number of genes being up-regulated and down-regulated, on account of the regenerative and degenerative nature of the disease. In our study, a comparison was made between a more affected biceps / quadriceps muscle and a less affected calf muscle from the same DMD affected patient. Even though both muscles were affected, we also found more genes were up-regulated in the biceps / quadriceps muscle when compared to the calf muscle. Whether

these genes are up-regulated as a result of the dystrophic process being more heightened in the biceps / quadriceps muscle is as yet unknown. Large scale studies would have to be performed on more patients' sample in order to accurately confirm these findings.

With respect to calpain3 being down-regulated in biceps / quadriceps, there has been much speculation as to the role of calpains in muscular dystrophies. It was thought that the calpains, particularly calpain3, the neutral protease plays a regulatory role in proteolysis in muscle cells, which in effect brings about muscle wasting (Blake *et al.*, 2002). Calpain levels are elevated early on in the dystrophic process and have been found in necrotic fibres initially and at the membrane of muscle fibres at the latter stages of the disease. The calpains are therefore thought to be involved in the pathophysiology of Duchenne muscular dystrophy (Tidball & Spencer, 2000).

Many transcription factors are differentially expressed in our study. The actual function of these factors is as yet unknown however some appear to play a significant role in signalling cascade pathways. It stands to reason that some transcription factors would be up-regulated as the protein turnover would be increased when the muscle is in a state of stress. The clustering data therefore opens up many possibilities for pathway studies to be performed.

The heat-shock proteins may have been over-expressed in the biceps / quadriceps muscle, which are in a constant state of stress, as these proteins have been associated with facilitating the "assembly of intracellular proteins" (Kim *et al.*, 2006). During a state of cellular stress, such as in dystrophic muscle, Hsps may aid in the process of restoring homeostasis in a cell (Frier & Locke, 2007).

When the Chen *et al.* (2000) data was compared to our data, several genes were discordant. One of these was NF-kB, which was previously shown to play an important role in initiating atrophy, in studies conducted on mice. Since it was over-expressed in biceps / quadriceps muscle in humans, which shows signs of weakness and progressive wasting, an NF-kB pathway may be responsible for the effects seen in the patient. It was also documented that non use and sepsis (Hunter *et al.*, 2002; Penner *et al.*, 2001) activates this pathway. Future studies should focus on the group of patients that are already in wheelchairs to try and unravel mechanisms that come into play when the child becomes immobile. It would be interesting to determine to what extent NF-kB, TNF-alpha and other cytokines such as the ILs are up-regulated in immobile DMD sufferers. These findings may help to direct therapy towards the use of NF-kB and cytokine antagonists (Cai *et al.*, 2004), which may reverse the atrophy seen in these patients or prevent further muscle wasting.

## 7.5.6    Differential expression of Hsp70

When our study data was projected against the data obtained by Chen *et al.* (2000) a gene that showed a surprising result was Hsp70. Much work has been done on this heat shock protein, which belongs to a family that is rapidly produced in the bodies of most organisms in response to "protein damaging stresses" (O'Neill *et al.*, 2006). Many authors have focussed on this protein owing to its presence in the cardiovascular system where it can be induced by in response to oxidative and mechanical stresses. It is also constitutively produced in the body to aid with "protein folding, facilitation of intracellular trafficking and signalling processes" (Zheng *et al.*, 2006).

Kim *et al.* (2006) where absence of Hsp70 was shown to increase cardiac hypertrophy. It appears that similar pathways may be activated and regulated when Hsp70 is absent to bring about hypertrophy in cardiac and smooth muscle.

Hypertrophy of the calf muscle in DMD patients may be due to a complex series of events. One of the pathways that play a role in maintaining this hypertrophic muscle is the MAPK/p28 pathway concert with Hsp70 reduction. Even though these genes have been implicated in the hypertrophic process, this may be just the beginning in unravelling the many mechanisms that are involved in hypertrophy. The next step would be to look at other genes that are up-regulated in spontaneously occurring models of hypertrophy such as the callipyge lambs. A paternally expressed protein coding genes *DLK*1 and *PEG*11 are thought to play an integral role in bringing about the hypertrophy seen in the callipyge lambs (Fleming-Waddell et al., 2007). Using gene expression profiling experiments, Fleming-Waddell *et al.* (2007) showed that these lambs had increased expression of "muscle-type phosphofructokinase (PFKM)", "phosphodiesterase 7A (PDE7A) is a high-affinity cAMPspecific phosphodiesterase that is found in high abundance in skeletal muscle" and "terminal deoxynucleotidyltransferase interacting factor 1 (DNTTIP1)", which may act to induce hypertrophy (Fleming-Waddell *et al.*, 2007). We would be able to obtain more insight into the pathways that regulate the process of hypertrophy by analysing data collected from studies like this one (Fleming-Waddell *et al.*, 2007) conducted in animals.

Skeletal muscle hypertrophy has received much attention of late owing to the discovery of the infant with unusually large muscle mass in 2004 (Schuelke *et al.*, 2004). A recent study aimed to determine how Hsp proteins influence muscle hypertrophy, by using rats that

were subjected to heat stress and overload. It has been previously documented that when skeletal muscle is faced with "overload", the muscle apparatus adapts by undergoing hypertrophy by increasing "structural and contractile protein content" and increasing type I myosin heavy chain. In this way, hypertrophy serves as a protective response by the muscle (Frier & Locke, 2007). The authors were able to show that an accumulation of Hsp proteins "inhibits increase in muscle mass" in those muscles in the process of undergoing hypertrophy. Therefore it stands to reason that a reduction / absence of Hsp70 will result in muscle hypertrophy. This gives credibility to the result that was obtained in our study where a comparison was done between the weaker biceps or quadriceps muscle as the stronger hypertrophied calf muscle in the same dystrophinopathy patient.

Many studies on muscle hypertrophy focus on the how the event can be prevented as the Hsp proteins are known to be activated by stress responses. The next group of studies should rather focus on the beneficial and protective aspects of skeletal muscle hypertrophy and all the pathways that are involved in bringing about this phenomenon. Even though studies on the myostatin gene and the use of IgF-1 to bring about hypertrophy have been performed, the underlying mechanisms that drive such processes still remain elusive. Microarray and gene profiling analyses therefore hold the key to understanding the mechanisms that regulate hypertrophy.

### 7.5.7    Differential expression of CYP2J2

CYP2J2 is cytochrome P450 epoxygenase that metabolises arachidonic acid to epoxyeicosatrienoic acids (EETs). These are subsequently "converted to dihydroxyeicosatrienoic acids (DHETs) by epoxide hydrolases". Many epoxygenases are

expressed in the heart but CYP2J2 is unique in that it is expressed primarily in cardiomyocytes. Quantitative real-time PCR was used to localise the expression of three P450 epoxyygenases CYP2C8, CYP2C9, and CYP2J2 in the heart, aorta and coronary artery samples with GAPDH serving as the control against which the results were weighted. CYP2J2 mRNA was found to be $10^3$ times higher in human heart than the other two, CYP2C9 levels was highest in aorta and relatively higher than the other two in coronary artery (DeLozier et al., 2007). Further to this, real-time reverse-transcriptase PCR was used to measure the levels of CYP1, CYP2, CYP3 in 22 different human tissues (Bie`che et al., 2007). With specific reference to CYP2J2, this P450 epoxygenase was expressed in heart, salivary gland, placenta and skeletal muscle.

A single nucleotide polymorphism (G-50T), located in the proximal promoter region of the CYP2J2 gene has been implicated in and associated with increased risk of coronary heart disease. This SNP is located in a region where there are four putative Sp1 transcriptional binding sites and the loss of one Sp1 binding site at the proximal promoter significantly reduces to the CYP2J2 gene (Spiecker et al., 2004). In 2004, Seubert et al. showed that transgenic mice exhibiting over-expression of CYP2J2 in cardiomyocytes caused increased expression of p42/p44 MAPK after ischaemia and in effect bestowing protection on the cardiac apparatus.

Since CYP2J2 was recently found to be expressed in skeletal muscle, the results from our microarrays data showing up-regulation of CYP2J2 in calf muscle suggests that it may be involved in protecting the skeletal muscle tissue together with the MAPK pathway.

## 7.5.8  Real-time PCR using the LightCycler 2

Initially, the Sybr green detection kit was used to determine if usable results could be obtained without having to use the UPL system or any other such probe based system. Unfortunately very poor results were obtained and the melting curve analysis could not be properly interpreted. Following this, an attempt was made to use the hybridisation probe detection master mix, together with the UPL mix and the adlican primers as the hybridisation probe kit was available in the laboratory since it was used in the assay of another disease. Once again the results were not satisfactory. Very low fluorescence signals (~0.1) were obtained and these results could not be used. In comparison, the TaqMan master mix using the hydrolysis probe approach produced excellent results on the first attempt.

When a comparison was done between the amounts of product that was obtained using two method of cDNA production, the random hexamer approach was found to be better than the gene specific primer approach. These results are shown in figure 88 above. The random hexanucleotide method of producing cDNA was used in all subsequent reactions.

As previously mentioned, the adlican gene or MXRA5 is a matrix remodelling precursor proteins. These proteins appear to play an active role in the pathological states, such as the muscular dystrophies. The matrix metalloproteinases are also associated with tissue remodelling in pathological processes such as metastasis, tissue repair and have been implicated in inflammatory diseases (Page-McCaw et al., 2007). This is seen in the graph above where 3 of the 4 (Figure 89, Table 43) polymyositis patients have a higher gene expression level than the DMD patients.

It can be speculated that the inflammatory condition of polymyositis patients would render the tissue remodelling more active in their muscle fibres than the muscle of the DMD patients. Also the patients in the polymyositis cohort are much older therefore the muscles may have endured more remodelling than the DMD patients. The age difference between cohorts may be a significant factor in contributing to gene expression changes as was shown by Kang *et al.* (2005) when a comparison was done between four muscles in different age groups.

One can speculate that the dystrophinopathy patients would show more regeneration (Schmalbruch, 1984) as opposed to necrosis as a result of tissue remodelling because they are much younger. The regenerative process is more pronounced at a younger age owing to satellite cell proliferation.

# CHAPTER 8

# GENERAL DISCUSSION AND CONCLUSIONS

The study involved 68 patients in total. All patients agreed to have muscle biopsies. The biopsy samples were subjected to immunohistochemical techniques and routine histological examination. The immunohistochemical test serves as the "gold standard" even at a time when molecular biology tools are becoming useful, and at times invaluable in diagnosing diseases such as Duchenne muscular dystrophy and other such debilitating disorders. The main problem encountered by a researcher working on the dystrophin gene is that mutations are found throughout the 79 exons of dystrophin. Even though 65% of mutations are deletions, which are located in hot-spot exons, the remaining 35% can be anything from a duplication to a point mutation that could be scattered anywhere throughout the 2.4 Mb gene.

This makes mutation detection a mammoth task for diagnostic laboratories. One aspect of the present study dealt with mutation detection, whilst the next focussed on the use of microarray analysis in attempting to elucidate the pathogenesis in DMD. The author chose to evaluate both deletion and point mutation detection techniques since one of the patient cohorts included in this study were found to have no deletions on conventional 18 exon multiplex PCR testing. The deletion detection study formed part of the author's MMedSc. thesis (K.D. Pillay, 2002). The reason for also focussing on deletion testing in this study was to determine whether increasing the number of exons screened would improve the deletion detection rate. Further to this, a novel technique called the MLPA assay was established by Schouten *et al.* (2002) just prior to the author's candidature. This technique

could be used to screen for deletions and duplications in all exons of the dystrophin gene, which would be useful in our setting.

## 8.1     Mutation detection

With respect to the mutation detection aspect of the project, 30-plex multiplex PCR was used to detect deletions in the suspected dystrophinopathy patients. This technique provides important data in a laboratory setting where large and expensive pieces of equipment such as a DNA sequencer would not readily be available for regular use. However, it works best in the hands of an experienced molecular scientist or laboratory technician whose sole responsibility would be to perform the technique. During our study, the technique was found to be less reproducible when a new and inexperienced member of staff was carrying out the procedure. On evaluation of the results obtained from the 30-exon multiplex PCR assay, it was found that increasing the number of exons tested did not significantly improve the diagnostic efficacy as the same numbers of patients were found to have deletions as with the conventional 18-exon screening assay. The only difference was that the area over which the exon deletion occurred increased in some cases. The actual span of the deletion was confirmed by testing more exons in the assay.

If the author were to design a deletion and duplication detection protocol for a DMD diagnostic laboratory, the following would be recommended. The first method of choice should be the MLPA assay if the laboratory has a genetic analyser at its disposal, such as the ABI 310 or ABI3100 from Applied Biosystems. This assay could serve a dual purpose as it would provide deletion and duplication results using the DNA from a suspected dystrophinopathy patient and it could also be used for carrier testing in the female relatives

of those patients that were shown to have a deletion. In this way, genetic counselling could be implemented for that group of patients and their families. The next recommendation would be to include the 30-plex technique in the deletion protocol if the MLPA assay yielded a result that required confirmation. In such a case, two entirely different methods would be employed thereby strengthening the confidence in the deletion that was found. If a single deletion was found in a patient's sample, it would be wise to perform DNA sequence analysis on the DNA sample from the patient by first obtaining a PCR product and subjecting it to sequencing analysis. This could be done by placing the primer binding site further away from the exon thereby creating a product if no deletion was present. Such a deletion may be the result of a primer site polymorphism that would be viewed as a deletion on MLPA or quantitative PCR. It could also be the result of a single nucleotide point mutation, which on sequence analysis might lead to a stop codon being produced. In this way, nonsense mutations could be found in patients' samples, with the aid of the MLPA assay. Such a result would be invaluable for families that would like their child to be considered for clinical trials based on nonsense mutations in the dystrophin gene or exon skipping clinical trials. Such trials are well underway in the USA, with the support of the DMD Parent Project.

For point mutation testing, there still appears to be no definitive testing method that could be referred to as the gold standard. The first method that was evaluated in this study was the single stranded conformation polymorphism analysis. This would be a cheap and relatively uncomplicated method to set-up in a resource limited setting by a researcher experienced in molecular biology methodology such as PCR, agarose and polyacrylamide gel preparations, purification of PCR products, DNA sequencing using capillary electrophoresis and analysis using Biotools or other bioinformatics software. However the

assay is time-consuming and labour-intensive. The author found that the assay was laborious as several gels were required to be run using various temperatures and gel concentrations until highly resolved bands were obtained. The author also found that SSCP bands were better resolved and more clearly visible when the Novex pre-cast gel system was utilised as opposed to conventional slab gels, which were run using the Hoefer system. Despite the negative attributes of the SSCP methodology, visual band shifts were found in 15 of the 28 exons tested with 17 patients showing abnormal band migration. DNA sequencing was performed for exons 6, 8, 52, 53, 60, 41, 42 and flanking sequences. DNA sequencing could not be performed on the other exons as the patients' DNA was not available. In exon 6 and flanking sequence of exon 5, three SNPs were found and in exon 52, two insertion mutations were found. It is possible that several more of those mutations that were detected in visual inspection could be confirmed using DNA sequencing if the patients' DNA was available for testing.

Realistically the SSCP assay should not be the method of choice for a gene as large as the dystrophin gene, since several patients' samples would need to be analysed and at least 25-30 hot-spot exons would need to be assessed as was attempted in Chapter 4 of the thesis. The SSCP method may be useful in detecting even more mutations than the slab gel method if it were performed using a capillary electrophoresis (CE) apparatus. However, the technique would only be useful if modifications to a CE apparatus such as the ABI 3100 could be performed without the warranty being affected. The modification is required as the 3100 is unable to reach low temperatures such as 4-10°C, which are vital temperatures to obtain and detect the single stranded conformers. Even in such a situation, the SSCP assay would require different temperatures for each exon to be tested and this would make it labour-intensive and very expensive. Such capillary electrophoresis modifications were

not possible at the Neuroscience laboratory, Inkosi Albert Luthuli Central Hospital, Durban, South Africa because the apparatus was not only used for the sole purpose of detecting mutations in the dystrophin gene. Ultimately, the SSCP assay is a useful technique in a resource limited setting and has the ability to produce data that is useful, provided all conditions are optimal.

In addition to the SSCP technique, the author attempted reverse-transcriptase (RT) PCRs on the RNA samples from patients and controls. The RNA samples were extracted from muscle tissue or blood samples. The RT-PCRs did not yield the expected results. A faint band or no band was present in the patients' samples when agarose gel electrophoresis was performed. This could be attributed to sample degradation.

On evaluation of this technique, the author would recommend that RNA samples be extracted immediately and stored at -80ºC if the RT-PCR assay is being considered for mutation detection. The cDNA should also be prepared soon after RNA extraction.

For those laboratories that have access to an ABI 3100 on a daily basis, it may be worth considering the possibility of performing DNA sequencing on the entire coding region of the dystrophin gene. This is a definitive method of detecting point mutations. By exploiting such technology, several types of mutations could be detected, including small deletions, insertions, spice-site mutations and stop codon mutations. The only drawback of such a technique is the cost of the reagents such as the sequencing kits as well as the reagents required to run the genetic analyser.

## 8.2    Genetic counselling

It is important that genetic counselling be offered to all mothers and female relatives of clinically affected dystrophinopathy patients. If DNA sequencing and analysis were performed, those families that were found to have no deletions and / duplications on MLPA analysis, would obtain a definitive result.

Previous studies that focussed on detecting cardiac abnormalities in carriers showed that the risk of cardiomyopathy is much lower than was previously documented. The recommendation would be to include both ECG and echocardiography as screening methods to clinically assess all patients (Grain *et al.*, 2001).

## 8.3    Gene profiling analysis

The mutation in our dystrophinopathy patients had to first be determined in order to better analyse the data generated from microarray analysis. If the mutation was not known it may become more difficult to assess the importance of specific genes being dysregulated. If for example the patient was found to have an in-frame deletion and there were specific genes being dysregulated, one could correlate the genes being over and under-expressed to the type of mutation found. If the patient had an out-of-frame deletion, once again the dysregulated genes on microarrays analysis could be better explained. If the mutation was not known, one would have to rely entirely on the gene expression profiles to understand the mechanisms that are regulating the gene expression in that individual. Once the mutation is know, the gene expression data can be analysed from a point of knowledge.

In our study, four dystrophinopathy patients agreed to have double biopsies. The biopsy samples were required to determine the usefulness of performing gene expression studies on two different muscle groups in the same individual thereby removing any genetic variability and significantly reducing bias during the statistical analyses. The biopsies were taken from a muscle that becomes progressively weaker in DMD (quadriceps / biceps) and a muscle group that remains invariably strong (gastrocnemius) despite muscle weakness and eventual wheelchair confinement.

Both the spotted oligonucleotide arrays and the Illumina beadchips showed a positive correlation between the molecular findings and immunohistochemical analyses. In order to determine the strength of our data, a comparative analysis between our study and that of Chen et al. (2000) was performed, where the Affymetrix system was utilised. The study by Chen et al. (2000) was one of the most extensive DMD studies performed however the drawback of the study was the use of pooled samples to obtain definitive results on the Affymetrix system as large amounts of starting material are required. In our study we aimed to elucidate the mechanisms that may influence the strength of the gastrocnemius muscle in DMD patients. This question may have been answered by the novel finding that homeobox transcription factors were differentially expressed in our study thus suggesting that it may be responsible for sparing the gastrocnemius when other muscle groups become progressively weaker.

Another important finding was that Hsp70 was up-regulated in our study (biceps or quadriceps vs. calf muscle) as opposed to being down-regulated, which was a finding in the Chen et al. (2000) study in DMD versus healthy. The absence of Hsp70 is responsible for induction of cardiac hypertrophy and increased MAPK signalling. Our finding allows

us to speculate that the increased MAPK/p38 signalling may be responsible for the calf hypertrophy seen in DMD patients. Yet another MAPK signalling associated finding included the dysregulation of the CYP2J2 gene in our study. CYP2J2 is a P450 epoxygenase that synthesizes arachadonic acid. It is known to activate the p42/p44 MAPK signalling cascade in cardiomyocytes, conferring cardioprotection after iscahemia. Interestingly, this gene has recently been found in skeletal muscle, thus suggesting that it may play a similar protective role in skeletal muscle. A more elaborate study focussing on these dysregulated genes is required to confirm these novel results.

In conclusion, with respect to mutation detection, the MLPA assay should be the initial screening method to be implemented in a laboratory working on DMD as it is able to detect both deletions and duplications. Once a deletion is found, it can be confirmed using multiplex PCR. This ensures that two different techniques are used to confirm a deletion, with the one utilising probes and the other using primer based methodology. However, the Southern blotting technique would still have to be utilised to confirm the presence of a duplication.

Gene profiling analysis using different muscle tissue samples from the same patient has proven to be useful in determining which pathways are being regulated in different tissues. This is especially important in the case where the different muscle groups are affected to varying degrees by the disease process as is the case with the biceps / quadriceps and calf muscles in DMD patients.

This project has set the scene for further studies to be performed in both mutation detection as well as gene profiling analysis. With respect to mutation detection, DNA sequencing of

the dystrophin gene in a South African cohort has not previously been undertaken. The results obtained could prove to be very useful as the data from our four unique South Africa racial groups could be compared to Caucasian populations and other such ethnic groups. Such data analyses could determine of there are variations in the mutation spectrum between different racial groups and different ethnicities.

With respect to the gene profiling analysis, it is the first study of this nature that has been performed using two muscle groups from the same patient. The study is therefore unique and internationally novel. There are several avenues that could not be pursued owing to the results that have thus far been obtained. The author is keen to compare the results obtained using a larger cohort of patients. If double biopsies from the same patient cannot be obtained, a large number of single biopsies from a calf and biceps muscle can be compared.

# REFERENCES

Aartsma-Rus, A., Janson, A.A., Kaman, W.E., Bremmer-Bout, M., van Ommen, G.J., den Dunnen, J.T., *et al.* (2003). Antisense-induced multiexon skipping for Duchenne muscular dystrophy makes more sense. *Am J Human Genet* **74**: 83-92.

Aartsma-Rus, A., van Deutekom, J.C.T., Fokkema, I.F., van Ommen, G.B., & den Dunnen, J.T. (2006). Entries in the Leiden Duchenne muscular dystrophy mutation database: an overview of mutation types and paradoxical cases that confirm the reading-frame rule. *Muscle Nerve* **34**: 135–144.

Acsadi, G., Lochmuller, H., Jani, A., Huard, J., Massie, B., Prescott, S. *et al.* (1996). Dystrophin expression in muscles of mdx mice after adenovirus-mediated in vivo gene transfer. *Hum Gene Ther* **7**: 129–140.

Altschul, S.F., Gish, W., Miller, W., Myers, E.W., & Lipman, D.J. (1990). Basic local alignment search tool. *J Mol Biol* **215(3)**: 403-410.

Amersham Biosciences. (2002). *Microarray handbook*. England.

Andersen, P. S., Jespersgaard, C, Vuust, J., Christiansen, M., & Larsen, L. A. (2003a) High-throughput single strand conformation polymorphism mutation detection by automated capillary array electrophoresis: validation of the method. *Hum Mutat* **21**: 116-122.

Andersen, P. S., Jespersgaard, C, Vuust, J., Christiansen, M., & Larsen, L. A. (2003b). Capillary electrophoresis-based single strand DNA conformation analysis in high-throughput mutation screening. *Hum Mutat* **21**: 455-465.

Anderson, J.L., Head, S.I., Rae, C., & Morley, J.W. (2002). Brain function in Duchenne muscular dystrophy. *Brain* **125**: 4-13.

Anderson, J.T., Rogers, R.P., & Jarrett, H.W. (1996). Ca2_-calmodulin binds to the carboxyl-terminal domain of dystrophin. *J Biol Chem* **271**: 6605–6610.

Arakawa, M., Shiozuka, M., Nakayama, Y., Hara, T., Hamada, M., Kondo, S. *et al.* (2003). Negamycin restores dystrophin expression in skeletal and cardiac muscles of mdx mice. *J Biochem* **134**: 751-758.

Armour, J.A., Sismani, C., Patsalis, P.C., & Cross, G. (2000). Measurement of locus copy number by hybridisation with amplifiable probes. *Nucleic Acids Res* **28(2)**: 605-609.

Axon Instruments Inc. (2003). *GenePix Pro 5.0. Microarray acquisition and analysis software for genepix microarray scanners. User's guide and tutorial.* California, USA.

Bakay, M., Zhao, P., Chen, J., & Hoffman, E.P. (2002). A web-accessible complete transcriptome of normal human and DMD Muscle. *Neuromuscular Disord* **12**: S125–S141.

Baker, P.E., Kearney, J.A., Gong, B., Merriam, A.P., Kuhn, D.E., Porter, J.D. *et al.* (2006). Analysis of gene expression differences between utrophin/ dystrophin-deficient vs mdx skeletal muscles reveals a specific upregulation of slow muscle genes in limb muscles. *Neurogenetics* 7: 81–91.

Bakker, E. (1989). *Duchenne muscular dystrophy: Carrier detection and prenatal diagnosis by DNA analysis. New mutation and mosaicism.* PhD thesis. The Netherlands.

Bakker, E., & van Ommen, G.J.B. (1999). "Duchenne and Becker muscular dystrophy," in *Neuromuscular disorders: Clinical and molecular genetics*, A.E.H Emery, ed., Wiley, Chichester, U.K.

Barton-Davis, E.R., Cordier, L., Shoturma, D.I., Leland, S.E., & Sweeney, H.L. (1999). Aminoglycoside antibiotics restore dystrophin function to skeletal muscle of mdx mice. J *Clin Invest* **104**: 375–81.

Baldwin, D., Cranetand, V., & Ricet, D. (1999). A comparison of gel-based, nylon filter and microarray techniques to detect differential RNA expression in plants. *Curr Opin Plant Biol* **2**: 96-1 03.

Bar, S., Barnea, E., Levy, Z., Neuman, S., Yaffe, D., & Nudel, U. (1990). A novel product of the Duchenne muscular dystrophy gene, which greatly differs from the known isoforms in structure and tissue distribution. *Biochem J* **272**: 557-560.

Bardoni, A., Felisari, G., Sironi, M., Comi, G., Lai, M., Robotti, M. *et al.*, (2000). Loss of Dp140 regulatory sequences is associated with cognitive impairment in dystrophinopathies. *Neuromuscul Disord* **10**: 194-199.

Barnea, E., Zuk, D., Simantov, R., Nudel, U., & Yaffe, D. (1990) Specificity of expression of the muscle and brain dystrophin gene promoters in muscle and brain cells. *Neuron* **5**: 881–888.

Baumbach, L.L., Chamberlain, J.S., Ward, P.A., Farwell, N.J., & Caskey, C.T. (1989). Molecular and clinical correlations of deletions leading to Duchenne and Becker muscular dystrophies. *Neurology* **39**: 465-474.

Baumeister, R., & Ge, L. (2002). The worm in us- Caenorhabtitis elegans as a model of human disease. *Trends Biotechnol* **20**: 147–148.

Beggs, A.H. Koenig, M. Boyce, F.M., & Kunkel, L.M. (1990). Detection of 98% of DMD/BMD gene deletions by polymerase chain reaction. *Hum Genet* **86**: 45-48.

Beggs, A.H., Hoffman, E.P., Snyder, J.R., Arahata, K., Specht, L., Shapiro, F. *et al.*, (1991). Exploring the molecular basis for variability among patients with Becker muscular dystrophy: dystrophin gene and protein studies. *Am J Hum Genet* **49**: 54-67.

Bertoni, C., Lau, C. & Rando, T.A. (2003). Restoration of dystrophin expression in mdx muscle cells by chimeraplast-mediated exon skipping. *Hum. Mol. Genet* **12**: 1087–1099.

Bie'che, I., Narjoz, C., Asselah, T., Vacher, S., Marcellin, P., Lidereau, R., Beaune, P., & de Waziers, I. (2007). Reverse transcriptase-PCR quantification of mRNA levels from cytochrome (CYP)1, CYP2 and CYP3 families in 22 different human tissues. *Pharmacogenet Genomics* **17**: 731–742.

Billard, C., Gillet, P., Barthez, M., Hommet, C., & Bertrand, P. (1998). Reading ability and processing in Duchenne muscular dystrophy and spinal muscular atrophy. *Dev Med Child Neurol* **40**: 12–20.

Blake, D.J., Tinsley, J.M., Davies, K.E., Knight, A.E., Winder, S.J., & Kendrick-Jones, J. (1995). Coiled-coil regions in the carboxy-terminal domains of dystrophin and related proteins: potentials for proteinprotein interactions. *Trends Biochem Sci* **20**: 133–135.

Blake, D. J., Weir, A., Newey, S.E., & Davies, K.E. (2002). Function and genetics of dystrophin and dystrophin-related proteins in muscle. *Physiol Rev* **82**: 291–329.

Blankinship, M.J., Gregorevic, P., & Chamberlain, J.S. (2006). Gene therapy strategies for Duchenne muscular dystrophy utilizing recombinant adeno-associated virus vectors. *Mol Ther* **13**: 241-9.

Bonni, A., Brunet, A., West, A.E., Datta, S.R., Takasu, M.A., Greenberg, M.E. (1999). Cell survival promoted by the Ras-MAPK signaling pathway by transcription-dependent and independent mechanisms. *Science* **286**:1358-1362.

Bork, P., & Sudol, M. (1994). The WW domain: a signalling site in dystrophin? *Trends Biochem Sci* **19**: 531.

Brandon, C., and Tooze, J. (1991). *Introduction to protein structure*, 1st edition. Garland Publishing, New York, USA.

Bredt, D.S., Snyder, S.H. (1994). Nitric oxide: a physiologic messenger molecule. *Annu Rev Biochem* **63**: 175–195.

Buetler, T. M., Renard, M., Offord, E. A., Schneider, H., & Ruegg, U.T. (2002). Green tea extract decreases muscle necrosis in mdx mice and protects against reactive oxygen species. *Am J Clin Nutr* **75(4)**: 749–753.

Bulfield, G., Siller, W.G., Wight, P.A., & Moore, K.J. (1984). X chromosomelinked muscular dystrophy (mdx) in the mouse. *Proc Natl Acad Sci USA* **81**: 1189-1192.

Byers, T.J., Lidov H.G.W., & Kunkel, L.M. (1993). An alternative dystrophin transcript specific to peripheral nerve. *Nat Genet* **4**: 77-81.

Cai, D., Frantz, J. D., Tawa, N. E., Jr., Melendez, P. A., Lidov, H. G.W., Hasselgren, P. O., *et al.* (2004). IKKbeta/NF-kappaB activation causes severe muscle wasting in mice. *Cell* **119**: 285–298.

Campanelli, J.T., Roberts, S.L., Campbell, K.P., Scheller, R.H. (1994). A role for dystrophin associated glycoproteins and utrophin in Agrin induced AchR clustering. *Cell* **77**: 663–674.

Campbell, K.P., & Kahl, S.D. (1989). Association of dystrophin and integral membrane glycoprotein. *Nature* **338**: 259-262.

Chamberlain, J.S. Gibbs, R.A. Ranier, J.E. Nguyen, P.N., & Caskey, C.T. (1988). Deletion screening of the Duchenne muscular dystrophy locus via multiplex DNA amplification. *Nucleic Acids Res* **16**: 11141-11156.

Chamberlain, J.S., Gibbs, R.A., Ranier, J.E., & Caskey, C.T. (1990). "Multiplex PCR for the diagnosis of Duchenne muscular dystrophy," in *PCR Protocols: A Guide to Methods and Applications*, M.A. Innis, D.H. Gelfand, J.J. Sninsky, T.J. White, eds., Academic Press, San Diego, USA, pp 272-281.

Chamberlain, J.S., Corrado, K., Rafael, J.A., Cox, G.A., Hauser, M., & Lumeng, C. (1997). Interactions between dystrophin and the sarcolemmal membrane. *Soc Gen Physiol Ser* **52**: 19-29.

Charlier, C., Coppieters, W., Farnir, F., Grobet, L., Leroy, P.L., Michaux, C. *et al.* (1995). The MH gene causing double muscling in cattle maps to bovine chromosome 2, *Mamm. Genome* **6**: 788–792.

Chen, R.H., Sarnecki, C. & Blenis, J. (1992). Nuclear localization and regulation of ERK- and Rsk-encoded protein kinases. *Mol Cell Biol* **12**: 915-927.

Chen, Y., Zhao, P., Borup, R., & Hoffman, E.P. (2000). Expression Profiling in the Muscular Dystrophies: Identification of Novel Aspects of Molecular Pathophysiology. *J Cell Biol* **151(6)**: 1321–1336.

Chelly, M., Gilgenkrantz, J. H., Lambert, M., Hamard, G., Chafey, P., Recan, D. *et al.*, (1990). Effect of dystrophin gene deletions on mRNA levels and processing in Duchenne and Becker muscular dystrophies. *Cell* **63**: 1239-1248.

Chelly, J., Hamard, G., Koulakoff, A., Kaplan, J.C., Kahn, A., & Berwald-Netter, Y. (1990). Dystrophin gene transcribed from different promoters in neuronal and glial cells. *Nature* **344**: 64–65.

Collins, C.A., & Morgan, J.E. (2003). Duchenne's muscular dystrophy: animal models used to investigate pathogenesis and develop therapeutic strategies. *Int J Exp Pathol* **84**: 165–172.

Collins, C.A., Olsen, I., Zammit, P.S., Heslop, L., Petrie, A., Partridge, T.A. *et al.* (2005). Stem cell function, self-renewal, and behavioral heterogeneity of cells from the adult muscle satellite cell niche. *Cell* **122**: 289-301.

Comi, G.P., Prelle, A., Bresolin, N., Moggio, M., Bardoni, A., Gallanti, A., Vita, G. *et al.* (1994). Clinical variability in Becker muscular dystrophy: Genetic, biochemical and immunohistochemical correlates. *Brain*, **117**: 1-14.

Cooke R. (2004). The sliding filament model: 1972-2004. *Journal of General Physiology* **123(6)**: 643-56.

Cotton, S., Voudouris, N.J., & Greenwood, K.M. (2001). Intelligence and Duchenne muscular dystrophy: Full-Scale, Verbal and Performance intelligence quotients. *Dev Med Child Neurol* **43**: 497–501.

Covone, A.E., Caroli, F., & Romeo, G. (1992). Screening Duchenne and Becker muscular dystrophy patients for deletions in 30 exons of the dystrophin gene by three-multiplex PCR. *Am J Hum Genet* **51**: 675-677.

Cozzi, F., Cerletti, M., Luvoni, G.C. Et Al. (2001). Development of muscle pathology in canine X-linked muscular dystrophy. II. Quantitative characterisation of histopathological progression during postnatal skeletal muscle development. *Acta Neuropathol. (Berl.)* **101**: 469–478.

Crosbie, R.H., Lebakken, C.S., Holt, K.H., Venzke, D.P., Straub, V., Lee, J.C. *et al.* (1999). Membrane targeting and stabilization of sarcospan is mediated by the sarcoglycans subcomplex. *J Cell Biol* **145**:153-165.

Crosbie, R. H., Straub, V., Yun, H. Y., Lee, J.C., Rafael, J. A., Chamberlain, J. S. *et al.* (1998). Mdx muscle pathology is independent of nNOS perturbation. *Hum. Mol. Genet* **7**: 823-829.

Deconinck, N., & Dan, B. (2007). Pathophysiology of Duchenne Muscular Dystrophy: Current Hypotheses. *Pediatr Neurol* 36(1): 1-7.

Deconinck, A.E., Potter, A.C., Tinsley, J.M., Wood, S.J., Vater, R., Young, C. *et al.* (1997) Postsynaptic abnormalities at the neuromuscular junctions of utrophin-deficient mice. *J Cell Biol* **136**: 883–894.

den Dunnen, J.T., & Antonarakis, S.E. (2000). Mutation Nomenclature Extensions and Suggestions to Describe Complex Mutations: A Discussion. *Hum Mutat* 15: 7-12

DeLozier, T.C., Kissling, G.E., Coulter, S.J., Dai, D., Foley, J.F., Bradbury, J. A. *et al.* (2007). Detection of human CYP2C8, CYP2C9, and CYP2J2 in cardiovascular tissues. *Drug Metab Dispos* 35: 682–688.

De Luca, A., Pierno, S., Liantonio, A. Centrone, M., Camerino, C., Fraysse, B. *et al.* (2003). Enhanced dystrophic progression in mdx mice by exercise and beneficial effects of taurine and insulin-like growth factor 1. *J Pharmacol Exp Ther* **304**: 453–463.

Dickson, G., Roberts, M.L., Wells, D.J., & Fabb, S.A. (2002). Recombinant micro-genes and dystrophin viral vectors. *Neuromuscular Disord* **12**: S40–S44.

Dixon, A.K., Tait, T.M., Campbell, E.A., Bobrow, M., Roberts, R.G., Freeman, T.C. (1997). Expression of the dystrophin-related protein 2 (Drp2) transcript in the mouse. *J Mol Biol* **270**: 551–558.

Dominique, J., & Gérard, C. (2006). Myostatin regulation of muscle development: Molecular natural mutations, physiopathological aspects. *Exp Cell Res* **312**: 2401–2414.

Dorchies, O. K., Wagner, S., Vuadens, O., Waldhauser, K., Buetler, T. M., Kucera, P., *et al.* (2006). Green tea extract and its major polyphenol (- )-epigallocatechin gallate improve muscle function in a mouse model for Duchenne muscular dystrophy. *American Journal of Cell Physiology* **290**: C616–C625.

Dubowitz, V. (1995). *Muscle disorders in childhood*, 2nd edition. W.B.Saunders Company, London.

Dunckley, M.G., Wells, D.J., Walsh, F.S., Dickson, G. (1993). Direct retroviral mediated transfer of a dystrophin minigene into mdx mouse muscle in vivo. *Hum Mol Genet* **2**: 717-723.

Ehmsen, J., Poon, E, & Davies, K. (2002). The dystrophin associated protein complex. *J Cell Sci* **115**: 2801-2803.

Emery, A.E. (1993) *Duchenne muscular dystrophy*. Oxford University Press, Edinburgh.

Emery, A.E.H. (2002). The muscular dystrophies. *Lancet* **359**: 687–95.

Emery, A.E., & Emery, M.L. (1993). Edward Meryon (1809-1880) and muscular dystrophy. *J Med Genet* **30**: 506-511.

Emery, A.E.H., & Skinner, R. (1976). Clinical studies in benign (Becker-type) muscular dystrophy. *Clin genet* **10**: 189-201.

Ervasti, J.M. (2003). Costameres: the Achilles' heel of Herculean muscle, *J Biol Chem* **278**: 13591.

Ervasti, J.M., Ohlendieck, K., Kahl, S.D., Gaver, M.G., & Campbell, K.P. (1990). Deficiency of a glycoprotein component of the dystrophin complex in dystrophic muscle, *Nature* **345**: 315.

Ervasti, J.M., & Campbell, K.P. (1991). Membrane organization of the dystrophin–glycoprotein complex, *Cell* **66**: 1121.

Ervasti, J.M. (2006). Dystrophin, its interactions with other proteins, and for muscular dystrophy. *Biochim Biophys Acta* 1772(2): 108-17.

Fabb, S.A., Wells, D.J., Serpente, P., Dickson, G. (2002). Adeno-associated virus vector gene transfer and sarcolemmal expression of a 144 kDa microdystrophin effectively restores the dystrophin-associated protein complex and inhibits myofibre degeneration in nude/mdx mice. *Hum Mol Genet* **11**: 733–741.

Fall, A.M., Johnsen, R., Honeyman, K., Iversen, P., Fletcher, S., & Wilton, S.D. (2006). Induction of revertant fibres in the mdx mouse using antisense oligonucleotides. *Genet Vaccines Ther.* **4**: 3.

Fanin, M., Danieli, G. A., Cadaldini, M., Miorin, M., Vitiello, L., &, Angelini, C. (1995). Dystrophin-positive fibers in duchenne dystrophy: origin and correlation to clinical course. *Muscle Nerve* **18**: 1115-1120.

Fassati, A., Wells, D.J., Walsh, F., Dickson, G. (1996). Transplantation of retroviral

producer cells for in vivo gene transfer into mouse skeletal muscle. *Hum Gene Ther* **7**: 595–602.

Fleming-Waddell, J. N., Wilson, L. M., Olbricht, G. R., Vuocolo, T., Byrne, K., Craig, B. A. *et al.* (2007). Analysis of gene expression during the onset of muscle hypertrophy in callipyge lambs. *Anim Genet* **38**: 28–36.

Forrest, S.M., Cross, G.S., Speer, A., Gardner-Medwin, D., Burns, J., & Davies, K.E. (1987). Preferential deletion of exons in Duchenne and Becker muscular dystrophies. *Nature* **329**: 638-640.

Fowler, E. G., Graves, M. C., Wetzel, G. T., & Spencer, M. J. (2004). Pilot trial of albuterol in Duchenne and Becker muscular dystrophy. *Neurology* **62(6)**: 1006–1008.

Frier, B.C., & Locke, M. (2007). Heat stress inhibits skeletal muscle Hypertrophy. *Cell Stress Chaperon* **12 (2)**: 132–141.

Glass, D.J. (2003). Signalling pathways that mediate skeletal muscle hypertrophy and atrophy. *Nat Cell Biol*: **5**: 87–90.

Glass, D. J. (2005). Skeletal muscle hypertrophy and atrophy signaling pathways. *The Int J Biochem Cell B* **37**: 1974–1984.

Glavač, D. & Dean, M. (1993). Optimization of the single-strand conformation polymorphism (SSCP) technique for detection of point mutations. *Hum Mutat* **2**: 404-414.

Gillard, E.F., Chamberlain, J.S., Murphy, E.G., Duff, C.L., Smith, B., Burghes, A.H.M. *et al.*, (1989). Molecular and phenotypic analysis of patients with deletions within the deletion-rich region of the Duchenne muscular dystrophy (DMD) gene. *Am J Hum Genet* **45**: 507-520.

Gorecki, D.C., Monaco, A.P., Derry, J.M., Walker, A.P., Barnard, E.A., & Barnard, P.J. (1992). Expression of four alternative dystrophin transcripts in brain regions regulated by different promoters. *Hum Mol Genet* **1**: 505–510.

Grady, R.M., Grange, R.W., Lau, K.S., Maimone, M.M., Nichol, M.C., Stull, J.T., Sanes, J.R. (1999). Role for α-dystrobrevin in the pathogenesis of dystrophin dependent muscular dystrophies. *Nat Cell Biol* **1**: 215–220.

Grain, L., Cortina-Borja, M., Forfar, C., Hilton-Jones, D., Hopkin, J, & Burch, M. (2001). Cardiac abnormalities and skeletal muscle weakness in carriers of Duchenne and Becker muscular dystrophies and controls. *Neuromuscular Disord* **11**: 186-91.

Granchelli, J. A., Pollina, C., & Hudecki, M. S. (2000). Pre-clinical screening of drugs using the mdx mouse. *Neuromusclular Disord* **10**: 235–239.

Gregorevic, P., Blankinship, M.J., Allen, J.M., & Chamberlain, J.S. (2008). Systemic microdystrophin gene delivery improves skeletal muscle structure and function in old dystrophic mdx mice. *Mol Ther* **16**: 657-664.

Grounds, M.D., & Davies, K.E. (2007). The allure of stem cell therapy for muscular dystrophy. *Neuromuscular Disord* **17**: 206–208.

Grounds, M. D., & Torrisi, J. (2004). Anti-TNF-α (Remicade) therapy protects dystrophic skeletal muscle from necrosis. *FASEB J 18*: 676–682.

Guyon, J.R., Steffan, L.S., Howell, M.H., Pusack, T.J., Lawrence, C., & Kunkel, L.M. (2006). Modeling human muscle disease in zebrafish. *Biochim Biophys Acta* **1772(2)**: 205-15.

Hack, A.A., Lam, M.Y., Cordier, L., Shoturma, D.I., Ly, C.T., Hadhazy, M.A., Hadhazy, M.R. *et al.* (2000). Differential requirement for individual sarcoglycans and dystrophin in the assembly and function of the dystrophin-glycoprotein complex. *J Cell Sci* **113**: 2535-2544.

Haider, M.Z., Bastaki, L., Habib, Y., & Moosa, A. (1998). Screening 25 dystrophin gene exons for deletions in Arab children with Duchenne muscular dystrophy. *Hum hered* **48**: 61-66.

Hall, D.A., Ptacek, J., & Snyder, M. (2007). Protein Microarray Technology. *Mech Ageing Dev* **128(1)**: 161–167.

Hall, T. A. (1999). BioEdit: a user-friendly biological sequence alignment editor and analysis program for Windows 95/98/NT. *Nucleic Acids Symp Ser* **41**: 95-98.

Han, J., Jiang, Y., Li, Z., Kravchenko, V.V. & Ulevitch, R.J. (1997). Activation of the transcription factor MEF2C by the MAP kinase p38 in inflammation. *Nature* **386**: 296-299.

Harper, S.Q., Hauser, M.A., DelloRusso, C., Duan, D., Crawford, R.W., Phelps, S.F., *et al.* (2002). Modular flexibility of dystrophin: implications for gene therapy of Duchenne muscular dystrophy. *Nat Med* **8**: 253–261.

Haslett, J.N., & Kunkel, L.M. (2002a). Microarray analysis of normal and dystrophic skeletal muscle. *Int J Dev Neurosci* **20**: 359–365.

Haslett, J.N., Sanoudou, D., Kho, A.T., Bennett, R.R., Greenberg, S.A., Kohane, I.S., et al. (2002b). Gene expression comparison of biopsies from Duchenne muscular dystrophy (DMD) and normal skeletal muscle. *PNAS* **99**: 15000-15005.

Hayashi, K., & Yandell, D.W. (1993). How sensitive is PCR-SSCP? *Hum Mutat* **2**: 338-346.

Hoffman, E.P., Brown, R.H., & Kunkel, L.M. (1987). Dystrophin: the protein product of the Duchenne muscular dystrophy locus. *Cell* **51**: 919–928.

Hoffman, E.P., & Escolar, D. (2006). Translating mighty mice into neuromuscular therapeutics. Is bigger muscle better? *A J Pathol* **168(6)**: 1775-78.

Holder, E., Maeda, M., & Bies, R.D. (1996). Expression and regulation of the dystrophin Purkinje promoter in human skeletal muscle, heart and brain. *Hum Genet* **97**: 232–239.

Hongyo, T. Buzard, G.S. Calvert, R.J. & Weghorst, C.M. (1993). "Cold-SSCP": a simple, rapid and non-radioactive method for optimised single-strand conformation polymorphism analyses. *Nucleic Acids Res* **21 (16)**: 3637-3642.

Howard, M.T., Shirts, B.H., Petros, L.M., Flanigan, K.M., Gesteland, R.F., Atkins, J.F. (2000). Sequence specificity of aminoglycoside-induced stop codon read-through: potential implications for treatment of Duchenne muscular dystrophy. *Ann Neurol* **48**: 164-9.

Huard, J., Cao, B., Qu-Petersen, Z. (2003). Muscle-derived stem cells: potential for muscle regeneration. *Birth Defects Res C Embryo Today* **69**: 230-237.

Hunter, R.B., Stevenson, E., Koncarevic, A., Mitchell-Felton, H., Essig, D.A., & Kandarian, S.C. (2002). Activation of an alternative Statistical Analyses NF-_B pathway in skeletal muscle during disuse atrophy. *FASEB J* **16**: 529–538.

Imanishi, T., Itoh, T., Suzuki, Y., O'Donovan, C., Fukuchi, S., Koyanagi, K.O. *et al.* (2004). Integrative Annotation of 21,037 human genes validated by full-length cDNA clones. *PLoS Biology* **2(6)**: 1-20.

Janssen, B., Hartmann, C., Scholz, V., Jauch, A., & Zschocke, J. (2005). MLPA analysis for the detection of deletions, duplications and complex rearrangements in the dystrophin gene: potential and pitfalls. *Neurogenetics* **6**: 29–35.

Jimenez-Mallebrera, C., Davies, K., Putt, W., Edwards, Y.H. (2003). A study of short utrophin isoforms in mice deficient for full-length utrophin. *Mamm Genome* **14**: 47–60.

Junqueira, L.C., Carneiro, J., & Kelly, R.O. (1998), *Basic histology*, 9th edition. Appleton and Lange, USA.

Kang, P.B., Kho, A.T., Sanoudou, D., Haslett, J.N., Dow, C.P., Han, M. *et al.* (2005). Variations in gene expression among different types of human skeletal muscle. *Muscle Nerve* **32**: 483–491.

Karpati, G., & Lochmuller, H. (2001). When running a stop sign may be a good thing. *Ann Neurol* **49(6)**: 693-694.

Kim, Y., Suarez, J., Hu, Y., McDonough, P.M., Boer, C., Dix D.J. *et al*. (2006). Hypertrophy cardiac contractile function and calcium handling associated with deletion of the inducible 70-kda heat shock protein genes in mice impairs. *Circulation* **113**: 2589-2597.

Kimura, S., Itoa, K., Miyagia, T., Hiranumaa, T., Yoshiokaa, K., Ozasaa, S., *et al*. (2005). A novel approach to identify Duchenne muscular dystrophy patients for aminoglycoside antibiotics therapy. *Brain Dev-JPN* **27**: 400–405.

Kingston, H.M., Harper, P.S., Pearson, P.L., Davies, K.E., Williamson, R., & Page, D. (1983). Localisation of gene for Becker muscular dystrophy. *Lancet* **2**: 1200.

Kneppers, A.L.J. Deutz-Terlouw, P.P. den Dunnen, J.T. van Ommen, G.J.B & Bakker, E. (1995). Point mutation screening for 16 exons of the dystrophin gene by multiplex single-strand conformation polymorphism analysis. *Hum Mutat* **5**: 235-242.

Koenig, M., Beggs, A.H., Moyer, M., Scherpf, S., Heindrich, K., Bettecken, T., *et al*. (1989). The molecular basis for Duchenne versus Becker muscular dystrophy: correlation of severity with type of deletion. *Am J Hum Genet* **45**: 498 –506.

Koenig, M., Hoffman, E.P., Bertelson, C.J., Monaco, A.P., Feener, C., & Kunkel, L.M. (1987). Complete cloning of Duchenne muscular dystrophy (DMD) cDNA and preliminary genomic organization of the DMD gene in normal and affected individuals. *Cell* **50**: 509-517.

Koenig, M., Monaco, A.P., & Kunkel, L.M. (1988). The complete sequence of dystrophin predicts a rod-shaped cytoskeletal protein. *Cell* **53**: 219-228.

Kuhlman, P.A., Hemmings, L., & Critchley, D.R. (1992). The identification and

characterization of an actin-binding site in alpha-actinin by mutagenesis. *FEBS Letter* **304**: 201-206.

Kunkel, L.M., Monaco, A. P., Middelsworth, W., Ochs, H.D., & Latt, S.A. (1985). Specific cloning of DNA fragments from the DNA from a patient with an X-chromosome deletion. *Proc Natl Acad Sci USA* **82**: 4778-4882.

Kunkel, L.M., Snyder, J.R., Beggs, A.H., Boyce, F.M., & Feener, C.A. (1991). "Searching for dystrophin gene deletions in patients with atypical presentations," in *Etiology of human diseases at the DNA level*, J. Lindsten, & U. Petterson, eds., Raven Press, New York, USA, pp. 51-60.

Kyte, J., & Doolittle, R.F. (1982). A simple method for displaying the hydropathic character of a protein. *J Mol Biol* **157**: 105-132.

Lai, K. V., Gonzalez, M., Poueymirou, W, T., Kline, W, O., Na, E., Zlotchenko, E. *et al.*, (2004). Conditional activation of AKT in adult skeletal muscle induces rapid hypertrophy. *Mol Cell Biol* **24(21)**: 9295–9304.

Lander, E.S., Linton, L.M., Birren, B., Nusbaum, C., Zody, M.C., Baldwin, J. *et al.* (2001). Initial sequencing and analysis of the human genome. *Nature* **409**: 860–921.

Lapidos, K.A., Kakkar, R., & McNally, E.M. (2004). The dystrophin glycoprotein complex: signaling strength and integrity for the sarcolemma. *Circ Res* **94**: 1023-1031.

Larsen, L.A. Andersen, P.S. Kanters, J.K. Jacobsen, J.R. Vuust, J. & Christiansen, M. (1999a). A single strand conformation polymorphism / heteroduplex (SSCP/HD) method for detection of mutations in 15 exons of the KVTQT1 gene, associated with long QT syndrome. *Clin Chim Acta* **280**: 113-125.

Larsen, L.A., Christiansen, M., Vuust, J., & Andersen, P.S. (1999b). High-throughput single-strand conformation polymorphism analysis by automated capillary electrophoresis:

robust multiplex analysis and pattern-based identification of allelic variants. *Hum Mutat* **12**: 318-327.

Lebakken, C.S., Venzke, D.P., Hrstka, R.F., Consolino, C.M., Faulkner, J.A., Williamson, R.A., & Campbell, K.P. (2000). Sarcospan-deficient mice maintain normal muscle function. *Mol Cell Biol* **20**: 1669-1677.

Lee, M.T. (2004). *Analysis of microarray gene expression data*, 1st edition. Kluwer Academic Publishers, USA.

Lee, S.J., & McPherron, A.C. (2001). Regulation of myostatin activity and muscle growth, *Proc Natl Acad Sci USA* **98**: 9306–9311.

Lenk, U. Hanke, R. & Speer, A. (1994). Carrier detection in DMD families with point mutations, using PCR-SSCP and direct sequencing. *Neuromuscular Disord* **4**: 411-418.

Lidov, H.G.W., Selig, S., & Kunkel, L.M. (1995). Dp140: a novel 140 kDa CNS transcript from the dystrophin locus. *Hum Mol Genet* **4**: 329-335.

Lin, J., Arnold, H.B., Della-Fera, M.A., Azain, M.J., Hartzell, D.L., & Baile, C.A. (2002). Myostatin knockout in mice increases myogenesis and decreases adipogenesis, *Biochem Biophys Res Commun* **291**: 701–706.

Liu, Y., Shen, T., Randall, W.R., & Schneider, M.F. (2005). Signaling pathways in activity-dependent fiber type plasticity in adult skeletal muscle. *J Muscle Res Cell M* **26**: 13–21.

Lu, Q.L., Mann, C.J., Lou, F., Bou-Gharios, G., Morris, G.E., Xue, S.A., *et al.* (2003). Functional amounts of dystrophin produced by skipping the mutated exon in the mdx dystrophic mouse. *Nat Med* **9**: 1009-1014.

Lu, Q.L., Rabinowitz, A., Chen, Y.C., Yokota, T., Yin, H., Alter, J., *et al.* (2005). Systemic delivery of antisense oligoribonucleotide restores dystrophin expression in body-wide skeletal muscles. *Proc Natl Acad Sci USA* **102**: 198-203.

Malhotra, S.B., Hart, K.A., Klamut, H.J., Thomas, N.S.T., Bodrug, S.E., Burghes, A.H.M. *et al.* (1988). Frameshift deletions in patients with Duchenne and Becker muscular dystrophy. *Science* **242**: 755-759.

Mayor, S. (2007). Fitting the drug to the patient. *BMJ* **334**: 452-453.

McCroskery, S., Thomas, M., Platt, L., Hennebry, A., Nishimura, T., McLeay, L. *et al.* (2005). Improved muscle healing through enhanced regeneration and reduced fibrosis in myostatin-null mice, *J Cell Sci* **118**: 3531–3541.

McPherron, A.C., & Lee, S.J. (2002). Suppression of body fat accumulation in myostatin-deficient mice, *J Clin Invest* **109**: 595–601.

Mendell, J.R. Buzin, C.H. Feng, J. Yan, J. Serrano, C. Wall, C. *et al.* (2001) Diagnosis of Duchenne dystrophy by enhanced detection of small mutations. *Neurology* **57**: 645-650.

Metzinger, L., Blake, D.J., Squier, M.V., Anderson, L.V., Deconinck, A.E., Nawrotzki, R., Hilton-Jones, D., And Davies, K.E. (1997). Dystrobrevin deficiency at the sarcolemma of patients with muscular dystrophy. *Hum Mol Genet* **6**: 1185–1191.

Michaud, J., Brody, L.C., Steel, G., Fontaine, G., Martin, L.S., Valle, D., and Mitchell, G., 1992. Strand-separating conformational polymorphism analysis: efficacy of detection of point mutations in the human ornithine delta-aminotransferase gene. *Genomics* **13**: 389-394.

Miller, S.A. Dykes, D.D. & Polesky, H.F. (1988). A simple salting out procedure for extracting DNA from human nucleated cells. *Nucleic Acids Res* **16(3)**: 1215.

Monaco, A.P., Bertolson, C.J., Middelsworth, W., Coletti, C.A., Aldridge, J., Fishbeck, K.

*et al.*, (1985). Detection of deletions spanning the DMD locus using a tightly linked DNA segment. *Nature* **316**: 842-845.

Monaco, A.P., Bertelson, C.J., Liechti-Gallati, S., Moser, H., & Kunkel, L.M. (1988). An explanation for the phenotypic differences between patients bearing partial deletions of the DMD locus. *Genomics* **2**: 90 –95.

Muntoni, F., Torelli, S., & Ferlini, A. (2003). Dystrophin and mutations: one gene, several proteins, multiple phenotypes. *Lancet Neurol* **2**: 731–740.

Musaro, A., McCullagh, K., Paul, A., Houghton, L., Dobrowolny, G., Molinaro, M. *et al.* (2001). Localized Igf-1 transgene expression sustains hypertrophy and regeneration in senescent skeletal muscle. *Nat Genet* **27**: 195–200.

Nguyen, F., Cherel, Y., Guiand, L., Goubault-Leroux, I. & Wyers, M. (2002). Muscle lesions associated with dystrophin deficiency in neonatal golden retriever puppies. *J Comp Pathol* **126**: 100–108.

Nicholas, K. B. & Nicholas, H. B. J. (1997). GeneDoc: a tool for editing and annotating multiple sequence alignments. Distributed by the author. Ref Type: Computer Program.

Nobile, C., Marchi, J., Nigro, V., Roberts, R.G., & Danieli, G.A. (1997). Exon–intron organization of the human dystrophin gene. *Genomics* **45**: 421-424.

Noegel, A., Witke, W., and Schleicherm, M. (1987). Calcium sensitive non-muscle alpha actinin EF hand structures and highly conserved regions. *FEBS Lett* **221**: 391-396.

Noguchi, S., Tsukahara, T., Fujita, M., Kurokawa, R., Tachikawa, M., Toda, T., Tsujimoto, A. *et al.* (2003). cDNA microarray analysis of individual Duchenne muscular dystrophy patients. *Hum Mol Genet* **12(6)**: 595–600.

Novel experimental technology. (1996). *ThermoFlow "Cold" SSCP applications notes.* Novex, San Diego, CA 92121.

Nudel, U., Robzyk, K., & Yaffe, D. (1988). Expression of the putative Duchenne muscular dystrophy gene in differentiated myogenic cell cultures and in the brain. *Nature* **331**: 635-638.

Odom, G.L., Gregorevic, P., Allen, J.M., Finn, E., & Chamberlain, J.S. (2008). Microutrophin delivery through rAAV6 increases lifespan and improves muscle function in dystrophic dystrophin/utrophin-deficient mice. *Mol Ther* **16**: 1539-45.

Ohlendieck, K., Ervasti, J.M., Matsumura, K., Kahl, S.D., Leveille, C.J., Campbell, K.P. (1991). Dystrophin-related protein is localized to neuromuscular junctions of adult skeletal muscle. *Neuron* **7**: 499-508.

O'Neill, D.E.T., Aubrey, F.K., Zeldin, D.A., Michel R.N. & Noble, E.G. (2006). Slower skeletal muscle phenotypes are critical for constitutive expression of Hsp70 in overloaded rat plantaris muscle. *J Appl Physiol* **100**: 981-987.

Orita, M. Iwahana, H. Kanazawa, H. Hayashi, K. & Sekiya, T. (1989). Detection of polymorphisms of human DNA by gel electrophoresis as single-stranded conformation polymorphisms. *P Natl Acad Sci USA* **86**: 2766-2770.

Ota, T., Suzuki, Y., Nishikawa, T., Otsuki, T., Sugiyama, T., Irie, R. *et al*. (2004). Complete sequencing and characterization of 21,243 full-length human cDNAs. *Nat Genet* **36**: 40-45.

Page-McCaw, A., Ewald, A.J., & Werb, Z. (2007). Matrix metalloproteinases and the regulation of tissue remodeling. *Nat Rev Mol Cell Bio* **8**: 221-233.

Parsons, S.A., Millay, D.P., Sargent, M.A., Mitchell, R., McNally, E.M., Crandall, D.L. *et al*. (2006). Age-dependent effect of myostatin blockage on disease severity in a murine model of limb-girdle muscular dystrophy. *Am J Pathol* **168**: 1975–1985.

Passos-Bueno, M.R., Vainzof, M., Marie, S.K., Zatz, M. (1994). Half the dystrophin gene

is apparently enough for a mild clinical course: confirmation of its potential use for gene therapy. *Hum Mol Genet* **3**: 919–922.

Patria, S.Y., Takeshima, Y., Suminaga, R., Nakamura, H., Iwasaki, R., Minagawa, T. *et al.*, (1999). A simple explanation for a case of incompatibility with the reading frame theory in Duchenne muscular dystrophy: failure to detect an aberrant restriction fragment in Southern blot analysis. *Brain Dev-JPN* **21**: 386-389.

Péault, B., Rudnicki, M., Torrente, Y., Cossu, G., Tremblay, J.P., Partridge, T. *et al.* (2007). Stem and Progenitor Cells in Skeletal Muscle Development, Maintenance, and Therapy. *Mol Ther* **15(5)**: 867–877.

Peters, M.F., O'brien, K.F., Sadoulet-Puccio, H.M., Kunkel, L.M., Adams, M.E., & Froehner, S.C. (1997). Beta-dystrobrevin, a new member of the dystrophin family. Identification, cloning, and protein associations. *J Biol Chem* **272**: 31561-31569.

Phimister, B. (1999) Going global. *Nat Genet Suppl* **21**: 1.

Pelosi, L., Giacinti, C., Nardis, C., Borsellino, G., Rizzuto, E., Nicoletti, C. *et al.* (2007). Local expression of IGF-1 accelerates muscle regeneration by rapidly modulating inflammatory cytokines and chemokines. *FASEB J* **21(7)**: 1393-402.

Penner, C.G., Gang, G., Wray, C., Fischer, J.E., & Hasselgren, P.O. (2001). The transcription factors NF-_B and AP-1 are differentially regulated in skeletal muscle during sepsis. *Biochem Biophys Res Commun* **281**: 1331–1336.

Poduslo, S.E. Dean, M. Kolch, U., & O'Brien, S.J. (1991). Detecting high-resolution polymorphisms in human coding loci by combining PCR and single-stranded conformation polymorphism (SSCP) analysis. *Am J Hum Genet* **49**: 106-111.

Ponting, C.P., Blake, D.J., Davies, K.E., Kendrick-Jones, J., Winder, S.J. (1996). ZZ and TAZ: new putative zinc fingers in dystrophin and other proteins, *Trends Biochem Sci* **21**: 11.

Porter, G.A., Dmytrenko, G.M., Winkelmann, J.C., & Bloch, R.J. (1992). Dystrophin colocalizes with β-spectrin in distinct subsarcolemmal domains in mammalian skeletal muscle, *J Cell Biol* **117**: 997.

Porter, J. D., Khanna, S., Kaminski, H. J., Rao, J. S., Merriam, A. P., & Richmonds, C. R. (2002). A chronic inflammatory response dominates the skeletal muscle molecular signature in dystrophin-deficient *mdx* mice. *Hum Mol Genet* **11**: 263–272.

Radley, H.G., De Luca, A., Lynch, G.S., & Grounds, M.D. (2007). Duchenne muscular dystrophy: Focus on pharmaceutical and nutritional interventions. *Int J Biochem Cell Biol* **39(3)**: 469-77.

Radley, H. G., & Grounds, M. D. (2006). Cromolyn administration to block mast cell degranulation) reduces necrosis of dystrophic muscle in mdx mice. *Neurobiol Dis* **23(2)**: 387–397.

Rando, T.A. (2001). The dystrophin–glycoprotein complex, cellular signaling, and the regulation of cell survival in the muscular dystrophies. *Muscle Nerve* **24**: 1575–1594.

Rafael, J.A., Tinsley, J.M., Potter, A.C., Deconinck, A.E., & Davies, K.E. (1998). Skeletal muscle specific expression of a utrophin transgene rescues utrophin-dystrophin deficient mice. *Nat Genet* **19**: 79–82.

Rafael, J.A., & Brown, S.C. (2000). Dystrophin and utrophin: genetic analyses of their role in skeletal muscle. *Microsc res techniq* **48**: 155–166.

Reid, A.G., Tarpey, P.S. & Nacheva, E.P. (2003). High-resolution analysis of acquired genomic imbalances in bone marrow samples from chronic myeloid leukemia patients by use of multiple short DNA probes. *Gene chromosome canc* **37**: 282–290.

Relling, M.V., & Hoffman, J.M. (2007). Should Pharmacogenomic Studies be Required for New Drug Approval? *Clin Pharmacol Ther* **81(3)**: 425-428.

Roberts, R.G. (1995). Dystrophin, Its gene, and the dystrophinopathies. *Adv Genet* **33**: 177-231.

Roberts, R.G. (2001). Dystrophins and dystrobrevins. *Genome Biol* **2(4)**: 1-7.

Roberts R.G., Barby, T.F.M., Manners, E., Bobrow, M., & Bentley D.R. (1991). Direct detection of dystrophin gene rearrangements by analysis of dystrophin mRNA in peripheral blood lymphocytes. *Am J Hum Genet* **49**: 298-310.

Roberts, R.G., Bobrow, M., & Bentley, D.R. (1992). Point mutations in the dystrophin gene. *Proc Natl Acad Sci USA* **89**: 2331-2335.

Roberts, R.G., Coffey, A.J., Bobrow, M., & Bentley, D.R. (1993). Exon structure of the human dystrophin gene. *Genomics* **16**: 536-538.

Roberts, R.G., Freeman, T.C., Kendall, E., Vetrie, D.L., Dixon, A.K., Shaw-Smith, C *et al.* (1996). Characterization of DRP2, a novel human dystrophin homologue. *Nat Genet* **13(2)**: 223-6.

Roberts, M.L., Wells, D.J., Graham, I.R., Fabb, S.A., Hill, V.J., Duisit, G. *et al.* (2002). Stable micro-dystrophin gene transfer using an integrating adeno-retroviral hybrid vector ameliorates the dystrophic pathology in mdx mouse muscle. *Hum Mol Genet* **11(15)**: 1719-30.

Rouger, K., Le Cunff, M., Steenman, M., Potier, M., Gibelin, N., Dechesne, C.A. *et al.*, (2002). Global/temporal gene expression in diaphragm and hindlimb muscles of dystrophin-deficient (*mdx*) mice. *Am J Physiol Cell Physiol* **253**: C773–C784.

Sadoulet-Puccio, H.M., Khurana, T.S., Cohen, J.B., & Kunkel, L.M. (1996). Cloning and characterization of the human homologue of a dystrophin related phosphoprotein found at the *Torpedo* electric organ post-synaptic membrane. *Hum Mol Genet* **5**: 489-496.

Sadoulet-Puccio, H.M., Rajala, M., & Kunkel, L.M. (1997). Dystrobrevin and dystrophin:

an interaction through coiled-coil motifs. *Proc Natl Acad Sci USA* **94**: 12413–12418.

Sampaolesi, M., Blot, S., D'Antona, G., Granger, N., Tonlorenzi, R., Innocenzi, A *et al.* (2006). Mesoangioblast stem cells ameliorate muscle function in dystrophic dogs. *Nature* **127**: 1304–6.

Sander, M., Chavoshan, B., Harris, S.A., Iannaccone, S.T., Stull, J.T., Thomas, G.D. *et al.* (2000). Functional muscle ischemia in neuronal nitric oxide synthase-deficient skeletal muscle of children with Duchenne muscular dystrophy. *Proc Natl Acad Sci USA* **97**: 13818 13823.

Sargiacomo, M., Bricarelli, F.D., Minetti, C., Sudol, M., & Lisanti, M.P. (2000). Caveolin-3 directly interacts with the C-terminal tail of beta-dystroglycan. Identification of a central WW-like domain within caveolin family members. *J Biol Chem* **275**: 38048–38058.

Schatzberg, S.J., Olby, N.J., Breen, M., Anderson, L.V., Langford, C.F., Dickens, H.F. *et al.* (1999). Molecular analysis of a spontaneous dystrophin"knockout" dog. *Neuromuscular Disord* **9**: 289–295.

Schuelke, M., Wagner, K.R., Stolz, L.E., Hübner, C., Riebel, T., Kömen, W. *et al.*, (2004). Myostatin mutation associated with gross muscle hypertrophy in a child. *New Engl J Med* **350**: 2682–2688.

Sharp N.J, Kornegay J.N, Van Camp S.D, Herbstreith M.H, Secore S.L, Kettle S, *et al.* (1992). An error in dystrophin mRNA processing in golden retriever muscular dystrophy, an animal homologue of Duchenne muscular dystrophy. *Genomics* **13**: 115–121.

Sheffield, V.C. Beck, J.S. Kwitek, A.E. Sandstrom, D.W. & Stone, E.M. (1993). The sensitivity of single-strand conformation polymorphism analysis for the detection of single base substitutions. *Genomics* **16**: 325-332.

Sicinski, P., Geng, Y., Ryder Cook, A.S., Barnard, E.A., Darlison, M.G., & Barnard, P.J. (1989). The molecular basis of muscular dystrophy in the mdx mouse: a point mutation. *Science* **244**: 1578–1580.

Seubert, J., Yang, B., Bradbury, J. A., Graves, J., Degraff, L.M., Gabel, S. et al. (2004). Enhanced postischemic functional recovery in CYP2J2 transgenic hearts involves mitochondrial ATP-sensitive K$^+$ channels and p42/p44 MAPK pathway. *Circ Res* **95**: 506-514.

Simonds, A.K., Muntoni, F., Heather, S., & Fielding, S. (1998). Impact of nasal ventilation on survival in hypercapnic Duchenne muscular dystrophy. *Thorax* **53**: 949–52.

Sollee, N.D., Latham, E.L., Kindlon, D.J., & Bresnan, M.J. (1985). Neuropsychological impairment in Duchenne muscular dystrophy. *J Clin Exp Neuropsychol* **5**: 486–496.

Southern, E.M. (1996). High-density gridding: techniques and applications. *Curr Opin Biotech* **7**: 85-88.

Spiecker, M., Darius, H., Hankeln, T., Soufi, M., Sattler, A.M., Schaefer, J.R. *et al.* (2004). Risk of coronary artery disease associated with polymorphism cytochrome P450 epoxygenase CYP2J2. *Circulation* **110**: 2132-2136.

Stedman, H.H., Sweeney, H.L., Shrager, J.B., Maguire, H.C., Panettieri, R.A., Petrof, B., Narusawa, M., Leferovich, J.M., Sladky, J.T., & Kelly, A.M. (1991). The mdx mouse diaphragm reproduces the degenerative changes of Duchenne muscular dystrophy. *Nature* **352**: 536-539.

Steelman, C.A., Recknor, J.C., Nettleton, D., & Reecy, J.M. (2006). Transcriptional profiling of myostatin-knockout mice implicates Wnt signaling in postnatal skeletal muscle growth and hypertrophy. *FASEB J* **20**: 580-582.

Sterrenburg, E., van der Wees, C.G.C., White, S.J., Turk, R., de Menezes, R.X., van Ommen, G.B. *et al.*, (2006). Gene expression profiling highlights defective myogenesis in DMD patients and a possible role for bone morphogenetic protein 4. *Neurobiol Dis* **23**: 228–236.

Schmalbruch, H. (1984). Regenerated muscle fibers in Duchenne muscular dystrophy: a serial section study. *Neurology* **34**: 60–65.

Schouten, J.P., McElgunn, C.J., Waaijer, R., Zwijnenburg, D., Diepvens, F., & Pals, G. (2002). Relative quantification of 40 nucleic acid sequences by multiplex ligation-dependent probe amplification. *Nucleic Acids Res* **30(12) e57**: 1-13.

Squire, S., Raymackers, J.M., Vandebrouck, C., Potter, A., Tinsley, J., Fisher, R. *et al.* (2002). Prevention of pathology in mdx mice by expression of utrophin: analysis using an inducible transgenic expression system. *Hum Mol Genet* **11**: 3333–3344.

Stewart, C.E.H., & Rittweger, J. (2006). Adaptive processes in skeletal muscle: Molecular regulators and genetic influences. *Journal of musculoskeletal and neuronal interactions* **6**: 73-86.

Straub, V. Bittner, R.E. Léger, J.J. Voit, T. (1992). Direct visualization of the dystrophin network on skeletal muscle fiber membrane, *J Cell Biol* **119**: 1183.

Surono, A., Van Khanh, T., Takeshima, Y Wada, H., Yagi, M., Takagi, M. *et al.* (2004). Chimeric RNA/ethylene-bridged nucleic acids promote dystrophin expression in myocytes of duchenne muscular dystrophy by inducing skipping of the nonsense mutation-encoding exon. *Hum gene ther* **15**: 749–757.

Suzuki, A., Yoshida, M., Hayashi, K., Mizuno, Y., Hagiwara, Y., & Ozawa, E. (1994). Molecular organization at the glycoprotein-complex-binding site of dystrophin. Three dystrophin associated proteins bind directly to the carboxy-terminal portion of dystrophin. *Eur J Biochem* **220**: 283-92.

Takemitsu, M., Ishiura, S., Koga, R., Kamakura, K., Arahata, K., Nonaka, I., & Sugita, H. (1991). Dystrophin-related protein in the fetal and denervated skeletal muscles of normal and mdx mice. *Biochem Biophys Res Commun* **180**:1179-1186.

Thanh, L.T., thi Man, N., Helliwell, T. R., & Morris, G. E. (1995). Characterization of revertant muscle fibers in duchenne muscular dystrophy, using exon-specific monoclonal antibodies against dystrophin. *Am J Hum Genet* **56**: 725-731.

Thompson, J. D., Gibson, T. J., Plewniak, F., Jeanmougin, F., & Higgins, D. G. (1997). The CLUSTAL_X windows interface: flexible strategies for multiple sequence alignment aided by quality analysis tools. *Nucleic Acids Res* **25**: 4876-4882.

Tidball, J.G., Albrecht, D.E., Lokensgard, B.E., & Spencer, M.J. (1995). Apoptosis precedes necrosis of dystrophin-deficient muscle. *J Cell Sci* **108**: 2197–2204.

Tidball, J.G., and Spencer, M.J. (2000). Calpains and muscular dystrophies. *Int J Biochem Cell B* **32**: 1-5.

Tidball, J.G., & Wehling-Henricks, M. (2007). The role of free radicals in the pathophysiology of muscular dystrophy. *J Appl Physiol* **102**:1677-1686.

Tinsley, J.M., Blake, D.J., Roche, A., Byth, B.C., Knight, A.E., Kendrick-Jones, J. *et al.* (1992). Primary structure of dystrophin related protein. *Nature* **360**: 591.

Tinsley, J.M., Potter, A.C., Phelps, S.R., Fisher, R., Trickett, J.I., & Davies, K.E. (1996). Amelioration of the dystrophic phenotype of mdx mice using a truncated utrophin transgene. *Nature* **384**: 349–353.

Tinsley, J., Deconinck, N., Fisher, R., Kahn, D., Phelps, S., Gillis, J.M., & Davies, K. (1998). Expression of full-length utrophin prevents muscular dystrophy in mdx mice. *Nat Med* **4**: 1441–1444.

Tkatchenko, A.V., PieÂtub, G., Crosa, N., Gannoun-Zakia, L., Auffrayb, C., LeÂgera, J.J. *et al.*, (2001). Identification of altered gene expression in skeletal muscles from Duchenne muscular dystrophy patients. *Neuromuscular Disord* **11**: 269-277.

Tong, W., Cao, X., Harris, S., Sun, H., Fang, H., Fuscoe, J. *et al.*, (2003). ArrayTrack Supporting Toxicogenomic Research at the U.S. Food and Drug Administration National Center for Toxicological Research. *Environ Health Persp* **111 (15)**: 1819-1826.

Tseng, B. S., Zhao, P., Pattison, J. S., Gordon, S. E., Granchelli, J. A., Madsen, R. W. *et*

*al.*, (2002). Regenerated *mdx* mouse skeletal muscle shows differential mRNA expression. *J Appl Physiol* **93**: 537–545.

Tskhovrebova, L., & Trinick, J. (2003). Titin: properties and family relationships. *Nat Rev Mol Cell Bio* **4(9)**: 679-89.

Tuffery-Giraud, S., Chambert, S., Demaille, J., & Claustres, M. (1999). Point Mutations in the Dystrophin Gene: Evidence for frequent use of cryptic splice sites as a result of splicing defects. *Hum Mutat* **14**: 359.368.

Tuffery-Giraud, S., Saquet, C., Chambert, S., Echenne, B., Cuisset, J. M., Rivier, F. *et al.*, (2004). The role of muscle biopsy in analysis of the dystrophin gene in Duchenne muscular dystrophy: experience of a national referral centre. *Neuromuscular Disord* **14**: 650–658.

Urish, K., Kanda, Y., & Huard J. (2005). Initial failure in myoblast transplantation therapy has led the way toward the isolation of muscle stem cells: potential for tissue regeneration. *Curr Top Dev Biol* **68**: 263-280.

van der Plas, M.C., Pilgram, G.S.K., de Jong, A.W.M., Bansraj, M.R.K.S., Fradkin, L.G., Noordermeer, J.N. (2007). Drosophila Dystrophin is required for integrity of the musculature. *Mech Develop* **124**: 617–630.

Venter, J.C., Adams, M.D., Myers, E.W., Li, P.W., Mural, R.J., Sutton, G.G. *et al.*, (2001). The sequence of the human genome. *Science* **291**: 1304-1351.

Verellen-Dumoulin, C., Freund, M., de Meyer, R., Laterre, Ch., Frederique, J., Thompson, M.W. *et al.* (1984). Expression of an X-linked muscular dystrophy in a female due to a translocation involving Xp21 and a non-random inactivation of the normal X-chromosome. *Hum Genet* **67**: 115-119.

Vincent, N., Ragot, T., Gilgenkrantz, H., Couton, D., Chafey, P., Grégoire, A. *et al.* (1993). Long-term correction of mouse dystrophic degeneration by adenovirus-mediated transfer of a minidystrophin gene. *Nat Genet* **5**: 130–134.

Vogel, H., & Zamecnik, J. (2005). Diagnostic Immunohistology of Muscle Diseases. *J Neuropath Exp Neur* **64(3)**: 181-93.

Wagers, A.J., & Conboy, I.M. (2005). Cellular and molecular signatures of muscle regeneration: current concepts and controversies in adult myogenesis. *Cell* **122**: 659-667.

Wagner, K.R., Cohen, J.B., & Huganir, R.L. (1993). The 87K postsynaptic membrane protein from torpedo is a protein–tyrosine kinase substrate homologous to dystrophin, *Neuron* **10**: 511.

Wagner, R.W., Hamed, S., Hadley, D.W., Gropman, A.L., Burstein, A.H., Escolar, D.M. *et al.* (2001). Gentamicin treatment of Duchenne and Becker muscular dystrophy due to nonsense mutations. *Ann Neurol* **49**: 706–11.

Wagner, K.R. Liu, X. Chang, X. Allen, R.E. (2005). Muscle regeneration in the prolonged absence of myostatin, *Proc Natl Acad Sci USA* **102 (7)**: 2519–2524.

Walz, T. Geisel, J. Bodis, M. Knapp, J. & Herrmann, W. (2000) Fluorescence-based single-strand conformation polymorphism analysis of mutations by capillary electrophoresis. *Electrophoresis* **21**: 375-379.

Wang, B., Li, J., & Xiao, X. (2000). Adeno-associated virus vector carrying human minidystrophin genes effectively ameliorates muscular dystrophy in mdx mouse model. *Proc Natl Acad Sci USA* **97**: 13714–13719.

Watkins, S.C., Hoffman, E.P., Slayer, H.S., & Kunkel, L.M. (1988). Immunoelectron microscopic localization of dystrophin in myofibres. *Nature* **333**: 863-66.

Weghorst, C.M., & Buzard, G.S. (1993). Enhanced single-strand conformation polymorphism (SSCP) detection of point mutations utilizing methylmercury hydroxide. *Biotechniques* **15**: 396-398.

Wells, D.J., & Wells, K.E. (2002). Gene transfer studies in animals: what do they really

tell us about the prospects of gene therapy for DMD? *Neuromuscul Disord* **12 (Suppl. 1)**:
11–22.

Widegren, U., Ryder, J.W., & Zierath, J.R. (2001). Mitogen-activated protein kinase signal
transduction in skeletal muscle: effects of exercise and muscle contraction. *Acta
Physiologica Scandinavica* **172(3)**: 227-38.

White, S.J. (2005). *Detecting copy number changes in genomic DNA – MAPH and MLPA*,
PhD thesis. Febodruk B.V., Enschede, The Netherlands.

White, S.J., Sterrenburg, E., van Ommen, G.J., den Dunnen, J.T., & Breuning, M.H.
(2003). An alternative to FISH: detecting deletion and duplication carriers within 24 hours.
*J Med Genet* **40**: e113 (http://www.jmedgenet.com/cgi/content/full/40/10e/e113)

White, S.J., Vink, G.R., Kriek, M., Wuyts, W., Schouten, J., Bakker, E. *et al.*, (2004).
Two-color multiplex ligation-dependent probe amplification: detecting genomic
rearrangements in hereditary multiple exostoses. *Hum Mutat* **24**: 86-92.

White, S.J., Aartsma-Rus, A., Flanigan, K.M., Weiss, R.B., Kneppers, A.L., Lalic, T. *et al.*
(2006). Duplications in the DMD Gene. *Hum Mutat* **27(9)**: 938-945.

Winder, S.J., Gibson, T.J., & Kendrick-Jones, J. (1995). Dystrophin and utrophin:
the missing links! *FEBS Lett* **369**: 27-33.

Winand, N.J., Edwards, M., Pradhan, D., Berian, C.A., & Cooper, B.J. (1994). Deletion of
the dystrophin muscle promoter in feline muscular dystrophy. *Neuromuscular Disord* **4**:
433–445.

Wilson, L.A., Cooper, B.J., Dux L., Dubowitz, V. & Sewry, C.A. (1994). Expression of
utrophin (dystrophin-related protein) during regeneration and maturation of skeletal muscle
in canine X-linked muscular dystrophy. *Neuropathol Appl Neurobiol* **20**: 359–367.

Wilton, S.D., Dye, D.E., Blechynden, L.M., & Laing, N.G. (1997). Revertant fibres: a

possible genetic therapy for Duchenne muscular dystrophy? *Neuromuscul Disord* **7(5)**: 329-35.

Worton, R.G. (1992). Duchenne muscular dystrophy: Gene and gene product; mechanism of mutation in the gene. *J Inherit Metab Dis* **15**: 539-550.

Worton, R.G., Duff, C., Sylvester, J.E., Schmickel, R.D., & Willard, H.F. (1984). Duchenne muscular dystrophy involving translocation of the DMD gene next to ribosomal DNA genes. *Science* **244**: 1447-1448.

Xing, J., Ginty, D.D. & Greenberg, M.E. (1996). Coupling of the RAS-MAPK pathway to gene activation by RSK2,a growth factor-regulated CREB kinase. *Science* **273**: 959-963.

Yagi, M., Takeshima, Y., Surono, A., Takagi, M., Koizumi, M., & Matsuo, M. (2004). Chimeric RNA and 2'-O, 4'-C- ethylene-bridged nucleic acid have stronger activity than phosophorothioate oligodeoxynucleotides in induction of exon 19 skipping in dystrophin mRNA. *Oligonucleotides* **14**: 33-40.

Yuasa, K., Miyagoe, Y., Yamamoto, K., Nabeshima, Y., Dickson, G., & Takeda, S. (1998). Effective restoration of dystrophin-associated proteins in vivo by adenovirus-mediated transfer of truncated dystrophin cDNAs. *FEBS Lett* **425**: 329–336.

Zhang, Y., Ye, J., Chen, D., Zhao, X., Xiao, X., & Tai, S. (2006). Differential expression profiling between the relative normal and dystrophic muscle tissues from the same LGMD patient. *J Transl Med* **4(53)**: 1-12.

Zheng, Y., Im, C.N., & Seo, J,S. (2006). Inhibitory effect of Hsp70 on angiotensin II induced vascular smooth muscle cell hypertrophy. *Exp Mol Med* **38**(5): 509-518.

Zhou, G., Xie, H., Zhang, S., & Yang, Z. (2006). Current understanding of dystrophin related muscular dystrophy and therapeutic challenges ahead. *Chinese Med J-Peking* **119(16)**: 1381-1391.

Zhu, X., Hadhazy, M., Wehling, M., Tidball, J.G., & McNally, E.M. (2000). Dominant negative myostatin produces hypertrophy without hyperplasia in muscle. *FEBS Lett* **474**: 71–75.

Zubrzycka-Gaarn, E.E., Bulman, D.E., Karpati, G., Burghes, A.H.M., Belfall, B., Klamut, H.J. *et al.* (1988). The Duchenne muscular dystrophy gene product is localized in sarcolemma of human skeletal muscle. *Nature* **333**: 466.

# APPENDICES

## APPENDIX A

### PRIMER SEQUENCES

### 1. Single stranded conformation polymorphism analysis.

Table 44: Actual primer sequences in the 5' – 3' orientation that were used in the PCR procedure to amplify the products for SSCP analysis.

| EXON NAME | SEQUENCE 5' – 3' | SIZE IN BASE PAIRS |
|---|---|---|
| 2 F | CAC TAACAC ATC ATA ATG G | 233 bp |
| 2 R | GAT ACA CAG GTA CAT AGT C | |
| 3 F | TCA TCC ATC ATC TTC GGC AGA TTA A | 410 bp |
| 3 R | CAG GCG GTA GAG TAT GCC AAA TGA AAA TCA | |
| 4 F | TTG TCG GTC TCC TGC TGG TCA GTG | 190 bp |
| 4 R | CAA AGC CCT CAC TCA AAC ATG AAG C | |
| 5 F | GGT TGA TTT AGT GAA TAT TGG AAG TAC | 114 bp |
| 5 R | CCA TTC ATC AGG ATT CTT ACC TGC C | |
| 6 F | CCA CAT GTA GGT CAA AAA TGT AAT GAA | 202 bp |
| 6 R | GTC TCA GTA ATC TTC TTA CCT ATG ACT ATG G | |
| 8 F | GTC CTT TAC ACA CTT TAC CTG TTG AG | 360 bp |
| 8 R | GGC CTC ATT CTC ATG TTC TAA TTA G | |
| 9 F | TCT ATC CAC TCC CGA ACC TCT CTG CAG | 278 bp |
| 9 R | AAC AAA CCA GCT CTT CAC GAG GAG A | |
| 12 F | GAT AGT GGG CTT TAC TTA CAT CCT TC | 331 bp |
| 12 R | GAA AGC ACG CAA CAT AAG ATA CAC CT | |
| 13 F | AAT AGG AGT ACC TGA GAT GTA GCA GAA AT | 238 bp |
| 13 R | CTG ACC TTA AGT TGT TCT TCC AAA GCA G | |
| 16 F | TCT ATG CAA ATG AGC AAA TAC ACG C | 290 bp |
| 16 R | GGT ATC ACT AAC CTG TGC TGT ACT C | |
| 17 F | GAC TTT CGA TGT TGA GAT TAC TTT CCC | 416 bp |
| 17 R | AAG CTT GAG ATG CTC TCA CCT TTT CC | |
| 20 F | GTG TTA ATG CAG ATA GCA TCA AAC | 239 bp |
| 20 R | ACA AAT TTT TAA CTG ACT TTT AAT TG | |
| 22 F | TTG ACA CTT TGC CAC CAA TGC GCT ATC | 140 bp |
| 22 R | CAA TTC CCC GAG TCT CTG CTC CAT G | |
| 32 F | GAC CAG TTA TTG TTT GAA AGG CAA A | 253 bp |
| 32 R | TTG CCA CCA GAA ATA CAT ACC ACA CAA TG | |
| 34 F | GTA ACA GAA AGA AAG CAA CAG TTG GAG AA | 171 bp |
| 34 R | CTT TCC CCA GGC AAC TTC AGA ATC CAA A | |
| 41 F | GTT AGC TAA CTG CCC TGG GCC CTG TAT TG | 274 bp |
| 41 R | TAG AGT AGT AGT TGC AAA CAC ATA CGT GG | |
| 42 F | CAC ACT GTC CGT GAA GAA ACG ATG ATG | 155 bp |

| | | |
|---|---|---|
| 42 R | TTA GCA CAG AGG TCA GGA GCA TTG AG | |
| 43 F | GAA CAT GTC AAA GTC ACT GGA CTT CAT GG | 357 bp |
| 43 R | ATA TAT GTG TTA CCT ACC CTT GTC GGT | |
| 44 F | GTT GTG TGT ACA TCG TAG GTG TGT A | 426 bp |
| 44 R | TCC ATC ACC CTT CAG AAC CTG ATC T | |
| 45 F | AAA CAT GGA ACA TCC TTG TGG GGA C | 547 bp |
| 45 R | CAT TCC TAT TAG ATC TGT CGC CCT AC | |
| 46 F | GCT AGA AGA ACA AAA GAA TAT CTT GTC | 148 bp |
| 46 R | CTT GAC TTG CTC AAG CTT TTC TTT TAG | |
| 47 F | CGT TGT TGC ATT TGT CTG TTT CAG TTA C | 181 bp |
| 47 R | GTC TAA CCT TTA TCC ACT GGA GAT TTG | |
| 50 F | CAC CAA ATG GAT TAA GAT GTT CAT GAA T | 271 bp |
| 50 R | TCT CTC TCA CCC AGT CAT CAC TTC ATA G | |
| 51 F | GAA ATT GGC TCT TTA GCT TGT GTT TC | 388 bp |
| 51 R | GGA GAG TAA AGT GAT TGG TGG AAA ATC | |
| 52 F | AAT GCA GGA TTT GGA ACA GAG GCG TCC | 113 bp |
| 52 R | TTC GAT CCG TAA TGA TTG TTC TAG CCT C | |
| 53 F | TTG AAA GAA TTC AGA ATC AGT GGG ATG | 212 bp |
| 53 R | CTT GGT TTC TGT GAT TTT CTT TTG GAT TG | |
| Pb F | TCT GGC TCA TGT GTT TGC TCC GAG GTA T AG | 332 bp |
| Pb R | CTT CCA TGC CAG CTG TTT TTC CTG TCA CTC | |
| Pm F | GAA GAT CTA GAC AGT GGA TAC ATA ACA AAT GCA TG | 535 bp |
| Pm R | TTC TCC GAA GGT AAT TGC CTC CCA GAT CTG AGT CC | |

## 2. 30-exon multiplex PCR.

**Table 45: Primer sequences for the adapted and optimised original Chamberlain set of exons for the first multiplex PCR set.**

| EXON NAME | SEQUENCE 5' - 3' | SIZE IN BASE PAIRS |
|---|---|---|
| 45 F<br>45 R | aaa cat gga aca tcc ttg tgg gga c<br>cat tcc tat tag atc tgt cgc cct ac | 547 |
| 48 F<br>48 R | ttg aat aca ttg gtt aaa tcc caa cat g<br>cct gaa taa agt ctt cct tac cac ac | 506 |
| 19 F<br>19 R | gat ggc aaa agt gtt gag aaa aag tc<br>ttc tac cac atc cca ttt tct tcc a | 459 |
| 44 F<br>44 R | gtt gtg tgt aca tcg tag gtg tgt a<br>tcc atc acc ctt cag aac ctg atc t | 426<br>(QmPCR) |
| 44 F<br>44 R | ctt gat cca tat gct ttt acc tgc a<br>tcc atc acc ctt cag aac ctg atc t | 268 |
| 17 F<br>17 R | gac ttt cga tgt tga gat tac ttt ccc<br>aag ctt gag atg ctc tca cCT TTT CC | 416 |
| 51 F<br>51 R | gaa att ggc tct tta gct tgt gtt tc<br>gga gag taa agt gat tgg tgg aaa atc | 388 |
| 8 F<br>8 R | ggc ctc att ctc atg ttc taa tta g<br>gtc ctt tac aca ctt tac CTG TTG AG | 360 |

298

| | | |
|---|---|---|
| 12 F | gat agt ggg ctt tac tta cat cct tc | 331 |
| 12 R | gaa agc acg caa cat aag ata cac ct | |
| 29 F | cca atg tat tta gaa aaa aaa gga g | 242 |
| 29 R | gca aat tag att aaa gag att ttc ac | |
| 4 F | ttg tcg gtc tct ctg ctg gtc agt g | 196 |
| 4 R | caa agc cct cac tca aac atg aag c | |
| 22 F | TTG ACA CTT TGC CAC CAA TGC GCT ATC | 140 |
| 22 R | CAA TTC CCC GAG TCT CTG CTC CAT G | (Covone) |
| 30 F | AGG CTG TAA GGA GGC AAA AGT TGC | 175bp |
| 30 R | GAT GTA CTT GCC TGG GCT TCC TGA GGC | (QmPCR) |

**Table 46: Table showing the primer sequences used for the adapted and optimised original Beggs set of exons for the second multiplex PCR set.**

| EXON NAME | SEQUENCE 5' – 3' | SIZE IN BASE PAIRS |
|---|---|---|
| Pm F | GAAGATCtagacagtggatacataacaaatgcatg | 535 |
| Pm R | ttctccgaaggtaattgcctcccagatctgagtcc | |
| 3 F | tcatccgtcatcttcggcagattaa | 410 |
| 3 R | caggcggtagagtatgccaaatgaaaatca | |
| 43 F | gaacatgtcaaagtcactggacttcatgg | 357 |
| 43 R | atatatgtgttacctacCCTTGTCGGTCC | |
| 21 F | gcaaaatgtaatgtatgcaaag | 319 |
| 21 R | atgttagtaccttctggatttc | |
| 50 F | ttaaaagaaattctacccactaaagtt | 337 (QmPCR) |
| 50 R | ctctctcacccagtcatcacttcata | |
| 50 F | cac caa atg gat taa gat gtt cat gaa t | 271 |
| 50 R | tct ctc tca ccc agt cat cac ttc ata g | |
| 13 F | aataggagtacctgagatgtagcagaaat | 238 |
| 13 R | ctgacCTTAAGTTGTTCTTCCAAAGCAG | |
| 6 F | ccacatgtagGTCAAAAATGTAATGAA | 202 |
| 6 R | gtctcagtaatcttcttacCTATGACTATGG | |
| 47 F | cgttgttgcatttgtctgtttcagTTAC | 181 |
| 47 R | gtctaacCTTTATCCACTGGAGATTTG | |
| 60 F | AGGAGAAATTGCGCCTCTGAAAGAGAACG | 139 |
| 60 R | CTGCAGAAGCTTCCATCTGGTGTTCAGG | |
| 52 F | AATGCAGGATTTGGAACAGAGGCGTCC | 113 |
| 52 R | TTCGATCCGTAATGATTGTTCTAGCCTC | |

**Table 47: Primer sequences for the adapted and optimised original Kunkel set of exons for the third multiplex PCR set.**

| EXON NAME | SEQUENCE 5' – 3' | SIZE IN BASE PAIRS |
|---|---|---|
| Pb F | TCTGGCTCATGTGTTTGCTCCGAGGTATAG | 332 |
| Pb R | CTTCCATGCCAGCTGTTTTTCCTGTCACTC | |
| 49 F | gtgcccttatgtaccaggcagaaattg | 439 |
| 49 R | gcaatgactcgttaatagccttaagatc | |
| 46 F | GCTAGAAGAACAAAAGAATATCTTGTC | 148 |
| 46 R | CTTGACTTGCTCAAGCTTTTCTTTTAG | |
| 16 F | tctatgcaaatgagcaaatacacgc | 290 |
| 16 R | ggtatcactaacCTGTGCTGTACTC | |
| 41 F | gttagctaactgccctgggccctgtattg | 274 |

| | | |
|---|---|---|
| 41 R | tagagtagtagttgcaaacacatacgtgg | |
| 32 F<br>32 R | gaccagttattgtttgaaaggcaaa<br>ttgccaccagaaatacatacCACACAATG | 253 |
| 20 F<br>20 R | GTG TTA ATG CAG ATA GCA TCA AAC<br>ACA AAT TTT TAA CTG ACT TTT AAT TG | 239 (Covone) |
| 42 F<br>42 R | CAC ACT GTC CGT GAA GAA ACG ATG ATG G<br>CTT CAG AGA CTC CTC TTG CTT AAA GAG AT | 195 |
| 42 F<br>42 R | CAC ACT GTC CGT GAA GAA ACG ATG ATG<br>tta gca cag agg tca gga gcA TTG AG | 155 |
| 34 F<br>34 R | GTAACAGAAAGAAAGCAACAGTTGGAGAA<br>CTTTCCCCAGGCAACTTCAGAATCCAAA | 171 |
| 1 F<br>1 R | [M13f]-GCAGGTCCTGGAATTTGA<br>[M13r]-caaactaaacgttatgccaca | 405 |
| 2 F<br>2 R | cac taa cac atc ata atg g<br>gat aca cag gta cat agt c | 233 (QmPCR) |
| 5 F<br>5 R | Ggt tga ttt agt gaa tat tgg aag tac<br>Cca ttc atc agg att ctt acc tgc c | 114 (QmPC |
| 62 F<br>62 R | gtc ttt cct gtt tgc gat gaa ttt gac c<br>ctc act tgt gaa tat aca ggt tag tca c | 191<br>(QmPCR) |

M13F = 5'-TGTAAAACGACGGCCAGT-3'.

M13R = 5'-CAGGAAACAGCTATGACC-3'.

The exon 1 primer in the third set contains a M13 tail to enable sequencing to be performed.

3. **Reverse transcription PCR primers.**

Table 48: Table showing the primers that were included in the reverse transcription PCR assays.

| EXON NAME | SEQUENCE 5' – 3' | cDNA position |
|---|---|---|
| 2F1(1A) | CAA AAG AAA ACA TTC ACA AAA TGG | 49-72 |
| 2F2(1C) | T7-TCT AAG TTT GGG AAG CAG CA | 88-107 |
| 9F1(1G) | CGA TTC AAG AGC TAT GCC TAC | 883-903 |
| 10F1 (1E) | T7-TTG CAA GCA CAA GGA GAG ATT | 1084-1104 |
| 11R2(1D) | TGA GGC ATT CCC ATC TTG A | 1285-1303 |
| 12R1(1H) | TTA GCC AGT CAT TCA ACT CTT TCA | 1370-1393 |
| 17F1(2A) | cgg atc cAC AAG GGA ACA GAT CCT GGT AA | 2068-2089 |
| 17F2(2C) | gcT7-AGG CAG ATT ACT GTG GAT TCT GA | 2134-2156 |
| 23F2(2G) | ATT GAG GGA CGC TGG AAG A | 3073-3091 |
| 23F1(2E) | gcT7-GAG CAT TGT CAA AAG CTA GAG GA | 3112-3134 |
| 18R1(1F) | CTT CTG AGC GAG TAA TCC AGC T | 2197-2218 |
| 18R2(1B) | ACT CTG CAA CAC AGC TTC TGA G | 2211-2232 |
| 25R1(2D) | CCC ACC TTC ATT GAC ACT GTT | 3316-3336 |
| 25R2(2H) | GTC TCA AGT CTC GAA GCA AAC TCT | 3363-3386 |

| | | |
|---|---|---|
| 30F2(3A) | TCA CAT TCA TTG ACA AGC AGT TGG | 4157-4180 |
| 31F1(3C) | gcT7-GCC CAA AGA GTC CTG TCT CA | 4309-4328 |
| 35R1(2Bw) | TTA TCT TCC ACC AAC GTC TCC TTC TTG | 4929-4955 |
| 35R2(2Dw) | CCT ACC TCT GTG ATA CTC TTC AGG TGC | 4878-4904 |
| 36F3(3G) | CAC AAA GTG GAT CAT TCA GGC | 5073-5093 |
| 36F2(3E) | T7-GCT GAC ACA CTT TTG GAT G | 5092-5110 |
| 38R1(3D) | TTA AAC TGC TCC AAT TCC TTC AA | 5338-5360 |
| 40R1(3H) | CAA TGT CAT CCA AGC ATT TCA G | 5668-5689 |
| 43F1(4A) | GCA ACG CCT GTG GAA AGG GTG | 6196-6216 |
| 44F2(4C) | T7-GCT GAA CAG TTT CTC AGA AAG ACA CAA | 6367-6393 |
| 45R3(3Dw) | CTG TCT GAC AGC TGT TTG CAG ACC TCC | 6579-6605 |
| 46R1(3B) | CTG CTT CCT CCA ACC ATA AAA C | 6670-6691 |
| 50F1(4G) | AGC TCC TGG ACT GAC CAC TAT T | 7281-7302 |
| 51F1(4E) | T7-TGG ACA GAA CTT ACC GAC TGG | 7435-7455 |
| 53R1(4Dw) | CTT TTG GAT TGC ATC TAC TGT ATA GGG | 7828-7854 |
| 54R1(4Bw) | TGC CAC TGG CGG AGG TCT TTG GCC AAC | 7875-7901 |
| 56/57F1(5A) | AAA AGT CTC TCA ACA TTA GGT CCC | 8372-8395 |
| 58F1(5C) | gcT7-ACA GAG CAG CCT TTG GAA G | 8620-8638 |
| 59R3(4F) | CTC TTG AAG TTC CTG GAG TCT TTC | 8800-8823 |
| 59R4(4B) | GTG ATC TTG GAG AGA GTC AAT GAG G | 8898-8922 |
| 63F1(5G) | ACG AGA CTC AAA CAA CTT GCT G | 9227-9248 |
| 67F2(5E) | gcT7-TGG GTG AAG TTG CAT CCT TTG G | 9743-9764 |
| 68R2(5D) | TGG ACA CTC TTT GCA GAT GTT AC | 9938-9960 |
| 73R1(5H) | ATC CAT TGC TGT TTT CCA TTT C | 10336-10357 |
| 79R1(5F) | ATC ATC TGC CAT GTG GAA AAG | 11064-11084 |
| 79R2(5B) | gcg aat tcT ATT CTG CTC CTT CTT CAT CTG TC | 11120-11143 |

The start codon ATG was at position 245 using the NM004006 dystrophin consensus sequence.

T7- gga tcc taa tac gac tca cta tag gaa cag acc acc atg

## 4. Lightcycler 2 adlican primers.

**Table 49: Table showing the primer set that was included in the Lightcycler 2 assays.**

| Primer name | Sequence 5' - 3' |
|---|---|
| Adlican forward | ctt ctt ttg caa atg cca ctc |
| Adlican reverse | tga tga atg ttc ctc aga tat cct at |

# APPENDIX B

## B1. ACCESSION NUMBERS

AF213406: Exon 6

AF213408: Exon 8

AF213429: Exon 41

AF213430: Exon 42

AF213437: Exon 52

AF213438: Exon 53

Z11860: Exon 60

NM_004006.1: cDNA reference sequence (dystrophin)

M18533: old cDNA reference sequence (dystrophin)

## B2. WEBSITES / INTERNET LITERATURE

http://www.chem.agilent.com/ - Bioanalyser lab-on-a-chip, Agilent technologies.

http://en.wikipedia.org/wiki/Image:Gastrocnemius.png – Image of gastrocnemius muscle.

http://en.wikipedia.org/wiki/Biceps_brachii_muscle - Image of biceps muscle.

http://en.wikipedia.org/wiki/Muscle

http://en.wikipedia.org/wiki/Image:Illu_lower_extremity_muscles.jpg – gastroc and quadriceps muscle image.

http://users.rcn.com/jkimball.ma.ultranet/BiologyPages/M/Muscles.html - Striated appearance of muscle.

www.harkema.ucla.edu/muscles.html - image of the rectus femoris.

http://en.wikipedia.org/wiki/H&E_stain - H+E staining protocol.

http://www.neuro.wustl.edu/neuromuscular/pics/biopsy/dmd/dmdmyopthgreg.jpg
Dystrophic images H+E staining.

http://missinglink.ucsf.edu/lm/ids_104_musclenerve_path/student_musclenerve/normal.ht
ml - normal muscle fibres from adult and child. 200X magnification.

http://www.usuhs.mil/pat/surg_path/nlhist/pictures/nl0004b.jpg&imgrefurl - Longitudinal
section of muscle fibre.

www.unm.edu/.../musclesarcomere.html - subcellular organisation of muscle.

(http://www.genetechhk.com/image/ser_spotting.jpg) – microarray spotting.

(http://www.ebi.uniprot.org:80/index.shtml) – universal protein knowledgebase.

http://frodo.wi.mit.edu/ - Primer3 software for primer design.

http://www.mdausa.org – muscular dystrophy association in the USA.

http://staff.science.nus.edu.sg/~scilooe/srp_2003/sci_paper/paediatrics/research_paper/liew
_yi_jin.pdf : Splice site selection in the dystrophin gene.

http://www.dmd.nl/dmd_all.html: All dystrophin mutations.

http://www.invitrogen.com/content.cfm?pageid=4082: Invitrogen RT-PCR manual

http://www.geospiza.com: FinchTV V 1.4.0

http://www.hgvs.org/mutnomen/recs-DNA.html: Human genome variation society